U.S. Department of Transportation

Federal Railroad Administration

Comparison of Major Parameters In Electrodynamic and Electromagnetic Levitation Transport Systems

National Maglev Initiative
Washington, D.C. 20590

W. S. Brown
C. R. Dauwalter
F. Heger
M. S. Weinberg

The Charles Stark Draper Laboratory, Inc.
555 Technology Square
Cambridge, Massachusetts 02139

DOT/FRA/NMI-92/15

September 1992

This document is available to the U.S. public through the National Technical Information Service, Springfield, Virginia 22161.

11 - Advanced Systems

Technical Report Documentation Page

1. Report No. DOT/FPA/NMI–92/15	2. Government Accession No.	3. Recipient's Catalog No.
4. Title and Subtitle COMPARISON OF MAJOR PARAMETERS IN ELECTRODYNAMIC AND ELECTROMAGNETIC LEVITATION TRANSPORT SYSTEMS		5. Report Date September 1992
		6. Performing Organization Code
7. Authors (s) W.S. Brown, C.R. Dauwalter, F. Heger, M.S. Weinberg		8. Performing Organization Report No. CSDL-R-2420
9. Performing Organization Name and Address The Charles Stark Draper Laboratory, Inc. 555 Technology Square Cambridge, MA 02139		10. Work Unit No. (TRAIS)
		11. Contract or Grant No. DTFR53-91-C-00055
12. Sponsoring Agency Name and Address U.S. Department of Transportation Federal Railroad Administration Office of Research and Development Washington, D.C. 20590		13. Type of Report and Period Covered Final Report July 1991-September 1992
		14. Sponsoring Agency Code

15. Supplementary Notes

Contracting Officer Technical Representative: Mr. Thomas D. Schultz

16. Abstract

This study compiles quantitative design information that can be used in selecting a high-speed magnetic levitation system. Analytic models were developed for three configurations of electromagnetic (EMS) and three electrodynamic (EDS) systems, and for linear induction and synchronous motors. The models permit comparisons based on consistent assumptions. The following results indicate that the hoped-for advantages of EDS are difficult to realize: 1) all of the systems studied require smooth guideways to achieve acceptable ride quality unless active control techniques are developed; 2) the estimated weight of the superconducting magnets for the EDS systems is surprisingly large and comparable to the weight of the EMS onboard electromagnets; and 3) real power consumption in sheet guideway null flux EDS is similar to EMS when practical configurations and end effects are considered.

17. Key Words	18. Distribution Statement
Electrodynamic suspensions Electromagnetic suspensions High-speed ground transportation Magnetic levitation Magnetic suspensions Linear induction motors Linear synchronous motors Ride comfort	This document is available to the U.S. public through the National Technical Information Service, Springfield, Virginia 22161

19. Security Classif. (of this report)	20. Security Classif. (of this page)	21. No. of Pages	22. Price
UNCLASSIFIED	UNCLASSIFIED	238	

Form DOT F 1700.7 (8-72) **Reproduction of completed page authorized**

METRIC/ENGLISH CONVERSION FACTORS

ENGLISH TO METRIC

LENGTH (APPROXIMATE)

1 inch (in.) = 2.5 centimeters (cm)
1 foot (ft) = 30 centimeters (cm)
1 yard (yd) = 0.9 meter (m)
1 mile (mi) = 1.6 kilometers (km)

AREA (APPROXIMATE)

1 square inch (sq in, in^2) = 6.5 square centimeters (cm^2)
1 square foot (sq ft, ft^2) = 0.09 square meter (m^2)
1 square yard (sq yd, yd^2) = 0.8 square meter (m^2)
1 square mile (sq mi, mi^2) = 2.6 square kilometers (km^2)
1 acre = 0.4 hectares (he) = 4,000 square meters (m^2)

MASS - WEIGHT (APPROXIMATE)

1 ounce (oz) = 28 grams (gr)
1 pound (lb) = .45 kilogram (kg)
1 short ton = 2,000 pounds (lb) = 0.9 tonne (t)

VOLUME (APPROXIMATE)

1 teaspoon (tsp) = 5 milliliters (ml)
1 tablespoon (tbsp) = 15 milliliters (ml)
1 fluid ounce (fl oz) = 30 milliliters (ml)
1 cup (c) = 0.24 liter (l)
1 pint (pt) = 0.47 liter (l)
1 quart (qt) = 0.96 liter (l)
1 gallon (gal) = 3.8 liters (l)
1 cubic foot (cu ft, ft^3) = 0.03 cubic meter (m^3)
1 cubic yard (cu yd, yd^3) = 0.76 cubic meter (m^3)

TEMPERATURE (EXACT)

[(x - 32) (5/9)] °F = y°C

METRIC TO ENGLISH

LENGTH (APPROXIMATE)

1 millimeter (mm) = 0.04 inch (in)
1 centimeter (cm) = 0.4 inch (in)
1 meter (m) = 3.3 feet (ft)
1 meter (m) = 1.1 yards (yd)
1 kilometer (km) = 0.6 mile (mi)

AREA (APPROXIMATE)

1 square centimeter (cm^2) = 0.16 square inch (sq in, in^2)
1 square meter (m^2) = 1.2 square yards (sq yd, yd^2)
1 square kilometer (kn^2) = 0.4 square mile (sq mi, mi^2)
1 hectare (he) = 10,000 square meters (m^2) = 2.5 acres

MASS - WEIGHT (APPROXIMATE)

1 gram (gr) = 0.036 ounce (oz)
1 kilogram (kg) = 2.2 pounds (lb)
1 tonne (t) = 1,000 kilograms (kg) = 1.1 short tons

VOLUME (APPROXIMATE)

1 milliliter (ml) = 0.03 fluid ounce (fl oz)
1 liter (l) = 2.1 pints (pt)
1 liter (l) = 1.06 quarts (qt)
1 liter (l) = 0.26 gallon (gal)
1 cubic meter (m^3) = 36 cubic feet (cu ft, ft^3)
1 cubic meter (m^3) = 1.3 cubic yards (cu yd, yd^3)

TEMPERATURE (EXACT)

[(9/5) y + 32] °C = x °F

QUICK INCH-CENTIMETER LENGTH CONVERSION

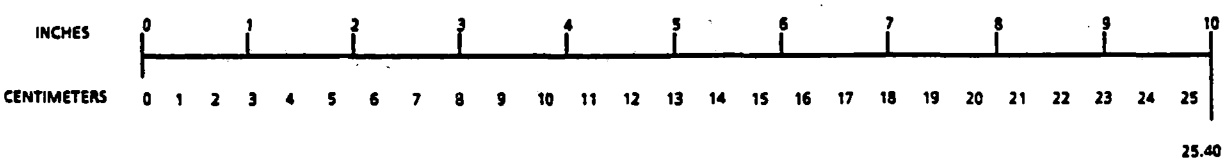

QUICK FAHRENHEIT-CELSIUS TEMPERATURE CONVERSION

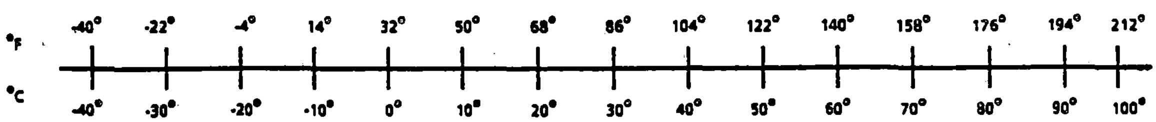

For more exact and or other conversion factors, see NBS Miscellaneous Publication 286, Units of Weights and Measures. Price $2.50. SD Catalog No. C13 10286.

DOT/FRA/NMI-92/15

COMPARISON OF MAJOR PARAMETERS IN ELECTRODYNAMIC AND ELECTROMAGNETIC LEVITATION TRANSPORT SYSTEMS

W. S. Brown
C. R. Dauwalter
F. Heger
M. Weinberg

September 1992

Contract No. DTFR53-91-C-00055

The Charles Stark Draper Laboratory, Inc.
Cambridge, Massachusetts 02139-3563

TABLE OF CONTENTS

TABLE OF CONTENTS (CONT.)

TABLE OF CONTENTS (CONT.)

TABLE OF CONTENTS (CONT.)

EXECUTIVE SUMMARY

Electrodynamic and Electromagnetic Levitation Transport Systems

Objective

The objective of this study is to compile quantitative design information on magnetic levitation transportation systems which will assist in the determination of the most promising direction to pursue for future system development.

Background

The choice between electromagnetic and electrodynamic systems is under deliberation. Electromagnetic systems incorporate conventional electromagnets which are servoed to lift the vehicle even at zero operating speeds. Electrodynamic systems fix a large magnetic field, generated by superconducting coils, to the vehicle. When the vehicle moves, currents are induced in the guideway that generate lift. Most effort in the U.S. has focused on electrodynamic systems.

Under this program, preliminary design and analysis was performed to quantify engineering parameters, such as ride quality, power, and vehicle weight and payload, to contribute factual information to the decision between electromagnetic and electrodynamic systems. To cover many possible variations and to obtain general results while limiting the work scope, these systems were analyzed:

<u>Electromagnetic Systems</u> (EMS)

I. Separate magnets for heave and lateral guidance and a separate linear induction motor.

II. Staggered magnets which combine lift and lateral guidance and a separate linear induction motor.

III. Combined heave and synchronous propulsion magnets with separate lateral magnets. The lift magnets are used as the moving element (rotor) for a linear synchronous motor, similar to Transrapid. This option, EMS III is preferred and is the basis for the results below.

Electrodynamic Systems (EDS)

1. Image flux in which the superconducting magnets move above a continuous circular arc cross section guideway (the Magneplane configuration). Because of its large air gaps, only the image flux configuration has no secondary suspension. The three options all include a linear synchronous motor with the armature winding in the guideway.

2. Null flux with coils in the guideway and on-board superconducting magnets . The coils are arranged so that at zero lift, no current flows through the guideway coils

3. Hybrid null flux, similar to null flux but with a continuous sheet guideway.

Results

In terms of required guideway smoothness, and passenger payload, the electromagnetic system (EMS III) and the electrodynamic systems EDS 1 and 2 (image flux and hybrid null flux) are comparable. The resistive power for EDS systems were higher than EMS while the reactive power was lower (EDS 1 and 3) and similar (EDS 2). In addition, the EDS systems require significant development (which implies risk) to demonstrate the feasibility of operation. **Until major developments in the technology of electrodynamic systems are realized, the electromagnetic system (EMS 3, similar to Transrapid) is preferred.** If EDS is to be competitive, further development will be required and significant risks addressed. Major results are summarized:

- All the systems require smooth guideways (equivalent to welded steel rails) to achieve acceptable ride quality (passive secondary suspensions were assumed except for image flux). The expectation that the EDS systems, because of the larger guideway-vehicle clearances, would permit rougher guideways was not realized.

- The weight of the superconducting magnets with shields, supports, and insulation for the EDS image and null flux systems was similar to that of EMS III at 25% total vehicle weight. For a 40 Mg vehicle, 113 passengers can be accommodated. Fewer passengers could be handled with the hybrid null flux (EDS 3).

- Total power dissipation for propulsion and magnetic drag was 1,500 W/m of powered guideway for EMS III (linear synchronous motor), 2,000 W/m of powered guideway for EDS 1 (image flux) and 1,000 W/m of powered guideway for EDS 3 (coil null flux). For a 40 Mg vehicle at 134 m/s, aerodynamic drag power was estimated at 5.4 MW. The reactive guideway power was larger in EMS III (25 kVA/m of powered guideway) than in the EDS systems (5 kVA/m of powered guideway for image flux, 22 kVA/m of powered guideway for hybrid null flux and 5.3 kVA/m of powered guideway for coil null flux).

- Little data was available to estimate the effect of guideway AC fields quenching EDS superconducting magnets, an important effect in superconducting generators. **Feasibility of electrodynamic systems cannot be fully determined until the issue of possible quenching of superconducting magnets due to AC guideway fields is resolved.**

Other important results include:

- Magnetic saturation limits the EMS III propulsion capability to 0.1 g, which makes operation at 134 m/s marginal, with negligible hill climbing capability at that speed.

- Because the relative displacements between the vehicle and the bogey are small, active secondary suspensions, which would enable rougher roadways, should be considered for EDS.

SECTION 1
INTRODUCTION

1.1 Objective

The objective of this study is to compile quantitative design information on magnetic levitation transportation systems which will assist in the determination of the most promising candidates for pursuit of future system development.

Background

The choice between electrodynamic and electromagnetic levitation systems for high speed ground transportation systems is under deliberation. Proponents of both Electrodynamic Systems (EDS) and Electromagnetic Systems (EMS) emphasize the advantages of their approach, but are not always quick to point out the disadvantages, both known and potential. This natural tendency makes objective evaluations difficult.

EDS generally feature larger mechanical clearances between vehicle and guideway and thus appear to be more tolerant of guideway roughness, suggesting the possibility of lower guideway cost (a major component of the cost of acquisition of a complete system, according to many studies). On the other hand, EMS require smaller clearances for efficient design and operation, but are magnetically self-shielding, can provide levitation at zero speed, and can have lower drag then EDS, except at very high velocities. In both types of levitation systems, the on-board magnets can be used to implement linear synchronous motors.

In order to provide objective information to aid in the selection of high speed magnetic levitation systems, this study compiled detailed quantitative design information based on assumptions which were consistent across all of the systems examined. The consistency of assumptions which were made provides results which can reliably identify significant differences between systems, even though their accuracy may be less than perfect. The results should be able to contribute to a rational first order evaluation of the viability, both technical and economic, of these levitation systems.

The parameters which were evaluated include

(1) Effect of guideway roughness and cross-winds on:

(a) Vehicle design requirements, e.g., adequate vehicle-guideway clearances.

(b) Passenger comfort.

(2) Mass of levitation and propulsion components

(a) In the vehicle.

(b) On the guideway.

(3) Mass of vehicle including structure, furnishings, utilities such as environmental control, on-board power conditioning equipment and batteries.

(4) Passenger capacity, including baggage.

(5) Power consumption from aerodynamic drag, eddy current losses in the guideway and ohmic power losses in both guideway and on-board the vehicle.

1.2. Assumptions

Six different configurations of magnetically levitated high speed ground transportation systems were selected for study and comparison. The selection includes the major system types presently under consideration. The intent of the study was, in addition to providing quantitative comparison information, to clarify the trade-offs between systems by holding some important system parameters invariant between the systems. These parameters are:

(1) Vehicle speed; two different speeds were examined for each system:

(a) 134 meters/second (300 miles per hour).

(b) 89 meters/second (200 miles per hour).

(2) Vehicle weight, frontal area and volume; A vehicle weight of 40 Mg was selected as being representative of the vehicles being studied elsewhere. Initially, a decision was necessary as to whether the vehicle weight or the vehicle payload should be maintained the same for all of the systems under comparison. Vehicle weight was selected for this study because it fixes the levitation capability requirement of the magnet system, leading to direct calculations of the magnet design. Fixing the payload capability would have required iterative solutions to the magnet design because the magnet size would depend on the total vehicle weight (which depends in turn on the magnet weight). With this choice, payload (which for this study consisted entirely of passengers and their baggage) for the fixed vehicle weight could be calculated because simple relationships were identified for estimating the weight of all vehicle components except the magnets, once the magnet weight was determined. This still required

iterative solutions for payload/passenger capacity, but these were much simpler than iterative solutions for the magnet designs would have been.

(3) Magnetic force capability; two sets of requirements for magnetic force capability were selected for the study, corresponding to the two design speeds addressed, 89 meters/second and 134 meters/second; these are shown in Table 1-1. They were selected to provide the vehicles studied with the capability to withstand the static and dynamic levitation and guidance loads which could be reasonably expected and to provide a propulsion margin above aerodynamic drag to provide for reasonable acceleration and permit negotiation of hills. The requirements differed for the two design speeds because the aerodynamic drag and the lateral component of the crosswind forces depend on the vehicle speed. The lateral force requirements were divided into two categories, continuous (e.g., force due to steady crosswind) and short term (e.g., force due to wind gusts). The duration of the short term lateral force was set at five seconds.

(4) Magnetic field in the passenger compartment; Magnetic field exposure might present a health risk. Even though, at the present time, there are no definitive standards for such exposure or unequivocal evidence of adverse consequences, public concern demands that factors with possible health implications be addressed. Consequently, estimates were made of the strength of the magnetic fields which riders would be exposed to in the passenger compartment of each of the vehicles and magnetic shielding provided, if necessary, to prevent exposure to high field levels.

(5) Ride quality; Ride comfort is expected to be an important determinant of public acceptance of Maglev transportation systems. While it is possible that an extremely comfortable ride may not itself attract passengers from alternative modes, it seems likely that significantly poorer ride quality may discourage public acceptance. Consequently, each of the vehicles studied was evaluated for ride quality according to the Pepler index, a frequently used measure for ride comfort.

Table 1-1. Vehicle force requirements.

Description	Units	Design Speed 89 m/s	Design Speed 134 m/s
Propulsion			
Aerodynamic drag (C_d = 0.3 assumed)†	g	0.044	0.1
Hill climbing (3% grade)	g	0.03	0.03
Acceleration at low speed	g	0.15	0.15
Acceleration at high speed	g	0.075	0.075
Net propulsion requirement (Propulsion minus magnetic drag)	g	0.15	0.21
Vertical support	g	1.1	1.1
Lateral Guidance			
27 m/s (60 mph) lateral wind loads	g	0.16	0.32
14 m/s (30 mph) lateral wind loads	g	0.08	0.16
6° banked curve (at standstill)	g	0.1	0.1
Lateral force requirement			
Short term (5 seconds)	g	0.26	0.42
Continuous	g	0.18	0.26

† Cd is the coefficient of Drag

SECTION 2

ELECTROMAGNETIC SYSTEMS

2.0 General

The electromagnetic systems described in this report are characterized by the effective confinement of the magnetic flux of the levitation and propulsion components within a ferromagnetic core, except for the leakage and air gap fluxes. The leakage flux density decreases rapidly with distance away from the device, with a characteristic distance of the order of the air gap. As a result, even though the fields may be as high as 1 Tesla in the air gap, because typical gaps are of the order of only 1 cm the magnetic fields experienced in the vehicle passenger compartment are small, and special shielding to control these fields is usually not necessary. The magnetic fluxes which produce the required levitation, guidance and propulsion forces are induced by electrical currents flowing in coils suitably placed on the iron cores; these coils are typically made from copper or aluminum wire, the latter often used when cost or weight are important.

The magnetic structures, or rails, on the guideway which provide the levitation and guidance functions alone are entirely made of iron, without any electrical conductors. This is in contrast with the guideway portion of the motors for propulsion, which do incorporate electrical conductors.

All of these electromagnetic components are characterized by an attractive magnetic force between the vehicle magnets structures and the iron guideway which is unstable; that is, as the air gap decreases, the attractive magnetic force tends to increase (this is not the case for lateral suspension of EMS II, as is discussed in Section 2.2). Consequently, it is necessary to implement a closed-loop controller for the magnet currents to enable stable operation of the suspension elements.

The three electromagnetic systems analyzed in this study are illustrated in Figures 2-1 through 2-4. The systems are termed EMS I, EMS II and EMS III in this report and are described in more detail in Sections 2-1 through 2-3, respectively. Electromagnets, such as the one shown in Figure 2-5, are located at the corners of the vehicles or along

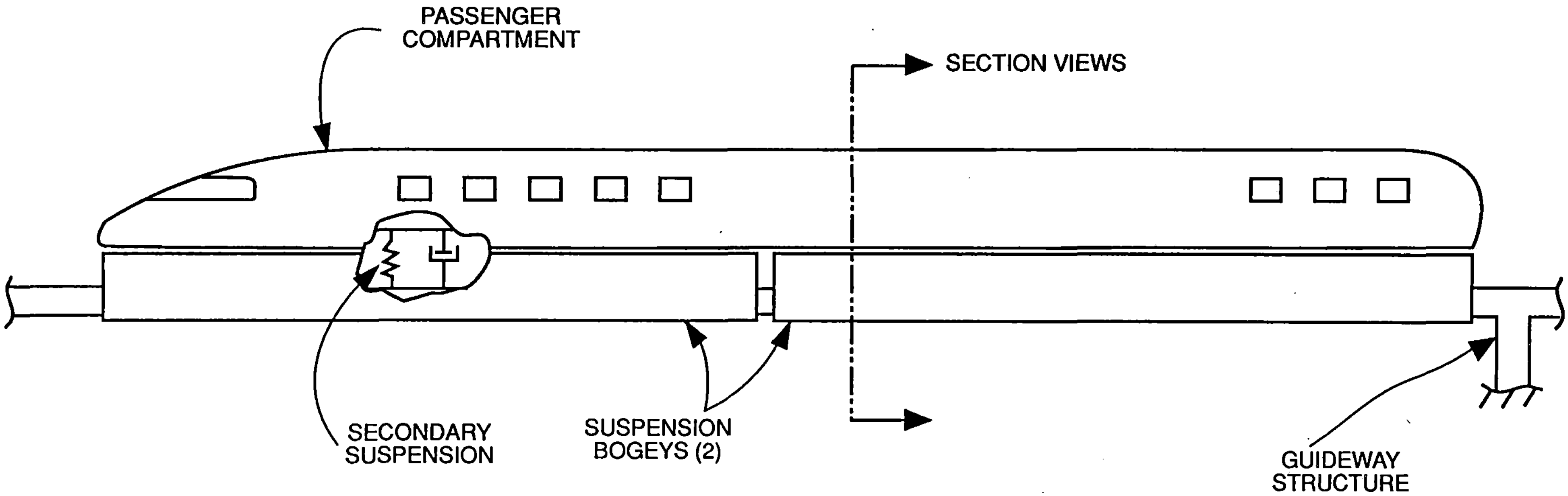

Figure 2-1. EMS Maglev vehicle, side view.

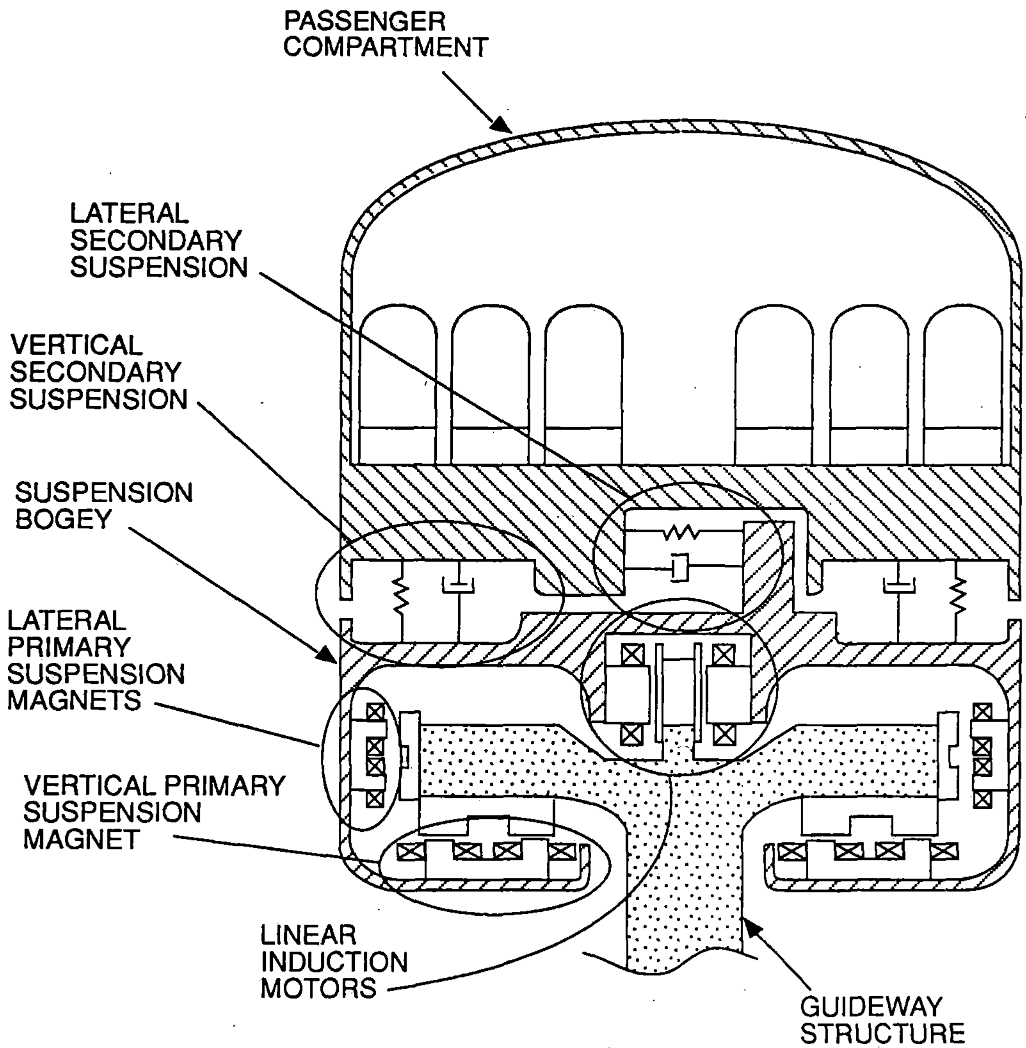

Figure 2-2. EMS I vehicle and guideway cross section.

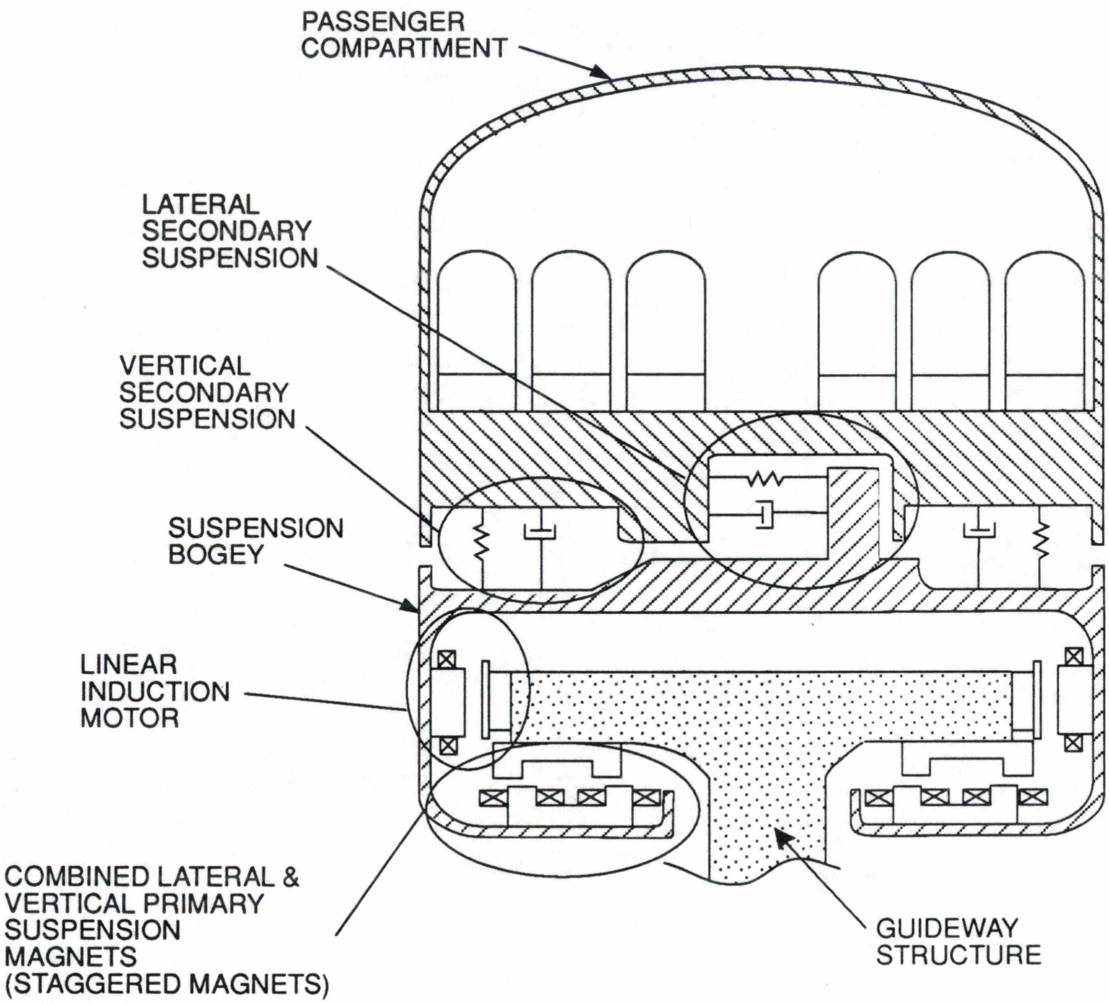

Figure 2-3. EMS II vehicle and guideway cross section.

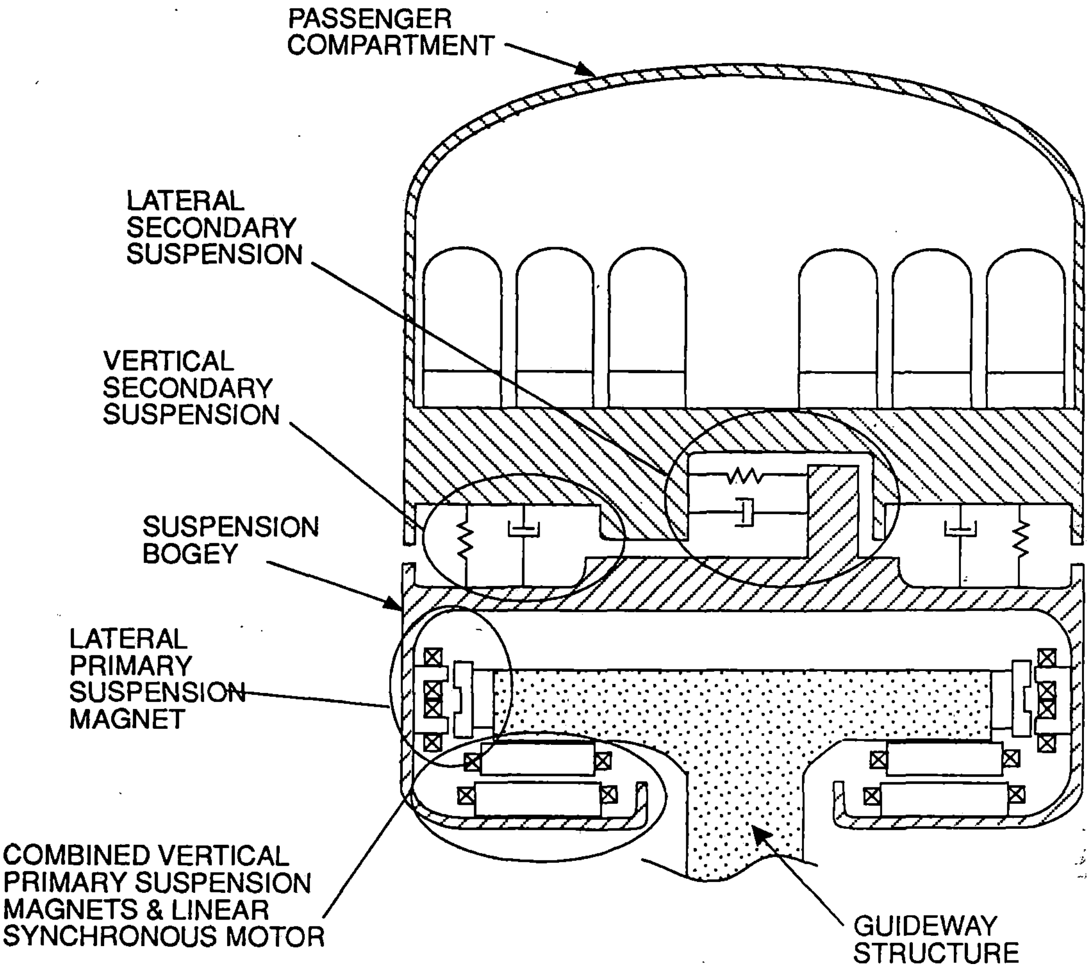

Figure 2-4. EMS III vehicle and guideway cross section.

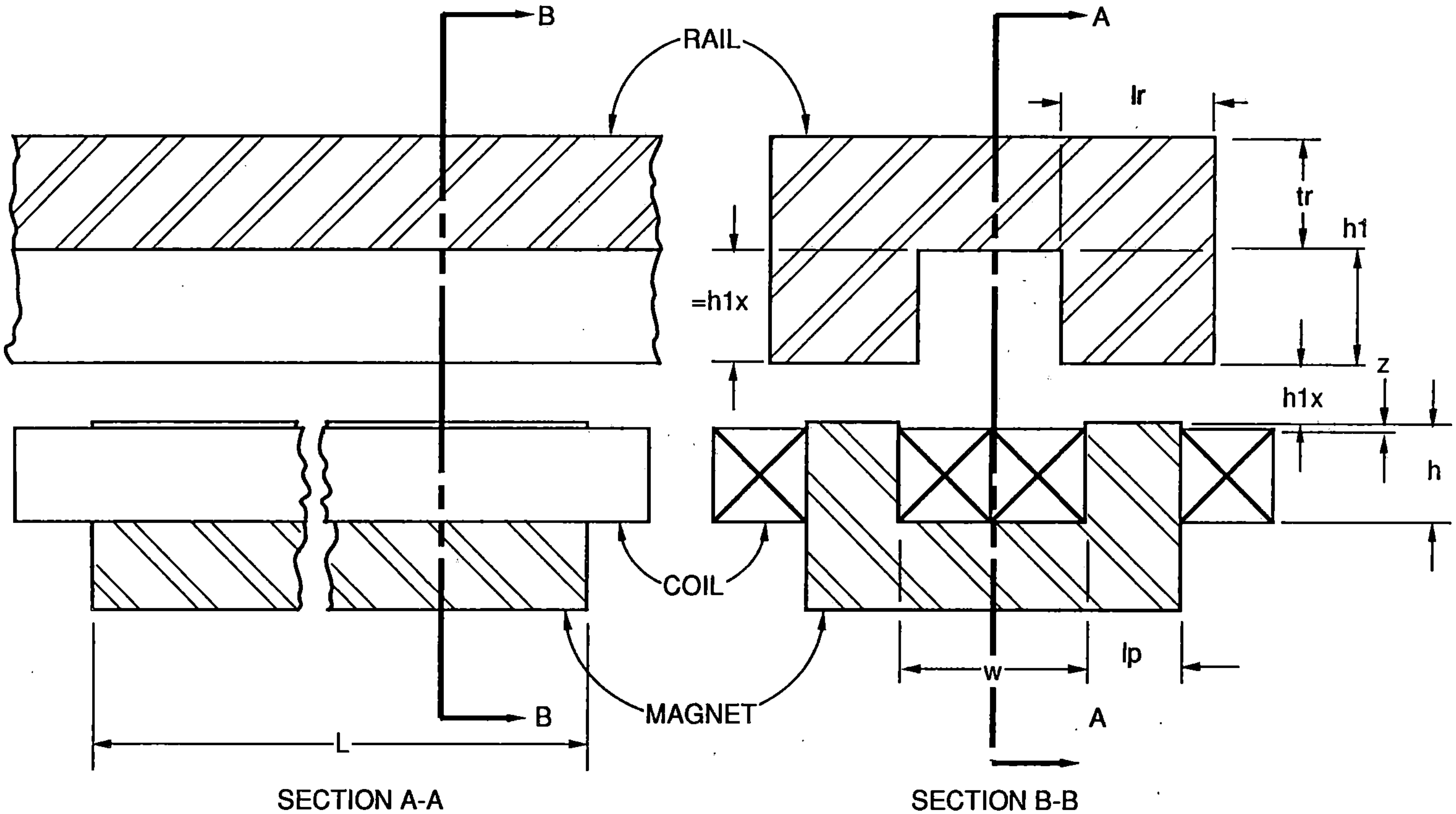

Figure 2-5. Nomenclature for simple electromagnet (EMS I & EMS III).

both sides to provide control of translational (vertical, sometimes termed heave, and horizontal, sometimes termed sway) and rotational (pitch,roll and yaw) motions. The guideway rail which interacts with each of these magnets is located symmetrically in the lateral or vertical direction with respect to the levitation and guidance magnets, respectively. For EMS I and EMS III, the poles of the guideway rail are usually somewhat wider than the poles of the vehicle magnet so that the air gap reluctance is, to first order, unaffected by the lateral (in the case of the levitation magnets) or vertical (in the case of the guidance magnets) motions of the vehicle.

In EMS I and EMS II, a separate magnetic structure which implements a Linear Induction Motor (LIM) is included to provide the propulsion forces. For the vehicle systems using the LIM, the full propulsion power, approximately five megawatts for velocities in the 134 meters/second range, must be transmitted by some means from the wayside to the vehicle, and converted on the vehicle into a form suitable for the LIM (in general, 3 phase power of controllable frequency and amplitude). The guideway portion of the LIM includes a layer of an electrical conductor, typically aluminum for reasons of cost, over the guideway iron. In EMS III, both the levitation and propulsion functions are provided by the same vehicle magnetic structure, which interacts with a guideway structure containing suitably excited conductors (like the LIM, 3 phase power of controllable frequency and amplitude) to produce a moving magnetic field to provide propulsion.

2.1. EMS I, Separate Lift and Lateral Magnets and Linear Induction Motor (LIM)

The first system, termed EMS I and illustrated in Figure 2-2, utilizes separate magnetic structures, both on the vehicle and on the guideway, to provide levitation, guidance and propulsion forces. The levitation and guidance structures are similar to the simple electromagnet illustrated in Figure 2-5, and interact with iron rails installed on the guideway. The propulsion function for this configuration is provided by a LIM, which is illustrated in Figure 2-6 (the illustrative figures define the nomenclature used in the spreadsheets which evaluate the major parameters; the models and the spreadsheets used to calculate the major parameters are described in Appendix A. The spreadsheets containing the numerical results appear in Appendix F, and Appendix E contains the formulas used for the calculations). EMS I is the only one of the 3 EMS configurations which utilizes a separate set of devices for each of the required functions, levitation, or lift, guidance and propulsion. The other two system configurations both utilize a

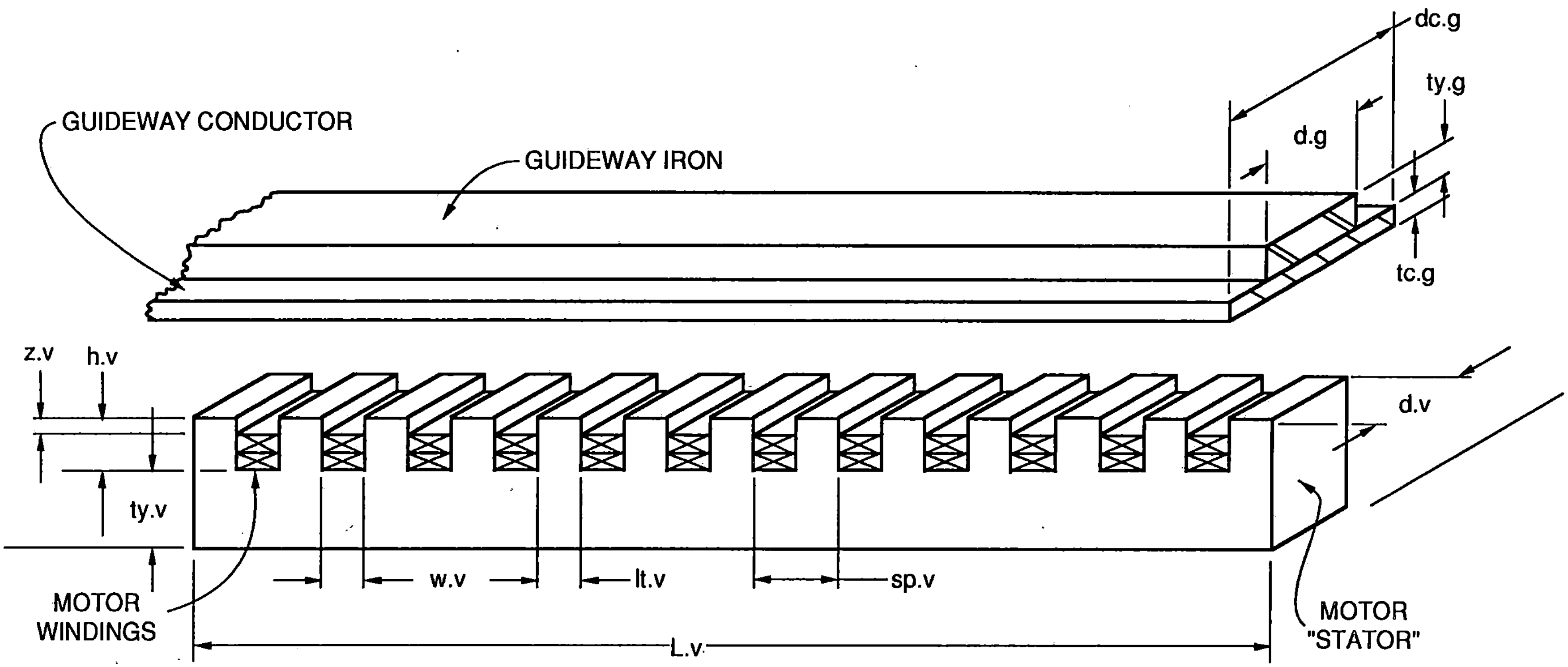

Figure 2-6. Nomenclature for linear induction motor.

common magnetic structure to provide two of the three necessary functions.

2.2. EMS II, Staggered Lift and Lateral Magnets with Linear Induction Motor

EMS II is characterized by pairs of magnets located at each corner of the vehicle. A single magnet of such a pair is illustrated in Figure 2.7. Each magnet of an individual pair is "staggered" or displaced laterally with respect to its mate, with both magnets of the pair interacting with a single rail on the guideway. Unlike the levitation and guidance magnets of EMS I, the poles of both the vehicle magnets and the guideway rails of this configuration have more or less the same width; the air gap reluctance in this system is consequently affected by both the vertical and lateral motions of the vehicle and both lift and guidance forces are produced. The lift forces of the simple electromagnet of Figure 2-5 are unstable in that, for a constant coil current, the attractive force increases as the magnet and rail approach each other more closely i.e., as the air gap (h1x in Figure 2-5) decreases. In contrast, the lateral force of the magnet is stable in that, as the magnet moves laterally with respect to the rail (increasing "del" in Figure 2-7) the magnetic force tends to return the magnet to the centered position ("del"=0, i.e., the magnet and rail centerlines coincident).

The separate magnet control systems for the vertical and lateral motion are so designed that both motions are stably controlled and, moreover, so that there is no cross-coupling between the two directions of motion. To accomplish this decoupling requires a specific gain value for the lateral magnet controller, called the decoupling gain [2]; and this determines the lateral natural stiffness and thus the natural frequency of the suspension. This frequency is often lower than might otherwise be chosen, based on tracking considerations only, and results generally in a softer ride but larger gap excursions than would be the case with higher natural frequency values. In general, the increased "gap" excursions (gap is somewhat a misnomer in this case, because the air gap, or perpendicular distance between the moving and stationary parts, does not change as a result of the lateral motions) can be acceptable because the lateral displacement limits are substantially larger than the air gap. For the configurations analyzed in this study, the range of lateral motions for which lateral force is a linear function of lateral displacement ranged from 1.5 to 1.9 times the air gap. Wormley, et al [2] have shown that the lateral force continues to increase for some distance beyond the linear range.

2.3. EMS III, Combined Lift and Synchronous Motor and Separate Lateral Guidance Magnets

EMS III is essentially similar to the German Transrapid System [8]. Illustrated in Figure 2-3; the model assumes four vehicle magnets, one at each corner (Transrapid has magnets distributed continuously along the vehicle length), which simultaneously provide the functions of levitation, or lift, and act as the "rotor" of a Linear Synchronous Motor (LSM) in conjunction with the windings installed in the guideway rails. These rails are slotted transversely and are provided with a winding consisting of 3 conductors which "meander" through the slots of the guideway. These conductors, when excited by three-phase wayside inverters, provide a moving magnetic field which acts against the field of the vehicle magnets, propelling them synchronously with the guideway field. Maglev systems using LSM are usually operated with the LSM excitation applied to a limited length of the guideway because, as will be seen in Section 2.5, the guideway power is quite high, of the same order of magnitude as the aerodynamic drag power, for a block length of only one kilometer. Thus, block lengths of many kilometers are impractical from an operating economy point of view. On the other hand, short block lengths are undesirable because the wayside power transmission, conditioning and control equipment is duplicated for each block so that short block lengths increase the capital cost of system acquisition. A proper balance between these two conflicting requirements will have to be resolved based on economic considerations, not addressed in this study. The combined lift magnet and linear synchronous motor configuration is illustrated in Figure 2-8.

The Transrapid Maglev system differs from the configuration studied here in having many independent magnets along the length of its vehicle. In addition, the Transrapid lateral magnets are suspended vertically and the lift magnets horizontally by rubber springs with a resonant frequency of about 1.5 Hz. This has the effect of somewhat isolating the magnets from motions of the bogey parallel to the air gap surfaces, thus reducing the effective unsprung weight for improved ride quality and reduced air gap variations.

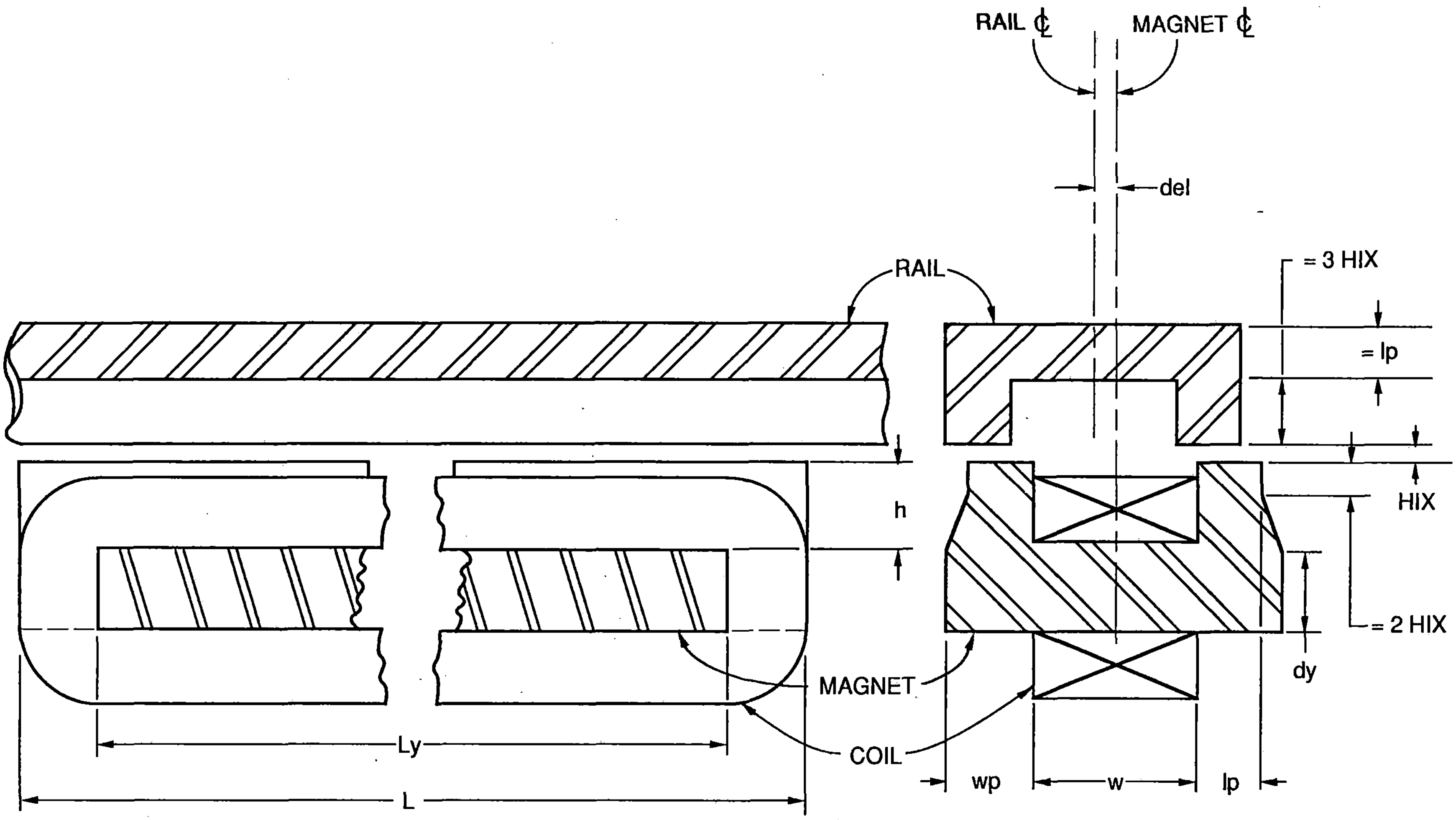

Figure 2-7. Nomenclature for combined (staggered) lift and guidance magnets (EMS II).

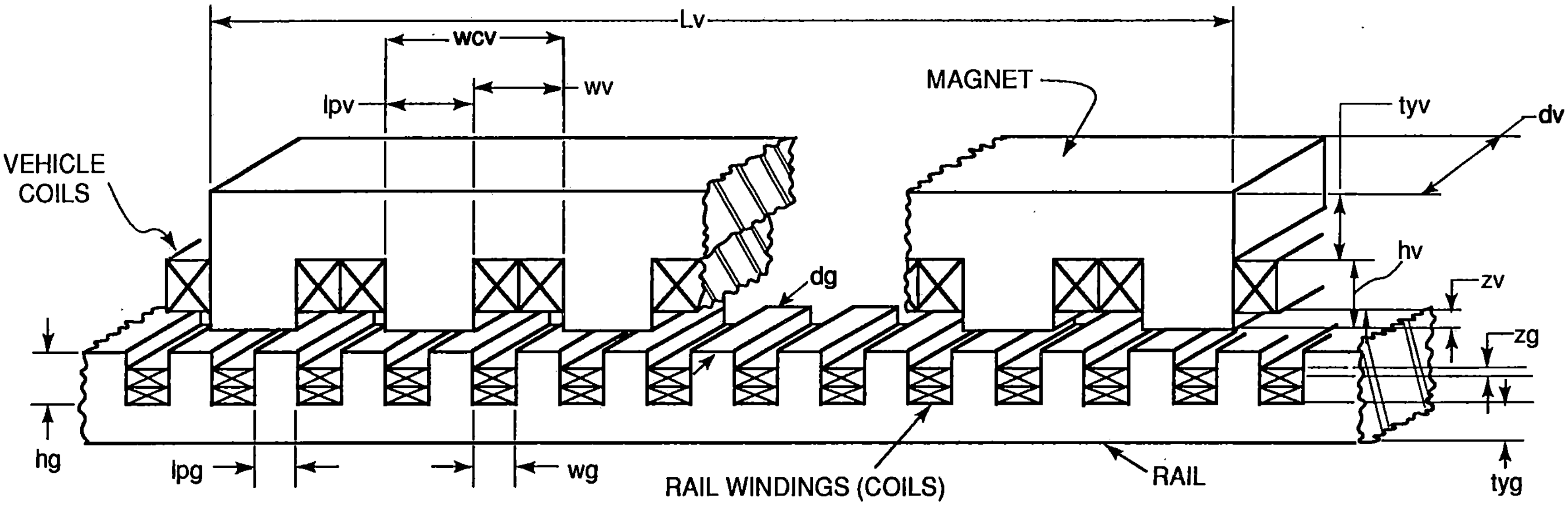

Figure 2-8. Combined lift magnets and linear synchronous motor (EMS III).

2.4 Assumptions, Constraints and Optimization

The suspension and propulsion performance requirements for all of the systems examined in this study are listed in Table 1-1, which also shows some of the selected conditions which determined those requirements. Some additional constraints were applied to the EMS studied. A major constraint on the design is the practical necessity for levitating the system from a power-off condition in which the vehicle has settled onto the skids, increasing the air gap beyond its normal operating value. In this study, the air gap at levitation is taken as twice the normal operating value. This constraint effectively determines the back iron dimensions necessary to prevent magnetic saturation.

The electromagnetic components of all three systems studied were optimized for operation at two design speeds, 134 meters/second and 89 meters/second; these optimized designs are termed Design 1, or baseline (b/l), on the spreadsheets. Optimization of a design can involve many different considerations, such as size, weight, power consumption, temperature rise, efficiency and others. Clearly, parameters such as power consumption and efficiency are important in the design of an economical operational system, but the scope of this study precluded inclusion of such economic considerations. In this study, optimization was limited to minimizing the weight of the individual magnetic components.

The constraints applied to the optimization were that the force capability be no less than the maximun requirement, that the winding insulation temperature be limited to the rating of the insulation, that the flux density in the iron portions of the magnets not exceed the saturation flux density of the material and that the coil window width to height ratio (w/h) be not greater than two, the approximate limit of validity of the expression used to evaluate interpole leakage permeance.

In the case of insulation temperature limitations, two conditions were considered for the lateral suspension magnets; these were short term requirements (5 seconds in this study) and continuous operation. As seen from Table 1-1, the short term requirements for lateral force are the more demanding. The study determined that the temperature rise from the continuous requirements was higher than that from the short term requirements. The remaining magnet dimensions were then systematically varied until the minimum value of magnet weight was achieved, consistent with the stated constraints.

In order to indicate the sensitivity of the optimization to two important magnet dimensions, two variations of the optimized designs, were examined; these are termed Design 2 and Design 3 on the spreadsheets. Design 2 has the additional constraint that the magnet pole width (lp), is 3/4 the value for Design 1, while Design 3 has an air gap (h1x) that is 80% that of Design 1 and the same magnet pole width. With these additional constraints, the remaining dimensions of Designs 2 and 3 were again systematically varied to determine the minimum magnet weight. After the three designs were optimized for each of the two operating speeds, the performance of each was then determined at a speed 2/3 the design speed (89 meters/second for the 134 meters/second optimization and 59 meters/second for the 89 meters/second optimization to provide an indication of the effect of operating speed on the performance parameters of each particular design.

2.5 Comparisons Between Electromagnetic Systems

All of the data generated in this study is contained in the spreadsheets for each of systems, which appear in Appendix F. The major results for each of the systems are extracted from the spreadsheets and appears in Tables 2-10 through 2-15 at the end of this section. These results for all of the systems are combined and presented below in the major categories of weight and power; each of these categories is subdivided into on-vehicle and on-guideway components. Finally, a relative ranking, from best to worst, for each of the categories is presented.

The Table 2-1 compares the weights of the on-vehicle electromagnetic components.

Table 2-1.

Electromagnetic on-vehicle component weight (Mg)

	EMS I		EMS II		EMS III	
Optimization Speed (m/s)	89	134	89	134	89	134
Levitation magnets	1.54	1.54	4.74	4.79	5.30	5.30
Guidance Magnets	1.55	1.93	Included in Levitation		1.55	1.93
Motor Stator	2.52	3.71	2.52	3.71	Included in Levitation	
Total	5.61	7.18	7.26	8.50	6.85	7.23

In every case, the weight of the guidance magnets is higher for designs optimized for operation at 134 meters/second, as compared with those optimized for 89 meters/second; the reason for this is that the guidance force requirements are higher for the 134 meters/second speed, as seen in Table 2-1. On the other hand, the levitation magnet weights are the same because the levitation force requirements are the same for both speeds. The Linear Induction Motor stator weight is higher for the 134 meters/second optimization speed because the propulsion force requirement is higher, as also shown in Table 2-1. The propulsion force for the Linear Synchronous Motor in EMS III was designed to 0.1 g, because the on-vehicle weight was so much larger for the 0.21 g requirement of Table 1-1 that it was judged to be impractical to design to the higher force level. With this restriction, the weight of the vehicle magnets for EMS III is comparable to that of the other two configurations.

The weights of the electromagnetic components mounted on the guideway is shown in Table 2-2.

Table 2-2.
Electromagnetic on-guideway component weight (Mg/km)

	EMS I		EMS II		EMS III	
Optimization Speed (m/s)	89	134	89	134	89	134
Levitation	113	113	48.8	48.9	271	271
Guidance	82.8	113	Included in Levitation		82.8	113
Propulsion Motor	159	180	159	180	Included in Levitation	
Total	512.8	586	365.8	408.8	353.8	384

As might be expected, the weight of the EMS III combined levitation/LSM guideway components is higher than that of the EMS I levitation magnets, since they provide two functions instead of one. The LIM guideway components comprise the heaviest single element. However, it is important to note that the propulsion capability of the LIM design meets the same requirements as the EDS at 0.21 g for 134 meters/second and 0.15 g for 89 meters/second, whereas that of the EMS III LSM is limited to 0.1g. Overall, total weight of the guideway mounted components of EMS III is the lightest of the three configurations, and that of the EMS I components is the heaviest, as might be expected since in the latter all of the functions are provided by separate components.

The power dissipation of the vehicle mounted components is shown in Table 2-3.

Table 2-3.
Electromagnetic on-vehicle power dissipation (kW)

	EMS I		EMS II		EMS III	
Optimization Speed (m/s)	89	134	89	134	89	134
Levitation magnets	119	119	74.4	75.1	51.3	47.9
Guidance Magnets	17.6	18.8	Included in Levitation		17.6	18.8
Motor Stator	60.0	82.8	60.0	82.8	Included in Levitation	
Total	196.6	220.6	134.4	157.9	65.5	66.7

EMS I vehicle mounted components have by far the largest power dissipation, followed by EMS II, with EMS III having the least power dissipation. The guidance magnets of EMS I and III have the same dissipation because they are of identical design, as are the Linear Induction Motor stators of EMS I and II. Note that the LIM on-vehicle power dissipation was not separated into vehicle and guideway components and includes that due to the eddy currents in the guideway conductor sheet and iron; due to the high LIM efficiency, guideway power dissipation is relatively small.

The reactive power of the on-vehicle components is summarized in Table 2-4. Reactive power was calculated because the rating, and thus size and weight, of the power conditioning equipment used to drive the electromagnetic components is determined, more or less, by the total volt-amperes which must be accommodated; the weight of the power conditioning equipment was included in the total vehicle weight, requiring reactive power to be calculated. Reactive power is also relevant to the sizing of the wayside power equipment and the electric utility requirements for the system, for the same reason. It is also potentially relevant to the cost of power for the system, because it affects the power factor of load presented by the system, and some electric utilities levy a charge for non-unity power factor.

Table 2-4
Electromagnetic on-vehicle reactive power (kVA)

	EMS I		EMS II		EMS III	
Optimization Speed (m/s)	89	134	89	134	89	134
Levitation magnets	N/A	N/A	N/A	N/A	N/A	N/A
Guidance Magnets	N/A	N/A	Included in Levitation		N/A	N/A
Motor Stator	1,570	3,220	1,570	3,220	Included in Levitation	
Total	1,570	3,220	1,570	3,220	N/A	N/A

EMS III reactive power is relatively small, of the order of kVA, and is due to the current variations in the vehicle magnets in response to guideway roughness and wind gusts. However, the guideway reactive power is nearly an order of magnitude larger than the on-board LIM reactive power. The reactive power associated with the eddy currents in the guideway of the LIM are, like the real power, included in the on-vehicle table.

Power dissipated in the guideway components is listed in Table 2-5.

Table 2-5.
Electromagnetic on-guideway power dissipation (kW)

	EMS I		EMS II		EMS III	
Optimization Speed (m/s)	89	134	89	134	89	134
Eddy Current Power Dissipation due to Vehicle Magnets						
Levitation magnets	29.3	66.3	14.0	31.6	11.1	23.6
Guidance Magnets	7.34	33.1	Included in Levitation		7.34	33.1
Total Eddy Current Power	36.64	99.4	14.0	31.6	18.14	57.5
Propulsion Motor Power Dissipation (1 km block length assumed)						
Guideway Windings	N/A	N/A	N/A	N/A	1,470	1,470
Guideway Eddy Currents	N/A	N/A	N/A	N/A	33.4	75.8
Total Guideway Power	36.64	99.4	14.0	31.6	1,522	1,603

Total system power dissipation is not listed, because the LSM power is stated in terms of the power dissipation per kilometer of excited guideway; thus the total EMS III power depends upon the length of an excited block. The choice of block length depends on a number of factors, mainly economic; major ones include the capital cost of the electric utilities required to supply the power, and the cost of wayside power conversion equipment (assuming this is duplicated for each block). The same considerations also apply to the EDS, which also use LSM and some of the factors also bear on the other EMS, but not necessarily in exactly the same way. Thus, the question of which system may be better in terms of dissipated power does not have a simple answer, although it is clear that EMS III will have the highest system dissipation unless the blocks are very short (probably impractically short).

Table 2-6 depicts the guideway reactive power per kilometer, which only applies to EMS III since it is the only EMS to utilize a linear synchronous motor having guideway excitation.

Table 2-6.
Electromagnetic on-guideway reactive power (kVA/km)

	EMS I		EMS II		EMS III	
Optimization Speed (m/s)	89	134	89	134	89	134
Winding Reactive Power						
Linear Synchronous Motor	N/A	N/A	N/A	N/A	16,600	25,000
Total Reactive Power	N/A	N/A	N/A	N/A	16,600	25,000

It is important to note that the reactive power for a 1 kilometer block of guideway for EMS III at 134 meters/second is approximately 5 times larger than the power required to propel the vehicle. This is an important consideration since the size, and cost, of the wayside power conditioning equipment is governed to a large extent by the total volt-amperes which it must handle. The motor efficiency at that speed is about 78%. The large reactive power and relatively low efficiency are a result of having to excite the windings of a considerable length of guideway while the vehicle traverses it. The actual values will, of course, depend upon the actual length of guideway block to be excited which depends, in turn, on considerations such as required headway between vehicles, desired passenger throughput, etc. Note that EMS I and II also have reactive power, which must also be processed by power conditioning equipment and is supplied from the wayside by electric utilities. However, reactive power for EMS I and II are roughly an order of magnitude lower than for EMS III because the latter requires excitation for a very long (relative to the LIM length of EMS I and II) motor stator.

Table 2-7 shows a comparison of the total electrical power dissipated on the vehicle and on the guideway with the aerodynamic drag power for systems optimized for operation at both 89 meters/second and 134 meters/second and operating at those design speeds; power dissipation is lower at lower operating speeds mostly because the eddy current power is lower and since the aerodynamic drag is lower, the propulsive power required is correspondingly lower.

Table 2-7.
Electrical Power Dissipation Comparison with Aerodynamic Drag Power

	Units	EMS I		EMS II		EMS III	
Optimization Speed	m/s	89	134	89	134	89	134
On-Vehicle Power	kW	196.6	220.6	134.4	157.9	65.5	66.7
Guideway Power	kW	36.6	99.4	14.0	31.6	1,522†	1,603†
Total Power Dissipation	kW	233.2	320.0	148.4	189.5	1,588†	1,670†
Aerodynamic Power	kW	1,520	5,200	1,520	5,200	1,520	5,200
Total Power/Aero Power		0.15	0.06	0.10	0.04	1.04	0.32

† 1 kilometer block length assumed

It can be seen that for EMS III optimized for operation at 89 meters /second and operating at that speed, the total power dissipation is approximately the same as the aerodynamic drag power, whereas for EMS I and EMS II also optimized for operation at 89 meters/second the electrical power dissipation is from 6 to 10 times lower than the aerodynamic drag power. This large discrepancy is entirely a result of the large guideway power dissipation of EMS III, a consequence of the necessity for powering a guideway block (long stator) which is a great deal longer than the length of the LIM stator (short stator) on the vehicle. As a result of this large guideway power dissipation, EMS III has by far the largest ratio of electrical power dissipation to aerodynamic drag power for a one kilometer guideway block length; for a 1 km block length, the guideway power dissipation is completely dominated by the LSM power, of which the winding resistive power is an order of magnitude larger than the rail eddy current power.

2.6 Summary

Of the three EMS configurations, EMS I has the lowest total weight of electromagnetic components mounted on the vehicle for 89 meters/second optimization, while EMS I and EMS III are comparable for optimization at 134 meters/second operation. EMS II is heaviest at both optimization speeds: 25% of EMS 1 and 105% of EMS III for 89 meters/second optimization and 118% of EMS I and 17% of EMS III for 134 meters/second. Since magnet weight is a major contributor to total vehicle weight, EMS I and III could be expected to have roughly equal payload capacity for 134 meters/second optimization, with EMS I slightly better at 89 meters/second optimization; EMS II would have the smallest payload at each of the speeds.

The weight of the components mounted on the guideway does not affect the payload capacity of the vehicles; rather, its major impact is on the capital cost of acquisition. In this comparison, EMS I has the greatest weight of guideway mounted components, EMS III the least and EMS II is ≈ 5% greater than EMS III for both optimization speeds. For 89 meters/second, EMS I weight is 145% of EMS III and 152% at 134 meters/second.

In terms of on-vehicle power dissipation, EMS III is lower by a substantial margin at both optimization speeds. For the 89 meters/second optimization, EMS I on-vehicle power is 300% of EMS III and EMS II is 205% of EMS III. For the 134 meters/second optimization, EMS I power is 330% of EMS III and EMS II is 237% of EMS III.

For reactive power, EMS I and EMS II are identical, since they have identical LIM, which is the source of the reactive power, while EMS III has no on-board reactive power.

The on-guideway power dissipation is due entirely to eddy currents induced in the rails by the vehicle magnets for EMS I and EMS II. In addition to this, EMS III also has eddy current dissipation due to the guideway LSM excitation, but its guideway total power dissipation is dominated by the LSM winding dissipation for block lengths greater than about twice the vehicle length, and is still an order of magnitude larger than EMS I and II even for the impractically short block length of 100 meters, which is only about three times the length of the vehicle. The guideway eddy current power dissipation due only to the vehicle magnets is about a factor of two lower for EMS III than for EMS I .

The above summary is condensed into relative rankings of the three systems in

Tables 2-8 and 2-9. In the rankings, 1 denotes best and 3 worst, where best denotes lowest weight, lowest power and lowest ratio of electrical power dissipation to aerodynamic drag power.

Table 2-8.
Rankings for 89 meters/second Optimizations

Parameter	EMS I	EMS II	EMS III
Weight On-Vehicle	1	3	2
Weight	3	2	1
Power Dissipation On-Vehicle	3	2	1
Power Dissipation On-Guideway	2	1	3†
Reactive Power On-Vehicle	3	3	N/A
Reactive Power On-Guideway	N/A	N/A	3
Electrical Power/Aero Drag Power	2	1	3

† 1 kilometer block length assumed

Table 2-9.
Rankings for 134 meters/second Optimizations

Parameter	EMS I	EMS II	EMS III
Weight On-Vehicle	1	3	2
Weight On-Guideway	3	2	1
Power Dissipation On-Vehicle	3	2	1
Power Dissipation On-Guideway	2	1	3†
Reactive Power On-Vehicle	3	3	N/A
Reactive Power On-Guideway	N/A	N/A	3
Electrical Power/Aero Drag Power	2	1	3

† 1 kilometer block length assumed

Table 2-10. EMS I Summary; Design optimized for operation at 89 m/s
Separate Lift and guidance magnets and Linear Induction Motor

ElectroMagnetic Suspension I Optimized for operation at 89 m/s maximum speed
(Separate vertical & lateral suspensions & linear induction motor)

DESCRIPTION	UNITS	89 m/s Optimization			89 m/s Optimization @ 59 m/s		
		DESIGN 1	DESIGN 2	DESIGN 3	DESIGN 1	DESIGN 2	DESIGN 3
		baseline (b/l)	slim pole (3/4 b/l)	small gap (0.8 b/l)	baseline	slim pole (3/4 b/l)	small gap (0.8 b/l)
EMS I Summary							
Weight on Vehicle							
Lift Magnets	kg	1.54E+03	1.99E+03	1.23E+03	1.54E+03	1.99E+03	1.23E+03
Guidance Magnets	kg	1.55E+03	2.17E+03	1.23E+03	1.55E+03	2.17E+03	1.23E+03
Linear Induction Motor	kg	2.52E+03	2.52E+03	2.28E+03	2.52E+03	2.52E+03	2.28E+03
Total	kg	5.61E+03	6.68E+03	4.75E+03	5.61E+03	6.68E+03	4.75E+03
Weight on Guideway							
Lift Magnets	kg/m	1.13E+02	7.17E+01	8.94E+01	1.13E+02	7.17E+01	8.94E+01
Guidance Magnets	kg/m	8.28E+01	5.36E+01	6.49E+01	8.28E+01	5.36E+01	6.49E+01
Linear Induction Motor	kg/m	1.59E+02	1.59E+02	1.39E+02	1.59E+02	1.59E+02	1.39E+02
Total	kg/m	3.55E+02	2.84E+02	2.93E+02	3.55E+02	2.84E+02	2.93E+02
Real Input Power Dissipation							
Ohmic Power Dissipation							
Lift Magnets	W	1.19E+05	1.95E+05	1.06E+05	1.19E+05	1.95E+05	1.06E+05
Guidance Magnets	W	1.76E+04	3.97E+04	2.18E+04	1.76E+04	3.97E+04	2.18E+04
Linear Induction Motor	W	6.00E+04	6.00E+04	5.62E+04	2.56E+04	2.56E+04	2.35E+04
Total Ohmic Power	W	1.96E+05	2.95E+05	1.84E+05	1.62E+05	2.60E+05	1.52E+05
Eddy current Power							
Lift Magnets	W	2.93E+04	4.94E+03	1.93E+04	1.29E+04	2.17E+03	8.47E+03
Guidance Magnets	W	7.34E+03	1.21E+03	4.72E+03	3.23E+03	5.31E+02	2.07E+03
Total eddy current Power	W	3.66E+04	6.14E+03	2.40E+04	1.61E+04	2.70E+03	1.05E+04
Total Real Power Dissipation	W	2.33E+05	3.01E+05	2.08E+05	1.78E+05	2.63E+05	1.62E+05
Reactive Input Power							
Linear Induction Motor	V-A	1.57E+06	1.57E+06	1.53E+06	4.68E+05	4.68E+05	4.57E+05
Total	V-A	1.57E+06	1.57E+06	1.53E+06	4.68E+05	4.68E+05	4.57E+05

Table 2-11. EMS I Summary; Design optimized for operation at 134 m/s
Separate Lift and guidance magnets and Linear Induction Motor

ElectroMagnetic Suspension I Optimized for operation at 134 m/s maximum speed
(Separate vertical & lateral suspensions & linear induction motor)

DESCRIPTION	UNITS	134 m/s Optimization			134 m/s Optimization @ 89 m/s		
		DESIGN 1	DESIGN 2	DESIGN 3	DESIGN 1	DESIGN 2	DESIGN 3
		baseline	slim pole (3/4 b/l)	small gap (0.8 b/l)	baseline	slim pole (3/4 b/l)	small gap (0.8 b/l)
EMS I Summary							
Weight on Vehicle							
Lift Magnets	kg	1.54E+03	1.99E+03	1.23E+03	1.54E+03	1.99E+03	1.23E+03
Guidance Magnets	kg	1.93E+03	2.58E+03	1.54E+03	1.93E+03	2.58E+03	1.54E+03
Linear Induction Motor	kg	3.71E+03	3.71E+03	2.89E+03	3.71E+03	3.71E+03	2.89E+03
Total	kg	7.18E+03	8.28E+03	5.67E+03	7.18E+03	8.28E+03	5.67E+03
Weight on Guideway							
Lift Magnets	kg/m	1.13E+02	7.17E+01	8.94E+01	1.13E+02	7.17E+01	8.94E+01
Guidance Magnets	kg/m	1.13E+02	7.17E+01	8.87E+01	1.13E+02	7.17E+01	8.87E+01
Linear Induction Motor	kg/m	1.80E+02	1.80E+02	1.56E+02	1.80E+02	1.80E+02	1.56E+02
Total	kg/m	4.06E+02	3.23E+02	3.34E+02	4.06E+02	3.23E+02	3.34E+02
Real Input Power Dissipation							
Ohmic Power Dissipation							
Lift Magnets	W	1.19E+05	1.95E+05	1.06E+05	1.19E+05	1.95E+05	1.06E+05
Guidance Magnets	W	1.88E+04	3.88E+04	2.08E+04	1.88E+04	3.88E+04	2.08E+04
Linear Induction Motor	W	8.28E+04	8.28E+04	8.00E+04	3.40E+04	3.40E+04	3.08E+04
Total Ohmic Power	W	2.20E+05	3.16E+05	2.07E+05	1.71E+05	2.68E+05	1.58E+05
Eddy current Power							
Lift Magnets	W	6.63E+04	1.12E+04	4.37E+04	2.93E+04	4.94E+03	1.93E+04
Guidance Magnets	W	3.31E+04	5.49E+03	2.16E+04	1.46E+04	2.42E+03	9.52E+03
Total eddy current Power	W	9.94E+04	1.67E+04	6.52E+04	4.39E+04	7.36E+03	2.88E+04
Total Real Power Dissipation	W	3.20E+05	3.33E+05	2.72E+05	2.15E+05	2.75E+05	1.87E+05
Reactive Input Power							
Linear Induction Motor	V-A	3.22E+06	3.22E+06	3.27E+06	9.47E+05	9.47E+05	9.32E+05
Total	V-A	3.22E+06	3.22E+06	3.27E+06	9.47E+05	9.47E+05	9.32E+05

Table 2-12. EMS II Summary; Design optimized for operation at 89 m/s
Combined Lift and guidance magnets (staggered) and Linear Induction Motor

ElectroMagnetic Suspension II Optimized for operation at 89 m/s maximum speed
(Combined vertical & lateral suspensions(staggered), Linear Induction Motor)

DESCRIPTION	UNITS	89 m/s Optimization			89 m/s Optimization @ 59 m/s		
		DESIGN 1	DESIGN 2	DESIGN 3	DESIGN 1	DESIGN 2	DESIGN 3
VEHICLE PARAMETERS		baseline (b/l)	slim pole (3/4 b/l)	small gap (0.8 b/l)	baseline (b/l)	slim pole (3/4 b/l)	small gap (0.8 b/l)
EMS II Summary							
Weight on Vehicle							
Lift/Guidance Magnets	kg	4.74E+03	5.60E+03	3.60E+03	4.74E+03	5.60E+03	3.60E+03
Linear Induction Motor	kg	2.52E+03	2.52E+03	2.28E+03	2.52E+03	2.52E+03	2.28E+03
Total	kg	7.26E+03	8.12E+03	5.88E+03	7.26E+03	8.12E+03	5.88E+03
Weight on Guideway							
Lift/Guidance Magnets	kg/m	4.88E+01	3.54E+01	4.07E+01	4.88E+01	3.54E+01	4.07E+01
Linear Induction Motor	kg/m	3.17E+02	3.17E+02	2.78E+02	3.17E+02	3.17E+02	2.78E+02
Total	kg/m	3.66E+02	3.53E+02	3.19E+02	3.66E+02	3.53E+02	3.19E+02
Real Input Power Dissipation							
Ohmic Power Dissipation							
Lift/Guidance Magnets	W	7.44E+04	1.08E+05	6.07E+04	7.44E+04	1.08E+05	6.07E+04
Linear Induction Motor	W	6.00E+04	6.00E+04	5.62E+04	2.56E+04	2.56E+04	2.35E+04
Total Ohmic Power	W	1.34E+05	1.68E+05	1.17E+05	1.00E+05	1.34E+05	8.41E+04
Eddy current Power							
Lift/Guidance Magnets	W	1.40E+04	3.77E+03	1.17E+04	6.17E+03	1.66E+03	5.12E+03
Total eddy current Power	W	1.40E+04	3.77E+03	1.17E+04	6.17E+03	1.66E+03	5.12E+03
Total Real Power Dissipation	W	1.48E+05	1.72E+05	1.29E+05	1.06E+05	1.36E+05	8.92E+04
Reactive Input Power							
Linear Induction Motor	V-A	1.57E+06	1.57E+06	1.53E+06	4.68E+05	4.68E+05	4.57E+05
Total	V-A	1.57E+06	1.57E+06	1.53E+06	4.68E+05	4.68E+05	4.57E+05

Table 2-13. EMS II Summary; Design optimized for operation at 134 m/s
Combined Lift and guidance magnets (staggered) and Linear Induction Motor

ElectroMagnetic Suspension II Optimized for operation at 134 m/s maximum speed
(Combined vertical & lateral suspensions(staggered), Linear Induction Motor)

DESCRIPTION	UNITS	134 m/s Optimization			134 m/s Optimization @ 89 m/s		
		DESIGN 1	DESIGN 2	DESIGN 3	DESIGN 1	DESIGN 2	DESIGN 3
VEHICLE PARAMETERS		baseline (b/l)	slim pole (3/4 b/l)	small gap (0.8 b/l)	baseline (b/l)	slim pole (3/4 b/l)	small gap (0.8 b/l)
<u>EMS II Summary</u>							
<u>Weight on Vehicle</u>							
Lift/Guidance Magnets	kg	4.79E+03	5.60E+03	3.60E+03	4.79E+03	5.60E+03	3.60E+03
Linear Induction Motor	kg	3.71E+03	3.71E+03	2.89E+03	3.71E+03	3.71E+03	2.89E+03
Total	kg	8.50E+03	9.31E+03	6.49E+03	8.50E+03	9.31E+03	6.49E+03
<u>Weight on Guideway</u>							
Lift/Guidance Magnets	kg/m	4.89E+01	3.54E+01	4.07E+01	4.89E+01	3.54E+01	4.07E+01
Linear Induction Motor	kg/m	3.60E+02	3.60E+02	3.12E+02	3.60E+02	3.60E+02	3.12E+02
Total	kg/m	4.09E+02	3.95E+02	3.52E+02	4.09E+02	3.95E+02	3.52E+02
<u>Real Input Power Dissipation</u>							
Ohmic Power Dissipation							
Lift/Guidance Magnets	W	7.51E+04	1.08E+05	6.07E+04	7.51E+04	1.08E+05	6.07E+04
Linear Induction Motor	W	8.28E+04	8.28E+04	8.00E+04	3.40E+04	3.40E+04	3.08E+04
Total Ohmic Power	W	1.58E+05	1.91E+05	1.41E+05	1.09E+05	1.42E+05	9.14E+04
Eddy current Power							
Lift/Guidance Magnets	W	3.16E+04	8.55E+03	2.65E+04	1.40E+04	3.77E+03	1.17E+04
Total eddy current Power	W	3.16E+04	8.55E+03	2.65E+04	1.40E+04	3.77E+03	1.17E+04
Total Real Power Dissipation	W	1.90E+05	2.00E+05	1.67E+05	1.23E+05	1.46E+05	1.03E+05
<u>Reactive Input Power</u>							
Linear Induction Motor	V-A	3.22E+06	3.22E+06	3.27E+06	9.47E+05	9.47E+05	9.32E+05
Total	V-A	3.22E+06	3.22E+06	3.27E+06	9.47E+05	9.47E+05	9.32E+05

Table 2-14. EMS III Summary; Design optimized for operation at 89 m/s
Separate guidance magnet,Combined lift magnet and LSM

ElectroMagnetic Suspension III Optimized for operation at 89 m/s maximum speed
(Separate vertical suspension & synchronous motor, lateral suspension)

DESCRIPTION	UNITS	89 m/s Optimization			89 m/s Optimization @ 59 m/s		
		DESIGN 1	DESIGN 2	DESIGN 3	DESIGN 1	DESIGN 2	DESIGN 3
		baseline	slim pole (3/4 b/l)	small gap (0.8 b/l)	baseline	slim pole (3/4 b/l)	small gap (0.8 b/l)
EMS III Summary							
Weight on Vehicle							
Lift Magnets/LSM	kg	5.67E+03	5.30E+03	3.40E+03	5.67E+03	5.30E+03	3.40E+03
Guidance Magnets	kg	1.55E+03	2.17E+03	1.23E+03	1.55E+03	2.17E+03	1.23E+03
Total	kg	7.22E+03	7.47E+03	4.64E+03	7.22E+03	7.47E+03	4.64E+03
Magnet Weight/Vehicle Weight	%	18.05%	18.67%	11.59%	18.05%	18.67%	11.59%
Weight on Guideway							
Lift Magnets/LSM	kg/m	2.71E+02	2.71E+02	2.71E+02	2.71E+02	2.71E+02	2.71E+02
Guidance Magnets	kg/m	8.28E+01	5.36E+01	6.49E+01	8.28E+01	5.36E+01	6.49E+01
Total	kg/m	3.54E+02	3.25E+02	3.36E+02	3.54E+02	3.25E+02	3.36E+02
Vehicle Real Power							
Ohmic Power Dissipation							
Lift Magnets/LSM	W	5.13E+04	4.79E+04	2.95E+04	5.13E+04	4.79E+04	2.95E+04
Guidance Magnets	W	1.76E+04	2.87E+04	1.58E+04	1.76E+04	2.87E+04	1.58E+04
Total Ohmic Power	W	6.88E+04	7.65E+04	4.53E+04	6.88E+04	7.65E+04	4.53E+04
Eddy current Power Dissipation							
Lift Magnets/LSM	W	1.11E+04	1.04E+04	6.41E+03	4.90E+03	4.57E+03	2.82E+03
Guidance Magnets	W	7.34E+03	1.21E+03	4.72E+03	3.23E+03	5.31E+02	2.07E+03
Total eddy current Power	W	1.85E+04	1.16E+04	1.11E+04	8.12E+03	5.10E+03	4.89E+03
Total Vehicle Power Dissipatic	W	8.73E+04	8.81E+04	5.64E+04	7.70E+04	8.16E+04	5.02E+04
Electrical Power/Aero Drag Powe	%	5.73%	5.79%	3.71%	17.35%	18.40%	11.31%
Guideway Power							
Real Power Dissipation							
Guideway LSM Winding	kW/m	1.47E+00	1.47E+00	1.47E+00	1.47E+00	1.47E+00	1.47E+00
Total	kW/m	1.47E+00	1.47E+00	1.47E+00	1.47E+00	1.47E+00	1.47E+00
Reactive Input Power							
Linear Synchronous Motor	kVA/m	1.66E+01	1.66E+01	1.66E+01	1.11E+01	1.11E+01	1.11E+01
Total	kVA/m	1.66E+01	1.66E+01	1.66E+01	1.11E+01	1.11E+01	1.11E+01

Table 2-15. EMS III Summary; Design optimized for operation at 134 m/s
Separate guidance magnet,Combined lift magnet and LSM

ElectroMagnetic Suspension III Optimized for operation at 134 m/s maximum speed
(Separate vertical suspension & synchronous motor, lateral suspension)

DESCRIPTION	UNITS	134 m/s Optimization			134 m/s Optimization @ 89 m/s		
		DESIGN 1	DESIGN 2	DESIGN 3	DESIGN 1	DESIGN 2	DESIGN 3
		baseline (b/l)	slim pole (3/4 b/l)	small gap (0.8 b/l)	baseline (b/l)	slim pole (3/4 b/l)	small gap (0.8 b/l)
EMS III Summary							
Weight on Vehicle							
Lift Magnets/LSM	kg	5.30E+03	5.58E+03	3.78E+03	2.22E+03	2.22E+03	2.22E+03
Guidance Magnets	kg	1.93E+03	2.58E+03	1.54E+03	1.93E+03	2.58E+03	1.54E+03
Total		7.23E+03	8.16E+03	5.32E+03	4.15E+03	4.80E+03	3.76E+03
Magnet Weight/Vehicle Weight	%	18.07%	20.40%	13.31%	10.38%	12.00%	9.41%
Weight on Guideway							
Lift Magnets/LSM	kg/m	2.71E+02	2.27E+02	2.57E+02	2.71E+02	2.27E+02	2.57E+02
Guidance Magnets	kg/m	1.13E+02	7.17E+01	8.87E+01	1.13E+02	7.17E+01	8.87E+01
Total	kg/m	3.84E+02	2.99E+02	3.46E+02	3.84E+02	2.99E+02	3.46E+02
Vehicle Real Power							
Ohmic Power Dissipation							
Lift Magnets/LSM	W	4.79E+04	6.07E+04	3.28E+04	4.79E+04	6.07E+04	3.28E+04
Guidance Magnets	W	1.88E+04	3.13E+04	1.68E+04	1.88E+04	3.13E+04	1.68E+04
Total Ohmic Power	W	6.66E+04	9.20E+04	4.96E+04	6.66E+04	9.20E+04	4.96E+04
Eddy current Power							
Lift Magnets/LSM	W	2.36E+04	1.96E+04	1.84E+04	1.04E+04	8.67E+03	8.10E+03
Guidance Magnets	W	3.31E+04	5.49E+03	2.16E+04	1.46E+04	2.42E+03	9.52E+03
Total eddy current Power	W	5.67E+04	2.51E+04	3.99E+04	2.50E+04	1.11E+04	1.76E+04
Total Real Power Dissipation	W	1.23E+05	1.17E+05	8.96E+04	9.16E+04	1.03E+05	6.72E+04
Guideway Power							
Real Power Dissipation							
Guideway LSM Winding	kW/m	1.47E+00	1.39E+00	1.44E+00	1.47E+00	1.39E+00	1.44E+00
Total	kW/m	1.47E+00	1.39E+00	1.44E+00	1.47E+00	1.39E+00	1.44E+00
Reactive Input Power							
Linear Synchronous Motor	kVA/m	2.50E+01	2.10E+01	2.42E+01	1.66E+01	1.40E+01	1.61E+01
Total	kVA/m	2.50E+01	2.10E+01	2.42E+01	1.66E+01	1.40E+01	1.61E+01

SECTION 3

ELECTRODYNAMIC SYSTEMS

3.0 General Description of the Electrodynamic Suspensions

This report considers three electrodynamic systems. These are image flux, hybrid null flux, and side wall null flux. Qualitative descriptions of these systems are in section 3.1.

Electrodynamic systems employ vehicle magnets that interact with conducting elements of a guideway. The electrodynamic vehicles considered in this report use superconducting magnets. While it is possible to consider permanent magnets or other vehicle magnets, superconducting vehicle magnets are the only choice. For magnets large enough for vehicle levitation and propulsion, superconducting magnets are much lighter than any alternative.

3.0.1 Image Flux

In an image flux system, superconducting vehicle magnets above a conducting sheet guideway provide lift when the vehicle is moving. Of the three electrodynamic systems, the image flux is the easiest to understand. If two permanent magnets come close to each other with the proper orientation, they push against each other. This is very close to what happens when an image flux vehicle is traveling at high speed. The conducting sheet guideway reflects an image of the vehicle magnets because at high speeds the vehicle magnet fields cannot diffuse through the conducting sheet of the stationary guideway. At high speeds the magnetic fields approach those that would result if an image of the vehicle were behind the guideway. (High speeds are those where the magnetic skin depth is less than the thickness of the guideway conducting sheet. For a two centimeter aluminum sheet and vehicle magnets with 1.5 meter pole pitch, speeds above 185 kilometer per hour are high speeds. For a one centimeter aluminum sheet, high speeds are above 738 kilometer per hour.) The high speed lift force can be calculated by finding the force from an image magnet.

Magnetic drag in an image flux system arises because the conducting sheet of the guideway carries electric currents while the vehicle is passing. The image fields are the result of these guideway currents. Magnetic drag on the vehicle must supply the energy dissipated in the guideway from resistive heating from these currents. If the resistive guideway suspension losses in any electrodynamic system are known, then magnetic drag is calculated as resistive losses divided by vehicle velocity. This is an energy balance. For an image flux system, a useful approximation for intermediate speeds is that the resistive losses are constant, independent of speed. This is reasonable since the current distribution needed to generate the image magnet field is roughly independent of speed, for some range of speed. (Intermediate speeds are below high speeds, as described above, and above the speed at which the guideway impedance is equally resistive and inductive. For a one centimeter thick guideway, and 1.5 meter pole pitch, this speed range is from 16 kilometer per hour to 738 kilometer per hour. For a two centimeter thick guideway this speed range is from 8 kilometer per hour to 185 kilometer per hour.) This implies that for these intermediate speeds, drag is inversely proportional to velocity. The intermediate speed range for which this is a good approximation is bounded at its upper limit by current distributions becoming non-uniform from near to far surface of the guideway sheet. When the magnetic skin depth becomes less than the guideway thickness, resistive losses increase with increasing speed. Magnetic drag continues to decrease with increasing speed, but not so quickly. The constant resistive loss approximation predicts unlimited drag as velocity approaches a stand-still. The drag does get very large at the bottom end of the intermediate speeds. But for speeds below the intermediate range, the image fields, resistive losses, lift, and drag decrease and approach zero as speed approaches zero.

Useful approximations for estimating the velocity dependence of forces in image flux systems have been published. Richards and Tinkham [38], which we used to develop our spreadsheets, is an example. Richard and Tinkham's approximations agree with other publications.

One complication of image flux force calculations for which we know of no easy solution involves forces from vehicle magnets near guideway edges. In any practical system, edge effects are important. This is certainly the case with the Magneplane configuration considered in this study.

One variation on the image flux system is to use guideway coils instead of a guideway sheet. The Japanese used this in their Miyazaki tests. The system is an image flux system because guideway coils reflect the vehicle fields that can not much penetrate the coils at normal operating speeds. The motivation for using coils instead of sheets is that lower drag is possible. One limitation of the guideway sheet implementation is magnetic skin depth at high speeds. For sheet guideways at low speeds, when the guideway thickness is less than the magnetic skin depth, increasing guideway thickness reduces drag. This strategy is unproductive if the skin depth is less than the guideway thickness. With wound coil guideways, skin depth limitations do not apply if the coils are wound with suitable fine wire. So the inductance to resistance ratio of wound coil guideways can be substantially better than for sheet guideways.

3.0.2 Null Flux

Null flux systems use superconducting vehicle magnets, and the guideway has coils, not sheets. The following are the most striking differences between image flux systems and null flux systems.

- Magnetic drag is lower.
- Suspension forces are stiffer.
- Either the vehicle magnets or the guideway coils have a more complicated shape.
- Suspension forces can either pull or push. There is a vehicle position of zero force.

The motivation for null flux is lower magnetic drag. The underlying principle that produces lower drag in both null flux and hybrid null flux systems, compared to image flux systems, is to produce lift using more powerful vehicle magnets with smaller guideway currents. Magnetic drag arises from guideway currents and associated resistive heating. Vehicle lift for any electrodynamic system depends in a complicated way on many parameters, but there is always a product of vehicle current and guideway current, or an equivalent. The essence of null flux systems is to use larger vehicle currents and smaller guideway currents. Vehicle currents are in superconductors and have essentially no resistive losses. They do not cause magnetic drag. Guideway currents produce magnetic drag. Thus a system that allows smaller guideway currents with larger vehicle currents is appealing.

If vehicle currents in an image flux system increase, the vehicle rises higher above the guideway and drag is approximately unchanged. So it is not possible to decrease magnetic drag by increasing vehicle current. Null flux systems are different in this regard. If vehicle currents increase in a null flux system, the vehicle will move slightly closer to a zero force position. Normal operation is typically about two centimeters from this zero force position. When the vehicle is in the zero force position, no guideway currents flow, by symmetry. That is, the shape of the vehicle and guideway coils is such that at the zero force position, the mutual inductance between vehicle and guideway coils is zero. This zero force position is a vertical position for lift force, or a horizontal position for guidance force. At the zero force position, mutual inductance is zero for all positions in the forward motion direction. This means that either the guideway or vehicle coil has a double loop topology, with the two loops near each other and opposed. In the configuration analyzed for this study, the vehicle coil is a single loop while the guideway coil has two loops in a figure eight configuration. Both coils are vertical. The classic configuration described by Powell and Danby[44] has a horizontal vehicle coil and connected guideway coils above and below the vehicle. This double coil in either the guideway or vehicle is the more complicated shape referred to above. The double coil provides a vertical position where, by symmetry typically, mutual inductance is zero. It is this arrangement that allows much higher vehicle currents than would be useful for image flux systems.

Suspension forces depend on vertical position in the following way. Lift and drag are both zero at the zero force position. Lift increases nearly linearly with displacement from the zero force position. This means that there can be both up and down forces on the vehicle. The suspension supports the vehicle, and traps it. Drag forces vary approximately as the square of the displacement from zero. One implication of these force dependencies is that talking about a lift to drag ratio is dangerous. If the suspension was providing a roll torque in response to either a cross wind, turning force, or vehicle weight unbalance, drag would increase due not only to increased lift forces for some cases, but to the uneven forces among vehicle magnets. Another consequence of the linear dependence and square dependence of lift and drag forces, respectively, on displacement is that there is a drag reduction incentive to have vehicle lift magnets spread over as much of the vehicle as possible. Richard and Tinkham[38] discuss the linear and square dependence of lift and drag forces.

Both high vehicle currents and more vehicle magnets reduce magnetic drag. Both these design strategies increase vehicle weight. This is a practical reason why magnetic drag can not be made arbitrarily small.

Magnetic drag force has a dependence on vehicle speed that is similar to image null flux. The difference is that there should not be any skin depth limitation. The coils will be wound with insulated strands of wires, so the product of magnetic drag and velocity will remain constant for normal operating speeds.

Another consequence of freedom from magnetic diffusion effects it that benefits from adding guideway conductor material are possible at high speeds. With an image flux system, if the guideway suspension sheets are made thicker than the magnetic skin depth, drag is not reduced significantly. With null flux there is no skin depth limitation. Guideway suspension coils can be wound with more turns and drag will decrease.

Magnetic coupling decreases limit this process. Thicker coils move guideway components away from the vehicle so that magnetic couplings between vehicle and guideway, measured by mutual inductances, fall. Another limit, of course, is guideway expense.

Null flux systems are easier to analyze than systems using sheet guideways. These latter systems are magnetic diffusion systems with three dimensional fields. Magnetic diffusion is not an important phenomenon in null flux systems, and the three dimensional fields of the other systems reduce to mutual inductances between coils that are easy to calculate.

3.0.3 Hybrid Null Flux

Hybrid null flux systems have characteristics that are similar to and different from the other two systems. The major points of comparison with image flux and straight null flux systems follow.

- Guideway suspension conductors are sheets like image flux, but thinner.
- Vehicle magnets have a double coil topology, like some null flux designs.
- Magnetic drag is typically less than image flux but greater than null flux.
- Suspension forces are stiff like null flux.
- Suspension forces push, pull, and have a zero force position like null flux.
- Each design has minimum drag at some velocity, unlike either image or null flux.

A simple hybrid null flux system, first described by Richards and Tinkham [38], is a vehicle with an upper and lower horizontal coil pair with opposing polarity. The currents in both coils are equal. The fields from this pair will have the pattern of an image flux system except both the upper and lower fields are present. In the plane half way between the upper and lower coil, magnetic fields are tangential. There are no vertical magnetic field components in this mid plane. The conducting guideway sheet is very close to this mid plane position.

The key to understanding the hybrid null flux concept is to recognize the absence of vertical field components in the mid plane, and to recognize some consequences of this condition.

If a very thin conducting sheet is in the mid plane, no currents will flow in the sheet as the vehicle passes, because of the absence of vertical magnetic fields. Choose any closed loop in the sheet. The passing vehicle causes no flux to pass through this loop, so no voltage is induced around it. No current flows.

The next feature of the fields to consider is that although there are no vertical fields, the fields tangential to the plane can be arbitrarily strong.

Now consider a thin guideway sheet displaced slightly from the center. In this position the guideway encounters vertical fields, and currents flow in the guideway. These guideway currents interact with the tangential fields to produce force that is in the direction to restore the guideway sheet to the center. Because the vehicle fields near the guideway can have very strong tangential components, the lift forces can be produced by strong vehicle currents and weak guideway currents compared to image flux systems. For this reason, hybrid null flux drag can be lower than image flux drag. This is the same result, coming from a similar mechanism, that makes the straight null flux system appealing.

To emphasize the connection between hybrid null flux and straight null flux, if coils in the plane of the sheet replace the sheet guideway of the hybrid null flux, lift is produced, and the system is a straight null flux system.

There are two drag components in a hybrid null flux system. Both arise from currents in the guideway sheet. The first component is due to currents that flow because the sheet is displaced from the mid plane. These currents produce lift. The second component is due to the thickness of the guideway sheet. The normal magnetic field is zero only in the mid plane. Since the guideway has thickness, it will see normal fields even when centered. These currents related to thickness do not produce lift.

The two components of guideway current present a conflict. If only the lift producing currents are considered, the guideway should be thick to decrease drag. If only the thickness currents are considered, the guideway should be thin. The best compromise between thick and thin is a function of vehicle speed. For any single guideway thickness, there will be a speed where drag is least. Figure 3.0 shows the

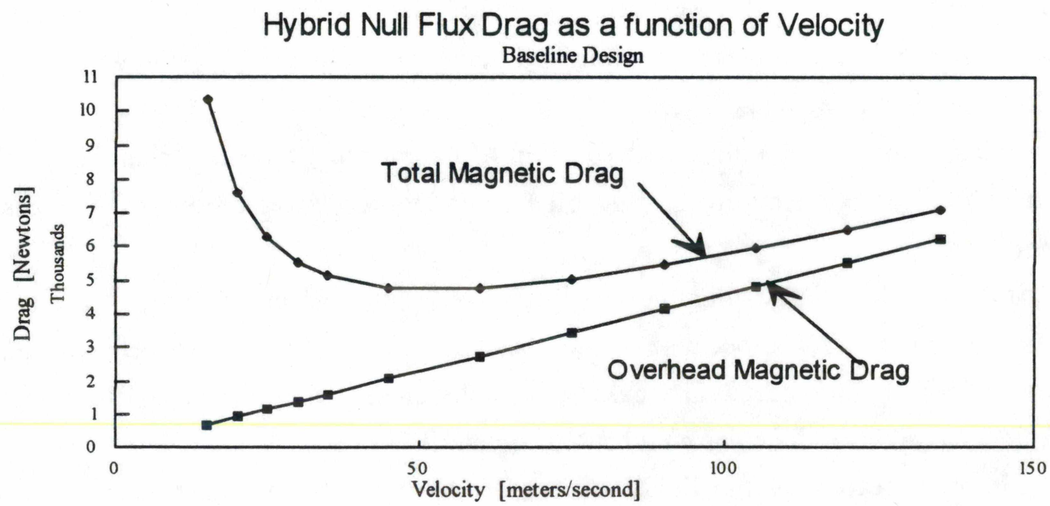

Figure 3.0

relationship between total magnetic drag, and overhead drag, at various speeds, with no side load. On this figure the thickness related drag is labeled "overhead drag." The curve shown in figure 3.0 is for the baseline design that is suited to low speed operation due to its thick guideway sheets.

For small displacements of the guideway relative to vehicle magnet centers, lift forces are proportional to displacement, and displacement drag forces are proportional to displacement squared. This is the same dependence shown by null flux suspensions. A major difference between null flux and hybrid null flux is that hybrid null flux has the thickness related, overhead drag, and null flux does not.

Modeling hybrid null flux forces is difficult. The paper by Richards and Tinkham [38] that introduced hybrid null flux has appealing approximate analytical expressions for lift and drag. They obtained these expressions by making some simplifying assumptions that appear to influence the results significantly. The major assumption is that the vehicle magnets are two dimensional. They are assumed to be very wide, so variations of the field from side to side are more gradual than variations in the direction of vehicle motion and in the vertical direction. The analytical result from this simplification says that making the vehicle magnets long in the direction of motion reduces drag. Both components of drag are improved by making the fields change slowly. If a system is designed following this guideline, the field variations that were assumed to be unimportant can become near dominant.

Urankar and Miericke [41] published an exact solution to yet a different simplified configuration. The simplification in this case was to ignore guideway edges, as did Richards and Tinkham, but at least the two dimensional assumption of Richards and Tinkham could be checked. They also used more than the fundamental spatial component of magnetic fields, unlike Richards and Tinkham. The result was substantially higher drag than Richards and Tinkham predict. Urankar and Miericke's result is not suitable for spreadsheet evaluation. For the working spreadsheet the analytical expressions of Richards and Tinkham were modified to approximately account for the third dimension, and the result was then in acceptable agreement with Urankar and Miericke.

3.1 Descriptions of the Electrodynamic Configurations

This report has calculated parameters for specific configurations. The choice of a particular configuration allows some degree of accuracy and realism that can not be obtained when considering general concepts, but these choices precluded other possibilities. Our results are valid for the particular configurations chosen. Within a configuration a parameter such as guideway sheet thickness can be varied to "optimize" the design. But different approaches to self shielding vehicle magnets, for example, can not be explored with a single configuration.

3.1.1 Image Flux

The image flux configuration analyzed here is Magneplane, but Magneplane is a developing system. The configuration used here is based on information available in the fall of 1991 when Henry Kolm gave a presentation at Professor Thornton's maglev seminars. Since then, the Magneplane System Concept Definition team has made changes, based on presentations at the second National Maglev Initiative conference at Argonne National Laboratory, April 1992. Abstracts are available from NMI.

Figures 3.1a, b, and c show the configuration analyzed.

One feature that this configuration shares with every Magneplane configuration known is stronger magnets in the center of the vehicle. The motivation for these magnets is to make coupling between the vehicle and motor efficient. The configuration shown here has four times more magnet current in the central sections than in the outer sections used for levitation and guidance. Any image flux system will face a similar need. Image flux vehicle magnets sized for levitation will be weaker than appropriate for the field of a linear synchronous motor. The need for stronger motor magnets is not necessarily a problem with image flux systems. The stronger magnets are easily provided. The linear motor described here for Magneplane is good. One cost that is not apparent is that the space occupied by the motor is not available for levitation. Another cost that deserves special attention is the effect of the linear synchronous motor on vehicle roll dynamics. A discussion of this follows.

The stronger magnets in the center of the vehicle interact with the guideway sheets to the side. This is a problem. Strong magnets must be in the center for the reasons above. Much space can not separate the two, because the motor should be wide, for good efficiency, and the levitation sheets need to be beneath the vehicle. The interaction pushes the stronger magnets to the center of the gap between the two levitation sheets, to the center of the motor. This to some extent prevents Magneplane from self-banking in turns. The roll stiffness produced by the interaction of the motor magnets and the levitation sheets limits roll motion of the vehicle. Stability from keel magnets is not needed for a self banking vehicle. Keel magnets degrade self banking.

The Magneplane configuration shown here limits passenger exposure to magnetic fields by separating passengers from high field regions. Figure 3.4 shows passenger

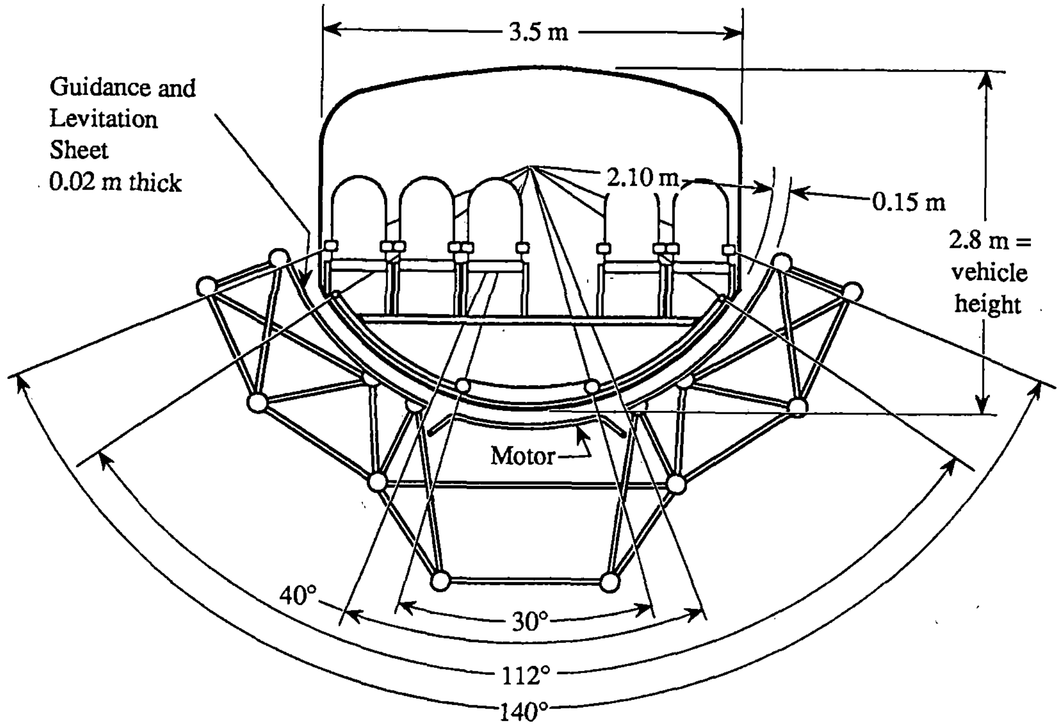

(a) Cross section

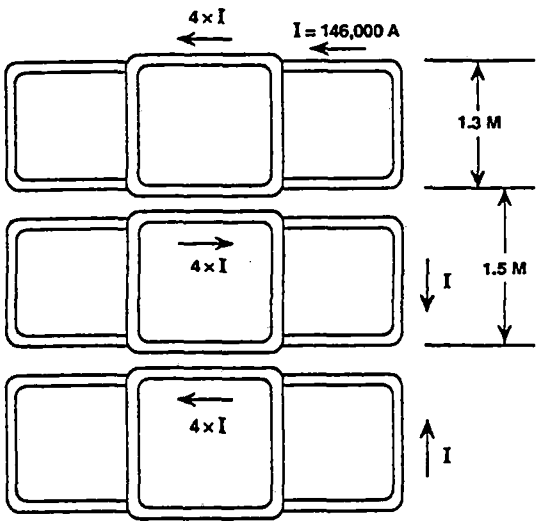

(b) Top view of a magnet cluster

Figure 3-1. Circular arc cross section guideway with image force levitation.

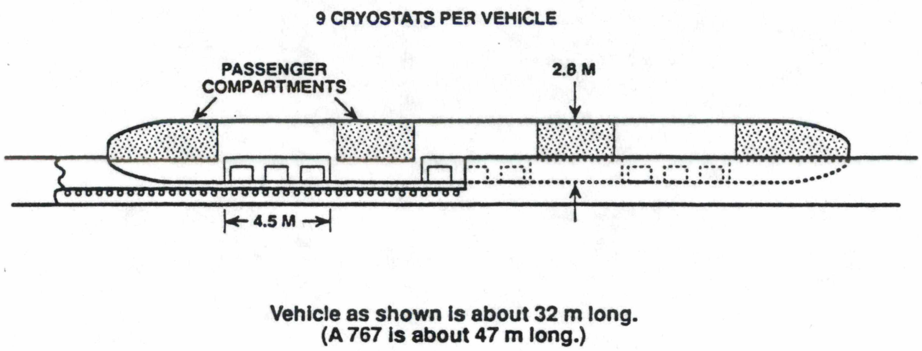

(c) Side view.

Figure 3-1. Circular arc cross section guideway with image force levitation. (Cont.)

compartment magnetic fields for all electrodynamic configurations. The second image flux field strength curve, described in the figure as "modified," achieves a noticeable improvement by simply making the first and second rows of magnets weaker while making the middle row stronger. Making the middle row carry twice the current of the first and third rows reduces the total dipole moment of the magnets to zero. The overall magnet strength was adjusted to provide similar motor and levitation behavior. The magnets can be modified to provide more self shielding. Judging from what was revealed at the Argonne meeting, the Magneplane team has pursued this.

One compelling characteristic of the Magneplane concept is simplicity. As shown here, and as Magneplane has been described traditionally, the vehicle is uncomplicated by secondary suspension. This is possible because the natural frequency of the primary suspension is approximately one hertz. The magnetic suspension is soft. But the suspension is not as simple as first appearances suggest. Not shown are aerodynamic control surfaces needed to achieve roll and pitch damping. The linear motor can provide heave damping. The first cut comparisons ignored aerodynamic differences among the systems. Section 3.2 discusses these differences.

Another complication is a landing gear. Vehicle weight estimates include landing gear. This estimate and other structural weight estimates were made using aircraft experience. Landing gear weight either increases vehicle weight or reduces payload.

A third complication is a restriction on tight, low speed turns. If the vehicles must pass through turns tighter than about 1 kilometer radius, the vehicles must be articulated or made shorter, or the system shown must be otherwise modified. For this study the vehicles were assumed to be unarticulated.

3.1.2 Null Flux

The configuration selected for the null flux system is based on the Japanese design. The Japanese used a single vehicle with two remarkably different guideways. The vehicle, MLU002, was used mostly with wound coil image flux guideway. It was also briefly used with a side wall null flux guideway. This is the configuration analyzed here.

Dimensions used in this analysis are from published descriptions of the Japanese system when available. Dimensions of the guideway levitation and guidance coils and motor windings are largely improvised.

The levitation coils analyzed here consist of an array of two interconnected loops of wire. The loops are vertical, one above the other on the side walls of the guideway. Each loop has many turns to achieve the desired winding cross section while avoiding

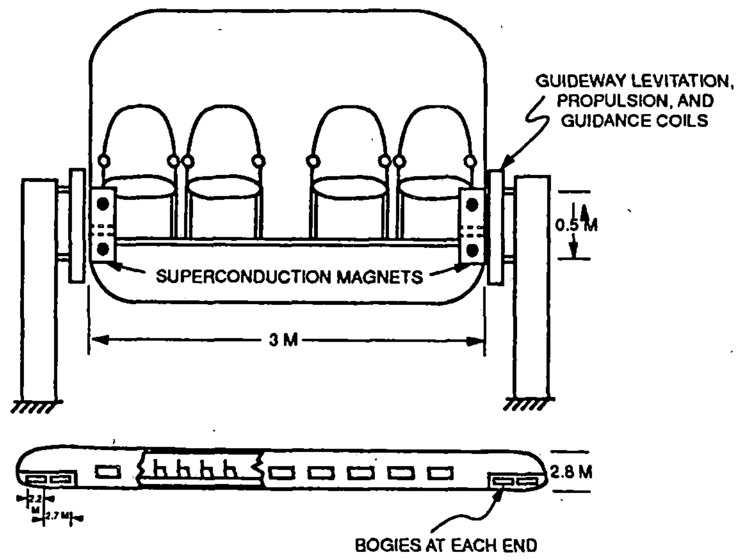

(a) Cross section and side view.

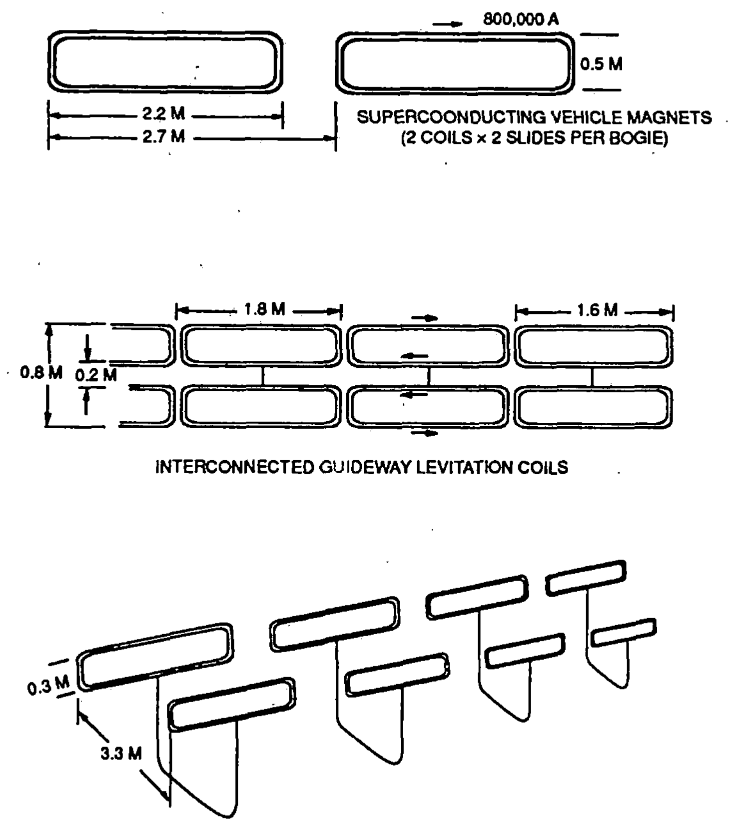

(b) Magnetic

Figure 3-2. Wide rectangular U-cross section guideway with vertical null flux coils.

magnetic skin depth effects. The results shown in table H-1 were obtained with levitation coil winding cross section diameters of 5.6 centimeter. The two loops are connected with two strands of the winding wire. The polarity of connection is such that if current flows, it flows in a figure eight pattern. The vehicle magnets are also vertical, on each side of the vehicle, facing the levitation coils. Normal operating position is for the vehicle magnets to be about two centimeters below the mid plane of the guideway levitation magnets. The vehicle and guideway coils are shown in figure 3.2.

The guideway guidance coils also consist of an array of interconnected pairs. Each pair consists of two thick loops wound with thinner wire. The interconnected guidance winding loop pairs are on either side of the guideway. The two interconnecting strands go below the vehicle. The polarity of interconnection is such that if the vehicle is centered from side to side in the guideway, the mutual inductances of the guidance coils and the vehicle magnets on the two sides cancel.

The linear synchronous motor windings are positioned between the levitation coils, which are closest to the vehicle, and the guidance windings. These coils are in each other's way due to their thickness. The levitation coil is 5.6 centimeters thick. The propulsion winding is 3 centimeters thick. Two gaps for insulation, each one centimeter thick, separate the three winding layers. These layers push the guidance windings back 10.6 centimeters and the magnetic coupling to the vehicle is significantly worse back that far. This configuration has space competition among levitation, guidance, and propulsion functions as does Magneplane.

One requirement for this configuration's safety is that superconducting coil pairs on two sides of the vehicle be linked so that if one quenches, the other goes down as well. If this is not done, then loss of one coil would result in a powerful side force.

Redundant vehicle magnets are desirable. The goal is to be able to continue operating a vehicle that loses a single magnet pair due to a quench until the vehicle reaches a station. The Japanese configuration with a pair of coils per side on each end of a vehicle is perhaps able to continue after a quench. This question was not pursued. If vehicle coils with the dimensions proposed by the Japanese are replaced by twice as many magnets half as long, then coil redundancy is almost certainly achieved.

Motor efficiency is another reason for changing the vehicle magnets as described above. The Japanese choice of pole pitch is too long for good motor efficiency for the single vehicles considered in this report. When used in trains with multiple cars, the Japanese pole pitch produces efficient motors.

3.1.3 Hybrid Null Flux

The hybrid null flux configuration is shown in figure 3.3, which shows the baseline values of the principal parameters.. The vehicle travels above a box beam guideway. The vehicle has superconducting magnets of a complicated shape. The hybrid null flux suspension requires a double coil magnet as described in section 3.0.3. This is formed by the inner four conductors shown in the cross section portion of figure 3.3. In addition, there are four outer superconducting loops per magnet unit. The purpose of these is to reduce magnetic fields in the passenger compartment by providing some self-shielding. The linear synchronous motor also uses these outer loops.

The self-shielding vehicle magnets considered in this study are much less effective than initial calculations indicated. Superconducting vehicle magnets can be self-shielding, up to a point. One self shielding magnet design considered for the Bechtel system produced fields in the passenger compartment no higher than 16 gauss, which is a substantial reduction in field compared with configurations that ignore passenger field reduction. The self shielding idea tried in the hybrid null flux configuration was based on two dimensional arguments. The position and magnitude of the currents shown in Figure 3.3 form a symmetrical arrangement that causes remarkably rapid drop off in magnetic field at distances that are larger than two meters from the magnet if only the longitudinal conductor segments are considered. When fields from end turns are included, as they must be, then fields are about 110 gauss at the passengers' feet instead of one sixth that without end turns.

To be self shielding, a magnet's dimensions should be small. This is a conflict for the present configuration. The dimensions from side to side should be large for other reasons. Width is needed to resist torques from side forces.

3.2 Aerodynamic Differences among Systems

The main results' tables are based on the assumption that each vehicle has a cross section three meters wide by four meters high. While this was a fast starting point and was in the spirit of evaluating technologies with even assumptions, some information is being lost. In particular, different technologies produce vehicles with different shapes. A box beam guideway uses taller vehicles than Magneplane.

The two charts below, figures 3.5 and 3.6, show aerodynamic, suspension, and motor losses for four systems, with and without aerodynamic corrections. The first four stacks in each chart use the three by four meter cross section assumption. The last four stacks estimate vehicle cross section and coefficient of aerodynamic drag based on

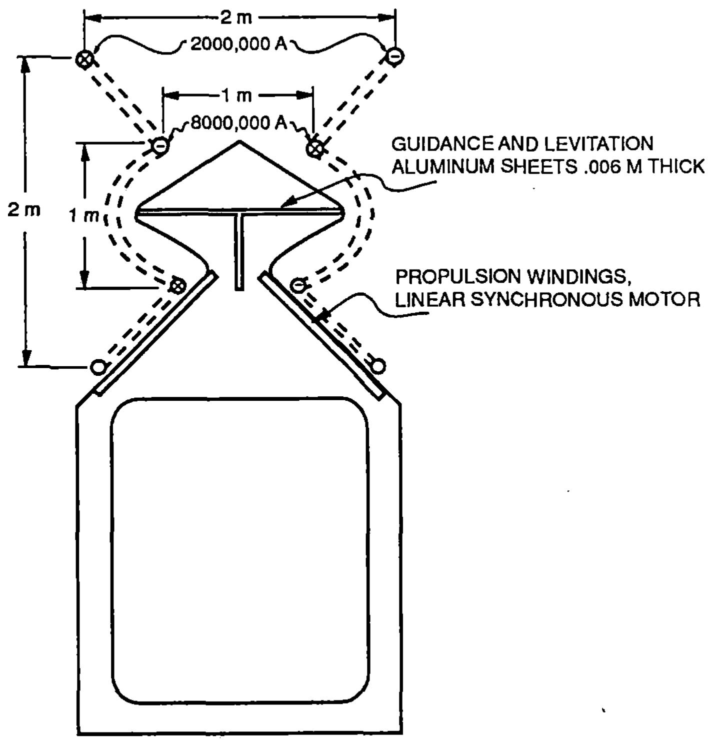

(a) Cross section.

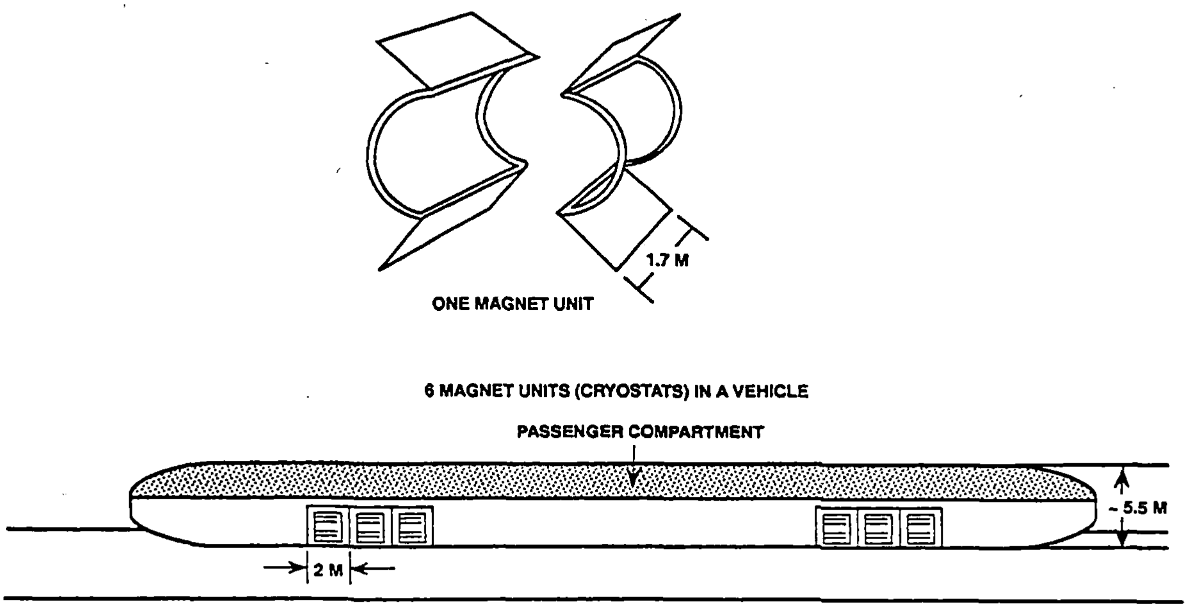

(b) Magnet unit and side view.

Figure 3-3. Small beam guideway with null flux.

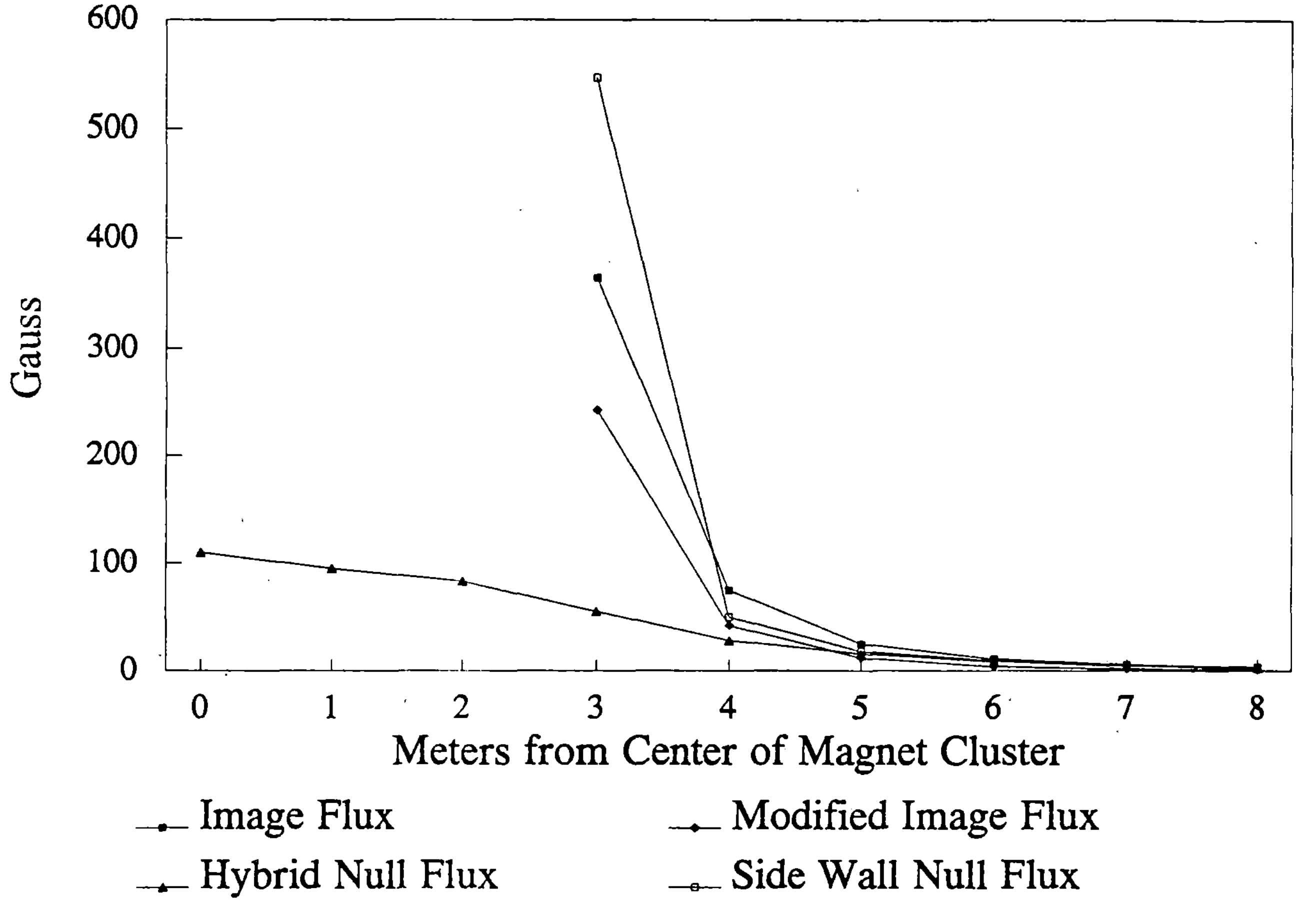

Figure 3-4. Passenger compartment B fields.

known parameters. The vertical scale has units of megawatts. Losses at 134 meters per second assume a .26 g side load. Losses at 89 meters per second assume a .18 g side load.

A number of basic design decisions affect aerodynamic characteristics. Channel guideways have higher drag. Aerodynamic control surfaces have drag. Secondary suspensions with irregular surfaces between bogies and passenger compartment will increase drag. Designs that have passengers above superconducting vehicle magnets will

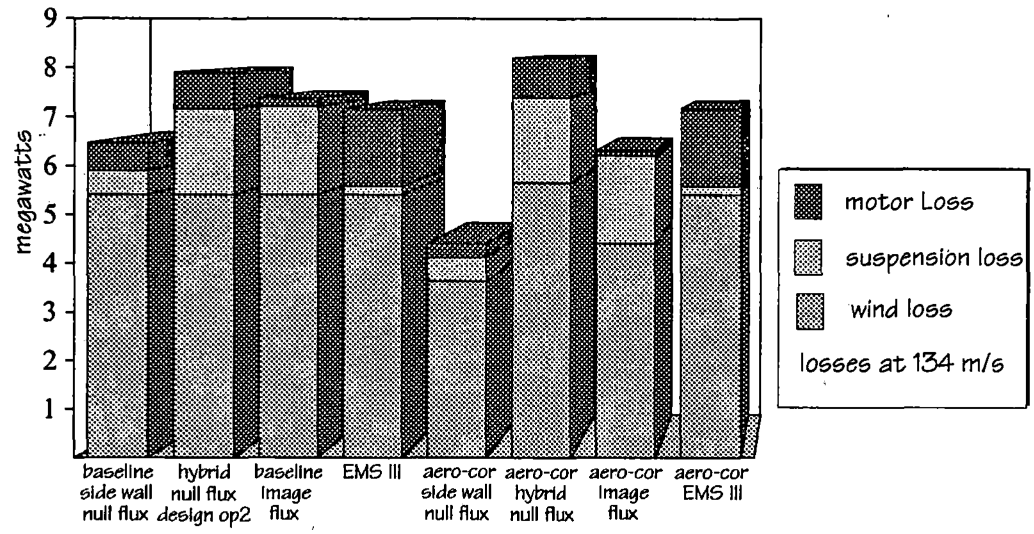

Figure 3.5. The importance of aerodynamic drag at 134 m/s

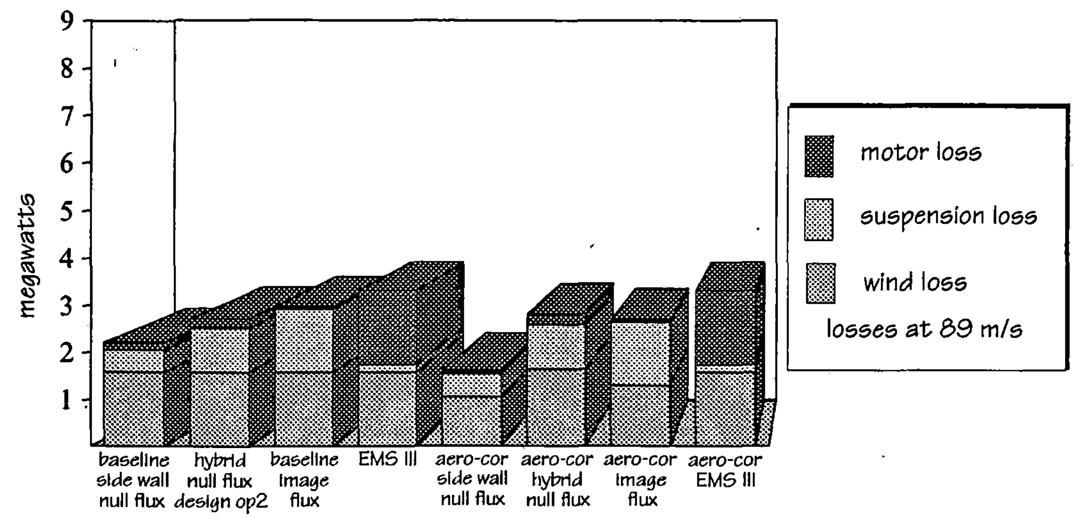

Figure 3.6. Aerodynamic drag is less important at 89 m/s

have higher vehicles and more aerodynamic drag from larger vehicle front area. Designs which separate passengers from magnetic components will have higher aerodynamic drag from increased vehicle length.

Since aerodynamic drag is the most important loss mechanism, small percentage differences in drag may be significant.

3.3 Superconducting Magnets and the Electrodynamic Systems

Superconducting magnets are necessary for any practical electrodynamic system. There is very little experience using them for vehicle suspension. There is concern that these magnets will be heavier than might be expected from projections based on static superconducting magnet applications, such as medical imaging systems.

Professor Joseph Smith of MIT's Mechanical Engineering Department, who has used superconducting magnets in rotating electrical machinery, has described these problems. Losses in the magnets are much higher in such an application than static thermal calculations predicted. The chief difficulty is that ac fields must be kept from the superconductors. This is done with normal metal shields which will probably be at cryogenic temperatures, but not superconducting temperatures. These shields need to be held very rigidly relative to the superconductor. Motion between shield and magnet will expose the magnet to ac fields, even though the original field, which may have caused the motion between shield and magnet, can not penetrate the shield. Lack of experience with such shields and supporting structures makes magnet calculations uncertain.

Another area of uncertainty is the weight of refrigeration equipment. Both the refrigeration load and refrigeration strategy are unknown. One design approach is to have on-board refrigeration. Another strategy is to have liquid helium supplied to the vehicle at stops, and to store warmed helium that is recycled through refrigeration equipment at stations.

Another uncertainty is the appropriate level of design margin for the magnets. A conservative design increases weight while decreasing the probability of magnet quench.

This study recognizes the importance and uncertainty of the superconducting magnet systems. No attempt was made to solve the above problems. To calculate cryosystem weight, the superconducting wire weight was calculated using the guidelines provided by the MIT Plasma Fusion Center as part of their current National Maglev Initiative work. These guidelines are understood to be conservative. Then the uncertainty was summarized in a "technology factor," T, the ratio of total cryogenic system weight to superconductor weight. A value of 5 was used for the technology factor in all calculations shown in this report. One estimate was T could be as low as three. Possibly the cryosystem weights could be twice as much as shown.

3.4 Side Wall Null Flux Trade-Offs

Table H-1 is a summary of eight side wall null flux designs. Seven of the designs show the effects of a limited change away from the design designated as "baseline." Boxes around numbers indicate design parameters that differ from baseline, and the more interesting consequences of these changes. Table H-1 has two parts. The first evaluates the eight designs at 134 meters per second; the second evaluates the designs at 89 meters per second.

3.4.1 Japanese Magnet Dimensions, Single Vehicle (J-single)

The published dimensions of the Japanese MLU002 were followed when available. This design was expected to be the baseline, but when the motor losses were calculated, the problem with this design was apparent. A new design with pole pitch half the Japanese pole pitch became the baseline.

The analysis assumes there are two magnets per bogie on each side, and the next closest bogie is far enough away that the guideway coils interact with only one bogie at a time. The guideway currents are assumed to die to zero between bogie encounters. This was a good assumption for the Japanese magnets, but when the magnet pole pitch was halved, twice as many magnets were needed. The effect of closer magnets is to improve the efficiency of the levitation system. Thus, the calculations for the baseline estimate lift low and drag high. Due to this, performance is better than calculations indicate.

The major differences between baseline and a Japanese single vehicle are summarized in the chart below, for 134 meters per second.

	Baseline	Japan, Single Vehicle
Pole Pitch (m)	1.35	2.7
Number of Bogies	4	2
Motor Constant (V/m/s)	30.2	13.4
Motor Losses (MW)	0.56	2.2
Motor Current (kA)	0.48	1.1
Motor Voltage (kV/phase)	4.1	1.8
Magnet Weight (Mg)	8.7	6.9
Motor Reactive Power (MVA)	5.3	12

The main difference is the motor, and the motor constant tells the whole story. The other motor parameters follow from the motor constant change.

This example can be used to discuss some concepts of linear synchronous motors. Linear synchronous propulsion motors require a strong magnetic field on the vehicle. The single vehicle electrodynamic designs considered in this report would all have better linear synchronous motors if the strengths of the vehicle magnets increased. Lower motor current is a desirable tradeoff for all vehicles considered except when insulation breakdown is approached.

The reason motor constant improves with shorter (by a factor of two) pole pitch is that the number of poles doubles, the number of active motor winding segments doubles, and the force per ampere and motor constant approximately doubles as well. This reduces current squared losses by about a factor of four.

One noticeable cost of the baseline magnet configuration is higher magnet weight. Another difference in the magnets that is not apparent at first is the baseline magnets have much shorter spacing between magnets in the direction of vehicle motion. This means the baseline has much stronger force between magnets. Presumably these magnets are in separate cryostats for redundancy, so that a quench will not cause the vehicle to crash. This means the magnetic forces between adjacent magnets must be carried to ambient temperature. The inner magnets in a bogie must be able to take this force even though it is balanced in normal operation. The force between adjacent magnets is approximately 210,000 newtons, which is 8.4 times the working force of supporting the vehicle. The Japanese magnet design has only 28,000 newtons between coils, which is .58 times the working force. This structure would be a source of heat leak and possibly added weight. The strength required to withstand this magnetic force may be less than the strength required for magnetic shielding as described in section 3.3.

3.4.2 Side Wall Null Flux Japanese Magnet Dimensions, 10 Car Train

As mentioned earlier, Japanese magnet dimensions are inappropriate for a single vehicle, but they work well for a train of vehicles. The reason is that the motor for a train has many additional field poles, and the current for a train is actually less than for a single vehicle, with everything possible held constant. A given guideway motor current produces a force per magnet coil. For a train the magnet coils are multiplied by the number of cars. The motor losses remain constant while the motor output goes as the number of cars. The most important parameters are summarized below for 134 meters per second.

	Baseline	Japan, 10 Car Train
Number of Bogies	4	20
Vehicle Weight (Mgram)	40	400
Pole Pitch (meters)	1.35	2.7
Coefficient of Aero Drag	0.3	1
Aero Drag Power (MW)	5.4	18
Motor Constant (volt/m/s)	30.2	134
Motor Losses (MW)	0.56	0.32
Motor Current (A)	490	410
Motor Voltage (kV back EMF)	4.1	17.9
Passengers	≈100	≈1000

The aerodynamic drag coefficient for the ten car train is a guess. This is an important number, but not the focus of this report.

The effect of greatest interest here is that the motor losses per passenger drop dramatically. With these reduced losses come higher motor voltages. The ten car train design shown here could be pushing insulation limits, and if so, the guideway could be wound with fewer turns of thicker wire to reduce motor voltages while keeping motor losses constant.

3.4.3 Side Wall Null Flux Baseline with Improved Estimate of Aerodynamic Drag

As part of the uniform assumptions, all vehicles were assumed to have equal vehicle sizes and shapes, and hence equal aerodynamic drag. The actual vehicles as developed for the calculations have different cross sections. As discussed in section 3.2, the side wall null flux and image flux vehicles developed here have lower cross sections than the box beam guideway. Future experience may indicate whether this is an inherent characteristic of box beam guideways, or just a consequence of the design decisions made for this report. At any rate, the effect of using calculated vehicle cross section is shown in the "BL-aero" column in the side wall null flux summary. The most important parameters are shown below, calculated for 134 meters per second.

	Baseline	Baseline-aero
Frontal Area (m^2)	12.2	8.2
Aero Drag Power (MW)	5.4	3.6
Motor Current (A)	490	340
Motor Losses (MW)	0.56	0.27

Motor losses drop simply because less current is needed to propel the smaller vehicle.

The aerodynamic drag is by far the most important loss mechanism. Section 3.2 discusses this.

3.4.4 Side Wall Null Flux Five Centimeter Mechanical Clearance

The side wall null flux configuration is surprisingly sensitive to the mechanical clearance allowed between the vehicle and guideway. The baseline has eight centimeters of clearance. The effect of changing this to five centimeters is shown in table H-1 in the column with "5cm clear" at the top. The most important parameter changes are shown below. Parameters shown are for 134 meters per second.

	Baseline	Five Centimeter Clearance
Mechanical Clearance (cm)	8	5
Vehicle Vertical Position (cm)	2.7	1.8
Motor Constant (V/m/s)	30.2	34
Motor Losses (MW)	0.56	0.42
Lift Losses (MW)	0.43	0.28
Lift/Drag (no guidance forces)	123	186

The explanation for the improvement is understandable. By reducing the mechanical clearance, the superconducting vehicle magnets are three centimeters closer to the guideway. The difference can be thought of as stronger fields at the guideway or better magnetic coupling between vehicle and guideway. Either way, both null flux levitation and synchronous motor propulsion do better with the smaller gap.

These results do not apply to other systems. Any linear synchronous motor will be better with closer spacing between field and armature. But neither the hybrid null flux nor the image flux suspensions improve with smaller mechanical clearance. The electromagnetic systems depend strongly on small clearance. Because the air gap field comes from normal metal conductors, the magnetic design is completely different and mechanical clearances need to be an order of magnitude smaller than electrodynamic systems.

The reduction in vehicle vertical position is a measure of primary suspension stiffness. Since the levitation force is nearly linear with vertical position, the natural frequency is, to a good approximation, the square root of gravity over vertical position. The primary natural frequency changes from 3 Hz for baseline to 3.7 Hz for the design with 5 centimeter clearance. Notice how lower suspension losses are associated with higher suspension natural frequencies. This is typically, but not always, the relationship between stiffness and efficiency for electrodynamic systems.

3.4.5 Side Wall Null Flux Magnet Current Reduced to 600 k Amps

Reducing the superconductor magnet current makes everything worse except magnet weight. The increase in motor and levitation losses is caused by exactly the same phenomena that made these losses smaller in the reduced clearance case above. The results are shown in the "600 kA" column of table H-1, and summarized below. Parameters are calculated at 134 meters per second.

	Baseline	600 kA Magnet Current
Magnet Current (kA)	800	600
Weight of Cryogenics (Mgram)	8.7	6.5
Motor Constant (V/m/s)	30.2	23.1
Motor Losses (MW)	0.56	1.08
Lift Losses (MW)	0.43	0.74
Lift/Drag (no guidance forces)	123	71
Vehicle Vertical Position (cm)	2.7	4.6

The 2.2 megagram saving in magnet weight is again based on a technology factor of 5 (section 3.3.) A 2.2 megagram weight reduction would allow perhaps 15 more passengers per 40 megagram vehicle. These numbers suggest that energy consumption per passenger seat would decrease about 2% with the lower magnet current. (Aerodynamic losses that dominate are constant and seats increase.) The uncertainty in the technology factor make this too close to call.

3.4.6 Side Wall Null Flux Reduced Guideway Levitation Conductor

The seventh column in table H-1, with "Rlc<BL" at the top, shows the effect of reducing the amount of aluminum in the guideway levitation conductors. As expected, levitation losses increase. The following table for 134 meters per second summarizes the results.

	Baseline	Reduced Levitation Aluminum
Levitation Coil Radius (cm)	2.8	2.4
Lift Losses (MW)	0.43	0.56
Lift to Drag Ratio	123	94
G'way Lev Aluminum (kg/m)	50	37
Vehicle Vertical Position (cm)	2.7	2.8

One curious feature of this example is that the vehicle vertical position did not greatly change while levitation losses increased significantly. In the previous two examples, this parameter was closely tied to levitation losses.

Analysis shows a slight improvement in the motor constant due to the motor windings moving closer to the vehicle due to decreased levitation coil diameter. However, motor losses increased due to lift losses requiring higher motor current.

3.4.7 Side Wall Null Flux Reduced Guideway Motor Aluminum

The last column in table H-1 shows that if guideway motor winding aluminum is reduced, motor losses increase. The table below summarizes the results for 134 meters per second.

	Baseline	Reduced Motor Aluminum
Motor Conductor Radius (cm)	1.5	1.3
G'way Motor Aluminum (kg/m)	115	86
Motor Resistance (mΩ/m)	0.8	1.06
Motor Losses (MW)	0.56	0.72

These last two cases illustrate that although any parameter can be improved, the cost of that improvement is probably a worsening of something else.

3.4.8 Baseline at 134 Meters per Second and at 89 Meters per Second

The second half of table H-1 evaluates the eight designs discussed above at 89 meters per second. Aerodynamic loss is much less important. Magnetic drag is higher at 89 meters per second for the side wall null flux designs and lift losses are also higher at the lower speed for all the side wall null flux designs considered. Magnetic losses associated with side loads are higher at 134 meters per second for the baseline because we assume higher side loads for the higher speed. For any linear synchronous motor, motor constant is not a function of speed. The table below summarizes baseline parameters.

	Baseline at 134 m/s	Baseline at 89 m/s
Aerodynamic Drag Loss (MW)	5.4	1.6
Magnetic Drag (kN)	3.6	5.4
Lift/Levitation Drag	123	78
Magnetic Losses (MW/vehicle)	0.49	0.48
Motor Losses (MW/km block)	0.56	0.15

3.5 Hybrid Null Flux Trade-Offs

Table H-2 shows twelve variations of the hybrid null flux configuration. The first column of numbers is a baseline, and most other columns differ from this design in only one respect. The parameters that differ from baseline, and the major effects of these differences, are in boxes.

3.5.1 Hybrid Null Flux Baseline at 134 Meters per Second with Side Load

The cryosystem is 35% of the vehicle weight, based on a technology factor of 5 (section 3.3.) This hybrid null flux configuration's cryosystem is especially heavy.

Magnetic losses are higher than side wall null flux losses, but lower than image flux losses. Baseline design has 1.8 MW magnetic losses at 134 meters per second with 0.26 g side load. The magnetic losses are mostly the result of two design characteristics. First, this system has continuous sheets instead of wound coils in the guideway. Second, the narrow box beam guideway balances torque from the side load with high forces. This lack of efficiency of the hybrid null flux design was not apparent before work began.

This configuration is notably inefficient when presented with a cross wind or other side load. The effects from side loads have two components that need explanation. Lateral drag is the drag that results from supporting the side force. This would be the only loss if the force acted at just the correct height low down on the vehicle so no torques were required from the levitation suspension elements. Wind and cornering forces are applied much higher than the lateral force center, so torques are involved. In fact, losses from lateral torque are substantially higher than the lateral force losses. This is characteristic of box beam configurations, which have suspension forces well toward the bottom of the vehicle, and a narrow track from which to balance torques.

The guidance guideway conductor crowds the motor of this design away from the best vehicle magnetic fields. Placing the guidance conductor above the levitation sheet would improve this. So placing the guidance conductor would also decrease losses from side load torques.

3.5.2 Hybrid Null Flux Baseline Operating Without Side Load

The next column in table H-2, labeled "134, no T" shows the effects of removing the side load from the baseline design. This is not a design option, of course, but clarifies where the baseline magnetic losses originate. The table below summarizes the differences between operating with and without side load.

	Baseline @ 134 m/s, side load	Baseline, no side load
Lateral force (g's)	0.26	0
Lateral drag loss (MW)	0.02	0
Lateral torque loss (MW)	0.8	0
Total magnetic losses	1.76	0.95
Motor winding losses	0.76	0.6

The above table does not explicitly show an overhead loss associated with the hybrid null flux configuration. Because of the sheet guideway conductors, there is magnetic drag if no levitation or guidance force is supplied by the system. So in the absence of side forces, there is still drag associated with the guidance conductor. This drag is included, arbitrarily, in lift losses. Sections 3.0.3 and 3.5.7 discuss this overhead drag.

3.5.3 Hybrid Null Flux Baseline at 89 Meters per Second with Side Load

The table H-2 column labeled "89 m/s" describes this case. The table below summarizes the major effects.

	Baseline at 134 m/s	Baseline at 89 m/s
Velocity (m/s)	134	89
Lateral force (g's)	0.26	0.18
Wind drag loss (MW)	5.4	1.58
Motor voltage (kV back EMF)	2.6	1.7
Total magnetic losses (MW)	1.76	0.88
Motor winding losses (MW)	0.76	0.2

Losses go down dramatically as velocity decreases. Besides the obvious wind drag losses, there are two additional reasons for this improvement. One is that the lateral force is lower, for a given cross wind, at lower speeds. The second factor is that the "overhead" magnetic drag for the baseline design decreases noticeably with speed.

Notice that motor open circuit voltage (back EMF) is lower at the lower speed. All synchronous electric motors, rotary or linear, have open circuit voltage proportional to relative air gap velocity.

3.5.4 Hybrid Null Flux Baseline operating without side load at 89 m/s

The column labeled "89, no T." in table H-2 describes this case. The table below shows the most interesting numbers.

	Baseline @ 89 m/s, side load	Baseline, 89 m/s, no side load
Lateral force (g's)	0.18	0
Lateral drag loss (MW)	0.01	0
Lateral torque loss (MW)	0.39	0
Total magnetic losses	0.88	0.48
Motor winding losses	0.2	0.14

Again, as at 134 meters per second, the major loss associated with side loads arises from the need to apply restoring torques with the levitation portions of the suspension.

Motor losses are higher with side forces due to the additional motor output required to overcome magnetic losses.

3.5.5 Hybrid Null Flux Baseline with Aerodynamic Corrections

The table H-2 column labeled "134 Aero" describes the effects of estimating the vehicle frontal area and using this to compute drag forces. The best estimate of vehicle frontal area, based on the known details of the design, is slightly greater than the standard assumption of 12.2 square meters. Section 3.2 discusses the 12.2 square meter assumption. The table below summarizes the differences between baseline and best estimate aerodynamic effects.

	Baseline, 134 m/s, no side load	Aero, 134 m/s, no side load
Vehicle frontal area (m^2)	12.2	12.7
Wind drag loss (MW)	5.4	5.64
Motor winding loss (MW)	0.6	0.64

3.5.6 Hybrid Null Flux Mechanical Clearance Reduced to 5 Centimeters

The column labeled "5 cm clear" shows the effects of reducing mechanical clearance between vehicle and guideway from 8 centimeters to 5 centimeters. The table below summarizes the effects.

	Baseline @ 134 m/s	Reduced clearance @ 134 m/s
Mechanical clearance (cm)	8	5
Motor voltage (kV back EMF))	2.6	2.9
Motor winding loss (MW)	0.76	0.59
Total magnetic losses (MW)	1.76	1.76

Compared with the side wall null flux configuration, the most surprising feature of this variation is that magnetic losses are unaffected by the reduced mechanical clearance. The difference is that the hybrid null flux operates mechanically centered with a small offset. Reduced mechanical clearances do not allow any improvement in the preferred operating position.

The motor does benefit from closer spacing between guideway motor windings and vehicle magnets.

3.5.7 Hybrid Null Flux Reduced Vehicle Magnet Current

The column labeled "600 kA" shows the effect of reducing the vehicle superconducting current from 800 kA to 600 kA. The table below summarizes the result.

	Baseline @ 134 m/s	Reduced magnet current
Main conductor current (kA)	800	600
Cryosystem weight (kg)	14,000	10,500
Motor voltage (kV)	2.6	2.1
Lift loss (MW)	0.95	0.68
Loss from lateral drag (MW)	0.02	0.03
Loss from lateral torque (MW)	0.8	1.41
Total magnetic losses (MW)	1.76	2.12
Motor winding losses (MW)	0.76	1.22
Primary natural freq. (Hz)	4.1	3.1

The reduction in cryosystem weight and motor voltage is predictable. Of more interest is the effect on magnetic loss. Some categories of magnetic loss increase, others decrease. The reason is there are two components of magnetic loss. One is the overhead component that exists independent of whether useful force is being supplied by the suspension. At a constant speed and fixed magnet current, the overhead loss is constant, independent of vehicle position or vehicle suspension force. The "lift loss" row of table H-2 and the table above includes the entire overhead loss. The other component increases with useful applied force, approximately proportionally with the square of the useful force. As a function of magnet current, overhead loss decreases and the proportional term increases with decreasing vehicle magnet current.

If the system only operated at a single velocity and side load, then the magnet current could be optimized to minimize some combination of loss and vehicle weight.

But the vehicle must operate over a range of states. The side load from wind is hard to control. The change from 800 to 600 kA looks attractive for magnetic losses if operating without side loads, but side loads favor the higher current. In addition, motor efficiency suffers from lower magnet currents. The lighter vehicle could carry about 30 additional passengers.

3.5.8 Hybrid Null Flux Thinner Guideway Conductor, at 134 Meters per Second

The table H-2 column labeled "d=.004" shows the effects of making the thickness of the conducting sheets in the guideway thinner by one third. The following table summarizes the effects. Overall, the results are similar to the last example. The overhead magnetic losses go down but the losses proportional to useful force squared go up.

	Baseline @ 134 m/s	Reduce g'way sheets @ 134 m/s
Guideway sheet thickness (mm)	6	4
Guideway sheet mass (kg/m)	39	26
Magnetic lift/drag, no lateral force	56	124
Lift loss (MW)	0.95	0.42
Loss from lateral drag (MW)	0.02	0.02
Loss from lateral torque (MW)	0.8	1.21
Total magnetic loss (MW)	1.76	1.65
Motor winding loss (MW)	0.76	0.74

The thinner guideway sheets are a better design at this speed. Absence of side forces enhances this advantage. The overhead drag goes down sharply, which accounts for the greatly improved lift to drag ratio for no lateral force. The loss associated with lateral force goes up because no overhead drag loss is included in this item.

3.5.9 Hybrid Null Flux Thinner Guideway Conductor at 89 Meters per Second

This case is the same as above except vehicle speed is 89 meters per second. It is in the table H-2 column labeled "4mm, 89m/s." The table below summarizes results.

The thinner guideway sheet is more attractive at 134 meters per second than at 89 meters per second. At the lower speed the loss difference between the two guideway sheet thicknesses is small. This is because at lower speeds the overhead loss term becomes less important and the loss proportional to useful suspension force squared is more important.

	Baseline @ 89 m/s	Reduced Guideway sheets @ 89 m/s
G'way sheet thickness (mm)	6	4
Guideway sheet mass (kg/m)	39	26
Magnetic lift/drag, no lateral force	72	121
Lift loss (MW)	0.48	0.29
Loss from lateral drag (MW)	0.01	0.01
Loss from lateral torque (MW)	0.39	0.58
Total magnetic loss (MW)	0.88	0.88
Motor winding loss (MW)	0.2	0.2

3.5.10 Hybrid Null Flux Reduced Pole Pitch, 134 Meters per Second

The table H-2 column labeled "P=1m" shows the effect of reducing the pole pitch to 1 meter. The overall effect is to reduce vehicle weight, but to increase losses. The table below shows the most interesting results.

	Baseline @ 134 m/s	Reduced pole pitch @ 134
Pole pitch (m)	2	1
Cryosystem weight (kg)	14,000	9,200
Motor open circuit voltage (kV)	2.6	2.4
Motor winding resistance (Ω)	0.29	0.37
G'way motor mass (kg/m)	46	58
Magnetic lift/drag, no side force	56	28
Lift loss (MW)	0.95	1.9
Loss from lateral drag (MW)	0.02	0
Loss from lateral torque (MW)	0.8	0.22
Total magnetic loss (MW)	1.76	2.12
Motor winding loss (MW)	0.76	1.2

The loss effects are similar to those produced by increasing vehicle magnet currents. The overhead loss increased while the term proportional to useful force squared decreased. With this combination of changes comes greater stiffness and a higher natural frequency. Ignoring overhead loss, the suspension efficiency improved, and this improvement is associated with higher stiffness. Notice that this trade substantially reduced the vehicle magnet weight. The results are complementary to reduced guideway sheet thickness. This suggests the next design.

3.5.11 Hybrid Null Flux Reduced Pole Pitch and Reduced Guideway Sheet Thickness, at 134 Meters per Second

The table H-2 column labeled "P&d<BL" shows the results of reducing the pole pitch to 1 meter and the guideway sheets to 4 mm. The table below shows the most interesting numbers.

The combination of reduced pole pitch and reduced guideway sheet thickness has reduced losses and reduced vehicle magnet weight compared with the baseline. Reactive power supplied by the motor is worse.

	Baseline @134 m/s	Reduced P and d
Pole Pitch (m)	2	1
Guideway sheet thickness (mm)	6	4
Cryosystem weight (kg)	14,000	9,200
Motor resistance (Ω)	0.29	0.37
Total guideway aluminum (kg/m)	84.8	83.8
Magnetic lift/drag (no side load)	56	87
Lift loss (MW)	0.95	0.6
Loss from lateral drag (MW)	0.02	0.01
Loss from lateral torque (MW)	0.8	0.34
Total magnetic losses (MW)	1.76	0.94
Motor winding loss (MW)	0.76	0.85
Primary natural frequency (Hz)	4.1	6.8
Motor reactive power (MVA)	24	45

3.5.12 Hybrid Null Flux Reduced Pole Pitch and Guideway Sheet Thickness, 89 m/s

The last column in table H-2 shows the design above operating at 89 meters per second. The results are similar. Magnetic losses are again down by about a factor of two, and motor winding losses are nearly unchanged. Motor reactive power increases by about 55%, not quite such a sharp increase as that at 134 meters per second.

3.5.13 Hybrid Null Flux Optimizations

For an operating condition of vehicle weight, speed, and side load, there are optimal thicknesses for the levitation and guidance sheets. Table H-2.1 shows four optimal designs and the conditions for which they are optimized. The optimization varied horizontal and vertical guideway sheet thicknesses while keeping other parameters, including pole pitch, at baseline values. The tables show performance for each design at two operating conditions.

The existence of the two components of magnetic drag leads to a best guideway thickness for an operating condition. The overhead component of drag increases with increasing sheet thickness. The lift related component of drag decreases with guideway sheet thickness. There is a thickness that minimizes magnetic drag.

The optimum is sensitive to operating conditions. Since the .26 g side-load at 134 meters per second and .18 g side load at 89 meters per second represent unusually high side loads, the system losses would be lower if a more typical side load was chosen as the optimizing point.

The following table summarizes the optimizations.

Design	Optimized for vel, side load	Lev sheet thickness	Guidance sheet t'ness	Mag loss @ conditions	Mag loss @ conditions
op1	134, 0.26	5.2 mm	2.3 mm	**1.48@134, 0.26**	.63@134, 0.09
op2	134, 0.09	3.6 mm	1.4 mm	1.74@134, 0.26	**.49@134, 0.09**
op3	89, 0.18	5.5 mm	2.4 mm	**.77@89, 0.18**	.37@89, 0.06
op4	89, 0.06	4.2 mm	1.4 mm	.85@89, 0.18	**.32@89 ,0.06**

The cells with bold font show the magnetic losses, in megawatts, at the optimizing conditions. For comparison, designs op1 and op2 are both evaluated at the same two operating points. Designs op3 and op4 are also both evaluated at two common points. The units of conditions are meters per second and gravities of side load.

3.6 Image Flux Trade-Offs

Table H-3 shows eight variations of the image flux configuration. The first column of numbers is the baseline. Other columns show the effects of deviating from the baseline by single parameters. Boxes show the changed parameters and the more interesting consequences of the changes.

3.6.1 Image Flux Baseline at 134 Meters per Second with Substantial Side Load

Table H-3 column labeled "134 m/s" shows this case.

This design follows the Magneplane design as it was understood in the fall of 1991, except for one important parameter. Following the level playing field convention, the vehicle is assumed to have a frontal area of 12.2 square meters. The realistic area is 8.5 square meters, based on vehicle geometry.

Notice that the motor losses are lower for this design than for either the side wall null flux or hybrid null flux designs at 134 meters per second.

3.6.2 Image Flux Baseline at 134 Meters per Second, No Side Load

The table H-3 column labeled "134, no T" shows this case.

Removing the side load has only a modest effect on magnetic drag and other parameters shown in the summary calculations table. However, there are dynamics and ride quality effects associated with side loads that are believed to be important but are difficult to calculate with great confidence. The motor magnets act as a keel held between the guideway levitation sheets. These concerns are described in appendix C.

The following table summarizes differences between the baseline at 134 meters per second with and without side force.

	Baseline @ 134 m/s	Baseline, 134, no side load
Lateral force (g's)	0.26	0
Total magnetic loss (MW)	1.79	1.36

3.6.3 Image Flux Baseline with Aerodynamic Corrections

Two aerodynamic corrections were made to the baseline to reflect what is believed to be the nature of Magneplane. The frontal area used for drag calculation is based on vehicle geometry. The coefficient of drag is increased to reflect the higher drag expected from channel guideways and Magneplane's aerodynamic control surfaces. Table H-3 in the column labeled "134 Aero" shows these changes. The table below summarizes the results. Wind drag is much lower.

The coefficient of drag for both the baseline and vehicle with aerodynamic corrections is an engineering estimate.

	Baseline @134 m/s	Aerodynamic corrections
Assumed frontal area (m^2)	12.2	8.5
Coefficient of drag	0.3	0.35
Wind drag power (MW)	5.4	4.4
Motor winding loss (MW)	0.17	0.13

The wind drag power is loss per vehicle, and the motor winding losses are for one vehicle on a block one kilometer long.

3.6.4 Image Flux Baseline at 89 Meters per Second

The fourth column table H-3 shows the effect of operating the baseline vehicle at 89 meters per second. Wind drag is 29 % of the 134 meters per second value. The table below summarizes this.

	Baseline @ 134 m/s	Baseline @ 89 m/s
Lateral force (g's)	0.26	0.18
Motor voltage (kV)	4.1	2.8
Motor reactive power (kVA)	5,100	1,200
Wind drag power (MW)	5.4	1.6
Total magnetic loss (MW)	1.8	1.35
Motor winding loss (MW)	0.17	0.06

Motor winding losses and motor reactive power are for a vehicle on a one kilometer long block. Wind drag power and magnetic loss is for a vehicle.

3.6.5 Image Flux Baseline at 89 Meters per Second, Magnet Current for 134 m/s

As an electrodynamic vehicle slows, it drops until wheels or the equivalent touch the guideway. For the baseline at 89 meters per second, the vehicle magnet currents increased just slightly compared with the baseline at 134 meters per second. The fifth column in table H-3, labeled "89, HSI," shows the vehicle dropping slightly if the magnet current stays at the 134 meters per second value. The model predicts almost no change, as summarized below.

	Baseline @89 m/s	Baseline@ 89 with 134 current
Vehicle vertical position (mm)	0	-0.05
Vehicle outer current (kA)	145.66	145.63

3.6.6 Image Flux Guideway Levitation Sheets Reduced to 1 Centimeter

The sixth column in the summary table, labeled "d=.01" shows the effects of reducing the thickness of the guideway levitation sheets, with the vehicle operating at 134 meters per second. This variation tests the possibility of reducing capital cost by increasing operating cost. One clear difference between image flux system and the other electrodynamic systems is image flux uses more aluminum in the guideway. If this aluminum is reduced, magnetic drag increases. With the thickness reduced from two to one centimeter the image flux design still uses more aluminum than the others.

The seventh column in table H-3, labeled "10mm, 89" shows the same variation operating at 89 meters per second.

The following two tables, one for each speed, summarize the thinner guideway. The columns on the right indicate that magnetic losses are nearly equal for the thin sheet guideway at 89 and 134 meters per second. For the thin sheet guideway, the speed at which magnetic skin depth is equal to 1 centimeter is 205 meters per second. So both 89 meters per second and 134 meters per second are in the intermediate speed range where levitation power is independent of speed, as described in section 3.0.1.

	Baseline at 134 m/s	Reduced guideway Al at 134 m/s
G'way sheet thickness (cm)	2	1
G'way lev. Aluminum, (kg/m)	213	106
Total magnetic losses (MW)	1.8	2.2

	Baseline at 89 m/s	Reduced guideway Al at 89 m/s
G'way sheet thickness (cm)	2	1
G'way lev. Aluminum, (kg/m)	213	106
Total magnetic losses (MW)	1.4	2.1

3.6.7 Image Flux Pole Pitch Reduced to 1 meter

The last column in table H-3, labeled "P=1 m" shows the effect of reducing the pole pitch from 1.5 meter to 1 meter. This reduces cryosystem weight and increases magnetic losses. The motor constant improves due primarily to higher currents in the vehicle magnets needed to levitate the vehicle with the smaller magnets. But motor resistance increases due to the increased number of meanders per block length. The table below summarizes this.

	Baseline @ 134 m/s	Reduced pole pitch @ 134 m/s
Pole pitch (m)	1.5	1
Magnet length (m)	1.3	0.8
Magnet outer current (kA)	146	155
Cryosystem weight (kg)	6,500	5,800
Motor voltage (kV back EMF)	4.1	4.5
Total magnetic losses (MW)	1.8	2.2
Motor winding losses (MW)	0.17	0.19

Magnetic losses are for a vehicle. Motor winding losses are for a vehicle on a one kilometer block.

3.7 Description of Electrodynamic Systems Spreadsheets, Overview

The three electrodynamic system spreadsheets differ in complexity. The hybrid null flux is the simplest. It is linear in the sense that the active formulas are in a single column. Consequently it is easy to see the structure and details of this spreadsheet by formatting the formulas as text.

The image flux spreadsheet is more complicated since portions of the spreadsheet dealing with the motor are two dimensional.

The side wall null flux is the most complicated. There are three separate spreadsheets that are linked together. A first spreadsheet computes levitation forces. Another spreadsheet computes motor parameters. A third spreadsheet computes guidance forces.

In addition, another spreadsheet computes magnetic fields in the passenger compartments.

3.7.1 Hybrid Null Flux Spreadsheet

Table G-1 shows the hybrid null flux spreadsheet in text format.

The suspension and propulsion calculations on this spreadsheet are suitable for hand calculations. As mentioned elsewhere, the suspension calculations are based on Richards and Tinkham. Their results were modified for three dimensional fields, using engineering judgment so the results agree with Urankar and Miericke.

3.7.2 Image Flux Spreadsheet

Tables G-2a, b, and c show the image flux spreadsheet in text format.

The suspension forces are based on Richards and Tinkham. For this configuration, calculating the high speed force limits directly using images avoids the problems of Richards and Tinkham's Fourier transforms of the coils.

The second and third sheets are motor related calculations. The large blocks of formulas are not legible with these spreadsheets printed in text format because of the length of the equations. These figures give some flavor of the calculations which are mostly two dimensional blocks of inductance calculations (Grover [40].)

3.7.3 Side Wall Null Flux Spreadsheet

Tables G-3a, b, c, and d show the side wall spreadsheets in text format.

The levitation, guidance, and propulsion forces are calculated with mutual inductances. As a consequence there is much less question of the reliability of the suspension forces for the side wall null flux compared with the other electrodynamic systems.

Each of the levitation, guidance, and propulsion spreadsheets has a two dimensional block of inductance calculations. Again these are based on Grover. A macro uses these inductance calculations, stepping position and recording inductance information for each position step in a table. The tables of inductance values, generally hundreds of steps long, are mostly not shown on the figures.

The more detailed motor calculations done for the side wall null flux configurations were compared to less exhaustive methods that were used for the hybrid null flux and image flux systems. The results were not significantly different.

3.7.4 Magnetic Fields Spreadsheets

Table G-4 represents the spreadsheets used to calculate magnetic fields in passenger compartments. A single string of formulas is shown although the actual spreadsheet is two dimensional.

The spreadsheets are organized with a core row that is used repeatedly, with different sources for each row. Each row represents a straight segment of vehicle magnet conductor. The formulas in each row are identical. Only the starting and ending coordinates of the conductor segment and the current differ. A single row shows the logic of the spreadsheet. A single row is transposed into a single column in table G-4. The formulas when formatted as text are thus legible.

The magnetic field from a straight line conducting filament is simply expressed in a coordinate system that has an axis lying on the filament. Most of the spreadsheet transforms vehicle coordinates to segment coordinates and then back again.

SECTION 4

COMPARISON OF SYSTEMS

4.0 Major parameters

The results of the calculations of major parameters of the EMS and EDS systems which were studied in this work are summarized in Tables 4-1 through 4-6. The following discussion will describe the tables and highlight the significant results. These results apply to the reference vehicle of 40 Mg mass and 35 meters length. While tables for forward speeds of 89 and 134 meters/second are included, the 134 meters/second results are emphasized. The optimization and trade-offs resulting in the designs listed in Tables 4-1 through 4-6 are discussed in Sections 2 and 3.

4.1 Weight comparison

Tables 4-1 and 4-2 summarize the weights for the six systems and use these results to project a passenger capacity for each system. The passenger capacity was determined by assuming that the total vehicle mass was 40 Mg. The magnet, shielding, and cryogenic insulation and refrigeration required to lift and guide 40 Mg (including the magnets) were than designed. The mass remaining after the magnet mass was subtracted from the 40 Mg was allotted to vehicle structure, utilities and furnishings, passengers and baggage and landing gear (EDS vehicles only), as calculated using aviation industry techniques [Ref. 48 and 49].

The weight of the superconducting magnets with shields, supports, and thermal insulation for the EDS 1 (image flux) and EDS 3 (coil null flux) systems was similar to that of EMS III at 25% total vehicle weight. Thus, the passenger payload for these systems was similar at 118, 113 and 113, respectively, passengers for the 40 tonne reference vehicle. For the EDS 2 (hybrid null flux) system, the magnets weighed more because of the complexity of conforming the magnets to a continuous sheet. At the beginning of this study, many expected that the superconducting magnets would weigh less than the iron cores for EMS. This study determined that the Dewars (vacuum insulation systems), magnetic shielding, and mechanical supports were quite heavy and end effects, neglected in simpler analyses and especially important for continuous sheet null flux designs, decreased lift. This large weight, along with other considerations, prevents the practical realization of the theoretically low power of null flux levitation systems [Ref 38].

The total weight of vehicle mounted magnetic components for EMS I (separate propulsion, lateral guidance, and lift) was smaller at 5.6 Mg than for EMS II (combined lateral and lift) and EMS III (combined lift and propulsion), which were similar at 7.2 and 7.3 Mg, respectively. Because EMS I and II require large powers to be brought on-board, EMS III is the preferred electromagnetic system and is emphasized throughout this report. However, it should be noted that, as mentioned below, this advantage is offset to some extent by the limitation of the maximum propulsion thrust to ≈0.1g in contrast to the other five systems, which provide the desired 0.21g.

4.2 Power comparison

Tables 4-3 and 4-4 summarize the results of the calculations of real and reactive power for the systems. Utility cost of energy depends mainly on real power and secondly on reactive power. In general, the size and cost of wayside electrical equipment such as transformers and inverters, as well as power transmission lines and on-board equipment, depends on total Volt-Amperes.

The propulsion power was that required to overcome the aerodynamic drag. Drag powers for lift and lateral guidance, which result from eddy currents in the guideway, are tabulated separately. As discussed in Section 1.2, the lateral drag was calculated for a maximum continuous lateral acceleration of 0.26 g for 134 meters/second and 0.15 g for 89 meters/second.

Because the large propulsion power must be transferred to the vehicle from the wayside, linear induction motors are not considered a viable candidate for either EMS (shown here as EMS I and II) or EDS. Linear induction motors require that the propulsion losses, plus the power used for overcoming aerodynamic drag, for hill climbing and for acceleration be transferred and conditioned on-board. This total power of ≈6 MW was one to two orders of magnitude higher than that which must be transferred on-board for the systems using linear synchronous motors with guideway propulsion excitation on the guideway.

Total real power for propulsion and drag was 1.6 kW/m of powered guideway for EMS III (linear synchronous motor) at 134 meters/second (300 mph). For EDS 1 (image flux), the real power consisted of 1.83 MW/vehicle drag and 170 W/m of powered guideway propulsion winding loss. For EDS 2 (image flux), the real power consisted of 2.18 MW/vehicle drag and 700 W/m of powered guideway propulsion winding loss. EDS 3 (sidewall coil null flux) real power consisted of of 491 kW/vehicle drag and 560

W/m of powered guideway winding loss. For a 40 Mg vehicle at 134 meters/second, wind drag power was estimated at 5.40 MW for all the vehicles.

In the electromagnetic systems, the largest power was dissipated in the EMS III guideway linear synchronous motor, in which the space (slots) for propulsion windings was small and the excitation currents must flow through relatively long distances of guideway. The iron guideway core resulted in high winding inductances and the reactive power was 25 kVA/m. Magnetic saturation limits the EMS propulsion capability, for reasonable size and weight, to ≈0.1 g, which makes operation at 134 meters/second marginal, with negligible hill climbing capability at that speed.

In the electrodynamic systems, the guideway power resulted from the eddy currents produced in the guideway by the magnetic fields required for lift and for lateral guidance and the power dissipation in the motor windings. The EDS linear synchronous motors had smaller inductances and generally more space for windings than the EMS III LSM, but required larger currents. Thus, for the EDS 1 (image flux) system, which provided the most winding space, the powers were the lowest of the EDS systems at 5 kVA/m of powered guideway reactive and 2 kW/m of powered guideway real. Because of the space constraints on the guideway winding of EDS 2 (hybrid null flux), the guideway propulsion reactive power was 22 kVA/m of powered guideway while the real power was 2.18 kW/m of powered guideway. In the EDS 3 (sidewall coil null flux) system, the coils were wound of small diameter filaments so that the penetration depth of magnetic fields was a greater fraction of the conductor diameter, reducing the effective resistance; the motor power dissipation at 134 meters/second was only 560 W/m of powered guideway, but the suspension stiffness was low. Because of the reduced volume available for motor windings, the current density was higher and the motor real power was 560 W/m of powered guideway with a reactive power of 5.3 kVA/m of powered guideway.

To summarize the power comparison, the resistive powers for EDS systems were higher than EMS while the reactive power was lower for EDS 1 and 3 and similar for EDS 2.

4.3 Ride Quality

Tables 4-5 and 4-6 summarize ride quality results for the six systems. It is essential that a practical system concept have the potential for providing its passengers with an acceptably comfortable ride. Guideway roughness equivalent to welded steel rails was assumed in this study. While Table 4-5 summarizes ride quality for forward speeds of 89 meters/second (200 mph), the discussion below focuses on the 134 meters/second (300 mph) results of Table 4-6.

In heave motion, the suspension parameters and ride quality of the three electromagnetic suspensions were similar. With a 1 cm nominal gap between the on-board magnets and the guideway rail, the closed loop controller was set to achieve stable operation and avoid rail-to-vehicle contact so that the bogey resonant frequency was 5 Hz and the damping ratio was 0.7. Passive secondary suspensions were assumed. Generally 1 Hz is accepted as the lowest practical natural frequency for a passive suspension. A damping ratio of 0.25 is an optimal trade off between ride quality and guideway tracking. The RMS (one sigma) passenger heave acceleration was 0.023 to 0.024 g for all of the EMS systems. The RMS gap variation was 20% and the current variation 21% to 25 %, acceptable figures since 100% represents vehicle to rail contact. The reactive power for EMS I was lower since the the spatial period of the lift-only magnets could be longer than for EMS II and EMS III, which combined two functions into one set of magnetic structures.

For sway and roll motion, parameters similar to those for heave were assumed with the exception of EMS II where decoupling of the vertical and sway modes required that the lateral suspension controller gain be set to a specific value, the decoupling gain; the resulting natural frequency for lateral displacements was 1.7 Hz when the eigenfrequency for vertical motion was set at 5 Hz. The parameters of the vertical suspension determine the roll stiffness and damping.

The variations in lateral primary suspension gap for EMS II (combined lift plus lateral, staggered magnets) was 45%, a permissible figure since the magnet moves parallel to, rather than normal to the rail for this motion. The RMS current and voltage variations were an order of magnitude smaller than for the other EMS cases because the magnetic forces are inherently stable whereas in the other configurations the magnet and rail move toward one another and the magnetic forces are unstable, requiring large control currents just to maintain stability.

Because the roll motion decouples the secondary from the primary, the passenger RMS lateral acceleration from guideway roughness was 0.015 g (less than for the vertical motion) for EMS II and III. The RMS lateral acceleration for EMS II (combined lift plus lateral, staggered magnets), was still lower because of the softer primary suspension. Similarly, the RMS roll rates were 0.8 and 0.4 degrees/second for EMS I for guideway roughness and wind inputs, respectively, and 0.5 and 0.3 degrees/second for EMS II. The which was 2.1 for EMS I (three separate functions) and EMS III (LSM propulsion combined with lift). Lower lateral primary suspension stiffness results in a Pepler index of 1.8, which is in the very comfortable to comfortable range, for EMS II.

For the EMS systems, which have primary suspension damping, the response to the design (high) wind input was generally half of that for the road inputs and did not have significant influence on ride quality.

The EDS 1 (image flux) system had a large 0.15 m clearance between the vehicle and guideway and soft 1 Hz natural frequency primary suspension with only passive control, so that no secondary suspension was assumed. The calculations assumed that the propulsion motor was used to provide vertical damping, as indicated in Section 3.1.1, with a damping ratio of 0.7 and the damping proportional to velocity relative to inertial space (rather than to the relative velocity between vehicle and guideway as in passive suspensions). The passenger acceleration of 0.012 g for heave motion in response to road inputs was superior to the other EDS systems because of the optimal damping. No damping was assumed for the lateral motion and roll damping was assumed to be produced by actively controlled aerodynamic surfaces resulting in a damping ratio of 0.7. The response to guideway roughness was 0.022 g (comparable to the EMS systems) but the response to the design maximum wind was high at 0.036 g. Roll rate responses were 1 and 1.9 degrees/second for lateral guideway and wind inputs, respectively. The large lateral motion responses were attributed to the lack of roll stiffness in the primary suspension. The Pepler comfort index in response to road inputs was 2.1, in the comfortable to somewhat comfortable range, comparable to the EMS systems. The RMS vehicle displacements relative to the guideway were less than 6% of the air gap.

The electrodynamic null flux cases (EDS 2 and 3) had stable, relatively stiff primary suspensions with no active control. Since simplicity is generally desirable, no primary damping was assumed in contrast to the image flux case; that is, the vehicle and suspension bogie motions were damped only by the passive secondary suspensions. For EDS 2 (hybrid null flux continuous guideway), the vertical and lateral primary suspension natural frequencies were 4.1 and 2.9 Hz, respectively. The heave and sway secondary suspensions for both EDS 2 and EDS 3 have damping ratios of 0.25 and resonant frequencies of 1 Hz. The heave RMS acceleration was large at 0.044 g, compared to 0.023-0.024 g for all the EMS, and was attributable to the lack of primary damping and the small ratio (1.28) of sprung to unsprung masses. The lower natural frequency of the lateral primary suspension resulted in lower RMS lateral accelerations of 0.012 g from guideway roughness inputs and 0.017 g from wind inputs. The Pepler index

0.012 g from guideway roughness inputs and 0.017 g from wind inputs. The Pepler index was an acceptable 2.6, again in the somewhat comfortable to comfortable range. As discussed in Section 4.1.3, the ratio of sprung to unsprung mass was only 1.28 so that passenger payload was poor compared to the other EDS systems and EMS III.

The primary suspension parameters of EDS 3 (sidewall coil null flux) differed from EDS 2 (hybrid null flux, continuous guideway), in that the sprung to unsprung mass ratio was higher, 3.6 compared to 1.3, and the natural frequencies were lower. Because of the channel guideway and magnet configuration, the lateral secondary suspension acted through the center of gravity of the unpsrung mass, so that lateral guideway roughness inputs did not directly cause roll. These parameters resulted in higher accelerations and lower roll rates than for EDS 2. The ride quality approached that of EMS III and EDS 1, with a Pepler index of 2.0, on the borderline between very comfortable and somewhat comfortable. The RMS lateral acceleration response to design maximum wind inputs was 0.035 g (a factor of five higher than for the EMS systems). While active primary suspensions are a necessary complexity for the EMS systems, to overcome the unstable magnetic attractive forces, it results in better ride performance. The soft undamped lateral primary suspension of EDS 3 resulted in relatively large lateral magnet-guideway RMS displacements of 10% and 17% of the nominal air gap for road and wind inputs, respectively; thus guideway roughness can be increased only by a factor of two if active secondary suspensions reduce passenger accelerations. The thin filaments, or laminations, of the guideway coils allow current to penetrate the conductors more completely, reducing the effective resistance, with the result that the effective guideway-vehicle clearance is increased; thus, the effective stiffnesses increases as the drag decreases.

In summary, all of the systems required smooth guideways (equivalent to welded steel rails) to achieve acceptable ride quality (passive secondary suspensions assumed except for EDS 1 (image flux)). At the beginning of this study, it had been expected that the EDS systems, because of their larger guideway-vehicle clearances, would permit rougher guideways while maintaining adequate ride comfort. The potential for guideway roughness increase for EDS 1 and EDS 3 is limited to a factor of two by passenger ride comfort considerations. To achieve adequate ride quality, EDS 1 (image flux, or Magneplane) curved guideway systems required aerodynamic roll damping. The large bogey masses of the EDS null flux systems also degraded ride quality. Because of the requirement to limit guideway-magnet contact, guideways rougher than welded steel rails will be difficult to accommodate unless the magnet control bandwith is increased substantially.

4.4 Other Considerations

Other important results include the following:

- No data was available to estimate the effect of AC fields produced by guideway eddy currents in inducing quenching or gradual decay of magnet fields of the superconducting magnets of EDS systems. Null flux systems with coils are particularly vulnerable to such effects, compared to EDS systems with sheet guideways. M.I.T.'s experience with superconducting generators indicate that this effect is very important. The feasibility of electrodynamic systems cannot be assured until these possible effects of AC guideway fields are resolved.

- EMS III (combined lift and LSM propulsion) is the most attractive electromagnetic system. Because of the large power required on-board the vehicle, which must be transferred from the wayside, systems using linear induction motors are considered to be secondary candidates. Variants of EMS I and EMS II built with a LSM with guideway propulsion windings are also secondary candidates. Such a variant of EMS I would be a poor candidate because of low passenger capacity resulting from the high on-board magnet weight of three separate magnetic cores. A LSM powered EMS II would incur the expense of two sets of laminated guideway cores. Weight, ride quality, and power estimates for LSM powered EMS I and II variations can be obtained from the cases studied and do not offer advantages over EMS III.

- Although guideway cost, like other economic issues, has not been considered here, several comments are offered. For EMS III, the guideway rails for the synchronous motor/lift magnets are constructed of laminated steel while the lateral rails may be constructed of solid steel. These structures have relatively small cross sections, and thus lower expected construction costs, compared to the guideway sheets and coils proposed for EDS systems.

- Active control for primary and secondary for EDS should be considered. While ride quality was near the Pepler index comfort limit, the displacements of the secondary suspensions were small. Active secondary suspensions would permit larger suspension strokes and reduced accelerations so that road roughness ($\propto\sqrt{A}$ in Appendix D) could increase by a factor of five compared to the 1 Hz natural frequency passive secondary suspensions assumed in this study. Active primary damping from aerodynamic control surfaces could improve ride quality as seen in the EDS 1 case. In EMS systems, active secondary suspensions can provide improved

In EMS systems, active secondary suspensions can provide improved ride quality but will not permit rougher guideways because the small guideway to magnet clearances will be limiting.

Table 4-1. EMS and EDS Vehicle Weight and Passenger Capacity Comparison; Designs optimized for operation at 89 m/s

Category / Description	Units	EMS I Separate heave & sway, LIM	EMS II Combined heave & sway, LIM	EMS III Separatate sway, combined heave & LSM	EDS I Image flux, LSM (Magneplane)	EDS II Hybrid null flux, LSM	EDS III Sidewall coil null flux, LSM
BASIC VEHICLE							
Vehicle body structure	Mg	9.8	9.8	8.9	9.4	5.5	8.9
Interior furnishings (seats, lavs, etc.)	Mg	4.6	4.6	4.2	4.4	2.2	4.2
HVAC,INSTRUMENTS, LANDING GEAR							
Basic equipment	Mg	0.5	0.5	0.5	0.5	0.3	0.5
Power conditioning & batteries	Mg	0.5	0.5	0.5	0.5	0.5	0.5
Instruments	Mg	0.2	0.2	0.2	0.2	0.2	0.2
Landing gear	Mg	N/A	N/A	N/A	1.2	1.2	1.2
Roll damper & actuator	Mg	N/A	N/A	N/A	0.1	N/A	N/A
LEVITATION & PROPULSION							
Levitation & guidance magnets	Mg	3.1	4.7	1.6 (guidance)	6.4	14.0	7.2
Motor stator	Mg	2.5	2.5	5.7 (& lev.)	inc. in Lev.	inc. in Lev.	inc. in Lev.
Bogie structure & secondary susp.	Mg	2.8	3.6	3.6	3.2	7.0	3.6
Power conditioning & batteries	Mg	1.6	1.1	1.1	N/A	N/A	N/A
CRYOGENIC REFRIGERATION							
Power conditioning & batteries	Mg	N/A	N/A	N/A	TBD	TBD	TBD
PAYLOAD							
Passenger weight	Mg	9.9	9.9	9.2	9.6	6.0	9.2
Carry-on baggage	Mg	1.1	1.1	1.0	1.1	0.7	1.0
Checked baggage	Mg	3.6	3.6	3.4	3.5	2.2	3.4
Total payload	Mg	14.6	14.6	13.6	14.2	8.9	13.6
SUMMARY							
Total Gross Weight, loaded	Mg	40.0	40.0	40.0	40.0	40.0	40.0
Passenger capacity		121	121	113	118	74	113

Table 4-2. EMS and EDS Vehicle Weight and Passenger Capacity Comparison; Designs optimized for operation at 134 m/s

Category / Description	Units	EMS I Separate heave & sway, LIM	EMS II Combined heave & sway, LIM	EMS III Separatate sway, combined heave & LSM	EDS I Image flux, LSM (Magneplane)	EDS II Hybrid null flux, LSM	EDS III Sidewall coil null flux, LSM
BASIC VEHICLE							
Vehicle body structure	Mg	8.8	8.8	8.9	9.4	5.5	8.9
Interior furnishings (seats, lavs, etc.)	Mg	4.1	4.1	4.2	4.4	2.2	4.2
HVAC,INSTRUMENTS, LANDING GEAR							
Basic equipment	Mg	0.5	0.5	0.5	0.5	0.3	0.5
Power conditioning & batteries	Mg	0.5	0.5	0.5	0.5	0.5	0.5
Instruments	Mg	0.2	0.2	0.2	0.2	0.2	0.2
Landing gear	Mg	N/A	N/A	N/A	1.2	1.2	1.2
Roll damper & actuator	Mg	N/A	N/A	N/A	0.1	N/A	N/A
LEVITATION & PROPULSION							
Levitation & guidance magnets	Mg	3.5	4.8	1.9 (guidance)	6.4	14.0	7.2
Motor stator	Mg	3.7	3.7	5.3 (& Lev.)	inc. in Lev.	inc. in Lev.	inc. in Lev.
Bogie structure & secondary susp.	Mg	3.6	4.3	3.6	3.2	7.0	3.6
Power conditioning & batteries	Mg	1.6	1.1	1.1	N/A	N/A	N/A
CRYOGENIC REFRIGERATION							
Power conditioning & batteries	Mg	N/A	N/A	N/A	TBD	TBD	TBD
PAYLOAD							
Passenger weight	Mg	9.1	9.1	9.2	9.6	6.0	9.2
Carry-on baggage	Mg	1.0	1.0	1.0	1.1	0.7	1.0
Checked baggage	Mg	3.4	3.4	3.4	3.5	2.2	3.4
Total payload	Mg	13.5	13.5	13.6	14.2	8.9	13.6
SUMMARY							
Total Gross Weight, loaded	Mg	40.0	40.0	40.0	40.0	40.0	40.0
Passenger capacity		112	112	113	118	74	113

Table 4-3. EMS and EDS Vehicle Power Comparison; Designs optimized for operation at 89 m/s

		EMS I Separate heave & sway, LIM	EMS II Combined heave & sway, LIM	EMS III Separatate sway, combined heave & LSM	EDS I Image flux, LSM (Magneplane)	EDS II Hybrid null flux, LSM	EDS III Sidewall coil null flux, LSM
LEVITATION							
Heave							
Real power @ 1 g	kW	119.0	74.4	51.3	1,100.0	330.0	450.0
Reactive power @ 1g	kVA	5.4	8.5	11.5	N/A	N/A	N/A
Sway							
Real power @ .26 g	kW	17.6	inc. in heave	17.6	240.0	440.0	31.0
Reactive power@ .26 g	kVA	3.1	"	5.6	N/A	N/A	N/A
PROPULSION							
Vehicle							
Dissipated power	kW	60.0	60.0	inc. in Lev.	0.0	0.0	0.0
Reactive power	kVA	1,570.0	1,570.0	inc. in Lev.	0.0	0.0	0.0
Guideway							
Dissipated power	W/m	36.6 (kW)	14.0 (kW)	1,489	62.0	190.0	160.0
Reactive power	VA/m	0	0	16,600	1,200	3,900	980
REFRIGERATION							
Hotel	kW	69.0	69.0	67.7	68.5	61.2	67.7
Cryogenic	kW	N/A	N/A	N/A	TBD	TBD	TBD
VEHICLE & GUIDEWAY TOTAL (1 km guideway assumed)							
Dissipated power	kW	233.2	148.4	1,557	1,402	960	641
Reactive power	kVA	1,578.5	1,578.5	16,617	1,200	3,900	980
AERODYNAMIC DRAG							
Power	kW	1,523	1,523	1,523	1,523	1,523	1,523

Table 4-4. EMS and EDS Vehicle Power Comparison; Designs optimized for operation at 134 m/s

		EMS I Separate heave & sway, LIM	EMS II Combined heave & sway, LIM	EMS III Separatate sway, combined heave & LSM	EDS I Image flux, LSM (Magneplane)	EDS II Hybrid null flux, LSM	EDS III Sidewall coil null flux, LSM
LEVITATION							
Heave							
Real power @ 1 g	kW	119.0	75.1	47.9	1,400.0	510.0	430.0
Reactive power @ 1g	kVA	12.3	17.7	22.1	N/A	N/A	N/A
Sway							
Real power @ .26 g	kW	18.8	inc. in heave	18.8	430.0	970.0	61.0
Reactive power@ .26 g	kVA	6.6	"	10.8	N/A	N/A	N/A
PROPULSION							
Vehicle							
Dissipated power	kW	82.8	82.8	inc. in Lev.	0.0	0.0	0.0
Reactive power	kVA	3,220.0	3,220.0	inc. in Lev.	0.0	0.0	0.0
Guideway							
Dissipated power	W/m	99.4 (kW)	31.6 (kW)	1,470	170.0	700.0	560.0
Reactive power	VA/m	0	0	25,000	5,000	22,000	5,300
REFRIGERATION							
Hotel	kW	67.5	67.5	67.7	68.5	61.2	67.7
Cryogenic	kW	N/A	N/A	N/A	TBD	TBD	TBD
VEHICLE & GUIDEWAY TOTAL (1 km guideway assumed)							
Dissipated power	kW	320.0	189.5	1,537	2,000	2,180	1,051
Reactive power	kVA	3,238.9	3,237.7	25,033	5,000	22,000	5,300
AERODYNAMIC DRAG							
Power	kW	5,400	5,400	5,400	5,400	5,400	5,400

Table 4-5. EMS and EDS Vehicle Ride Quality Comparison; Designs optimized for operation at 89 m/s

		EMS I Separate heave & sway, LIM		EMS II Combined heave & sway, LIM		EMS III Separatate sway, combined heave & LSM		EDS I Image flux, LSM (Magneplane)		EDS II Hybrid null flux, LSM		EDS III Sidewall coil null flux, LSM	
Sprung/Unsprung mass ratio		2.7		3.94		3.12		N/A		1.28		3.6	
Gap		0.01		0.01		0.01		0.150		0.08		0.08	
HEAVE MOTION													
Primary natural frequency	Hz	5.0		5.0		5.0		1.0		4.1		2.7	
Primary damping ratio	-	0.7		0.7		0.7		0.0		0.0		0.0	
Secondary natural frequency	Hz	1.0		1.0		1.0		N/A		1.0		1.0	
Secondary damping ratio	-	0.25		0.25		0.25		N/A		0.25		0.25	
Passenger RMS acceleration	g	0.019		0.019		0.019		0.010		0.034		0.022	
Primary RMS gap change	%	15.2		16.7		18.8		2.7		3.5		3.9	
Secondary suspension stroke	m	0.004		0.004		0.004		N/A		0.005		0.005	
Control current variation	%	15.9		17.6		19.6		N/A		N/A		N/A	
Control reactive power	kVA	5.4		8.5		11.5		N/A		N/A		N/A	
SWAY/ROLL MOTION													
Primary natural frequency	Hz	5.0		1.7		5.0		1.0		2.9		1.7	
Primary damping ratio	-	0.25		0.25		0.25		0.10		0.00		0.00	
Secondary natural frequency	Hz	1.0		1.0		1.0		N/A		1.0		1.0	
Secondary damping ratio	-	0.25		0.25		0.25		N/A		0.25		0.25	
		Road	Wind	Road	Wind	Road	Wind	Road	Wind	Road	Wind	Road	Wind
Passenger RMS acceleration	g	0.012	0.007	0.008	0.006	0.012	0.007	0.018	0.032	0.009	0.017	0.016	0.035
Passenger RMS roll rate	°/s	0.7	0.4	0.4	0.3	0.7	0.4	0.8	1.7	1.0	2.1	0.4	0.8
Primary RMS gap change	%	15.0	7.6	35.6	26.3	17.7	8.4	3.0	5.8	5.5	3.6	7.7	16.7
Secondary suspension stroke	m	0.005	0.004	0.004	0.003	0.005	0.004	N/A	N/A	0.010	0.028	0.005	0.010
Control current variation	%	16.4	8.0	36.2	26.6	19.1	8.9	N/A	N/A	N/A	N/A	N/A	N/A
Control reactive power	kVA	3.1	0.3	11.4	2.2	5.6	0.4	N/A	N/A	N/A	N/A	N/A	N/A
Peplar Index from road inputs		1.8		1.7		1.9		1.9		2.2		1.8	

Table 4-6. EMS and EDS Vehicle Ride Quality Comparison; Designs optimized for operation at 134 m/s

		EMS I		EMS II		EMS III		EDS I		EDS II		EDS III	
		Separate heave & sway, LIM		Combined heave & sway, LIM		Separatate sway, combined heave & LSM		Image flux, LSM (Magneplane)		Hybrid null flux, LSM		Sidewall coil null flux, LSM	
Sprung/Unsprung mass ratio		2.7		3.94		3.12		N/A		1.28		3.6	
Gap	m	0.01		0.01		0.01		0.150		0.08		0.08	
HEAVE MOTION													
Primary natural frequency	Hz	5.0		5.0		5.0		1.0		4.1		2.7	
Primary damping ratio	-	0.7		0.7		0.7		0.7		0.0		0.0	
Secondary natural frequency	Hz	1.0		1.0		1.0		N/A		1.0		1.0	
Secondary damping ratio	-	0.25		0.25		0.25		N/A		0.25		0.25	
Passenger RMS acceleration	g	0.024		0.024		0.023		0.012		0.044		0.027	
Primary RMS gap change	%	20.3		21.7		23.7		3.3		4.7		4.9	
Secondary suspension stroke	m	0.005		0.005		0.005		N/A		0.083		0.006	
Control current variation	%	21.4		23.0		24.8		N/A		N/A		N/A	
Control reactive power	kVA	12.3		17.7		22.1		N/A		N/A		N/A	
SWAY/ROLL MOTION													
Primary natural frequency	Hz	5.0		1.7		5.0		1.0		2.9		1.7	
Primary damping ratio	-	0.25		0.25		0.25		0.70		0.00		0.00	
Secondary natural frequency	Hz	1.0		1.0		1.0		N/A		1.0		1.0	
Secondary damping ratio	-	0.25		0.25		0.25		N/A		0.25		0.25	
		Road	Wind	Road	Wind	Road	Wind	Road	Wind	Road	Wind	Road	Wind
Passenger RMS acceleration	g	0.015	0.007	0.009	0.006	0.015	0.007	0.022	0.036	0.012	0.017	0.020	0.035
Passenger RMS roll rate	°/s	0.8	0.4	0.5	0.3	0.8	0.4	1.0	1.9	1.3	2.1	0.5	0.8
Primary RMS gap change	%	20.2	7.7	44.2	25.6	22.7	8.5	3.7	6.4	7.1	4.0	9.6	17.0
Secondary suspension stroke	m	0.006	0.004	0.005	0.003	0.007	0.004	N/A	N/A	0.012	0.026	0.006	0.010
Control current variation	%	22.4	8.1	45.0	25.9	24.6	9.0	N/A	N/A	N/A	N/A	N/A	N/A
Control reactive power	kVA	6.6	0.4	21.0	2.4	10.8	0.5	N/A	N/A	N/A	N/A	N/A	N/A
Peplar Index from road inputs		2.1		1.8		2.1		2.1		2.6		2.0	

SECTION 5

SUMMARY

5.1 Unanticipated Results

Several results were obtained in this study which were unanticipated at the beginning. These results indicate that the hoped-for advantages of EDS will be difficult to realize.

- Perhaps the most surprising was that all of the systems studied require smooth guideways to achieve acceptable ride quality. At the outset, it had been expected that the EDS systems, because of the larger guideway-vehicle clearances, would exhibit better ride quality. As mentioned in Section 4.3, this advantage is negated by the combined effects of stiffer primary suspensions, relative to the secondary suspensions, and the absence of primary damping.
- The estimated weight of the superconducting magnets for the EDS systems was surprisingly large, relative to initial expectations.
- It was initially expected that the hybrid null flux levitation system would be quite efficient due to the high magnet strength employed, but this was not the case for the configuration studied.

5.2 Discussion

EMS 3, combined lift and synchronous propulsion, is the most attractive electromagnetic system and is the EMS system employed for comparisons with EDS. Because of the large power required on board the vehicle, linear induction models (EMS 1 and 2) are secondary candidates. EMS 1 and 2 built with a synchronous motor with guideway propulsion windings could be secondary candidates. The synchronous EMS 1 is poor because of high on board magnet weight (low passenger load) from three separate magnetic cores. A synchronous EMS 2 would require two sets of laminated guideway cores. Weight, ride quality, and power estimates of synchronous EMS 1 and 2 can be obtained from the cases studied and do not offer any advantages over EMS 3.

For comparable guideway roughness, the ride quality of those EDS systems with 1 Hz secondary suspensions is similar or higher to that of EMS systems, notwithstanding the larger vehicle-guideway clearances typical of EDS. This is a result of the lack of damping in all the EDS systems and the high stiffness, relative to the secondary suspensions, of the EDS 2 and EDS 3 primary suspensions. While the EMS systems need high primary stiffness to avoid magnet-to-guideway contact, the active control which they employ makes it possible to optimize the primary damping, thus offering improved ride quality. Thus, a perceived advantage of EDS systems i.e., that guideway roughness requirements can be relaxed with resulting lower construction and maintenance costs, may be limited by the requirement to maintain adequate ride comfort for passengers. To achieve ride quality, the Magneplane curved guideway systems need aerodynamic damping, a development area. The large bogey masses of the EDS null flux systems also degraded ride quality. Because the relative displacements between the vehicle and the bogey are small, active secondary suspensions, which would enable rougher roadways, should be considered for EDS.

A major advantage of the image flux (EDS 1, Magneplane type) systems is that the vehicle and guideway geometry appear to be very feasible, both in terms of construction and operation. However, these systems also have some potential disadvantages. The relatively close proximity of the passenger compartment to the levitation/propulsion magnets tends to increase the level of magnetic field intensity to which the passengers are exposed. Thus, if it is shown that magnetic fields affect humans, it will be important to carefully address the control of magnetic fields by providing adequate magnetic shielding, which may exact a weight penalty in comparison with other EDS systems, by vehicle design which distances the magnets from passengers, and by magnet designs which provide some measure of magnetic field cancellation. While this type of system offers the advantage of self-banking in negotiating curves, the roll freedom which makes this possible is not inherently damped and the undamped roll motions can be large enough to adversely affect passenger ride comfort. Consequently, an auxiliary means of roll damping must be provided, such as by means of actively controlled aerodynamic actuators, with the accompanying weight and power penalty. A similar consideration applies to the sway (lateral motion) degree of freedom.

An expected advantage of the hybrid null flux systems was that high lift-to-drag ratios could be realized. This expectation was based upon simplified analyses which did not include end effects. When these are properly included, the lift efficiency is degraded, and the expected advantage is not realized. To achieve an effective system the relatively complex geometry of the magnet/guideway must be carefully addressed, particularly with respect to the modeling of the magnetic interaction in providing levitation and guidance. Additionally, because this configuration utilizes higher magnetic strength to achieve efficient levitation, the issue of passenger shielding must also be carefully addressed. Also, because the primary suspension has high stiffness and is undamped, some provisions may be required to achieve adequate ride comfort.

All of the EDS designs must address the problem of shielding the superconducting magnets from the AC fields generated in the guideway. Guideway roughness and wind gusts impinging on the vehicle result in these AC fields, which can cause losses in the superconducting magnets. These losses decrease the thermal margin in the magnets and, unless adequately designed for, can result in magnet quench and loss of levitation. It is also possible that these AC fields can result in gradual decay of the magnet current, which would require periodic recharging of the magnets. These problems may be particularly significant for coil guideway designs, which produce perturbations even in the absence of guideway and wind inputs, because of their discrete structure. M.I.T.'s experience with superconducting generators indicate that this effect is very important.

The sidewall discrete coil null flux system exhibits better levitation efficiency than the other EDS systems, for example, the primary suspension stiffness is approximately 7 times higher than the image flux system and the drag is approximately 3 times lower. However, the discrete nature of the guideway has an unfavorable impact on ride quality, due to the periodic variations of primary suspension stiffness, and AC fields effects, as discussed above. These effects must still be addressed.

The weight of the superconducting magnets with shields, supports, and insulation for the EDS image and null flux systems was similar to that of EMS 3 at 25% total vehicle weight. For a 40 Mg vehicle, 120 passengers can be accommodated. For the hybrid null flux, the magnets weighed more because of the complexity of wrapping the magnets around a continuous sheet.

Total power at 134 m/s for propulsion and magnetic drag was 1.5 kW/m for EMS 3 (linear synchronous motor) and 2 kW/m for EDS 1 (image flux), 2.2 kW/m for EDS 2 (Hybrid null Flux) and 1 kW/m for EDS 3 (coil null flux). For a 40 Mg vehicle at 134 m/s wind drag power was estimated at 5.4 MW. In the electromagnetic systems, the largest power was dissipated in the guideway linear synchronous motor and, in the electrodynamic, the power was consumed in the eddy currents required for lift or propulsion winding losses. The reactive guideway power was larger in EMS (25 kVA/m) than in the EDS systems (5 kVA/m for image flux, 22 kVA/m for hybrid null flux and 5.3 kVA/m for coil null flux).

Magnetic saturation limits the EMS 3 propulsion capability, for reasonable size and weight, to ≈ 0.1g, which makes operation at 134 m/s marginal, with negligible hill climbing capability at that speed.

All of the systems studied, except the two EMS systems using Linear Induction Motors (LIM), use Linear Synchronous Motors (LSM), in which propulsion power is supplied to the guideway. LIM's require the transfer of propulsion power to the vehicle from the wayside by means such as third rail or overhead catenary systems. This power transfer, at the very high speeds envisioned, can be troublesome in terms or reliability and maintenance, and require the addition of the power collection apparatus, with its weight penalty. It should be noted, however, that wayside power transfer to the vehicle at station stops was postulated for all of the systems studied, to avoid the substantial weight penalty which would otherwise be incurred by batteries to supply power at stations.

5.3 Observations

Models of sufficient detail were obtained or developed to perform the desired quantitative comparisons. Calculations for the EMS components are relatively straightforward and provide good approximations for levitation magnets and LSM. This is a result of the maturity of this technology and the large literature base which supports it.

The performance estimates obtained for the image flux system approximately matches the results cited in the literature and estimates in this study are judged to be good.

While the null flux concept promises a number of advantages, including high levitation efficiency, practical physical realizations lead to complicated configurations, especially when attempts are made to provide field cancellation to minimize the requirements for shielding passengers from stray magnetic fields. These complicated conductor and guideway configurations are not adequately treated by the closed form solutions appearing in the literature, requiring expensive numerical integration or finite element techniques for adequate analysis.

APPENDIX A
MODELS FOR ELECTROMAGNETIC SUSPENSION SYSTEMS

A.1 Model for a Single Function Electromagnet

The model and nomenclature for the single function electromagnet follows closely the development in Weinberg [1]. The geometry and nomenclature for the dimensional details of the model are shown in Figure 2-5. The vehicle magnet basically consists of a channel shaped iron body having coils of magnet wire mounted on each of the legs of the channel. The coils are connected in series, aiding, so that the magnetomotive force of the two coils is additive. The guideway mounted component is a continuous channel-shaped iron rail, the legs (also called poles) of which are the same distance apart as those of the vehicle magnet, but are shorter, usually from 2 to 3 times the gap dimension. The poles of the rail are wider than those of the magnet.

The computational model for this magnet is implemented in Microsoft Excel and may be found in Table E-1 of Appendix E, which is similar to the results spreadsheets of Appendix F, except that, instead of showing numerical values, it presents the formulas used to calculate those values. Each of the variables is described by name in column B, the units of the variable are shown in column C and the variable name appears in column D; these variable names correspond to the nomenclature of Figure 2-5.

The process of solution in the spreadsheet is as follows:

First, the values of the input variables are entered (the description of these variables is preceded by an asterisk (*) in column B).

The first step in the computation is to determine the coil ampere-turns which correspond to saturation in the stator iron. This computation is made with the air gap set at the maximum permissible value of twice the normal gap because this is the worst case for magnet back iron saturation.

Next, the dimensions of the vehicle magnet back iron and rail are determined to place the flux density in those parts at the saturation value(diminished by the saturation safety factor if entered) with the air gap at the normal operating value

The coil parameters are calculated, including the resistance, and the coil power and temperature.

Finally, the magnet length is calculated such that the developed levitation of guidance force is that required.

This procedure yields a single design point for the input parameters, but this will generally not be an optimum value. The design is next optimized using the Solver add-in of Excel. The pole width, window width and window height are varied, subject to the specified constraints, such that the weight of the magnet is minimized. The constraints applied are that the coil temperature not exceed the maximum allowed value for the wire insulation and that the window width-to-height ratio not exceed 2 (the approximate maximum value for which the pole-to-pole leakage permeance function is valid) and that the magnet length lie between 5m and 15m (1/2 the vehicle length). The minimum value of L is chosen so that the rail eddy current losses are not too high. The constraint that the flux density in the iron not exceed the saturation value is implicit in the relationships determining the relevant dimensions of the magnet and rail. The optimization procedure is followed for both the levitation and guidance magnets, for the baseline case and also for Design 2 and Design 3, in which the pole width is 3/4 the baseline value and the air gap 80% of the baseline value, respectively. These latter two cases are provided to give some indication of the sensitivity of magnet weight to non-optimum values of the pole width and air gap.

A.2 Model for Combined Lift and Lateral Magnets (Staggered Magnets)

In contrast to the EMS I system which implements lift and guidance functions with separate, independent, magnets and magnet control systems, this configuration implements both lift and guidance with a single set of magnets and an integrated control systems for the vertical and lateral directions of motion. In addition to reducing the complexity of the control system, certain other advantages can be obtained with this system. These include lower total weight of magnets for a given force and air gap requirement and longer allowable stroke for the lateral motion of the system.

The model and parameter nomenclature for this configuration is shown in Figure 2-7. The model follows closely the development given in Wormley, et al [2], with a number of corrections of typographical errors appearing in that report. Proper operation of this system requires the lateral controller gain to be set to a particular value to decouple lateral forces from vertical forces. When the gain is set at this value, the vertical force is independent of the lateral force and the lateral force is a linear function of the lateral displacement, independent of the vertical displacement, up to a maximum value of lateral displacement called y^*, the decoupling displacement limit. Although, in general, the lateral force continues to increase somewhat after the lateral displacement exceeds y^*, in normal operation the displacement would probably be limited to this value to avoid problems with controller instability due to the nonlinearity, etc.; the increasing force beyond y^* provides a safety margin in normal operation.

The computational model for this magnet is also implemented in Microsoft Excel and may be found in Table E-2 of Appendix E, which is similar to the results spreadsheets of Tables F-3 and F-4 of Appendix F, except that instead of showing numerical values, it presents the formulas used to calculate those values. As for the EMS I model, each of the variables is described in column B, the units of the variable are shown in column C and the variable name appears in column D.

The solution procedure for this model is similar to that for EMS II with the following exception: after setting the dimensions of the model, the value of y^*, the decoupling displacement limit, is determined as the value which equates alpha(g, delta) with alpha(g, delta+y^*) using the Excel goal seeker. Then the optimization process proceeds as in EMS I using the Solver add-in.

A.3 Model for Lift Magnets Combined with Synchronous Motor

The model and nomenclature for lift magnets combined with the "rotor" of the Linear Synchronous Motor (LSM) is shown in Figure 2-8. The computational model for this magnet is also implemented in Microsoft Excel and may be found in Table E-3 of Appendix E, which is similar to the results spreadsheets of Tables F-5 and F-6 of Appendix F, except that instead of showing numerical values, it presents the formulas used to calculate those values. Each of the variables is described in column B, the units of the variable are shown in column C and the variable name appears in column D.

The solution procedure for this model closely follows that of EMS I.

APPENDIX B

MODEL FOR LINEAR INDUCTION MOTOR

The literature on Linear Induction Motors (LIM) is fairly extensive at the present time [References 13-37]. However, those with a level of detail useful for design and analysis are not numerous. Since the typical configuration of LIM for high speed transportation vehicles includes an iron secondary covered by a conducting layer between the wound primary structure and the secondary iron, accurate calculations of performance necessarily involve solution of the electromagnetic field equations in the secondary region; the same configuration is used in this study. Among the more useful of these papers are the work of Skobelev, et al [36], Epifanov, et al [33], Gieras, et al[27] and Tevan, et al [23]. With the exception of the last, these describe rather elaborate computations and do not furnish much detail about programs for implementing the calculations, even though they do offer the promise of accurate results. In any event, the programs which had been developed to perform the calculations described in those works were not available to us. Tevan, et al on the other hand describe a relatively simple algorithm for the calculations which could be implemented within the scope of this study.

It was initially planned to implement the LIM calculations in the same spreadsheet format as used for the other EMS and EDS calculations, but this proved to be impractical because many of the parameters are complex numbers and the calculations proved to be impractically complicated in the spreadsheet format. It was therefore decided to utilize the MatLab® program for the calculations. MatLab®, which was also used for the ride comfort computations, handles complex numbers in a natural and convenient way, making the programming relatively straightforward and simple.

The program developed to implement the calculations described by Tevan, et al is shown in Table B-1. The numbers in parentheses following some statements are the numbers of the Tevan equations which the statement evaluates. The program calculates motor performance at constant primary current with a one turn per coil winding; it was assumed that the number of turns and wire size could subsequently be adjusted as required to accommodate the requirements of a reasonable drive electronics design.

One of the major characteristics of single-sided LIM is the presence of a substantial normal force, which is usually attractive at the low values of slip at which maximum tractive force and efficiency are realized; at higher values of slip, and for particular configurations, the normal forces can be repulsive, and several authors have proposed to use these repulsive forces to augment, or replace, the lift function of the vehicle's magnetic suspension. In this study,the normal forces, while calculated in the analysis, are not further considered. This implies that either the vehicle configuration utilizes LIM primaries in opposing pairs, as shown in Figures 2-2 and 2-3, so that the normal forces cancel, or that the configuration is such that the normal forces aid the lift forces of the vertical magnetic suspensions. In the latter case, this could have a beneficial effect on the overall design by providing some of the required lift in the erection phase of operation (one of the constraints assumed in the design of the levitation magnets is that the entire 1g lift force be provided at twice the operating air gap; this determines the back iron thickness, a major contributor to the core weight, from saturation considerations). Relaxing this requirement by utilizing the attractive force of the LIM would lead to smaller levitation magnet core weight. This possibility was not included in this study. The basic design of vehicles utilizing LIM in this study uses four LIM, arranged in two pairs; the primary (the vehicle mounted portion, usually termed the "stator" in rotating machinery terminology) cores of a pair are arranged "face-to-face" with the secondaries (guideway portion, corresponding to the rotor of rotating machines) between them. Two such pairs are used on each vehicle so that the bogies can move independently in negotiating curves and cresting hills.

The model was used to establish optimum LIM designs for the system configurations selected for comparison. Optimization has, of course, many possible considerations including weight, physical size, cost of acquisition, cost of operation, maintenance cost, etc. While operating cost (cost of electrical energy) is obviously a strong consideration in the design of an operating system, economic considerations were beyond the scope of this study and the design optimization consisted primarily of minimizing the on-vehicle weight, subject to the constraints which were applied. Weight of the guideway components was also addressed, but was given secondary importance. These same comments also apply to the optimizations of the levitation and guidance electromagnets described in Appendix A. The design requirements for the propulsion motors are listed in Table 1-1

The LIM configuration which was addressed in selecting optimum designs for the various systems studied was a single-sided design with a primary having a laminated core of M-19 silicon iron with half-filled slots at each end, and a two layer, fractional pitch, distributed winding. The configuration is illustrated in Figure 2-6. The secondary consisted of a solid rail of low carbon steel covered with an aluminum cap. Four optimum designs were identified, for maximum operating speeds of 89 meters/second and 134 meters/second and mechanical clearances between primary and secondary of 0.01 meters and 0.008 meters, corresponding to the variations of the levitation and guidance magnets which were studied.

Some of the results of the design optimization process for the LIM designed for operation at 134 m/s are summarized in Figure B-1 which plots approximate motor weight, and insulation and core and surface temperatures as a function of pole pitch with constant stack height and maximum traction force. The plotted weight neglects the weight of the end sections of the primary which contain half-filled slots; this weight is included in the motor weight for the final optimization results. The major impact of pole pitch on the motor design is very apparent as is the importance of insulation temperature constraints.

A major constraint on the design of any electromagnetic device is the necessity for maintaining the maximum wire insulation temperature within the rating of the insulation material. As will be seen, for a given traction force capability the insulation temperature rating has a significant impact on the weight of the motor. In this study, Class H insulation (rated at 220°C continuous operation) was selected to minimize the weight of the vehicle mounted electromagnets. The approximate motor weight is plotted vs maximum insulation temperature as pole pitch is varied in Figure B-2 which clearly shows the favorable effect on motor weight of increasing the insulation temperature rating. A limit of 200 °C was selected for the coil surface temperature in the calculations to allow for the internal temperature rise in the coils; a maximum ambient temperature of 50°C (122°F) was assumed.

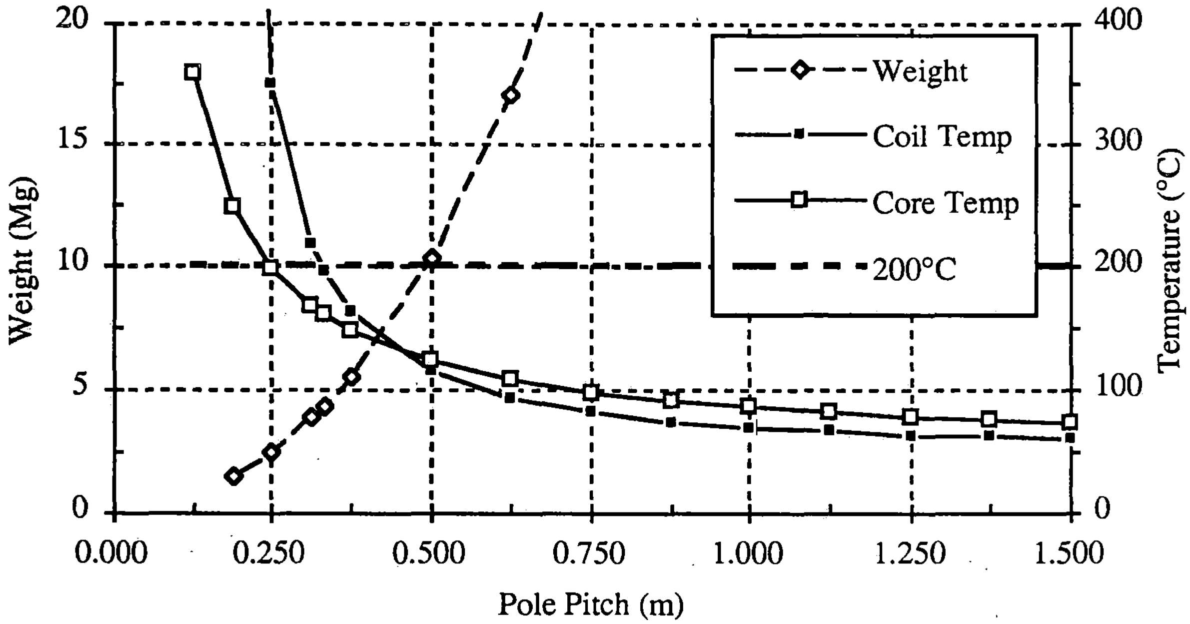

Surface Temperatures and Approximate Motor Weight vs Pole Pitch
Figure B-1

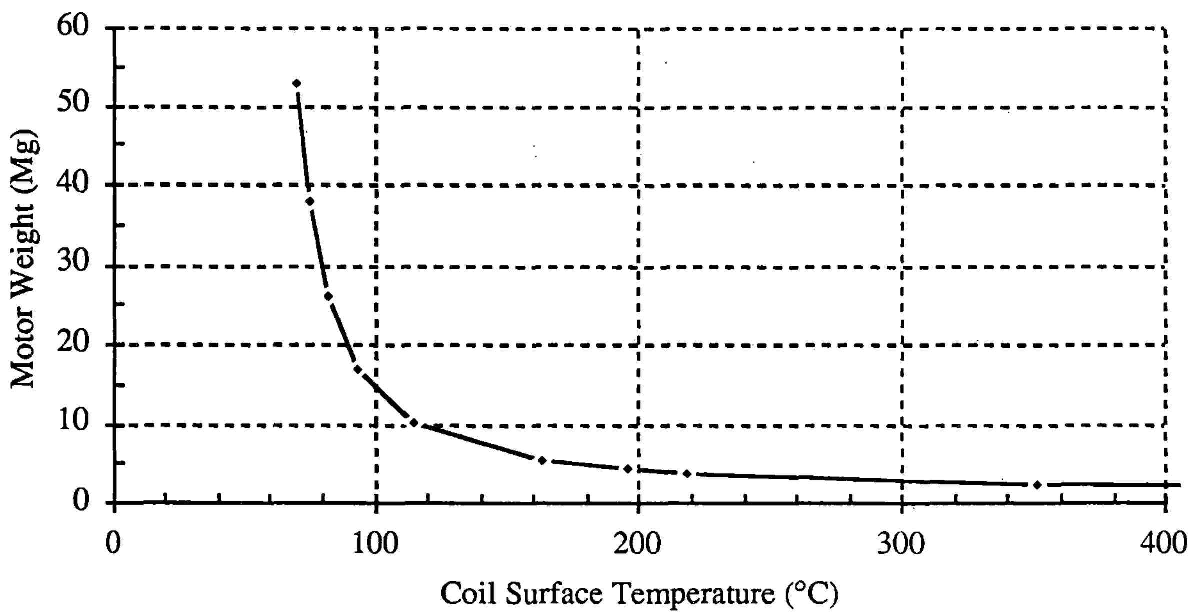

Approximate Motor Weight vs Coil Surface Temperature as Pole Pitch is Varied
Figure B-2

The motor parameters which resulted from the optimization procedure were for the most part quite close to the design recommendations presented by Nonaka and Higuchi[18]; for example, the optimized pole pitches were between 0.28 meters and 0.33 meters compared with their recommendation of "about 300mm regardless of the speed" and the stack heights of 0.18 meters to 0.22 meters is comparable to their recommended values of 0.22 meters to 0.23 meters. Such comparisons confirm the appropriateness of the model for the purposes of this study.

```
%filename:   FINAL_LIM
%Linear Induction Motor with constant current excitation
%after Tevan & Toth, Acta Technica (Hungaricae), Tomus 86(3-4), pp.331-362(1978)
%parameter names, mostly, are same as in the Toth paper; (xx) are T&T equations
%by C.R. Dauwalter, 3/21/92
%rev 5/18/92 6:45 P.M.
%MOST RECENT RUN 6/28/92 12:06 PM
%PARAMETERS FROM "LINEAR INDUCTION MOTOR" EXCEL SPREADSHEET

format compact
%Following are outputs of "LINEAR INDUCTION MOTOR" Excel spreadsheet
a=.281;                 % pole pitch
f0=160;                 % excitation frequency (Hz)
Iw=3.482e3;             % total current/slot @s=0, limited by core saturation
Icirc=7.42e4;           % nominal"circumferential" current linear density (A/m)
kc=1.18;                % Carter factor
g=2.56E-02;             % slot width
coreloss=4.11e3,        % coreloss power(from spreadsheet)
l=0.220;                % guideway iron width
alpha=1.65;             %primary leakage reactance proportionality factor(check this!)
b=0.008;                % mechanical air gap clearance
d=1.0;                  % 2*guideway conductor overreach beyond iron;
p=8;                    % number of pole pairs
v=0.005;                % thickness of guideway conductor
rho1=4.16E-08;          % primary resistivity (AT OPERATING TEMPERATURE!!)
%End of spreadsheet output

ff=3.14159/4;           % primary winding fill factor
gamma=1/(0.37e-7);      % conductivity of guideway conductor
%gamma=1/(0.27e-7);     % conductivity of guideway conductor
hred=0.045;             % reduced conductor height (primary)
l1= 1.05*a*2/3;         % length of one end turn (2/3 fractional pitch)
mu0=4*3.14159e-7;       % permittivity of free space
nomslip=0.01;           % nominal slip
q1=2;                   % number of slots/phase/pole
s=0.025;                % slip
v0=2*a*f0;              %synchronous velocity
                        %vzero=0.5*v0;     % onset velocity for end effect changes of thrust &
Z, etc.
```

```
diary  off

%PRELIMINARY CALCULATIONS (FOR VARIABLES NOT CHANGED INSIDE FOR LOOPS)

dslot=hred;                                 % depth of slot
A1=g*dslot*ff;                              % area of copper in 1 slot
area=2*p*a*l;                               % area of motor core
circumItotal=2*p*q1*3*Iw;                   % not used in calculations
dI=3*Iw*q1/a;                               % (41)
h=3*q1*A1*l/(a*(l+l1));                     % (36)
lambda=[0.44  0.28*(1-3.14159*3.14159/(108*p*p))  0.28*(1-3.14159*3.14159/(108*p*p))];      % (58)
nu=[1  1+1/(2*p)  1-1/(2*p)];
R1=rho1*l/(h*a/(3*q1));                     % (37)

%slip=[0:0.01:1];                           %CAUTION!! slip MUST have one zero value!!
slip=[0:0.001:0.1];
%slip(1)=1e-6;
w0=2*3.14159*f0;                            % excitation angular frequency
Xt1=alpha*w0*R1/(2*3.14159*50);             % (38)
[YY,II]=min(abs(slip-nomslip));             % II is the index of nominal slip
Nslots=q1*p*2*3;                            % total slots in the machine

%PRE-ALLOCATES VECTORS, WITH ZERO VALUES, TO SAVE COMPUTATION TIME LATER
FF=zeros(slip);
nFF=FF;                                     % Added 6/24/92
currentratio=FF;
Eab=FF;
eta=FF;
FFn=FF;
I2=FF;
I1=FF;
km=FF;
ke=FF;
ktemp=FF;
normalF=FF;
Pmech=FF;
ratio=FF;
R2prime=FF;
sigma=[0 0 0];
```

```
speed=FF;
tractionF=FF;
tractionForce_per_slot=FF;
TotalTractionForce=FF;
Vin=FF;
X2prime=FF;
zeta=[0 0 0];
Z2prime=FF;

%END OF PRELIMINARY CALCULATIONS

for iii=1:length(slip)                                  % beginning of main outside loop
s=slip(iii);
speed(iii)=3.6*v0*(1-slip(iii));                        % vehicle speed (km/hr)
for i=1:3
m(i)=(a/nu(i))*(a/nu(i))*gamma*mu0*w0*s/(3.14159*3.14159);                          %(10)
kinf(i)=1/(sqrt(1+j*m(i))*tan(-j*sqrt(1+j*m(i))*3.14159*v*nu(i)/a));                 %(14)
c1(i)=real((3.14159*l*nu(i)*sqrt(1+j*m(1))/(2*a))/tanh(3.14159*l*nu(i)*sqrt(1+j*m(i))/(2*a)));
                                                        %(24)
c2(i)=imag((3.14159*l*nu(i)*sqrt(1+j*m(i))/(2*a))/tanh(3.14159*l*nu(i)*sqrt(1+j*m(i))/(2*a)));
q(i)=3.14159*l*nu(i)/(2*a)*(exp(3.14159*d*nu(i)/a)-1)/(exp(3.14159*d*nu(i)/a)+1);         %(25)
ka(i)=j*a/(3.14159*v*nu(i))/((1+j*m(i))*(c1(i)+q(i)+j*(c2(i)+m(i)*q(i))));     %(26b)
end
k=kinf-ka;
ktemp(iii)=k(1);                                        % value of k(iii); added for diagnostics
bprime=b*sqrt(1+0.554*a*a/(l*l));                       % (32a)
K=[0 0 0];
for i=1:3
K(i)=(k(i)+j*tanh(3.14159*bprime*nu(i)/a))/(1-j*k(i)*tanh(3.14159*bprime*nu(i)/a));        % (32b)
end

% REACTANCE/IMPEDANCE CALCULATIONS

r=[0 0 0];
km=[0 0 0];
FFtemp1=0;
FFtemp2=0;
for i=1:3
```

```
zeta(i)=sin(nu(i)*3.14159/6)*sin(nu(i)*3.14159*g/(2*a))/(nu(i)*3.14159*g/(2*a)*(q1*sin(nu(i)*3.14159/(6*q1))));
                                                  % (40)
sigma(i)=(k(i)*conj(k(i))-1)/(2*real(k(i)));                    % (62a)
FFtemp1=FFtemp1+sigma(i)*lambda(i)*zeta(i)*zeta(i)*real(K(i));
FFtemp2=FFtemp2+lambda(i)*zeta(i)*zeta(i)*real(K(i));
L(i)=3.14159*l*nu(i)/(2*a);
V(i)=3.14159*v*nu(i)/a;

vprime(i)=(a/(3.14159*nu(i)))*atanh(V(i)*(L(i)/tanh(L(i))+q(i)));          %(45)
r(i)=3*q1*zeta(i)^2*w0*mu0*l/3.1459;                            % (51)
km(i)=k(i)/(1+j*k(i)*tanh(3.14159*vprime(i)*nu(i)/a));
chi0(i)=1/(tanh(3.14159*vprime(i)*(nu(i)/a))*cosh(3.14159*bprime*(nu(i)/a)+sinh(3.14159*bprime*(nu(i)/a))));
                                                  %(48)
chi1(i)=tanh(3.14159*bprime*(nu(i)/(2*a))*(1+chi0(i)*tanh(3.14159*vprime(i)*(nu(i)/a))));
                                                  %(49)
chi2(i)=chi0(i)*(cosh(3.14159*bprime*(nu(i)/a)-1));                        % (50)
end

% CALCULATE THE SLOT IMPEDANCES (without end effect)

temp=0;
for i=1:3
temp=temp+lambda(i)*zeta(i)*zeta(i)*K(i)/nu(i);
end

Zwi(iii)=(3*q1/3.14159)*w0*mu0*l*temp;            % (60)
Zw(iii)=R1+j*Xt1+Zwi(iii);                        % (39)
Zin(iii)=Zw(iii)*Nslots;                          % Total input impedance,added 5/18/92

%END OF REACTANCE/IMPEDANCE CALCULATIONS (without end effect)

% FORCE CALCULATIONS FOR CONSTANT INPUT CURRENT (without end effect)

% FF=tractive force per unit area
FF(iii)=mu0*dI*dI*FFtemp2;                        % (61)
nFF(iii)=FF(iii)*FFtemp1/FFtemp2;                 % Added 6/24/92
tractionF(iii)=FF(iii)*2*p*a*l;                   % (62a)
normalF(iii)=tractionF(iii)*FFtemp1/FFtemp2;            % (62b)
```

```
%BEGIN CALCULATIONS FOR CONSTANT INPUT VOLTAGE

Vin(iii)=Iw*Zin(iii);

% CALCULATE SLOT POWERS AND EFFICIENCY

Pin(iii)=Iw*Iw*real(Zin(iii));                % real input Power
Pinx(iii)=Iw*Iw*imag(Zin(iii));               % reactive input Power
Pout(iii)=tractionF(iii)*v0*(1-s);            % output Power
eta(iii)=100*Pout(iii)/Pin(iii);              % efficiency
PF(iii)=Pin(iii)/sqrt(Pin(iii)*Pin(iii)+Pinx(iii)*Pinx(iii));     %Power Factor

end                   % end of main outside loop (with index=iii)

diary on
%CALCULATE PARAMETERS FOR SPREADSHEET INPUT
[ZZ,JJ]=max(tractionF);
legend
a,f0,Iw,Icirc,coreloss,rho1,kc,g,l,alpha,b,d,p,v
velout=f0*2*a
slipout=slip(JJ)
tractionFout=tractionF(JJ)
tractionFperA=FF(JJ)
normalFout=normalF(JJ)
normalFperA=nFF(JJ)
realPout=Pout(JJ)
reactPin=Pinx(JJ)
realPin=Pin(JJ)
primaryIsqR=Iw^2*R1*2*3*q1*p
secondaryPin=realPin-realPout-primaryIsqR
efficiency=100*realPout/(realPin+coreloss)
```

APPENDIX C
DYNAMICS OF SIMPLE SUSPENSION MODELS

C.1 Summary of Pepler Ride Quality Index

Research into ride quality of transportation systems has resulted in the development of quantitative indices for the assessment of passenger comfort and ride acceptability. A particular ride comfort index, which has become widely known as the "Pepler Index", was specified as the standard to be used in this work for comparison of ride quality among the vehicle systems studied. The comfort rating C', or "Pepler Index", is defined as

$$C' = 1.0 + 0.5\omega_R + 0.1[db(A) - 65] + 17a_T + 17a_V$$

where

ω_R = passenger roll rate (angular velocity about longitudinal axis) (°/sec)
a_T = passenger lateral acceleration (m/sec^2)
a_V = passenger vertical acceleration (m/sec^2)
db(A) = sound level (db(A))

Comfort ratings of between 2 and 3, corresponding to subjective assessments of ride comfort of "comfortable" and "somewhat comfortable", respectively, are generally viewed as representing a satisfactory ride (comfort ratings of 2 and 3 correspond to ≈92% and ≈97%, respectively, of passengers satisfied with ride comfort). A comfort rating of 4 corresponds to a neutral assessment of ride comfort.

C.2 Assumed Spectral Densities for Ride and Cross Wind Inputs

<u>Guideway roughness</u>

Guideway surface irregularities are modeled as a stationary random process with a (single sided) spectral density function of the form

$$S_{y0}(F) = KF^{-n} \qquad \text{(units of } m^2/\text{(cycle/m))} .$$

where F = $1/\lambda$ is the spatial frequency and λ is the roughness wavelength.

Typical values for welded steel railroad rails were used in this study:

$$K = 6.1 \times 10^{-8}$$

$$n = 2.0$$

With this definition, the mean square value of x is

$$\overline{x^2} = \int_0^\infty S_x(f)df$$

For a vehicle moving at velocity V, the temporal frequency of the disturbance produced by the irregularity is

$$f = FV$$

with a spectrum of

$$S_{y0}(f) = \frac{KV}{f^2}$$

With angular frequency $\omega = 2\pi f$, the spectrum becomes

$$S_{y0}(\omega) = \frac{2\pi KV}{\omega^2}$$

Setting $A = \pi K$, the spectrum becomes

$$S_{y0}(\omega) = \frac{2AV}{\omega^2} = 2\Phi_{y0}(\omega)$$

where

$$\Phi_{y0}(\omega) = \frac{AV}{\omega^2}$$ is the double-sided spectrum in ω, used in this study

Wind

Wind is modeled as a first order Markov process (low-pass filtered white noise) in which the break frequency is determined by the correlation distance, assumed to be 200 meters in this study. Cross wind velocity is assumed to be 4.5 meters/second (10 miles/hour).

C.3 Vehicle Suspension Dynamic Models

Since assessment of the ride quality of each of the vehicle systems being considered was necessary, dynamic models of the systems were developed. The original intention was to develop a single model for determining the heave, lateral and roll motions of the vehicles, but to keep the model sufficiently simple for ready analysis, it was subsequently decided to use two separate models, one for only heave motions, and the second for combined lateral motions and roll.

C.3.1 Heave Model

The simple single degree of freedom model developed for heave is shown in Figure C-1(a). This model is used, with appropriate adjustment of parameters, for evaluating the performance of both EMS and EDS systems. The vehicle primary suspension is represented by the spring k_{y1} and the secondary suspension by the parallel combination of a spring, k_{y2}, and damper, b_{y2}. Although the primary suspension is indicated on the figure as a simple spring, in the model k_{y1} can be implemented as an active controller with selectable dynamics (to model EMS systems which utilize such control for the primary) and provision is also made to include passive damping if desired (although in the EDS systems, without active primary control, the damping is usually considered to be negligible, which is assumed in this study). The guideway is assumed to be perfectly rigid. y_0 represents the guideway roughness amplitude, which has a spectrum represented by AV/ω^2.

This single degree of freedom, four state model was implemented in MatLab®, a linear systems dynamics computer code. The secondary suspension can be represented either by passive damping proportional to relative motion between the vehicle passenger compartment, represented by m_2, and the suspension bogie, represented by m_1, or (not indicated on the figure) by active damping proportional to the passenger compartment velocity relative to inertial space. The model incorporates a finite magnet length filter to

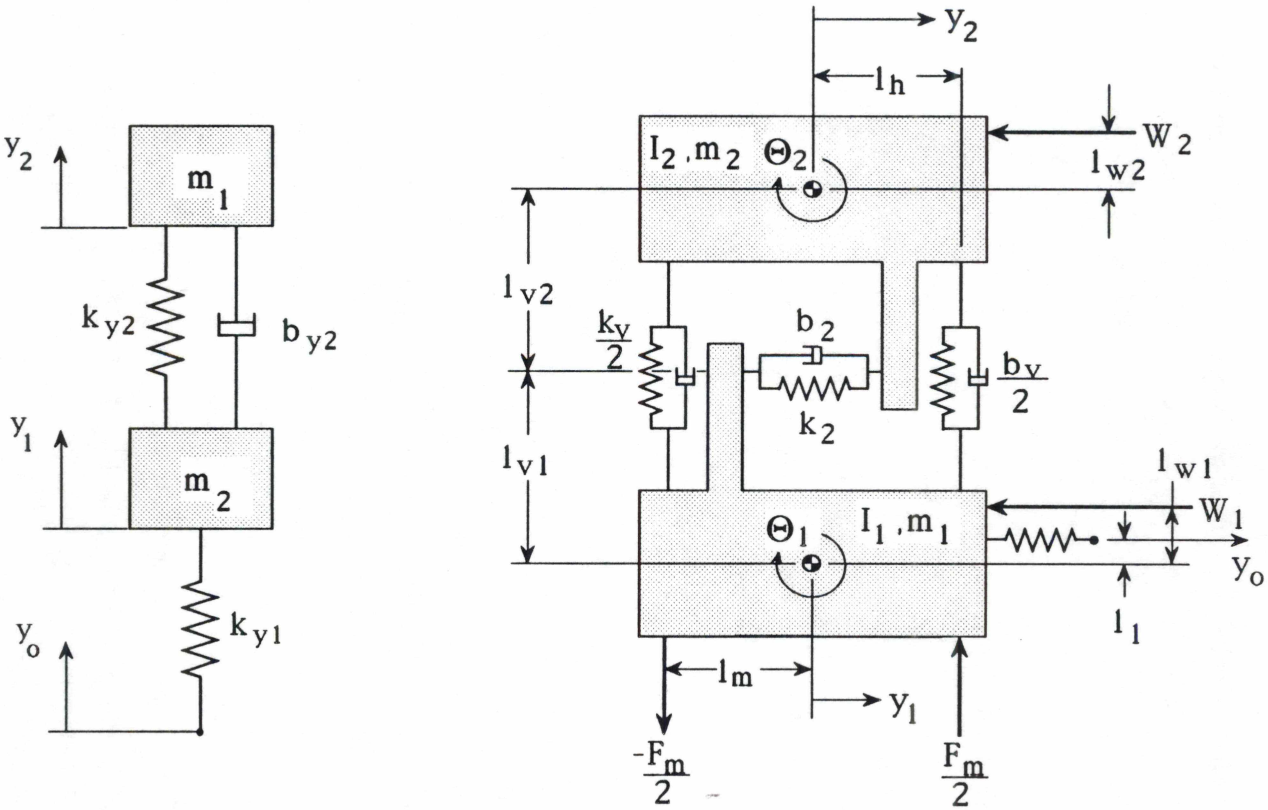

(a) Heave Model

(b) Lateral/Roll Model

Figure C-1. Vehicle Suspension Dynamic Models simulate the effect of averaging the short wavelength guideway roughness components over the length of the primary suspension magnets.

The input to the model is a guideway roughness spectrum as described in section C.2, the vehicle velocity, the relevant vehicle dimensional and mass property information and pertinent parameters of the suspension and controllers.

The model provides numerous outputs, numerically in the form of total RMS values and, if desired, as plots vs frequency of the spectra of magnitude and phase (plots only) of significant responses:

- Accelerations of passenger compartment (m_1) and suspension bogie (m_2).
- RMS Clearance variations between guideway and suspension bogie, and between suspension bogie and passenger compartment. The former is provided to permit assessment of probability of vehicle-guideway contact, and the latter to assess the probability of secondary suspension "bottoming" (the model is a strictly linear one, and cannot be used to quantitatively evaluate the effect on ride quality of "bottoming"; thus the suspension parameters must be selected to prevent it from occurring).
- RMS Current and voltage of the primary suspension magnet controller and the secondary suspension active control forcer. These permit assessment of the power (active and reactive) of the controllers, used in the estimation of their weight.

Additionally, RMS values are calculated for a number of the model responses; these include:

- Primary suspension to guideway clearance.
- Passenger compartment and bogie accelerations.
- Primary suspension controller current, voltage and reactive power.

The MatLab code for the model used for all of the EMS systems and for EDS 2 and EDS 3 appears in Table C-1. The code for the model used for EDS 1 appears in Table C-2

C.3.2. Lateral Motion/Roll Model

The Pepler Index includes lateral acceleration and roll rate. In all of the systems studied (with the exception of the image flux system) the centers of gravity of the bogie and passenger compartment (unsprung and sprung masses) are separated. Thus, a lateral guideway input moves the bogie laterally which causes the passenger compartment to both translate and rotate, coupling lateral acceleration and roll rates. A two mass, two rotational inertia, eight state model was developed, since none was available in the maglev literature.

The model is shown in Figure C-1(b). In this model, the roll degree of freedom is coupled to the lateral inputs of both the guideway and the wind. However, the roll is not coupled to the vertical disturbances from the guideway, in particular, differential guideway roughness between right and left sides does not excite the roll motions of bogie and passenger compartment.

The vehicle primary lateral suspension is represented by the spring k_1. The displacement y_0 of the guideway end of k_1 provides for guideway roughness inputs, which are represented as in the heave model. k_1 is located a distance l_{w1} above the center of mass of the bogie, providing roll moment inputs. As in the heave model, the primary suspension is indicated on the figure as a simple spring, but can be implemented in the model as an active controller with selectable dynamics, including damping if appropriate. Finite magnet length filtering of guideway roughness is also provided.

The primary vertical suspension is represented by reaction forces $\pm F_m/2$, located a distance l_m from the bogie center of mass. The reaction forces are produced by springs $k_m/2$ at those locations; as mentioned above, these are not excited by guideway roughness and hence produce roll moments on the bogie only in response to the bogie roll displacements.

The secondary lateral suspension is represented by the spring k_2 and parallel damper b_2, located distances l_{v1} above the bogie center of mass and l_{v2} below the passenger compartment center of mass. When $l_{v2} \neq 0$, they also provice roll restraint for the passenger compartment.

The secondary vertical suspension is represented by two pairs of parallel springs $k_v/2$ and dampers $b_v/2$; each pair of parallel spring and damper is located a horizontal distance l_h from the passenger compartment center of gravity and provides roll restraint.

Wind force inputs W_1 to the bogie and W_2 to the passenger compartment are provided, with relative magnitudes proportional to their respective lateral areas exposed to the wind and with points of application located distances l_{w1} and l_{w2} above the bogie and passenger compartment centers of mass, respectively.

The inputs to the model are parameter values for the guideway roughness and wind force spectra, the vehicle velocity and pertinent suspension and controller parameters. Outputs are similar to those of the heave model, except describing the horizontal responses, and with the addition of the roll responses.

Each of the RMS responses is calculated separately for guideway roughness and for wind inputs since the roughness inputs are always present, but the wind inputs are not necessarily. In subsequent calculations of the Pepler index, only the outputs due to guideway roughness are used. Since the guideway roughness and wind inputs are statistically independent, RMS responses to the combined inputs can be obtained as the

RSS of the individual components.

The MatLab code for the model used for all of the EMS systems and for EDS 2 and EDS 3 appears in Table C-3. The code for the model used for EDS 1 (image flux) appears in Table C-4

Determination of optimal performance is complicated, compared to the heave model, because of the larger number of degrees of freedom and forcer/torquer options and because of questions concerning the location of sensors such as accelerometers and relative position sensors. Consequently, the study was restricted to passive suspension springs and dampers, except for EDS 1 (image flux, or Magneplane, system). In the case of EDS 1, active roll damping was employed by the use of aerodynamic control surfaces. The model, however, is capable of modeling active secondary suspensions in which the damping force is determined by signals from accelerometers located at the centers of gravity of suspension bogey and passenger compartment. These active secondary suspensions can be implemented either through actuators (e.g., hydraulic) between the passenger compartment and bogey, or by aerodynamic control surfaces in which the damping forces act between the passenger compartment and inertial space.

Accuracy of both models was assessed by exercising them with model parameters taken from Wormley, et al [47] and comparing the results with theirs. Since their results were for a heave-only model without wind excitations, the lateral motion/roll model parameters were selected to prevent excitation of the roll motion and the wind input was set to zero. For both models, the resulting RMS values of accelerations and displacements and the ISO-type plots (RMS accelerations in one-third octave bands) were substaitially identical to those reported by Wormley, thus validating the models.

Table C-1. MatLab Code for Two Degree of Freedom Heave Model

```
%/MATLAB/MW/EM1.M
%TWO DEGREE OF FREEDOM MODEL FOR ELECTROMAGNETIC
SUSPENSION
%MARC S. WEINBERG 9/16/91
%LATEST REVISION MARC S. WEINBERG 12/12/91
%LATEST RUN 12/13/91
format short e
format compact
diary em.dia
clg
i=sqrt(-1);
dtr=pi/180;
g=9.8;
%PARAMETERS FOR DIMENSIONLESS SCALING
mass=4e4
gap=0.01
wsc=sqrt(g/gap)
vsc=sqrt(g*gap)
psc=2*mass*g*vsc
%UNSPRUNG MASS IS #1
m1=1
%SPRUNG MASS IS #2
m2=6
k2=m2*(6.283/wsc)^2
b2=2*m2*.25*(6.283/wsc)
k1=-2*(1+m2/m1)
b1=0
%
%MAGNET PARAMETER
%FORCE COEFFICENT
fi=2*(1+m2/m1)
%INDUCTANCE
l1=2.18
%RESISTANCE
r1=0.0
%r1=0.26
%CHANGE IN INDUCTANCE WITH AIR GAP
lh=1
%
%MAGNETIC FIELD CONTROLLER
%EXTRA PROOF MASS
win=6.283*20
mc11=0
mc12=0
%LAG FREQUENCY
w1=10000*win/wsc
%PRIMARY CONTROLLER-DAMPING & STIFFNESS
kc1=-k1+m1*(win/wsc)^2
bc1=2*0.7*win/wsc*m1
%HIGH PASS FILTER FOR VELOCITY INTEGRATION-BREAK FREQUENCY
wv=0
```

```
%
%SECONDARY FORCER CONTROLLER
mc22=0
mc21=0
%LAG FREQUENCY
w2=w1
kc2=0
bc2=2*m2*0.7*(6.283/wsc)*0.0001
%FINITE LENGTH FILTERING
%LENGTH
l=2
%VELOCITY
v=134
%MAGNITUDE OF ROAD ROUGHNESS SPECTRA (DOUBLED SIDED IN R/S)
av=6.283e-7*v*2*.3048/(gap*vsc)
%WIND INPUT SPECTRA
fw=0.053
nuw=6.283/wsc
numw=2*nuw*fw^2/pi*[1]
denw=[-1 0 nuw^2]
%WIND FACTOR (PER CENT OF TOTAL WIND LOAD ON UNSPRUNG MASS)
aw=1
%
%STATE VECTOR IS [Y1DOT H1 F1 Y2DOT H2 F2 Y1DOTINT]
%INPUT VECTOR IS [Y0DOT W AN]
%OUTPUT VECTOR IS [Y1DD H1 I1 V1 Y2DD H2 F2]
%DEFINE THE COEFFICIENTS OF D /DT
ix=zeros(7,7);
ix(1,1)=m1;
ix(2,2)=1;
ix(3,:)=[mc11 0 1/w1 mc12 0 0 0];
ix(4,4)=m2;
ix(5,5)=1.;
ix(6,:)=[mc21 0 0 mc22 0 1/w2 0];
ix(7,:)=[-1 0 0 0 0 0 1]
%DEFINE THE STATE MATRIX
at=zeros(7,7);
at(1,:)=[-b1-b2 -k1 1 b2 k2 -1 0];
at(2,1)=1;
at(3,:)=[0 -kc1 -1 0 0 0 -bc1];
at(4,:)=[b2 0 0 -b2 -k2 1 0];
at(5,:)=[-1 0 0 1 0 0 0];
at(6,:)=[0 0 0 -bc2 -kc2 -1 0];
at(7,7)=-wv
aa=inv(ix);
a=aa*at
[evec,eval]=eig(a);
poles=diag(eval)
%DEFINE THE INPUT MATRIX
bt=zeros(7,3);
bt(1,:)=[b1 aw 0];
```

```
bt(2,:)=[-1 0 0];
bt(3,:)=[0 0 -mc11];
bt(4,:)=[0 1-aw 0];
bt(7,:)=[0 0 1]
b=aa*bt
%WORK THE OUTPUTS
c=zeros(7,7);
d=zeros(7,3);
c(1,:)=a(1,:);
d(1,:)=b(1,:);
c(2,2)=1;
c(3,3)=1/fi;
%NOTE THAT H1=Y1-Y0 DIFFERENT FROM MSW THESIS
c(4,:)=a(3,:)*l1/fi+r1/fi*[0 0 1 0 0 0 0]+lh*[1 0 0 0 0 0 0];
d(4,:)=b(3,:)*l1/fi+lh*b(2,:);
c(5,:)=a(4,:);
c(6,5)=1;
c(7,6)=1
d(5,:)=b(4,:)
%FREQUENCY RESPONSE FOR ROAD INPUTS
%[num,den]=ss2tf(a,b,c,d,1)
%zeroy1dot=roots(num(1,1:7))
%zeroh1=roots(num(2,1:7))
%zeroy2dot=roots(num(5,1:7))
%zeroh2=roots(num(6,1:7))
%poles=roots(den)
%[z,p,k]=ss2zp(a,b,c,d,1)
%[z,p,k]=tf2zp(num,den)
w=logspace(-2,1,100);
%w=[0.1:0.1:20];
[mag,phase]=bode(a,b,c,d,1,w);
output1=[w;mag';phase'];
%FINITE LENGTH FILTERING
finl=sin(0.5*w*l*wsc/v)./(0.5*w*l*wsc/v);
breakw=2.764*v/(l*wsc)
temp=log(finl*(1+0*i))';
mf=exp(real(temp));
pf=imag(temp)/dtr;
%clg,subplot(211)
%plot(w,mf)
%plot(w,pf)
%pause
%GENERATE VECTOR TO CONTROL THE PLOTTING AXES
n=length(w)
v=[log10(w(1)),log10(w(n)),-3,2];
%OBTAIN CLEARANCE AT POINT BELOW MAGNET
t1=mag(:,1).*mf.*exp(i*dtr*phase(:,1)).*exp(i*pf*dtr)./(-w.*w)';
t2=ones(n,1)./(i*w');
temp=log(t1-t2);
pypt=imag(temp/dtr);
magypt=exp(real(temp));
```

```
%OBTAIN RMS VALUES FOR ROAD INPUTS
phiroad=av*ones(n,1);
rmshpt=rms(magypt,phiroad,w)
phiroad=phiroad.*mf.*mf;
rmsh1=+rms(mag(:,2),phiroad,w)
rmsh2=+rms(mag(:,6),phiroad,w)
rmsy1dd=rms(mag(:,1),phiroad,w)
rmsy2dd=rms(mag(:,5),phiroad,w)
rmsi=rms(mag(:,3),phiroad,w)
rmsv=rms(mag(:,4),phiroad,w)
rmsf2=rms(mag(:,7),phiroad,w)
iv=rmsi*rmsv*psc
h2m=rmsh2*gap
%PLOT THE ACCELERATIONS
axis(v),clg,subplot(211);
loglog(w,mag(:,1).*mf,w,mag(:,5).*mf),xlabel('angular freq. (rad/sec)')
ylabel('acceleration'),grid
title('ACCEL OF MASSES IN RESPONSE TO ROAD INPUT'),axis;
semilogx(w,phase(:,1)+pf,w,phase(:,5)+pf)
xlabel('angular freq. (rad/sec)'),ylabel('phase'),grid
pause
%PLOT THE CLEARANCES
axis(v),clg,subplot(211);
loglog(w,mag(:,2).*mf,w,mag(:,6).*mf,w,magypt),
xlabel('angular freq. (rad/sec)'),ylabel('clearance'),grid
title('CLEARANCE OF MASSES IN RESPONSE TO ROAD INPUT'),axis;
semilogx(w,phase(:,2)+pf,w,phase(:,6)+pf,w,pypt)
xlabel('angular freq. (rad/sec)'),ylabel('phase'),grid
pause
%PLOT THE MAGNET CURRENT AND VOLTAGE AND SECONDARY FORCER
axis(v);clg,subplot(211)
loglog(w,mag(:,3).*mf,w,mag(:,4).*mf,w,mag(:,7).*mf),
xlabel('angular freq. (rad/sec)'),ylabel('I, V, & F2'),grid
title('MAG. CURRENT, VOLT., & F2 ,IN RESPONSE TO ROAD INPUT'),axis;
semilogx(w,phase(:,3).*mf,w,phase(:,4).*mf,w,phase(:,7).*mf),
xlabel('angular freq. (rad/sec)'),ylabel('phase'),grid
pause
diary off
```

Table C-2. MatLab Code for Two Degree of Freedom Heave Model for EDS 1 (image flux)

```
%/MATLAB/MW/EDSIM1.M  NAME CHANGED FROM EDS1.M TO NAME ON
DISK (edsim1), 3/29/92
%TWO DEGREE OF FREEDOM MODEL FOR ELECTRODYNAMIC IMAGE FLUX
SUSPENSION
%SECONDARY SET TO ZERO BY M2 = 0
%IDENTICAL TO EM1.M EXCEPT FOR SUSPENSION PARAMETERS
%MARC S. WEINBERG 11/13/91
%BAA VEHICLE PARAMETERS FROM S. BROWN ADDED BY CRD, 3/29/92
%LATEST REVISION MARC S. WEINBERG 12/13/91
%LATEST RUN 8/13/92 by C. R. Dauwalter
format short e
format compact
diary edsim1_89.dia
clg
i=sqrt(-1);
dtr=pi/180;
g=9.8;
%PARAMETERS FOR DIMENSIONLESS SCALING
mass=4e4
gap=0.15
wsc=sqrt(g/gap)
vsc=sqrt(g*gap)
psc=2*mass*g*vsc
%UNSPRUNG MASS IS #1
m1=1
%SPRUNG MASS IS #2
win=6.283*1.04
m2=1e-4
k2=m2*(628.3/wsc)^2
b2=2*m2*.25*(628.3/wsc)
k1=-2*(1+m2/m1)*0+m1*(win/wsc)^2
b1=2*m1*win/wsc*0                % Zero primary heave damping for magneplane
%
%MAGNET PARAMETER
%FORCE COEFFICENT
fi=2*(1+m2/m1)
%INDUCTANCE
l1=2.18
%RESISTANCE
r1=0.0
%r1=0.26
%CHANGE IN INDUCTANCE WITH AIR GAP
lh=1
%
%MAGNETIC FIELD CONTROLLER
%EXTRA PROOF MASS
mc11=0
mc12=0
%LAG FREQUENCY
w1=10000*win/wsc
```

Table C-2 (continued). MatLab Code for Two Degree of Freedom Heave Model for EDS 1 (image flux)

```
%PRIMARY CONTROLLER-DAMPING & STIFFNESS
kc1=(-k1+m1*(win/wsc)^2)*0
bc1=2*0.7*win/wsc*m1
%HIGH PASS FILTER FOR VELOCITY INTEGRATION-BREAK FREQUENCY
wv=0
%
%SECONDARY FORCER CONTROLLER
mc22=0
mc21=0
%LAG FREQUENCY
w2=w1
kc2=0
bc2=2*m2*0.7*(6.283/wsc)*0.0001
%FINITE LENGTH FILTERING
%LENGTH
l=4.5
%VELOCITY
v=134
%MAGNITUDE OF ROAD ROUGHNESS SPECTRA (DOUBLED SIDED IN R/S)
av=6.283e-7*v*2*.3048/(gap*vsc)
%WIND INPUT SPECTRA
fw=0.053
nuw=6.283/wsc
numw=2*nuw*fw^2/pi*[1]
denw=[-1 0 nuw^2]
%WIND FACTOR (PER CENT OF TOTAL WIND LOAD ON UNSPRUNG MASS)
aw=0
%
%STATE VECTOR IS [Y1DOT H1 F1 Y2DOT H2 F2 Y1DOTINT]
%INPUT VECTOR IS [Y0DOT W AN]
%OUTPUT VECTOR IS [Y1DD H1 I1 V1 Y2DD H2 F2]
%DEFINE THE COEFFICIENTS OF D /DT
ix=zeros(7,7);
ix(1,1)=m1;
ix(2,2)=1;
ix(3,:)=[mc11 0 1/w1 mc12 0 0 0];
ix(4,4)=m2;
ix(5,5)=1.;
ix(6,:)=[mc21 0 0 mc22 0 1/w2 0];
ix(7,:)=[-1 0 0 0 0 0 1]
%DEFINE THE STATE MATRIX
at=zeros(7,7);
at(1,:)=[-b1-b2 -k1 1 b2 k2 -1 0];
at(2,1)=1;
at(3,:)=[0 -kc1 -1 0 0 0 -bc1];
at(4,:)=[b2 0 0 -b2 -k2 1 0];
at(5,:)=[-1 0 0 1 0 0 0];
at(6,:)=[0 0 0 -bc2 -kc2 -1 0];
at(7,7)=-wv
aa=inv(ix);
```

Table C-2 (continued). MatLab Code for Two Degree of Freedom Heave Model for EDS 1 (image flux)

```
a=aa*at
[evec,eval]=eig(a);
poles=diag(eval)
%DEFINE THE INPUT MATRIX
bt=zeros(7,3);
bt(1,:)=[b1 aw 0];
bt(2,:)=[-1 0 0];
bt(3,:)=[0 0 -mc11];
bt(4,:)=[0 1-aw 0];
bt(7,:)=[0 0 1]
b=aa*bt
%WORK THE OUTPUTS
c=zeros(7,7);
d=zeros(7,3);
c(1,:)=a(1,:);
d(1,:)=b(1,:);
c(2,2)=1;
c(3,3)=1/fi;
%NOTE THAT H1=Y1-Y0 DIFFERENT FROM MSW THESIS
c(4,:)=a(3,:)*l1/fi+r1/fi*[0 0 1 0 0 0 0]+lh*[1 0 0 0 0 0 0];
d(4,:)=b(3,:)*l1/fi+lh*b(2,:);
c(5,:)=a(4,:);
c(6,5)=1;
c(7,6)=1
d(5,:)=b(4,:)
%FREQUENCY RESPONSE FOR ROAD INPUTS
%[num,den]=ss2tf(a,b,c,d,1)
%zeroy1dot=roots(num(1,1:7))
%zeroh1=roots(num(2,1:7))
%zeroy2dot=roots(num(5,1:7))
%zeroh2=roots(num(6,1:7))
%poles=roots(den)
%[z,p,k]=ss2zp(a,b,c,d,1)
%[z,p,k]=tf2zp(num,den)
w=logspace(-2,1,100);
%w=[0.1:0.1:20];
[mag,phase]=bode(a,b,c,d,1,w);
output1=[w;mag';phase'];
%FINITE LENGTH FILTERING
finl=sin(0.5*w*l*wsc/v)./(0.5*w*l*wsc/v);
breakw=2.764*v/(l*wsc)
temp=log(finl*(1+0*i))';
mf=exp(real(temp));
pf=imag(temp)/dtr;
%clg,subplot(211)
%plot(w,mf)
%plot(w,pf)
%pause
%GENERATE VECTOR TO CONTROL THE PLOTTING AXES
n=length(w)
```

```
v=[log10(w(1)),log10(w(n)),-3,2];
%OBTAIN CLEARANCE AT POINT BELOW MAGNET
t1=mag(:,1).*mf.*exp(i*dtr*phase(:,1)).*exp(i*pf*dtr)./(-w.*w)';
t2=ones(n,1)./(i*w');
temp=log(t1-t2);
pypt=imag(temp/dtr);
magypt=exp(real(temp));
%OBTAIN RMS VALUES FOR ROAD INPUTS
phiroad=av*ones(n,1);
rmshpt=rms(magypt,phiroad,w)
phiroad=phiroad.*mf.*mf;
rmsh1=+rms(mag(:,2),phiroad,w)
rmsh2=+rms(mag(:,6),phiroad,w)
rmsy1dd=rms(mag(:,1),phiroad,w)
rmsy2dd=rms(mag(:,5),phiroad,w)
rmsi=rms(mag(:,3),phiroad,w)
rmsv=rms(mag(:,4),phiroad,w)
rmsf2=rms(mag(:,7),phiroad,w)
iv=rmsi*rmsv*psc
h2m=rmsh2*gap
%PLOT THE ACCELERATIONS
axis(v),clg,subplot(211);
loglog(w,mag(:,1).*mf,w,mag(:,5).*mf),xlabel('angular freq. (rad/sec)')
ylabel('acceleration'),grid
title('ACCEL OF MASSES IN RESPONSE TO ROAD INPUT'),axis;
semilogx(w,phase(:,1)+pf,w,phase(:,5)+pf)
xlabel('angular freq. (rad/sec)'),ylabel('phase'),grid
pause
%PLOT THE CLEARANCES
axis(v),clg,subplot(211);
loglog(w,mag(:,2).*mf,w,mag(:,6).*mf,w,magypt),
xlabel('angular freq. (rad/sec)'),ylabel('clearance'),grid
title('CLEARANCE OF MASSES IN RESPONSE TO ROAD INPUT'),axis;
semilogx(w,phase(:,2)+pf,w,phase(:,6)+pf,w,pypt)
xlabel('angular freq. (rad/sec)'),ylabel('phase'),grid
pause
%PLOT THE MAGNET CURRENT AND VOLTAGE AND SECONDARY FORCER
axis(v);clg,subplot(211)
loglog(w,mag(:,3).*mf,w,mag(:,4).*mf,w,mag(:,7).*mf),
xlabel('angular freq. (rad/sec)'),ylabel('I, V, & F2'),grid
title('MAG. CURRENT, VOLT., & F2 ,IN RESPONSE TO ROAD INPUT'),axis;
semilogx(w,phase(:,3).*mf,w,phase(:,4).*mf,w,phase(:,7).*mf),
xlabel('angular freq. (rad/sec)'),ylabel('phase'),grid
pause
diary off
```

Table C-3. MatLab Code for Four Degree of Freedom Lateral/Roll Model

```
%/MATLAB/MW/EM2.M
%FOUR DEGREE OF FREEDOM MODEL FOR ELECTROMAGNETIC
SUSPENSION AND SECONDARY
%IN RESPONSE TO LATERAL INPUTS
%MARC S. WEINBERG 10/10/91
%LATEST REVISION C.R.D., per MARC S. WEINBERG 4/5/92
%LATEST RUN 4/5/92 by C.R.D.
format short e
format compact
diary em.dia
clg
i=sqrt(-1);
dtr=pi/180;
g=9.8;
%PARAMETERS FOR DIMENSIONLESS SCALING
mass=4e4
gap=.01
wsc=sqrt(g/gap)
vsc=sqrt(g*gap)
psc=2*mass*g*vsc
%LOCATIONS OF SUSPENSION FORCES
%VERTICAL MAGNET CG TO RAIL CENTER
lm=1.5/gap
%LATERAL RAIL FORCE ABOVE CG OF MASS 1
l1=0/gap
%VERTICAL SECONDARY SUSPENSION FROM CG
lh=1.5/gap
%LATERAL SECONDARY SUSPENSION-DISTANCE ABOVE CG 1
lv1=0.7/gap
%LATERAL SECONDARY SUSPENSION-DISTANCE BELOW CG 2
lv2=1.3/gap
%UNSPRUNG MASS IS #1
m1=1
%SPRUNG MASS IS #2
m2=6
m=m1+m2
%MOMENTS OF INERTIA ABOUT ROLL AXIS
lr=2/gap
i1=m1*lr^2/3
i2=m2*lr^2/3
%LATERAL SECONDARY SUSPENSION
k2=m2*(6.283/wsc)^2
b2=2*m2*.25*(6.283/wsc)
%VERTICAL SECONDARY SUSPENSION
kv=m2*(6.283/wsc)^2
bv=2*m2*.25*(6.283/wsc)
%LATERAL MAGNET CHARACTERISTICS
%RATIO OF NOMINAL CURRENT TO THAT REQUIRED FOR LIFT
ilat=0.5
win=6.283*5
k1=(-2*2*(1+m2/m1)*ilat^2)
```

Table C-3 (continued). MatLab Code for Four Degree of Freedom Lateral/Roll Model

```
b1=0
%FORCE COEFFICENT-EXTRA TWO ASSUMES PUSH-PULL OPERATION
fi=2*2*(1+m2/m1)*ilat^2
%INDUCTANCE
l1x=2.18*ilat^2                % *ilat^2 added 4/5/92 per MSW
%RESISTANCE
r1=0.0*ilat^2                  % *ilat^2 added 4/5/92 per MSW
%r1=0.26*ilat^2                 % *ilat^2 added 4/5/92 per MSW
%CHANGE IN INDUCTANCE WITH AIR GAP
lhx=1
%
%LATERAL MAGNETIC FIELD CONTROLLER
%EXTRA PROOF MASS
%PRIMARY CONTROLLER-DAMPING & STIFFNESS
kh1=(-k1+m1*(win/wsc)^2)
bh1=2*0.7*win/wsc
%PRIMARY VERTICAL CONTROLLER
winv=6.283*5
km=m1*(winv/wsc)^2
%LATERAL SECONDARY FORCER CONTROLLER
ks2=0
bs2=2*m2*0.7*(6.283/wsc)*1e-6
%FINITE LENGTH FILTERING
%LENGTH
l=2
%VELOCITY
v=134
%MAGNITUDE OF ROAD ROUGHNESS SPECTRA (DOUBLED SIDED IN R/S)
av=6.283e-7*v*2*.3048/(gap*vsc)
%WIND INPUT SPECTRA
fw=0.053
%CORRELATION LENGTH
lc=200
nuw=2*pi*v/(lc*wsc)
numw=2*nuw*fw^2/pi*[1]
denw=[-1 0 nuw^2]
%WIND FACTOR (PER CENT OF TOTAL WIND LOAD ON UNSPRUNG MASS)
aw=0
%CENTER OF LATERAL WIND FORCES ABOVE THE CG.
lw1=0
lw2=0
%
%STATE VECTOR IS [Y1DOT H1 Y2DOT H2 THETA1DOT THETA1 THETA2DOT
THETA2]
%INPUT VECTOR IS [Y0DOT W]
%OUTPUT VECTOR IS
% [Y1DOT H1 Y2DOT H2 THETA1DOT THETA1 THETA2DOT THETA2 i1, V1,
FM, FS]
%DEFINE THE COEFFICIENTS OF D /DT
ix=diag([m1,1,m2,1,i1,1,i2,1])
```

```
%DEFINE THE STATE MATRIX
at=zeros(8,8);
at(1,:)=[-b1-b2-bh1 k1+kh1 b2+bs2 -k2 -b2*lv1-b1*l1 -k2*lv1+m1....
     -b2*lv2 -k2*lv2];
at(2,:)=[-1 0 0 0 -l1 0 0 0];
at(3,:)=[b2 0 -b2-bs2 k2 b2*lv1 k2*lv1 b2*lv2 k2*lv2+m2];
at(4,:)=[1 0 -1 0 0 0 0 0];
at(5,:)=[-b2*lv1-l1*(b1+bh1) l1*(k1+kh1) +lv1*(bs2+b2) -k2*lv1 0 0 0 0];
at(5,5)=-b2*lv1^2-bv*lh^2-b1*l1^2;
at(5,6)=-k2*lv1^2-kv*lh^2-km*lm^2;
at(5,7)=-b2*lv1*lv2+bv*lh^2;
at(5,8)=-k2*lv1*lv2+kv*lh^2;
at(6,5)=1;
at(7,:)=[-b2*lv2 0 lv2*(b2+bs2) -k2*lv2 at(5,7) at(5,8) -b2*lv2^2-bv*lh^2 ....
      -k2*lv2^2-kv*lh^2];
at(8,7)=1
aa=inv(ix);
a=aa*at
[evec,eval]=eig(a);
poles=diag(eval)
eigenvectors=evec
%DEFINE THE INPUT MATRIX
bt=zeros(8,2);
bt(1,:)=[b1 aw];
bt(2,:)=[1 0];
bt(3,:)=[0 1-aw];
bt(5,:)=[l1*b1 lw1*aw];
bt(7,:)=[0 lw2*(1-aw)]
b=aa*bt
%WORK THE OUTPUTS
%OUTPUT VECTOR IS
% [Y1DOT H1 Y2DOT H2 THETA1DOT THETA1 THETA2DOT THETA2 i1, V1,
FM, FS]
c=[diag(ones(1,8)); zeros(4,8)];
d=zeros(12,2);
c(1,:)=a(1,:);
d(1,:)=b(1,:);
c(3,:)=a(3,:);
d(3,:)=b(3,:);
c(9,:)=[-bh1 kh1 zeros(1,6)]/fi;
c(10,:)=l1x*(-bh1*a(1,:)+kh1*a(2,:))/fi-lhx*a(2,:)+r1*c(9,:);
d(10,:)=l1x*(-bh1*b(1,:)+kh1*b(2,:))/fi-lhx*b(2,:)
c(11,:)=[zeros(1,5) -lm*km 0 0];
c(12,:)=[0 0 -bs2 0 0 0 0 0]
%NOTE THAT H1=Y0-Y1-l1*theta DIFFERENT FROM MSW THESIS
%FREQUENCY RESPONSE FOR ROAD INPUTS
%[num,den]=ss2tf(a,b,c,d,1)
%zeroy1dot=roots(num(1,1:7))
%zeroh1=roots(num(2,1:7))
%zeroy2dot=roots(num(5,1:7))
```

Table C-3 (continued). MatLab Code for Four Degree of Freedom Lateral/Roll Model

```
%zeroh2=roots(num(6,1:7))
%poles=roots(den)
%[z,p,k]=ss2zp(a,b,c,d,1)
%[z,p,k]=tf2zp(num,den)
w=logspace(-2,1,100);
%w=[0.1:0.1:20];
[mag,phase]=bode(a,b,c,d,1,w);
output1=[w;mag';phase'];
%FINITE LENGTH FILTERING
finl=sin(0.5*w*l*wsc/v)./(0.5*w*l*wsc/v);
breakw=2.764*v/(l*wsc)
temp=log(finl*(1+0*i))';
mf=exp(real(temp));
pf=imag(temp)/dtr;
%clg,subplot(211)
%plot(w,mf)
%plot(w,pf)
%pause
%GENERATE VECTOR TO CONTROL THE PLOTTING AXES
n=length(w)
vv=[log10(w(1)),log10(w(n)),-3,2];
%OBTAIN CLEARANCE AT POINT BELOW MAGNET
%t1=mag(:,1).*mf.*exp(i*dtr*phase(:,1)).*exp(i*pf*dtr)./(-w.*w)';
t1=(mag(:,1).*exp(i*dtr*phase(:,1))./(-w.*w)'+...
  l1*mag(:,6).*exp(i*dtr*phase(:,6))).*mf.*exp(i*pf*dtr);
t0=ones(n,1)./(i*w');
temp=log(t0-t1);
pypt=imag(temp/dtr);
magypt=exp(real(temp));
%OBTAIN RMS VALUES FOR ROAD INPUTS
phiroad=av*ones(n,1);
rmshpt=rms(magypt,phiroad,w)
phiroad=phiroad.*mf.*mf;
rmsh1=+rms(mag(:,2),phiroad,w)
rmsh2=+rms(mag(:,4),phiroad,w)
h2m=rmsh2*gap
rmsy1dd=rms(mag(:,1),phiroad,w)
rmsy2dd=rms(mag(:,3),phiroad,w)
rmst1d=rms(mag(:,5),phiroad,w)
rmst1=rms(mag(:,6),phiroad,w)
rmst2d=rms(mag(:,7),phiroad,w)
t2ddps=rmst2d*wsc/dtr
rmst2=rms(mag(:,8),phiroad,w)
rmsi=rms(mag(:,9),phiroad,w)
rmsv=rms(mag(:,10),phiroad,w)
rmsfs=rms(mag(:,12),phiroad,w)
%OBTAIN RMS VALUES FOR WIND INPUTS
[phiw,phasew]=bode(numw,denw,w);
%rmstest=rms(ones(n,1),phiw,w)
rmsh1w=+rms(mag(:,2),phiw,w)
```

Table C-3 (continued). MatLab Code for Four Degree of Freedom Lateral/Roll Model

```
rmsh2w=+rms(mag(:,4),phiw,w)
h2wm=rmsh2w*gap
rmsy1ddw=rms(mag(:,1),phiw,w)
rmsy2ddw=rms(mag(:,3),phiw,w)
rmst1dw=rms(mag(:,5),phiw,w)
rmst1w=rms(mag(:,6),phiw,w)
rmst2dw=rms(mag(:,7),phiw,w)
t2ddpsw=rmst2dw*wsc/dtr
rmst2w=rms(mag(:,8),phiw,w)
rmsiw=rms(mag(:,9),phiw,w)
rmsvw=rms(mag(:,10),phiw,w)
rmsfsw=rms(mag(:,12),phiw,w)
iv=rmsi*rmsv*psc*2   % added 4/5/92 per MSW
%PLOT THE ACCELERATIONS
axis(vv),clg,subplot(211);
loglog(w,mag(:,1).*mf,w,mag(:,3).*mf),xlabel('angular freq. (rad/sec)')
ylabel('acceleration'),grid
title('ACCEL OF MASSES IN RESPONSE TO ROAD VELOCITY'),axis;
semilogx(w,phase(:,1)+pf,w,phase(:,3)+pf)
xlabel('angular freq. (rad/sec)'),ylabel('phase'),grid
pause
%PLOT THE CLEARANCES
axis(vv),clg,subplot(211);
loglog(w,mag(:,2).*mf,w,mag(:,4).*mf,w,magypt),
xlabel('angular freq. (rad/sec)'),ylabel('clearance'),grid
title('CLEARANCE OF MASSES IN RESPONSE TO ROAD VELOCITY'),axis;
semilogx(w,phase(:,2)+pf,w,phase(:,6)+pf,w,pypt)
xlabel('angular freq. (rad/sec)'),ylabel('phase'),grid
pause
%PLOT THE MAGNET CURRENT AND VOLTAGE AND SECONDARY FORCER
axis(vv);clg,subplot(211)
loglog(w,mag(:,9).*mf,w,mag(:,10).*mf,w,mag(:,12).*mf),
xlabel('angular freq. (rad/sec)'),ylabel('I, V, & F2'),grid
title('MAG. CURRENT, VOLT., & F2 ,IN RESPONSE TO ROAD VELOCITY'),axis;
semilogx(w,phase(:,3)+pf,w,phase(:,4)+pf,w,phase(:,7)+pf),
xlabel('angular freq. (rad/sec)'),ylabel('phase'),grid
pause
%PLOT THE ANGLES
vv=[log10(w(1)),log10(w(n)),-4,0];
axis(vv),clg,subplot(211);
loglog(w,mag(:,6).*mf,w,mag(:,8).*mf),
xlabel('angular freq. (rad/sec)'),ylabel('clearance'),grid
title('ROTATION OF MASSES IN RESPONSE TO ROAD VELOCITY'),axis;
semilogx(w,phase(:,6)+pf,w,phase(:,8)+pf)
xlabel('angular freq. (rad/sec)'),ylabel('phase'),grid
diary off
```

Table C-4. MatLab Code for Four Degree of Freedom Lateral/Roll Model for EDS 1 (image flux)

```
%/MATLAB/MW/EDSIM2.M%FOUR DEGREE OF FREEDOM MODEL FOR
MAGNEPLANE IMAGE AND SECONDARY IN RESPONSE TO LATERAL INPUTS
%MARC S. WEINBERG 12/14/91
%LATEST REVISION MARC S. WEINBERG 3/31/92
%BAA VEHICLE PARAMETERS FROM S. BROWN ADDED BY CRD,3/29/92
%LATEST RUN 8/13/92 by C. R. Dauwalter
format short e
format compact
diary edsim2_89.dia
clg
i=sqrt(-1);
dtr=pi/180;
g=9.8;
%PARAMETERS FOR DIMENSIONLESS SCALING
mass=4e4
gap=0.15
wsc=sqrt(g/gap)
vsc=sqrt(g*gap)
psc=2*mass*g*vsc
%LOCATIONS OF SUSPENSION FORCES
%VERTICAL MAGNET CG TO RAIL CENTER
%lm=1.5/gap
l1=0/gap
%VERTICAL SECONDARY SUSPENSION FROM CG
lh=1.5/gap
%LATERAL SECONDARY SUSPENSION-DISTANCE ABOVE CG 1
lv1=0.7*1e-4/gap
%LATERAL SECONDARY SUSPENSION-DISTANCE BELOW CG 2
lv2=1.3*1e-4/gap
%UNSPRUNG MASS IS #1
m1=1
%SPRUNG MASS IS #2. SMALL FOR MAGNEPLANE WHICH HAS NO
SECONDARY SUSPENSION.
m2=1e-6
m=m1+m2
%MOMENTS OF INERTIA ABOUT ROLL AXIS
lr=2/gap
%i1=m1*lr^2/3
i2=m2*lr^2/3
%LATERAL SECONDARY SUSPENSION
k2=m2*(6283/wsc)^2
b2=2*m2*.25*(6283/wsc)
%VERTICAL SECONDARY SUSPENSION
kv=m2*(6283/wsc)^2
bv=2*m2*.25*(6283/wsc)
%SPECIAL SECTION FOR MAGNEPLANE
%ANGLE OF CENTER OF LIFT COIL FROM CENTER
th=45*dtr
%KM DROPS OUT OF MAGNEPLANE ANALYSIS BY LM = 0
win=6.283*1.0
```

```
km=m1*(win/wsc)^2
k1=km*(tan(th))^2
b1=2*(win/wsc)*m*0.1
%R=RADIUS OF MAGNEPLANE
r=2.1/gap
lm=0
%POSITION OF VERTICAL SUSPENSIONS FROM CENTER
xmag=r*sin(th)/gap
lcg=0.9/gap
%SINCE FORCE ACTS THROUGH CYLINDER CENTER LCG IS OFTEN
ANALOGOUS TO OLD L1
l1=lcg
%LATERAL RAIL FORCE ABOVE CG OF MASS 1
%INERTIA ABOUT CG
%inertia about cg=5e4 per S. Brown;
%expressing i1 as m1*lbar^2 results in lbar=1.18m
%i1=(m1*r^2/4 )
i1=m1*(1.18/gap)^2
%INERTIA ABOUT CYLINDER CENTER
ic=i1+m1*lcg^2
%ROLL STIFFNESS ADDED 3/31/92
kroll=km*lm^2
wroll=sqrt((kroll+m1*lcg)/(i1+m1*lcg^2))
broll=2*(i1+m1*lcg^2)*wroll*0.7        % 0.7 is arbitrary-aero control assumed for BAA
%LATERAL MAGNET CHARACTERISTICS
%RATIO OF NOMINAL CURRENT TO THAT REQUIRED FOR LIFT
ilat=0.5
%FORCE COEFFICENT
fi=2*2*(1+m2/m1)*ilat^2
%INDUCTANCE
l1x=2.18
%RESISTANCE
r1=0.0
%r1=0.26
%CHANGE IN INDUCTANCE WITH AIR GAP
lhx=1
%
%LATERAL MAGNETIC FIELD CONTROLLER
%EXTRA PROOF MASS
%PRIMARY CONTROLLER-DAMPING & STIFFNESS
kh1=(-k1+m1*(win/wsc)^2)*0
bh1=2*0.7*win/wsc*0
%PRIMARY VERTICAL CONTROLLER
%winv=6.283*5
%km=m1*(winv/wsc)^2
%LATERAL SECONDARY FORCER CONTROLLER
ks2=0
bs2=2*m2*0.7*(6.283/wsc)*1e-6
%FINITE LENGTH FILTERING
%LENGTH
```

Table C-4 (continued). MatLab Code for Four Degree of Freedom Lateral/Roll Model for EDS 1 (image flux)

```
l=4.5
%VELOCITY
v=134
%MAGNITUDE OF ROAD ROUGHNESS SPECTRA (SINGLE SIDED IN R/S)
av=6.283e-7*v*2*.3048/(gap*vsc)
%WIND INPUT SPECTRA
fw=0.053
%CORRELATION LENGTH
lc=200
nuw=2*pi*v/(lc*wsc)
numw=2*nuw*fw^2/pi*[1]
denw=[-1 0 nuw^2]
%WIND FACTOR (PER CENT OF TOTAL WIND LOAD ON UNSPRUNG MASS)
aw=1
%CENTER OF LATERAL WIND FORCES ABOVE THE CG.
lw1=0
lw2=0.7
%STATE VECTOR IS [Y1DOT H1 Y2DOT H2 THETA1DOT THETA1 THETA2DOT
THETA2]
%INPUT VECTOR IS [Y0DOT W]
%OUTPUT VECTOR IS
% [Y1DOT H1 Y2DOT H2 THETA1DOT THETA1 THETA2DOT THETA2 i1, V1,
FM, FS]
%DEFINE THE COEFFICIENTS OF D /DT
ix=diag([m1,1,m2,1,i1,1,i2,1])
%DEFINE THE STATE MATRIX
at=zeros(8,8);
at(1,:)=[-b1-b2-bh1 k1+kh1 b2+bs2 -k2 -b2*lv1-b1*l1 -k2*lv1+m1....
     -b2*lv2 -k2*lv2];
at(2,:)=[-1 0 0 0 -l1 0 0 0];
at(3,:)=[b2 0 -b2-bs2 k2 b2*lv1 k2*lv1 b2*lv2 k2*lv2+m2];
at(4,:)=[1 0 -1 0 0 0 0 0];
at(5,:)=[-b2*lv1-l1*(b1+bh1) l1*(k1+kh1)  +lv1*(bs2+b2) -k2*lv1...
     0 0 0 0];
at(5,5)=-b2*lv1^2-bv*lh^2-b1*l1^2-broll;
at(5,6)=-k2*lv1^2-kv*lh^2-km*lm^2
at(5,7)=-b2*lv1*lv2+bv*lh^2;
at(5,8)=-k2*lv1*lv2+kv*lh^2;
at(6,5)=1;
at(7,:)=[-b2*lv2 0 lv2*(b2+bs2) -k2*lv2 at(5,7) at(5,8) -b2*lv2^2-bv*lh^2 ....
      -k2*lv2^2-kv*lh^2];
at(8,7)=1
aa=inv(ix);
a=aa*at
[evec,eval]=eig(a);
poles=diag(eval)
eigenvectors=evec
%DEFINE THE INPUT MATRIX
bt=zeros(8,2);
bt(1,:)=[b1 aw];
```

```
bt(2,:)=[1 0];
bt(3,:)=[0 1-aw];
bt(5,:)=[l1*b1 lw1*aw];
bt(7,:)=[0 lw2*(1-aw)]
b=aa*bt
%WORK THE OUTPUTS
%OUTPUT VECTOR IS
% [Y1DOT H1 Y2DOT H2 THETA1DOT THETA1 THETA2DOT THETA2 i1, V1,
FM, FS]
c=[diag(ones(1,8)); zeros(4,8)];
d=zeros(12,2);
c(1,:)=a(1,:);
d(1,:)=b(1,:);
c(3,:)=a(3,:);
d(3,:)=b(3,:);
c(9,:)=[-bh1 kh1 zeros(1,6)]/fi;
c(10,:)=l1x*(-bh1*a(1,:)+kh1*a(2,:))/fi-lhx*a(2,:)+r1*c(9,:);
d(10,:)=l1x*(-bh1*b(1,:)+kh1*b(2,:))/fi-lhx*b(2,:)
%THIS LINE MAY NOT BE VALID FOR MAGNEPLANE
c(11,:)=[zeros(1,5) -lm*km 0 0];
c(12,:)=[0 0 -bs2 0 0 0 0 0]
%NOTE THAT H1=Y0-Y1-l1*theta DIFFERENT FROM MSW THESIS
%FREQUENCY RESPONSE FOR ROAD INPUTS
%[num,den]=ss2tf(a,b,c,d,1)
%zeroy1dot=roots(num(1,1:7))
%zeroh1=roots(num(2,1:7))
%zeroy2dot=roots(num(5,1:7))
%zeroh2=roots(num(6,1:7))
%poles=roots(den)
%[z,p,k]=ss2zp(a,b,c,d,1)
%[z,p,k]=tf2zp(num,den)
w=logspace(-1,1,250);
%w=[0.1:0.1:20];
[mag,phase]=bode(a,b,c,d,1,w);
output1=[w;mag';phase'];
%FINITE LENGTH FILTERING
finl=sin(0.5*w*l*wsc/v)./(0.5*w*l*wsc/v);
breakw=2.764*v/(l*wsc)
temp=log(finl*(1+0*i))';
mf=exp(real(temp));
pf=imag(temp)/dtr;
%clg,subplot(211)
%plot(w,mf)
%plot(w,pf)
%pause
%GENERATE VECTOR TO CONTROL THE PLOTTING AXES
n=length(w)
vv=[log10(w(1)),log10(w(n)),-3,2];
%OBTAIN CLEARANCE AT POINT BELOW MAGNET
%t1=mag(:,1).*mf.*exp(i*dtr*phase(:,1)).*exp(i*pf*dtr)./(-w.*w)';
```

```
t1=(mag(:,1).*exp(i*dtr*phase(:,1))./(-w.*w)'+...
  l1*mag(:,6).*exp(i*dtr*phase(:,6))).*mf.*exp(i*pf*dtr);
t0=ones(n,1)./(i*w');
temp=log(t0-t1);
pypt=imag(temp/dtr);
magypt=exp(real(temp));
%OBTAIN RMS VALUES FOR ROAD INPUTS
phiroad=av*ones(n,1);
rmshpt=rms(magypt,phiroad,w)
phiroad=phiroad.*mf.*mf;
rmsh1=+rms(mag(:,2),phiroad,w)
%rmsh2=+rms(mag(:,4),phiroad,w)
%h2m=rmsh2*gap
rmsy1dd=rms(mag(:,1),phiroad,w)
rmsy2dd=rms(mag(:,3),phiroad,w)
rmst1d=rms(mag(:,5),phiroad,w)
rmst1=rms(mag(:,6),phiroad,w)
rmst2d=rms(mag(:,7),phiroad,w)
t2ddps=rmst2d*wsc/dtr
%rmst2=rms(mag(:,8),phiroad,w)
%rmsi=rms(mag(:,9),phiroad,w)
%rmsv=rms(mag(:,10),phiroad,w)
%rmsfs=rms(mag(:,12),phiroad,w)
%OBTAIN RMS VALUES FOR WIND INPUTS
[phiw,phasew]=bode(numw,denw,w);
%rmstest=rms(ones(n,1),phiw,w)
rmsh1w=+rms(mag(:,2),phiw,w)
%rmsh2w=+rms(mag(:,4),phiw,w)
%h2wm=rmsh2w*gap
rmsy1ddw=rms(mag(:,1),phiw,w)
rmsy2ddw=rms(mag(:,3),phiw,w)
rmst1dw=rms(mag(:,5),phiw,w)
rmst1w=rms(mag(:,6),phiw,w)
rmst2dw=rms(mag(:,7),phiw,w)
t2ddpsw=rmst2dw*wsc/dtr
%rmst2w=rms(mag(:,8),phiw,w)
%rmsiw=rms(mag(:,9),phiw,w)
%rmsvw=rms(mag(:,10),phiw,w)
%rmsfsw=rms(mag(:,12),phiw,w)
%PLOT THE ACCELERATIONS
axis(vv),clg,subplot(211);
loglog(w,mag(:,1).*mf,w,mag(:,3).*mf),xlabel('angular freq. (rad/sec)')
ylabel('acceleration'),grid
title('ACCEL OF MASSES IN RESPONSE TO ROAD VELOCITY'),axis;
semilogx(w,phase(:,1)+pf,w,phase(:,3)+pf)
xlabel('angular freq. (rad/sec)'),ylabel('phase'),grid
pause
%PLOT THE CLEARANCES
axis(vv),clg,subplot(211);
loglog(w,mag(:,2).*mf,w,mag(:,4).*mf,w,magypt),
```

```
xlabel('angular freq. (rad/sec)'),ylabel('clearance'),grid
title('CLEARANCE OF MASSES IN RESPONSE TO ROAD VELOCITY'),axis;
semilogx(w,phase(:,2)+pf,w,phase(:,6)+pf,w,pypt)
xlabel('angular freq. (rad/sec)'),ylabel('phase'),grid
pause
%PLOT THE MAGNET CURRENT AND VOLTAGE AND SECONDARY FORCER
axis(vv);clg,subplot(211)
loglog(w,mag(:,9).*mf,w,mag(:,10).*mf,w,mag(:,12).*mf),
xlabel('angular freq. (rad/sec)'),ylabel('I, V, & F2'),grid
title('MAG. CURRENT, VOLT., & F2 ,IN RESPONSE TO ROAD VELOCITY'),axis;
semilogx(w,phase(:,3)+pf,w,phase(:,4)+pf,w,phase(:,7)+pf),
xlabel('angular freq. (rad/sec)'),ylabel('phase'),grid
pause
%PLOT THE ANGLES
vv=[log10(w(1)),log10(w(n)),-3,1];
axis(vv),clg,subplot(211);
loglog(w,mag(:,6).*mf,w,mag(:,8).*mf),
xlabel('angular freq. (rad/sec)'),ylabel('clearance'),grid
title('ROTATION OF MASSES IN RESPONSE TO ROAD VELOCITY'),axis;
semilogx(w,phase(:,6)+pf,w,phase(:,8)+pf)
xlabel('angular freq. (rad/sec)'),ylabel('phase'),grid
diary off
```

APPENDIX D
WEIGHT AND POWER ESTIMATES FOR ON-BOARD EQUIPMENT

D.1 Weight

D.1.1 Weight of Vehicle Structure

The weight of the vehicle structure, interior furnishings, certain equipment, and landing gear (in the case of the EDS vehicles) was estimated based on aircraft practice, since Maglev vehicles are expected to more closely resemble, in terms of weight criticality, aircraft than rail vehicles. A NASA Study[49] has demonstrated that there is a very good correlation between the weight of transport aircraft structures and subsystems with such basic parameters as the number of passengers and vehicle takeoff gross weight. Simple equations were developed in that study which, when applied to three existing transport aircraft covering the range from small to very large, predicted weight to within $\approx\pm 5\%$ of the actual values.

Table D-1 summarizes the equations which were used in estimating vehicle weight and passenger capacity; these equations are those contained in the spreadsheets appearing as Tables 4-1 and 4-2. As may be seen, total loaded vehicle weight was assumed to be 40 Mg. An iterative procedure was used to determine passenger capacity for that vehicle weight, since the weight of major elements (particularly cabin structure and vehicle furnishings) depends on the number of passengers.
The following sections provide additional explanation of the weight estimation details.

D.1.2 Vehicle Structure and Furnishings

The estimated weight of the cabin structure was arbitrarily increased by 50% over the value predicted by the equations from the reference, to account for the different service conditions expected to be encountered by Maglev vehicles, especially those which might be operated in multi-car trains. These conditions include especially the moving vehicle-to-vehicle contact which may be expected to occur.

The vehicle furnishings include seats, floor covering, insulation, side panels & ceiling structure, coat/baggage compartments, complete lavatory installation, complete

Category	Description	Units	Symbol	Formula (EMS I Separate heave & sway, LIM)
BASIC VEHICLE				
	Vehicle body structure	Mg	m_body	=1.5*0.0004536*IF(N_pass<=100,(110*N_pass),(161*N_pass-5110))
	Interior furnishings (seats, lavs, etc.)	Mg	m_furn	=0.0004536*IF(N_pass<=80,(62.3*N_pass+290),(118.4*N_pass-4190))
HVAC, INSTRUMENTS, LANDING GEAR				
	HVAC			
	Basic equipment	Mg	m_hvac	=0.0004536*(1-0.29)*(13.6*N_pass)
	Power conditioning & batteries	Mg	m_batt_hvac	=0.0004536*P_hvac*lb_per_kW
	Instruments	Mg	m_inst	=0.0004536*(1.872*N_pass+128)
	Landing gear	Mg	m_land	=IF(ldg_gear="N/A","N/A",(1-0.038*(10-6))*0.0004536*(0.044*1000/0.4536*m_total-672))
	Roll damper & actuator	Mg	m_roll	=IF(A_tail="N/A","N/A",(5.03*A_tail+87+2.17*A_tail^0.973)*0.0004536)
LEVITATION & PROPULSION				
	Levitation & guidance magnets	Mg	m_mag	=1.54+1.93
	Motor stator	Mg	m_motor	3.71
	Bogie structure & secondary susp.	Mg	m_bogie	=f_bogie*SUM(m_mag,m_motor)
	Power conditioning & batteries	Mg	m_batt_lev	=(P_hvac+P_lev)*lb_per_kW*0.0004536
CRYOGENIC REFRIGERATION				
	Power conditioning & batteries	Mg	m_cyro	=IF(P_cryo="N/A","N/A",0.0004536*P_cryo*lb_per_kW)
PAYLOAD				
	Passenger weight	Mg	m_pass	=0.0004536*N_pass*180
	Carry-on baggage	Mg	m_carry	=0.0004536*N_pass*20
	Checked baggage	Mg	m_chek	=0.0004536*N_pass*66
	Total payload	Mg	m_pay	=SUM(m_pass:m_chek)
SUMMARY				
	Total Gross Weight, loaded	Mg	m_total	40
	Passenger capacity		N_pass	=IF(m_add>fuzz,N_pass+1,IF(m_add<-fuzz,N_pass-1,N_pass))
MISCELLANEOUS				
	Atail	ft^2	A_tail	N/A
	Additional payload	Mg	m_add	=m_total-SUM(m_body:m_chek)
	HVAC power	kW	P_hvac	=0.001*(48770+N_pass*167.5)
	Levitation power	kW	P_lev	=119+18.8
	Pwr cond + battery	lb/kW	lb_per_kW	17.4
	Refrigeration powe	kW	P_cryo	N/A
	Bogie structure & sec. susp. (fraction of magnet weight)		f_bogie	0.5
	Limit of weight erro	Mg	fuzz	=0.0004536*(200+20+66+110+290)
	Landing gear		ldg_gear	N/A

Table D-1. Vehicle Weight and Passenger Capacity with equations galley installation, attendant seats, fire warning and extinguishing system, exterior finish and miscellaneous emergency equipment (excluding emergency exit slides).

D.1.3 Passengers and Baggage

Each passenger was assumed to weigh 81.7 kg (180 pounds), carry-on baggage 9.07 kg (20 pounds) per passenger and checked baggage 29.9 kg (66 pounds) per passenger.

Landing Gear

Landing gear were provided for all of the EDS vehicles, since the EDS levitation generally does not provide sufficient lift to support the vehicle at low speeds. The estimated landing gear weight for aircraft is a function of the takeoff gross weight; a gross vehicle weight of 40 Mg was used here for estimating gear weight. The landing gear weight for aircraft was estimated on the basis of a sink speed (vertical velocity) of 10 feet/second at touchdown[48]. This was deemed excessive for maglev vehicles, and a value of 6 feet/second was assumed (this is the vertical velocity at contact after a 6 inch free fall); gear weight was derated to this value using the formula provided for sink speeds greater than 10 feet/second.

Roll Damper Aerodynamic Actuator

The Image Flux system (Magneplane type) has no inherent damping for roll motion (through proper design, this system can implement either heave damping or roll damping, but not both, through suitable modulation of the propulsion windings; this study assumed that heave damping was thus provided). Consequently, an aerodynamic control surface was provided to implement the roll damping assumed in the ride quality evaluations. The weight of this surface and its control actuator was based on a surface area of 1.115 m^2 (12 ft^2).

Batteries and Power Conditioning Equipment

Batteries

In all cases, wayside power was considered to be available at station stops, and the battery system was therefore assumed to be the power source when away from stations, except for EMS with Linear Induction Motors (LIM), which utilize wayside power pickup at all times, except for emergency operation. Emergency power requirements are assumed to be the same for all vehicle types. Nickel-cadmium wet cells were assumed, having a specific power of 25.35 Watt-hour/kg (11.5 Watt-hour/pound).

Maximum safe discharge current for these batteries is conservatively the amp-hour rating ÷ 15.

There are two separate constraints on battery sizing; battery weight was taken as the larger of the weight determined by each of the constraints.

(a) Minimum allowable operating time to discharge; this was assumed to be 12 minutes.

$$W' = \frac{\text{Power x operating time}}{\text{Specific Power}} = \frac{1\ \text{kW} \times \frac{12}{60}}{25.35\ \text{kW/kg}} = 7.88\ \frac{\text{kg}}{\text{kW}}\ (17.4\ \frac{\text{lb}}{\text{kW}})$$

(b) Maximum allowable discharge current.

Assuming 170 kW total power at a system operating voltage of 700 volts, the discharge current is

$$\text{discharge} = \frac{170 \times 10^3}{700} = 243\ \text{Amperes}$$

The minimum battery Ampere-hour rating is

$$(I \times t)_{rated} = \frac{243}{15} = 16\ \text{Ampere-hour}$$

Battery system rated energy storage is then

$$E_{rated} = 16 \times 700\ \text{volts} = 11.33\ \text{kW-hours}$$

and battery weight is

$$W_{battery} = \frac{11.33 \times 10^3}{25.35} = 447\ \text{kg (985 pounds)}$$

For this battery, the time to discharge is

$$t_{discharge} = \frac{16}{243} \times 60 = 3.9\ \text{minutes}$$

Thus, the determining consideration was the minimum operating time at full power, and the specific weight of the battery system was $7.88 \frac{kg}{kW}$ $(17.4 \frac{lb}{kW})$.

Power Conditioning

Power conditioning for three purposes was required in this study. In all cases, wayside power was considered to be available at station stops, and the battery system was therefore assumed to be the sole power source when away from stations, except for EMS with LIM.

(a) EMS Levitation: here the power conditioning system provides the active control power required for stable levitation of the primary suspension electromagnets. A conceptual design for this system was 60 pounds.

(b) Hotel Power: HVAC, lighting, instrumentation, etc. Maximum HVAC power was much larger than any of the other components, which were therefore assumed negligible. A single phase Pulse Width Modulated inverter was assumed, whose weight was negligible in comparison with the batteries which provide the power during the operating periods when wayside power was not available.

(c) Propulsion for EMS with LIM, in which the total propulsion power was conditioned on-board. In this case, wayside power pickup was assumed, and the power conditioning converted wayside power (assumed to be 700 VDC) to three phase AC for driving the LIM. A basic 3-phase Pulse Width Modulated inverter was designed, using Insulated Gate BiPolar transistors and simple LC filters for transient and noise suppression. The weight of this system was estimated to be 493 kg (1,087 pounds).

Heating, Ventilation and Air Conditioning (HVAC)

Estimates of both the power requirements and weight of the HVAC system is described. Following are the assumptions made about the parameters of the system:

Passenger compartment surface area:	124.5 m^2 (1,340 ft^2) - 3.96 meter (13 ft) diameter, half-cylinder, 20 meters (65.6 ft) long
Surface reflectivity	90%
Window area:	5% of outside skin area = 6.21m^2 (66.9 ft^2)
Window optical transmissibility	25%
Temperature	23.9C (75°F) inside

	37.8C (100F) outside (summer)
Relative humidity	85% outside 50% inside
Mean solar constant	0.7948 kW/m^2 (252 BTU/hr/ft^2) (42°N, June)[50]
Thermal conductivities	
Windows	0.313 kW/m^2/°C (0.45 BTU/hr/ft^2/°F)
Walls & floor	0.147 kW/m^2/°C (0.5 BTU/hr/ft^2/°F) (R-2)
Air changes per hour:	10
Passenger heat output	0.117 kW (400 BTU/hr)/person[50]
HVAC overall efficiency	70%

Using these parameters, the total HVAC power input for the vehicle was equal to (48.7 + 0.168 x number of passengers) kW, the value used in Table D-1. It is noted that the HVAC power requirement was dominated by the power required for dehumidification of the incoming ambient air.

D.1.5 Bogey Structure and Secondary Suspension Elements

The weights of the secondary suspension system elements (springs, dampers and actuators for active control) and the structure of the bogey were not individually estimated, since they would vary considerably in detail between the various system configurations. Instead, the combined weight of these elements was estimated at 50% of the weight of the magnets (including weight of cryostats for the EDS systems).

APPENDIX E

SPREADSHEETS FOR ELECTROMAGNETIC SYSTEMS WITH FORMULAS

Table E-1. EMS I with formulas used to calculate the dependent parameters.

	A	B	C	D	E
1		**ElectroMagnetic Suspensio**			Optimized for operation at 134 m/s maximum speed
2		*(Separate vertical & lateral suspensioi*			
3		=NOW()			
4		Asterisk (*) before description Indicat			
5		2 Asterisks (**) after description indic			
6					
7					
8		DESCRIPTION	UNITS	SYMBOL	DESIGN 1
9					baseline
10					
11	VE				
12	*Ds*				
13		*Vehicle mass	kg	m	40000
14		*Vehicle length	m	l_vehicle	30
15		*Design speed	m/s	V	134
16		*frontal area	m^2	Af	12
17		*air density	kg/m^3	roair	1.2
18		*drag coefficient	---	Cd	0.3
19		wind drag force	N	Fd	=0.5*CD*ROAIR*V^2*AF
20		wind drag power	W	Pd	=FD*V
21		*Max. Lift Force(@Max disp.)	g	max_Fz	1.1
22		*Max. Lateral Force(*)(cont.)	g	max_F.l	0.26
23		*Max. Lateral Force(*)(short term)	g	max_sF.l	0.42
24		*Time of Max. (short)Lateral F	sec	t_max	5
25		*Max propulsive force	g	max_Fp	0.21
26		*Maximum ambient temperature	°C	maxTamb	50
27					
28	*Pe*				
29		Power, (ohmic+eddy)/aero. drag	%		=(QC+qc.l+PR+Pr.l+Nmotor*(Pin.real-P.tract))/PD
30		Weight, (magnet+coil)/vehicle	%		=(MMAG+Mmag.l+mmotor)/M
31		eddy/lift amp-T (up. bound)	%		=NIE/NI
32		Aerodynamic drag/lift force	%		=FD/(9.8*M)
33					
34	CC				
35		*air permeability	N/A^2	mu	=PI()*0.0000004
36					
37	<u>Su</u>				
38		*Construction materials*			
39		*rail			steel
40		*magnet			2V Perm.
41		*coil			alum.
42		*Materials properties*			
43		mass density			
44		*rail	kg/m^3	ror	7506.3662183
45		*magnet	kg/m^3	rom	7784.3797819
46		*coil	kg/m^3	roc	2780.1356364
47		maximum flux density			
48		*rail	T	Bsatr	1.6
49		*magnet	T	Bsatm	2.3
50		*Saturation Safety Factor(<1)	---	SF	1
51		electrical resistivity			
52		*rail @20°C	ohm-m	rr	0.0000004061
53		*Temp. coefficient of rail	ohm-m/°C	rr_tc	
54		*coil @140 deg C	ohm-m	rc_	0.0000000406
55		*Temp. coefficient of coil	ohm-m/°C	rc_tc	
56		Thermal			
57		*magnet heat transfer coef.	W/C-m^2	k	=0.009*39.4^2
58		*Coil Specific heat	J/(kg°C)	cp	118.85
59		*Maximum wire insulation temp	°C	maxTins	200
60					
61	<u>Ur</u>				
62		*Construction materials*			
63		*rail			steel
64		*rail conductor(s)			aluminum

Table E-1. EMS I with formulas used to calculate the dependent parameters.

	A	B	C	D	E
1		**ElectroMagnetic Suspensio**			Optimized for operation at 134 m/s maximum speed
2		*(Separate vertical & lateral suspensio*			
3		=NOW()			
4		Asterisk (*) before description indicat			
5		2 Asterisks (**) after description indic			
6					
7					
8		DESCRIPTION	UNITS	SYMBOL	DESIGN 1
65		*magnet			M-19
66		*magnet coil			aluminum
67		*Materials properties*			
68		Mass density			
69		*rail	kg/m^3	rom.g	7506.3662183
70		*rail conductor(s)	kg/m^3	roc.g	2780.1356364
71		*magnet	kg/m^3	rom.v	7650
72		*coil	kg/m^3	roc v	2780.1356364
73					
74		maximum flux densities			
75		*rail	T	bsat.g	1.6
76		*magnet	T	bsat.v	1.5
77		Magnetic permeability			
78		rail	---	mu.g	3500
79		Vehicle (short) stator		mu.v	
80					
81		Core Loss @ 1.0T, 100 Hz	W/kg	refc.loss	2.87
82		Core loss frequency exponent	-	freq.exp	1.5
83		Core loss Induction exponent	-	B.exp	2.1
84		Core loss @ fsync & Bcore	W/kg	c.loss	=refc.loss*(fsync/100)^freq.exp*(Bcore.v/1)^B.exp
85					
86		electrical resistivity			
87		*Magnet laminations @ 140°C	ohm-m	rm.v	=0.0000005*1.4
88		*rail @20 deg C	ohm-m	rm.g	0.0000004061
89		*vehicle coil @20 deg C	ohm-m	rcRT.v	0.00000002781
90		*vehicle coil temperature coefficient	1/°C	alpha.v	0.0041
91		vehicle coil @operating temperature	ohm-m	rc.v	=rcRT.v*(1+alpha.v*(Tw.lim-20))
92		*Guideway conductor @20 deg c	ohm-m	rc.g	=0.000000028
93					
94		Heat transfer coefficients			
95		*magnet heat transfer coef.	W/C-m^2	k.v	=3*k.g
96		*rail heat transfer coef.	W/C-m^2	k.g	=0.009*39.4^2
97					
98	CC				
99	Vg				
100		*Geometric dimensions*			
101		*pole width	m	lp	0.0254
102		*air gap	m	H1x	0.01
103		*window width	m	w	0.084
104		*window height	m	h	0.045
105		Window width/height	---		=W/H
106			---		=IF(E105<2,"OK","TOO LARGE!")
107		*coil packing factor	---	f	0.7
108		*pole-coil clearance*	m	z	=0.2/39.4
109		*Number magnets required	---	nmag	4
110		magnet length	m	L	=9.8*M*max_Fz*2*MU/(B0^2*LP*2*NMAG)
111		Magnet length/vehicle length ratio			=IF(L/l_vehicle<=0.5,"OK","TOO LONG!")
112					
113		*Magnet design*			
114		*leakage/fringing flux ratios*			
115		√ fringing (across air gap)	---	nuf	=PF/PU
116		√ leakage (between poles)	---	nul	=PL/PU
117		√total	---	nut	=1+(NUL+nuf)
118		√nominal field in air gap(@2*H1x)	T	Bo	=BSATM/(1+2*(nuf+NUL))
119		√Max. Force per magnet(@2*H1x)	N	Fpm	=2*LP*L*B0^2/(2*MU)
120		√Max. vertical g's @ twice nom. gap	g		=IF(4*Fpm/(M*9.8)>=max_Fz,"OK","TOO SMALL!")

Table E-1. EMS I with formulas used to calculate the dependent parameters.

	A	B	C	D	E
1		**ElectroMagnetic Suspensio**			Optimized for operation at 134 m/s maximum speed
2		*(Separate vertical & lateral suspensio*			
3		-NOW()			
4		Asterisk (*) before description indicat			
5		2 Asterisks (**) after description indice			
6					
7					
8		DESCRIPTION	UNITS	SYMBOL	DESIGN 1
121		√Max amp turns per coil(@ 2H1x)	A	NI	-(2*H1X)*B0/MU
122		√Max. steady state NI (1 coil@1g)		NI_ss	-B0*SQRT(1/max_Fz)*H1X/MU
123		√core mass (1 mag)	kg	Mcore	-ROM*L*(W*LP+2*LP*(H+LP))
124		√mass core + coil (4 mag)	kg	Mmag	-4*(MCORE+2*Mc)
125		√Total magnet weight/vehicle wt.		%	-MMAG/M
126					
127		*Coil Design*			
128		√resist (1 coil, of 2 on magnet)	ohm	resc	-RC_*LC/AC
129		√Max. St. st. ohmic power(N mags)	W	qm_ss	-2*RESC*NMAG*(NI_ss)^2
130		√Max coil ohmic power (N magnets)	W	qc	-2*RESC*NI^2*NMAG
131		√Maximum coil power(1 coil)	W	qc_max	-NI^2*RESC
132		√Max. steady state coil power(1 coil)	W	qc_ss	-NI_ss^2*RESC
133		√Steady state temperature rise	°C	Tm_ss	-qc_ss/(NMAG*ADIS*K)
134		√Short term temperature rise	°C	Tm_st	-QC*t_max/(Mc*cp)
135		Maximum coil temperature	°C	Tc_max	-maxTamb+Tm_ss
136		√mass(one coil)	kg	Mc	-ROC*AC*LC
137					
138		*Rail design*			
139		√rail thickness	m	tr	-LP*(BSATM/BSATR)
140		√rail pole tip width	m	lr	-TR+2*H1X
141		rail mass/length(2 rails)	kg/m	mr	-2*ROR*(2*(TR+H1X)+TR*(W+LP-lr))
142					
143		nominal rail flux density	T	Br	-B0*(1+nuf)*(LP/TR)
144		eff. freq. for eddy anal.	Hz	Fe	-0.5*V/L
145		dB/dt amp. first harmonic	T/s	B1x	-4*FE*BR
146		eddy current power	W	Pr	-B1X^2*TR^3*L*(W+LP)*NMAG/(24*RR)
147		rms eddy amp turn			
148		(upper bound, 1 magnet)	A	NIe	-0.7071*B1X*TR^2*(W+LP)/(8*RR)
149		√Total continuous power	W	P.v	-PR+qm_ss
150					
151	*La*				
152		*Geometric dimensions*			
153		*pole width	m	lp.l	0.023
154		*window width	m	w.l	0.08
155		*window height	m	h.l	0.075
156		Window width/height ratio	---		-w.l/h.l
157		*	---		-IF(w.l/h.l<2,"OK","TOO LARGE!")
158		*coil packing factor	---	f.l	0.7
159		*air gap	m	H1x.l	0.01
160		*pole-coil clearance	m	z.l	-0.2/39.4
161		*Number magnets required	---	nmag.l	4
162		magnet length	m	L.l	-9.8*M*max_sF.l/(nmag.l/2)*2*MU/(2*(B0.l^2*lp.l))
163		Magnet length/vehicle length			-IF(L.l/l_vehicle<=0.5,"OK","TOO LONG!")
164					
165		*Magnet design*			
166		flux leakage coefficients			
167		fringing (across air gap)	---	nuf.l	-Pf.l/Pu.l
168		leakage (between poles)	---	nul.l	-Pl.l/Pu.l
169		total	---	nut.l	-1+(nuf.l+nuf.l)
170		nominal field in air gap	T	B0.l	-BSATM/(1+2*(nuf.l+nul.l))
171		√Max. Force per magnet(@2*H1x.l)	N	Fpm.l	-2*lp.l*L.l*B0.l^2/(2*MU)
172		Max. lateral g's @ twice nom. gap	g		-IF(2*Fpm.l/M>=max_sF.l,"OK","TOO SMALL!")
173		Max. amp turns per coil(@2H1x.l)	A	NI.l	-2*H1x.l*B0.l/MU
174		√Max. steady state NI (one coil)		NI_ss.l	-B0.l*SQRT(max_F.l/max_sF.l)*H1x.l/MU
175		core mass (1 mag)	kg	Mcore.l	-ROM*L.l*(w.l*lp.l+2*lp.l*(h.l+lp.l))
176		√mass core + coil (4 mag)	kg	Mmag.l	-4*(Mcore.l+2*Mc.l)

Table E-1. EMS I with formulas used to calculate the dependent parameters.

	A	B	C	D	E
1		**ElectroMagnetic Suspensio**			Optimized for operation at 134 m/s maximum speed
2		*(Separate vertical & lateral suspensioi*			
3		-NOW()			
4		Asterisk (*) before description indicat			
5		2 Asterisks (**) after description indic			
6					
7					
8		DESCRIPTION	UNITS	SYMBOL	DESIGN 1
177		Total magnet weight/vehicle wt.		%	-Mmag.l/M
178					
179		*Coil design*			
180		√resist(1 coil, of 2 on magnet)	ohm	resc.l	-RC_*lc.l/ac.l
181		√Max. St. st. ohmic power(N/2 mags)	W	qm_ss.l	-2*qc_ss.l*nmag.l/2
182		√Max. ohmic power (N/2 magnets)	W	qc.l	-2*qc_max.l*nmag.l/2
183		√Maximum coil power(1 coil)	W	qc_max.l	-Ni.l^2*resc.l
184		√Max. steady state coil power(1 coil)	W	qc_ss.l	-NI_ss.l^2*resc.l
185		√Steady state temperature rise	°C	Tm_ss.l	-qc_ss.l/(adis.l*K)
186		√Short term temperature rise	°C	Tm_st.l	-qc.l*t_max/(Mc.l*cp)
187		Maximum coil temperature	°C	Tc_max.l	-maxTamb+MAX(Tm_ss.l,Tm_st.l)
188		√mass(one coil)	kg	Mc.l	-ROC*ac.l*lc.l
189					
190		*Rail design*			
191		√rail thickness	m	tr.l	-lp.l*(B0.l*BSATR)*(1+2*nuf.l)
192		√rail pole tip width (-tr)	m	lr.l	-lp.l+2*H1x.l
193		rail mass/length(two rails)	kg/m	mr.l	-2*ROR*(2*lr*(tr.l+H1x.l)+tr.l*(w.l+lp.l-lr.l))
194					
195		nominal rail flux density(centered?)	T	Br.l	-B0.l*SQRT(max_F.l/max_sF.l)*(1+nuf.l)*(lp.l/tr.l)
196		*eff. freq. for eddy anal.*	Hz	Fe.l	-0.5*V/L.l
197		dB/dt amp. first harmonic	T/s	B1x.l	-4*Fe.l*Br.l
198		eddy current power	W	Pr.l	-B1x.l^2*tr.l^3*L.l*(w.l+lp.l)*nmag.l/(24*RR)
199		rms eddy amp turn			
200		(upper bound, 1 magnet)	A	Nie.l	-0.7071*B1x.l*tr.l^2*(w.l+lp.l)/(8*RR)
201		*Maximum continuous Power*	W	P.l	*-Pr.l+qc_ss.l*2*nmag.l/2*
202		Peak Power(@ V, max F & displ.)	W		
203					
204	*Lir*				
205					
206		Design maximum thrust	g	max.g	0.21
207		Design maximum thrust	N	max.thr	-max.g*M*9.8
208		Nominal excitation frequency	Hz	fsync	-V/(2*tau.v*(1-nom.slip))
209		Synchronous speed	m/s	vsync	-V/(1-nom.slip)
210		Nominal slip		nom.slip	0.01
211					
212		*General*			
213		*Number of motors		Nmotor	4
214		*Number of poles		Np.v	16
215		*Geometric dimensions*			
216		*Air gap (mechanical clearance)	m	cl.v	0.01
217		*Pole pitch	m	tau.v	-1/3
218		*Slots/pole/phase		Nslots	2
219		*Core width	m	d.v	0.21
220		*Tooth width/slot width ratio		tsr.v	1.2
221		*Slot depth	m	h.v	0.05
222		*Lamination thickness	m	tlam.v	0.000356
223		Magnetic gap (entrefer)	m	g.mag	-cl.v+tc.g
224		Carter factor		Kcarter	-sp.v*(5*g.mag+w.v)/(sp.v*(5*g.mag+w.v)-w.v*w.v)
225		Effective magnetic gap	m	ge.lim	-g.mag*Kcarter
226		Back iron thickness, vehicle	m	ty.v	-Fpp/(2*d.v*bsat.v)
227		Tooth width	m	lt.v	-w.v/tsr.v
228		Slot width	m	w.v	-tau.v/(Nslots*Nphase.v*(1+1/tsr.v))
229		Slot pitch (-tooth pitch)	m	sp.v	-lt.v+w.v
230		Number of laminations		Nlams.v	-INT(d.v/tlam.v)
231		Motor effective length	m	Leff	-Np.v*tau.v
232		Motor physical length	m	Lphys	-Leff+2*(Nphase.v*Nslots-1)*sp.v

Table E-1. EMS I with formulas used to calculate the dependent parameters.

	A	B	C	D	E
1		**ElectroMagnetic Suspensio**			Optimized for operation at 134 m/s maximum speed
2		*(Separate vertical & lateral suspensio*			
3		=NOW()			
4		Asterisk (*) before description indicat			
5		2 Asterisks (**) after description indic			
6					
7					
8		DESCRIPTION	UNITS	SYMBOL	DESIGN 1
233		Effective air gap area	m^2	Aface	=Leff*d.v
234		Core exposed surface area	m^2	Acore	=2*(d.v*(h.v+ty.v)+d.v*Lphys+(h.v+ty.v)*Lphys-h.v*w.v*Nphase.v*ncoils.v*Np.v)
235					
236		*Winding parameters*			
237		*Number of phases		Nphase.v	3
238		*Coil pitch/pole pitch ratio(fraction)		cp_tau	=2/3
239		*Number of winding layers		Nlayers.v	2
240		*Number of coils/pole/phase		ncoils.v	2
241		*Coil packing factor		f.v	0.785
242		*Pole/coil clearance	m	z.v	0.005
243		*Turns/coil		Npc.v	1
244		*End turn angle	degrees	alpha	30
245		*End turn projection	m	b	0.01
246		Distribution factor(distributed windin		Kd	=SIN(PI()/Nphase.v)/(Nslots*SIN(PI()/(Nslots*Nphase.v)))
247		Pitch factor(fractional pitch coils)		Kp	=COS(PI()*(1-cp_tau)/2)
248		Winding factor(for distributed winding		Kw	=Kd*Kp
249		Coil pitch	m	tau_c.v	=tau.v*cp_tau
250		Mean conductor length	m/coil	lcoil.v	=2*(tau.v*cp_tau/COS(alpha*PI()/180)+d.v+2*b)
251		Coil thickness	m	tcoil.v	=(h.v-z.v)/Nlayers.v
252		Conductor x-section area/slot/layer	m^2	Acoil.v	=tcoil.v*w.v*f.v
253		Coil Resistance	ohm	Rcoil.v	=Npc.v*rc.v*lcoil.v/Acoil.v
254		Heat transfer area (1 coil)	m^2	Aht.v	=2*(w.v+tcoil.v)*(d.v+2*(tau.v*cp_tau/COS(alpha*PI()/180)+2*b))
255		Peak MMF per coil RMS amp-turns	-	MMFperNI	=2*SQRT(2)*Nphase.v*Kw*Nslots/PI()
256		Core operating flux density	T	Bcore.v	=bsat.v*E25/max_Fp
257		Coil RMS amp-turns @ Bsat of tooth	Amp-turn	NIcoil.v	=bsat.v*lt.v*ge.lim/(MU*sp.v*MMFperNI)
258		Total flux per pole @ Bsat of tooth	Webers	Fpp	=2*MMFperNI*NIcoil.v*MU*d.v*tau.v*(1+nuf.lim)/(ge.lim*PI())
259		RMS phase current @ Bsat of tooth	A	Iphase.v	=NIcoil.v/Npc.v
260		Total RMS slot current @ Bsat of tooth	A	Islot .v	=Nlayers.v*Iphase.v
261		Coil power (1coil)	W	Pcoil.v	=Rcoil.v*Iphase.v^2
262		Coil surface temperature rise	°C	delTavg.v	=Pcoil.v/(Aht.v*k.v)
263		Maximum coil surface temperature	°C	Tw.lim	=maxTamb+delTavg.v
264		Slot current	A-conduct.	I.slot	=NIcoil.v*Nlayers.v
265		Linear current loading	A/m	I.load	=NIcoil.v*Nlayers.v/sp.v
266					
267		*Stator Leakage Reactance Calculations*			
268		Slot Leakage	ohm	Xslot	=(8*PI()*PI()*0.0000001)*fsync*(Nlayers.v*Npc.v)^2*d.v*(Nslots*Np.v)*(z.v/w.v+(h.v-z.v)/(3*w.v))
269		End turn leakage	ohm	Xec	=(1.418*0.0000001*fsync*SQRT(2)*Kd^2*(Npc.v*Nlayers.v)^2*Nphase.v*((PI()*cp_tau-SIN(PI()*cp_tau))/PI()*cp_tau)/(PI()*(Np.v/2)^2))*tau_c.v*TAN(alpha*PI()/180)/2
270		Total Primary Leakage Reactance	ohm	Xleak	=SUM(E268:E269)
271					
272		Stator Leakage Reactance @ 50 Hz.			
273		Leakage Reactance @ 50 Hz.	ohm/phase	X50_	=Xleak*50/fsync
274		Coil Resistance	ohm/phase	Rone	=Rcoil.v*ncoils.v*Np.v*Nlayers.v
275		Reactance/Resistance ratio @ 50 Hz.	-	alpha50	=X50_/Rone
276					
277		Series turns/phase		stp.lim	=Npc.v*ncoils.v*Np.v
278		Resistance, Primary	ohm/phase	rp.lim	=ncoils.v*Nlayers.v*Np.v*Rcoil.v
279					
280		Motor iron weight, single stator	kg	mi.v	=rom.v*Lphys*d.v*(ty.v+h.v/(1+1/tsr.v))
281		Motor conductor weight, single stator	kg	mc.v	=roc.v*Nslots*Nphase.v*Np.v*Acoil.v*lcoil.v
282		Total motor weight(Nmotor motors)	kg	mmotor	=Nmotor*(mi.v+mc.v)
283					
284		Core loss power, single stator	W	Pcore	=c.loss*mi.v
285		Core temperature rise	°C	delTcore	=Pcore/(Acore*k.v)
286		Core surface temperature	°C	Tcore	=maxTamb+delTcore
287					
288		Motor Secondary (guideway) Design Pa			

Table E-1. EMS I with formulas used to calculate the dependent parameters.

	A	B	C	D	E
1		**ElectroMagnetic Suspensio**			Optimized for operation at 134 m/s maximum speed
2		*(Separate vertical & lateral suspensioi*			
3		-NOW()			
4		Asterisk (*) before description indicati			
5		2 Asterisks (**) after description indice			
6					
7					
8		DESCRIPTION	UNITS	SYMBOL	DESIGN 1
289		Iron			
290		Back iron thickness, guideway	m	ty.g	-Fpp/(2*d.g*bsat.g)
291		Back iron width	m	d.g	-d.v+2*g.mag
292		Guideway iron specific weight	kg/m	mi.g	-rom.g*1*d.g*ty.g
293		Conductor			
294		*Conductor overlap factor		coll.g	0.4
295		*Conductor thickness	m	tc.g	0.005
296		Conductor width	m	dc.g	-d.g+2*coll.g*tau.v
297		*Guideway conductor specific weight*	*kg/m*	*mc.g*	*-roc.g*1*dc.g*tc.g*
298		Total guideway added weight	kg/m	m.gw	-Nmotor*(mc.g+mi.g)
299					
300	Pe				
301		Individual Motor Parameters at Maximu			
302		Thrust**	N	Thrust	20427
303		Slip**	-	slip	41358
304		Traction Power**	W	P.tract	2736900
305		Real input Power**	W	Pin.real	2819700
306		Reactive input Power**	V-A	Pin.react	3219400
307		Efficiency**	%	eff.v	96.5392
308		Power Factor		PwrFac	-COS(ATAN(Pin.react/Pin.real))
309					
310					
311					
312		**AUXILIARY CALCULATIONS**			
313		**LIFT MAGNETS**			
314		***permeances***			
315		√Air gap fringing permeance/length		Pf	1.92
316		√Ideal air gap permeance/length		Pu	-LP/H1X
317		?Inter-pole leakage perm./length		Pl	-(H-H1X)/W
318		***coil dimensions***			
319		√Mean turn length	m	lc	-2*(L+PI()*W/4+LP)
320		√*Coil crossectional area(one coil)*	m^2	ac	-(H-Z)*W/2*F
321		√Coil Surface area(for 1 coil)	m^2	adis	-0.5*(4*L*(LP+W+H)+4*H*LP+2*LP*(2*LP+W)+4*LP*W+PI()*W*W+2*(H-Z)*PI()*W)
322		**GUIDANCE MAGNETS**			
323		***permeances***			
324		√Air gap fringing permeance/length		Pf.l	1.92
325		√Ideal air gap permeance/length		*Pu.l*	*-lp.l/H1x.l*
326		?Inter-pole leakage perm./length		Pl.l	-(h.l-H1x.l)/w.l
327		***coil dimensions***			
328		√ Mean turn length(one coil)	m	lc.l	-2*(L.l+PI()*w.l/4+lp.l)
329		√Coil crossectional area(one coil)	m^2	ac.l	-(h.l-z.l)*w.l/2*f.l
330		√Coil Surface area(for one coil)	m^2	adis.l	-0.5*(4*L.l*(lp.l+w.l+h.l)+4*h.l*lp.l+2*lp.l*(2*lp.l+w.l)+4*lp.l*w.l+PI()*w.l*w.l+2*(h.l-z.l)*PI()*w.l)
331		**LINEAR INDUCTION MOTOR**			
332		***permeances***			
333		Ideal air gap permeance/length		Pu.lim	-d.v/ge.lim
334		*Air gap fringing permeance/length*		*Pf.lim*	*-1.92*
335		Fringing permeance ratio		nuf.lim	-Pf.lim/Pu.lim
336					
337					
338	El				
339	We				
340		Lift Magnets	kg		-MMAG
341		Guidance Magnets	kg		-Mmag.l
342		Linear Induction Motor	kg		-mmotor
343		***Total***	kg		-SUM(E340:E342)
344	We				

Table E-1. EMS I with formulas used to calculate the dependent parameters.

	A	B	C	D	E
1		**ElectroMagnetic Suspensio**			Optimized for operation at 134 m/s maximum speed
2		*(Separate vertical & lateral suspensior*			
3		=NOW()			
4		Asterisk (*) before description indicat			
5		2 Asterisks (**) after description indic			
6					
7					
8		DESCRIPTION	UNITS	SYMBOL	DESIGN 1
345		Lift Magnets	kg/m		=mr
346		Guidance Magnets	kg/m		=Mmag.l
347		Linear Induction Motor	kg/m		=m.gw
348		**Total**	kg/m		=SUM(E345:E347)
349	*Re*				
350		*Ohmic Power Dissipation*			
351		Lift Magnets	W		=qm_ss
352		Guidance Magnets	W		=qm_ss.l
353		Linear Induction Motor	W		=Pin.real-P.tract
354		Total Ohmic Power	W		=SUM(E351:E353)
355		*Eddy current Power*			
356		Lift Magnets	W		=PR
357		Guidance Magnets	W		=Pr.l
358		Total eddy current Power	W		=SUM(E356:E357)
359		**Total Real Power Dissipation**	W		=SUM(E358,E354)
360	*Re*				
361		Linear Induction Motor	V-A		=Pin.react
362		**Total**	V-A		=SUM(E361:E361)

Table E-2. EMS II with formulas used to calculate the dependent parameters.

	A	B	C	D	E
1		ElectroMagnetic Suspension IIA			
2		(Combined vertical & lateral suspensi			
3		=NOW()			
4		Asterisk (*) before description indicat			
5		2 Asterisks (**) after description indic			
6					
7					
8		DESCRIPTION	UNITS	SYMBOL	DESIGN 1
9					baseline
10					
11	VEH				
12	*Desi*				
13		*Vehicle mass	kg	m	40000
14		*Vehicle length	m	l_vehicle	30
15		*Design speed*	m/s	V	134
16		*frontal area	m^2	Af	12
17		*air density	kg/m^3	roair	1.2
18		*drag coefficient		Cd	0.3
19		*wind drag force*	N	Fd	=0.5*CD*ROAIR*V^2*AF
20		wind drag power	W	Pd	=FD*V
21		*Max. Lift Force(@Max disp.)	g	max_Fz	1.1
22		*Max. Lateral Force(*)(cont.)	g	max_F.l	0.26
23		*Max. Lateral Force(*)(short term)*	g	max_sF.l	0.42
24		*Time of Max. (short)Lateral F	sec	t_max	5
25		*Max propulsive force	g	max_Fp	0.21
26		*Maximum ambient temperature	°C	maxTamb	50
27					
28	*Perf*				
29		Power, (ohmic+eddy)/aero. drag	%		=(QC+PR)/PD
30		Weight, (magnet+coil)/vehicle	%		=MMAG/M
31		*eddy/lift amp-T (up. bound)*	%		*=NIE/NI*
32		Aerodynamic drag/weight	%		=FD/(9.8*M)
33					
34	CON				
35	*Gen*				
36		*air permeability	N/A^2	mu	=PI()*0.0000004
37					
38	*Susi*				
39		*Construction materials*			
40		*rail			steel
41		*magnet			2V Perm.
42		*coil			alum.
43		*Materials properties*			
44		*mass density*			
45		*rail	kg/m^3	ror	7850
46		*magnet	kg/m^3	rom	7850
47		*coil	kg/m^3	roc	2550
48		*Saturation flux density*			
49		*rail	T	BsatR	1.4
50		*magnet	T	BsatM	1.4
51		*Saturation Safety Factor(<1)	--	SF	1
52		*Electrical resistivity*			
53		*rail @20 deg C	ohm-m	rr	0.0000002
54		*coil @190 deg C	ohm-m	rc_	0.0000000472
55		*Thermal*			
56		*magnet heat transfer coef.	W/°C-m^2	h_s	20
57		*Conductor thermal conductivity	W/(°C m^2)	k_c	220
58		*Insulation thermal conductivity	W/°C-m^2	k_ins	0.173
59		*coil packing factor	...	f	=PI()/4
60		*Coil Width packing factor	...	f_y	=SQRT(F)
61		*Coil thickness packing factor	...	f_z	=SQRT(F)
62		*Maximum ambient temperature	°C	T	55
63		*Coil Specific heat	J/(kg*C)	cp	118.85
64		*Maximum wire insulation temp	°C	maxTins	220
65					
66	*Line*				
67		*Construction materials*			
68		*rail			steel
69		*rail conductor(s)			aluminum
70		*magnet*			M-19
71		*magnet coil			aluminum
72		*Materials properties*			
73		*Mass density*			

Table E-2. EMS II with formulas used to calculate the dependent parameters.

	A	B	C	D	E
1		ElectroMagnetic Suspension IIA			
2		(Combined vertical & lateral suspensi			
3		=NOW()			
4		Asterisk (*) before description indicat			
5		2 Asterisks (**) after description indic			
6					
7					
8		DESCRIPTION	UNITS	SYMBOL	DESIGN 1
74		*rail	kg/m^3	rom.g	7506.3662183
75		*rail conductor(s)	kg/m^3	roc.g	2780.1356364
76		*magnet	kg/m^3	rom.v	7650
77		*coil	kg/m^3	roc.v	2780.1356364
78		*maximum flux densities*			
79		*rail	T	bsat.g	1.6
80		*magnet	T	bsat.v	1.5
81		*Magnetic permeability*			
82		rail		mu.g	3500
83		Vehicle (short) stator		mu.v	
84		*Core loss*			
85		Core Loss @ 1.0T, 100 Hz	W/kg	refc.loss	2.87
86		Core loss frequency exponent		freq.exp	1.5
87		Core loss induction exponent		B.exp	2.1
88		Core loss @ fsync & Bcore	W/kg	c.loss	=REFC.LOSS*(FSYNC/100)^FREQ.EXP*(BCORE.V/1)^B.EXP
89					
90		*Electrical resistivity*			
91		*Magnet laminations @ 140°C	ohm-m	rm.v	=0.0000005*1.4
92		*rail @20 deg C	ohm-m	rm.g	0.0000004061
93		*vehicle coil @20 deg C	ohm-m	rcRT.v	0.00000002781
94		*vehicle coil temperature coefficient	1/°C	alpha.v	0.0041
95		vehicle coil @operating temperature	ohm-m	rc.v	=RCRT.V*(1+ALPHA.V*(TW.LIM-20))
96		*Guideway conductor @20 deg c	ohm-m	rc.g	=0.000000028
97					
98		*Heat transfer coefficients*			
99		*magnet heat transfer coef.	W/C-m^2	k.v	=3*K.G
100		*rail heat transfer coef.	W/C-m^2	k.g	=0.009*39.4^2
101					
102	COA				
103	*Vert*				
104		*Geometric dimensions*			
105		*Lateral stagger	m	del	0.015
106		*pole width	m	lp	0.04
107		*window width	m	w	0.229
108		*window height	m	h (or d)	0.092
109		*air gap	m	H1x	0.0125
110		*pole-coil clearance	m	z	=0.2/39.4
111		*Number magnet sets required	...	nmag.N.sets	4
112		*Number individual magnets/set	.	N.mags	2
113					
114	*Perf*				
115		Individual magnet total weight	kg	W_mag_coil	=MCORE+MCOIL
116		Lift-to-weight ratio	...	LTWR	=(M/8)/W_MAG_COIL
117		Power-to-lift ratio	kW/tonne	PTLR	=8*OC/M
118		Total weight of magnet assemblies	kg	M_magnets	=8*W_MAG_COIL
119		Magnet-to-Vehicle weight ratio	...	MVWR	=M_MAGNETS/M
120		Max. lateral force @y*(1 set)	kg	F_y_star	=4*F_CLASS*(2*H1X/(PI()*LP))*ALPHA_G.DEL.Y_S
121		Required max lateral force(1 set)	kg	F_ymax	=M*9.8*MAX_SF.L/NMAG_N.SETS
122		Max. lift force @y*(1 set)	kg	Fz_y_star	=4*F_CLASS*(1+(2*H1X/(PI()*LP))*(1-(DEL+Y_STAR)/H1X)*ATAN((DEL+Y_STAR)/H1X))
123		Required max. lift force(1 set)	kg	F_zmax	=M*9.8*MAX_FZ/NMAG_N.SETS
124		Classical lift force (1 mag, y=0)	kg	F_class	=MU*NI^2*L*LP/(4*H1X^2)
125		Lateral stiffness (4 sets)	N/m	K_lateral	=4*F_Y_STAR/Y_STAR
126					
127		*Maganet design*			
128		Decoupling displacement limit	m	y_star	0.021
129		magnet length	m	L	=M*9.8*MAX_FZ*4*H1X^2/(NMAG_N.SETS*N.MAGS*MU*NI^2*LP*ALPHA_G.DEL)
130		width of pole base	m	w_p	=LP*(1+(NU_L.P/NU_G))
131		Magnet yoke length	m	L_y	=L-2*H__OR_D_
132		Magnet yoke height	m	d_y	=LP*(1+LAMBDA)/(1-(2*H__OR_D_/L))
133		Yoke area	m^2	A_yoke	=L_Y*D_Y
134					
135		fringing (across air gap)	...	nuf	=PF/PU
136		leakage (between poles)	...	nul	=PL/PU
137		total	...	nut	=1+(NUL+NUF)
138		Nominal air gap flux density	T	B0	=BSATM*SF*(1+LAMBDA)/MAX(NU_T.MAX1,NU_T.MAX2)

Table E-2. EMS II with formulas used to calculate the dependent parameters.

	A	B	C	D	E
1		ElectroMagnetic Suspension IIA			
2		(Combined vertical & lateral suspensi			
3		=NOW()			
4		Asterisk (*) before description indicat			
5		2 Asterisks (**) after description indic			
6					
7					
8		DESCRIPTION	UNITS	SYMBOL	DESIGN 1
139		Nominal pole tip flux density	T		=B0*NU_G
140		Nominal pole base flux density	T		=B0*(NU_G+NU_L.P)
141		Nominal yoke flux density	T		=B0*NU_T
142		Force per magnet	N	Fpm	=LP*L*B0^2/MU
143		amp turns per magnet	A	NI	=2*H1X*B0/MU
144		core mass (1 mag)	kg	Mcore	=ROM*V_MAG
145		mass core + coil (4 mag)	kg	Mmag	=8*(MCORE+MCOIL)
146					
147		*Coil design*			
148		resistance (1 magnet, 1 turn)	ohm	resc	=RC_*LC/AC
149		coil ohmic power (1 magnet)	W	qc	=RESC*NI^2
150		Surface temperature rise	°C	deltaT_sur	=RC_*NI^2/(F*W*H__OR_D_*(2*H__OR_D_+W)*H_S)
151		Surface temperature	°C	T_s	=MAXTAMB+DELTAT_SUR
152		Internal temperature rise	°C	deltaT_int	=RC_*NI^2/(4*F*W*H__OR_D_*(2*H__OR_D_*F_Y/W)+W*F_Z/(2*H__OR_D_))
153		Maximum internal temperature	°C	T_int	=T+DELTAT_SUR+DELTAT_INT
154		mass(one coil)	kg	Mcoil	=ROC*F*V_COIL
155		Total ohmic power, Nmag*n_mags	W	P_total	=QC*N.MAGS*NMAG_N.SETS
156					
157		*Rail design*			
158		rail thickness	m	tr	=LP*(B0/BSATR)*(1+2*NUF)
159		rail mass/length	kg/m	mr	=2*ROR*(2*E289*(TR+H1X)+TR*(W-2*H1X))
160		nominal rail flux density	T	Br	=B0*(1+NUF)*(LP/TR)
161		eff. freq. for eddy anal.	Hz	Fe	=0.5*V/L
162		dB/dt amp. first harmonic	T/s	B1x	=4*FE*BR
163		eddy current power	W	Pr	=B1X^2*TR^3*L*(W+LP)*NMAG_N.SETS/(24*RR)
164		rms eddy amp turn			
165		(upper bound, 1 magnet)	A	NIe	=0.7071*B1X*TR^2*(W+LP)/(8*RR)
166		Total continuous power	W	P.v	=PR+QC
167					
168					
169					
170	*Line*				
171					
172					
173		Design maximum thrust	g	max.g	0.21
174		Design maximum thrust	N	max.thr	=MAX.G*M*9.8
175		Nominal excitation frequency	Hz	fsync	=V/(2*TAU.V*(1-NOM.SLIP))
176		Synchronous speed	m/s	vsync	=V/(1-NOM.SLIP)
177		Nominal slip		nom.slip	0.01
178		*General*			
179		*Number of motors		Nmotor	4
180		*Number of poles		Np.v	16
181		*Geometric dimensions*			
182		*Air gap (mechanical clearance)	m	cl.v	0.01
183		*Pole pitch	m	tau.v	=1/3
184		*Slots/pole/phase		Nslots	2
185		*Core width	m	d.v	0.21
186		*Tooth width/slot width ratio		tsr.v	1.2
187		*Slot depth	m	h.v	0.05
188		*Lamination thickness	m	tlam.v	0.000356
189		Magnetic gap (entrefer)	m	g.mag	=CL.V+TC.G
190		Carter factor		Kcarter	=SP.V*(5*G.MAG+W.V)/(SP.V*(5*G.MAG+W.V)-W.V*W.V)
191		Effective magnetic gap	m	ge.lim	=G.MAG*KCARTER
192		Back iron thickness, vehicle	m	ty.v	=FPP/(2*D.V*BSAT.V)
193		Tooth width	m	lt.v	=W.V/TSR.V
194		Slot width	m	w.v	=TAU.V/(NSLOTS*NPHASE.V*(1+1/TSR.V))
195		Slot pitch (=tooth pitch)	m	sp.v	=LT.V+W.V
196		Number of laminations		Nlams.v	589
197		Motor effective length	m	Leff	=NP.V*TAU.V
198		Motor physical length	m	Lphys	=LEFF+2*(NPHASE.V*NSLOTS-1)*SP.V
199		Effective air gap area	m^2	Aface	=LEFF*D.V
200		Core exposed surface area	m^2	Acore	=2*(D.V*(H.V+TY.V)+D.V*LPHYS+(H.V+TY.V)*LPHYS-H.V*W.V*NPHASE.V*NCOILS.V*NP.V)
201					
202	*Win*				
203		*Number of phases		Nphase.v	3

Table E-2. EMS II with formulas used to calculate the dependent parameters.

	A	B	C	D	E
1		ElectroMagnetic Suspension IIA			
2		(Combined vertical & lateral suspensi			
3		=NOW()			
4		Asterisk (*) before description indicat			
5		2 Asterisks (**) after description indic			
6					
7					
8		DESCRIPTION	UNITS	SYMBOL	DESIGN 1
204		*Coil pitch/pole pitch ratio(fraction)		cp_tau	=2/3
205		*Number of winding layers		Nlayers.v	2
206		*Number of coils/pole/phase		ncoils.v	2
207		*Coil packing factor		f.v	0.785
208		*Pole/coil clearance	m	z.v	0.005
209		*Turns/coil		Npc.v	1
210		*End turn angle	degrees	alpha	30
211		*End turn projection	m	b	0.01
212		Distribution factor(distributed windin		Kd	=SIN(PI()/NPHASE.V)/(NSLOTS*SIN(PI()/(NSLOTS*NPHASE.V)))
213		Pitch factor(fractional pitch coils)		Kp	=COS(PI()*(1-CP_TAU)/2)
214		Winding factor(for distributed windin		Kw	=KD*KP
215		Coil pitch	m	tau_c.v	=TAU.V*CP_TAU
216		Mean conductor length	m/coil	lcoil.v	=2*(TAU.V*CP_TAU/COS(ALPHA*PI()/180)+D.V+2*B)
217		Coil thickness	m	tcoil.v	=(H.V-Z.V)/NLAYERS.V
218		Conductor x-section area/slot/layer	m^2	Acoil.v	=TCOIL.V*W.V*F.V
219		Coil Resistance	ohm	Rcoil.v	=NPC.V*RC.V*LCOIL.V/ACOIL.V
220		Heat transfer area (1 coil)	m^2	Aht.v	=2*(W.V+TCOIL.V)*(D.V+2*(TAU.V*CP_TAU/COS(ALPHA*PI()/180)+2*B))
221		Peak MMF per coil RMS amp-turns	-	MMFperNI	=2*SQRT(2)*NPHASE.V*KW*NSLOTS/PI()
222		Core operating flux density	T	Bcore.v	=BSAT.V*SQRT(E25/MAX_FP)
223		Coil RMS amp-turns @ Bsat of tooth	Amp-turn	NIcoil.v	=BSAT.V*LT.V*GE.LIM/(MU*SP.V*MMFPERNI)
224		Total flux per pole @ Bsat of tooth	Webers	Fpp	=2*MMFPERNI*NICOIL.V*MU*D.V*TAU.V*(1+NUF.LIM)/(GE.LIM*PI())
225		RMS phase current @ Bsat of tooth	A	Iphase.v	=NICOIL.V/NPC.V
226		Total RMS slot current @ Bsat of tooth	A	Islot .v	=NLAYERS.V*IPHASE.V
227		Coil power (1coil)	W	Pcoil.v	=RCOIL.V*IPHASE.V^2
228		Coil surface temperature rise	°C	delTavg.v	=PCOIL.V/(AHT.V*K.V)
229		Maximum coil surface temperature	°C	Tw.lim	=MAXTAMB+DELTAVG.V
230		Slot current	A-conduct.	I.slot	=NICOIL.V*NLAYERS.V
231		Linear current loading	A/m	I.load	=NICOIL.V*NLAYERS.V/SP.V
232					
233		*Stator Leakage Reactance Calculation:*			
234		Slot Leakage	ohm	Xslot	=(8*PI()*PI()*0.0000001)*FSYNC*(NLAYERS.V*NPC.V)^2*D.V*(NSLOTS*NP.V)*(Z.V/W.V+(H.V-Z.V)/(3*W.V))
235		End turn leakage	ohm	Xec	=(1.418*0.0000001*FSYNC*SQRT(2)*KD^2*(NPC.V*NLAYERS.V)^2*NPHASE.V*((PI()*CP_TAU-SIN(PI()*CP_TAU))/PI()*CP_TAU)/(PI()*(NP.V/2)^2))*TAU_C.V*TAN(ALPHA*PI()/180)/2
236		Total Primary Leakage Reactance	ohm	Xleak	=SUM(E234:E235)
237		Stator Leakage Reactance @ 50 Hz.			
238		Leakage Reactance @ 50 Hz.	ohm/phase	X50_	=XLEAK*50/FSYNC
239		Coil Resistance	ohm/phase	Rone	=RCOIL.V*NCOILS.V*NP.V*NLAYERS.V
240		Reactance/Resistance ratio @ 50 Hz.	-	alpha50	=X50_/RONE
241		Series turns/phase		stp.lim	=NPC.V*NCOILS.V*NP.V
242		Resistance, Primary	ohm/phase	rp.lim	=NCOILS.V*NLAYERS.V*NP.V*RCOIL.V
243		*Weight*			
244		Motor iron weight, single stator	kg	mi.v	=ROM.V*LPHYS*D.V*(TY.V+H.V/(1+1/TSR.V))
245		Motor conductor weight, single stator	kg	mc.v	=ROC.V*NSLOTS*NPHASE.V*NP.V*ACOIL.V*LCOIL.V
246		Total motor weight(Nmotor motors)	kg	mmotor	=NMOTOR*(MI.V+MC.V)
247		*Power*			
248		Core loss power, single stator	W	Pcore	=C.LOSS*MI.V
249		Core temperature rise	°C	delTcore	=PCORE/(ACORE*K.V)
250		Core surface temperature	°C	Tcore	=MAXTAMB+DELTCORE
251					
252		*Motor Secondary (guideway) Design P.*			
253		Iron			
254		Back iron thickness, guideway	m	ty.g	=FPP/(2*D.G*BSAT.G)
255		Back iron width	m	d.g	=D.V+2*G.MAG
256		Guideway iron specific weight	kg/m	mi.g	=ROM.G*1*D.G*TY.G
257		Conductor			
258		*Conductor overlap factor		colf.g	0.4
259		*Conductor thickness	m	tc.g	0.005
260		Conductor width	m	dc.g	=D.G+2*COLF.G*TAU.V
261		Guideway conductor specific weight	kg/m	mc.g	=ROC.G*1*DC.G*TC.G
262		Total guideway added weight	kg/m	m.gw	=NMOTOR*(MC.G+MI.G)
263					
264	*Perf*				
265		Individual Motor Parameters at Maxim			
266		Thrust**	N	Thrust	20427
267		Slip**	-	slip	41358
268		Traction Power**	W	P.tract	2736900

Table E-2. EMS II with formulas used to calculate the dependent parameters.

	A	B	C	D	E
1		ElectroMagnetic Suspension IIA			
2		(Combined vertical & lateral suspensi			
3		=NOW()			
4		Asterisk (*) before description indicat			
5		2 Asterisks (**) after description indic			
6					
7					
8		DESCRIPTION	UNITS	SYMBOL	DESIGN 1
269		Real input Power**	W	Pin.real	2819700
270		Reactive input Power**	V·A	Pin.react	3219400
271		Efficiency**	%	eff.v	96.5392
272		Power Factor		PwrFac	=COS(ATAN(PIN.REACT/PIN.REAL))
273					
274					
275	AUX				
276		*Lift/guidance magnets*			
277		*permeances*			
278		√Air gap fringing permeance/length		Pf	1.92
279		√Ideal air gap permeance/length		Pu	=LP/H1X
280		?Inter-pole leakage perm./length		Pl	=(H__OR_D_-H1X)/W
281		alpha(g,delta)		alpha_g.del	=1+2*H1X*(1-(DEL/H1X)*ATAN(DEL/H1X))/(PI()*LP)
282		alpha(g,delta+y*)		alpha_g.del.y_sta	=1+2*H1X*(1-((DEL+Y_STAR)/H1X)*ATAN((DEL+Y_STAR)/H1X))/(PI()*LP)
283		example using function "alpha(y,g,l_p)		0	0
284		*Coil dimensions*			
285		Average turn length		lc	=2*L_Y+2*D_Y+PI()*H__OR_D_
286		Coil conductor crossectional area		ac	=H__OR_D_*W*F
287		Effective surface area/heat trans.		adis	=4*L*(LP+W+H__OR_D_)+4*H__OR_D_*LP+2*LP*(2*LP+W)+4*LP*W+PI()*W*W+2*(H__OR_D_-Z)*PI()*W
288		Coil volume	m^3	V_coil	=W*(2*H__OR_D_*L_Y+2*H__OR_D_*D_Y+PI()*H__OR_D_^2)
289					
290		*Magnet parameters*			
291		Magnet volume	m^3	V_mag	=L*(2*2*H1X*LP+2*(H__OR_D_-2*H1X)*(LP+W_P)/2+2*W_P*D_Y)+L_Y*D_Y*W
292		flux leakage coefficients			
293		Gap fringing flux coefficient		nu_g	=1+2*H1X/(PI()*LP)*(1+0.5*LN(1+(DEL/H1X)^2)-(DEL/H1X)*ATAN(DEL/H1X))
294		Pole leakage flux coefficient		nu_l.p	=2*H__OR_D_*H1X/(W*LP)
295		Yoke leakage flux coefficient		nu_l.y	=2*H1X/(PI()*LP)
296		Total leakage & fringing flux coef.		nu_t	=NU_G+NU_L.P+NU_L.Y
297		Total leakage flux coefficient		nu_l	=NU_L.P+NU_L.Y
298		Total leakage flux/gap flux		Lambda	=NU_L/NU_G
299		nu_t @ g=2go, y=0		nu_t.max1	=(1+2*(2*H1X)/(PI()*LP)*(1+LN(1+(DEL/(2*H1X))^2)-(DEL/(2*H1X))*ATAN(DEL/(2*H1X))))+2*NU_L
300		nu_t @ g=go, y=y_star		nu_t.max2	=2*(1+2*H1X/(PI()*LP)*(1+0.5*LN(1+((DEL+Y_STAR)/H1X)^2)-((DEL+Y_STAR)/H1X)*ATAN((DEL+Y_STAR)/H1X)))+2*NU_L
301					
302		*Linear induction motor*			
303		*permeances*			
304		Ideal air gap permeance/length		Pu.lim	=D.V/GE.LIM
305		Air gap fringing permeance/length		Pf.lim	=1.92
306		Fringing permeance ratio		nuf.lim	=PF.LIM/PU.LIM
307					
308					
309	EMS				
310	Wek				
311		Lift/Guidance Magnets	kg		=MMAG
312		Linear Induction Motor	kg		=MMOTOR
313		Total	kg		=SUM(E311:E312)
314	Wek				
315		Lift/Guidance Magnets	kg/m		=MR
316		Linear Induction Motor	kg/m		=MGW
317		Total	kg/m		=SUM(E315:E316)
318	Rea				
319		*Ohmic Power Dissipation*			
320		Lift/Guidance Magnets	W		=L
321		Linear Induction Motor	W		=PIN.REAL-P.TRACT
322		Total Ohmic Power	W		=SUM(E320:E321)
323		*Eddy current Power*			
324		Lift/Guidance Magnets	W		=PR
325		Total eddy current Power	W		=SUM(E324:E324)
326		Total Real Power Dissipation	W		=SUM(E325,E322)
327	Rea				
328		Linear Induction Motor	V·A		=PIN.REACT
329		Total	V·A		=SUM(E328:E328)

Table E-3. EMS III with formulas used to calculate the dependent parameters.

	A	B	C	D	E
1		ElectroMagnetic Suspension IIIA		filename:	Final EMS III, 134 m/s Optimization
2		(Separate vertical suspension & synchronous mc			
3		=NOW()			
4		Asterisk (*) before description indicates input.			
5					
6		DESCRIPTION	UNITS	SYMBOL	DESIGN 1
7					baseline
8					
9	VE				
10	*De*				
11		*Vehicle mass	kg	m	40000
12		*Vehicle length	m	l_vehicle	30
13		*Design speed	m/s	V	134
14		*frontal area	m^2	Af	9
15		*air density	kg/m^3	roair	1.2
16		*drag coefficient	---	Cd	0.3
17		wind drag force	N	Fd	=0.5*CD*ROAIR*V^2*AF
18		wind drag power	W	Pd	=FD*V
19		*Max. Lift Force(@Max disp.)	g	max_Fz	1.1
20		*Max. Lateral Force(*)(cont.)	g	max_F.l	0.26
21		*Max. Lateral Force(*)(short)	g	max_sF.l	0.42
22		*Time of Max. (short)Lateral F	sec	t_max	5
23		*Maximum ambient temp.	°C	maxTamb	50
24					
25		Payload	kg	Pload	
26		Total Power	kW	Pt	0
27		Total Power/weight	kW/kg		
28					
29		Propulsion/suspension system			
30		Added guideway weight/length	kg/m		0
31		Added vehicle weight	kg		0
32					
33					
34					
35	CC	*air permeability	N/A^2	mu	=PI()*0.0000004
36	*Ge*				
37		*Construction materials*			
38	*La*	*rail			steel
39		*magnet			2V Perm.
40		*coil			alum.
41		*Materials properties*			
42		*mass density*			
43		*rail	kg/m^3	ror	7506.3662183
44		*magnet	kg/m^3	rom	7784.3797819
45		*coil	kg/m^3	roc	2780.1356364
46		*maximum flux density*			
47		*rail	T	Bsatr	1.6
48		*magnet	T	Bsatm	2.3
49		*Saturation Safety Factor(<1)	---	SF	1
50		*Electrical resistivity*			
51		*rail @20 deg C	ohm-m	rr	0.0000004061
52		*coil @140 deg C	ohm-m	rc_	0.0000000406

Table E-3. EMS III with formulas used to calculate the dependent parameters.

	A	B	C	D	E
1		ElectroMagnetic Suspension IIIA		filename:	Final EMS III, 134 m/s Optimization
2		(Separate vertical suspension & synchronous mc			
3		=NOW()			
4		Asterisk (*) before description indicates input.			
5					
6		DESCRIPTION	UNITS	SYMBOL	DESIGN 1
53		*coil @220 deg C	ohm-m	rc_220	
54		*Thermal*			
55		*magnet heat transfer coef.	W/C-m^2	k	=0.009*39.4^2
56		*Coil Specific heat	J/(kg°C)	cp	118.85
57		*Maximum wire insulation temp	°C	maxTins	200
58					
59					
60		*Construction materials*			
61	Lil	*rail			steel
62		*rail windings			copper
63		*magnet			2V Perm.
64		*magnet coil			aluminum
65		*Densities*			
66		*rail	kg/m^3	rogm	7506.3662183
67		*rail windings	kg/m^3	rogc	8900
68		*magnet	kg/m^3	rovm	7784.3797819
69		*coil	kg/m^3	rovc	2780.1356364
70		*Maximum flux densities*			
71		*rail	T	bsatg	1.6
72		*magnet	T	bsatv	2.3
73		*Magnetic permeabilities*			
74		Rail	---	mug	3500
75		*Electrical Resistivity*			
76		*rail @20 deg C	ohm-m	rmg	0.0000004061
77		*vehicle coil @140 deg C	ohm-m	rcv	0.0000000406
78		*rail coil *140 deg c	ohm-m	rcg	=0.00000001673*1.47
79		*Thermal*			
80		*magnet heat transfer coefficient	W/C-m^2	kv	=0.009*39.4^2
81		*rail heat transfer coef.	W/C-m^2	kg	=0.009*39.4^2
82					
83					
84					
85	CC	*Geometric dimensions*			
86	La	*pole width	m	lp.l	0.0238
87		*window width	m	w.l	0.119
88		*window height	m	h.l	0.0594
89		Window width/height ratio	---		=W.L/H.L
90		*coil packing factor	---	f.l	0.7
91		*air gap	m	H1x.l	0.01
92		*pole-coil clearance	m	z.l	=0.2/39.4
93		*Number magnets required	---	nmag.l	4
94		magnet length	m	L.l	=9.8*M*MAX_SF.L/(NMAG.L/2)*2*MU/(B0.L^2*LP.L*2)
95		Magnet length/vehicle length			=IF(L.L/l_vehicle<=0.5,"OK","TOO LONG!")
96		*Magnet Design*			
97		flux leakage coefficients			
98		fringing (across air gap)	---	nuf.l	=PF.L/PU.L

Table E-3. EMS III with formulas used to calculate the dependent parameters.

	A	B	C	D	E
1		ElectroMagnetic Suspension IIIA		filename:	Final EMS III, 134 m/s Optimization
2		(Separate vertical suspension & synchronous mc			
3		=NOW()			
4		Asterisk (*) before description indicates input.			
5					
6		DESCRIPTION	UNITS	SYMBOL	DESIGN 1
99		leakage (between poles)	- - -	nul.l	=PL.L/PU.L
100		total	- - -	nut.l	=1+(NUL.L+NUF.L)
101		nominal field in air gap	T	B0.l	=BSATM/(1+2*(NUF.L+NUL.L))
102		Force per magnet	N	Fpm.l	=LP.L*L.L*B0.L^2/MU
103		amp turns per magnet	A	NI.l	=2*H1X.L*B0.L/MU
104		core mass (1 mag)	kg	Mcore.l	=ROM*L.L*(W.L*LP.L+2*LP.L*(H.L+LP.L))
105		mass core + coil (4 mag)	kg	Mmag.l	=4*(MCORE.L+MC.L)
106					
107		*Coil Design*			
108		resist (1 magnet, 1 turn)	ohm	resc.l	=RC_*LC.L/AC.L
109		St. state coil power(N/2 mags)	W	qc_ss.l	=QC.L*(1/4)*(MAX_F.L/MAX_SF.L)
110		Max. coil power (N/2 magnets)	W	qc.l	=2*RESC.L*NI.L^2*NMAG.L/2
111		Steady state temperature rise	°C	Tm_ss.l	=(1/2)*QC_SS.L/(ADIS.L*K)
112		Short term temperature rise	°C	Tm_st.l	=QC.L/(NMAG.L/2)*T_MAX/(MC.L*CP)
113		Maximum coil temperature	°C	Tc_max.l	=MAXTAMB+MAX(TM_SS.L,TM_ST.L)
114		mass(one coil)	kg	Mc.l	=ROC*AC.L*LC.L
115					
116		*Rail Design*			
117		rail thickness	m	tr.l	=LP.L*(BSATM/BSATR)
118		rail pole tip width (=tr)	m	lr.l	=TR.L
119		rail mass/length(two rails)	kg/m	mr.l	=2*ROR*(2*LR.L*(TR.L+H1X.L)+TR.L*(W.L+LP.L-LR.L))
120					
121		nominal rail flux density	T	Br.l	=B0.L*(1+NUF.L)*(LP.L/TR.L)
122		eff. freq. for eddy anal.	Hz	Fe.l	=0.5*V/L.L
123		dB/dt amp. first harmonic	T/s	B1x.l	=4*FE.L*BR.L
124		eddy current power	W	Pr.l	=B1X.L^2*TR.L^3*L.L*(W.L+LP.L)*NMAG.L/(24*RR)
125		rms eddy amp turn			
126		(upper bound, 1 magnet)	A	NIe.l	=0.7071*B1X.L*TR.L^2*(W.L+LP.L)/(8*RR)
127		Total power	W	P.l	=PR.L+QC.L
128					
129					
130		*Geometric Dimensions-on board magnet*			
131	Lif	*Xpole thickness	m	tpv	=LPV
132		Xpole to pole distance	m	wcv	=WV+LPV-TPV
133		*pole face width	m	lpv	0.2
134		Xface to face dist.	m	wv	=0.5*LPV
135		*window height	m	hv	0.08
136		*magnet depth	m	dv	0.1
137		*yoke thickness	m	tyv	0.085
138		*coil packing factor	- - -	ffv	0.7
139		*air gap	m	H1v	0.01
140		*pole-coil clearance	m	zv	=0.2/39.4
141		*number laminations	- - -	nlammv	5
142		lamination thickness	m	tmv	=DV/NLAMMV
143		*Number magnets required	- - -	nmagv	10
144		*number of poles per mag	- - -	nsegv	10

Table E-3. EMS III with formulas used to calculate the dependent parameters.

	A	B	C	D	E
1		ElectroMagnetic Suspension IIIA		filename:	Final EMS III, 134 m/s Optimization
2		(Separate vertical suspension & synchronous mc			
3		=NOW()			
4		Asterisk (*) before description indicates input.			
5					
6		DESCRIPTION	UNITS	SYMBOL	DESIGN 1
145		magnet length	m	Lv	=NSEGV*(LPV+WV)
146					
147		*Geometric Dimensions-guideway*			
148		*pole width	m	lpg	=0.4*LPV
149		*slot width	m	wg	=0.1*LPV
150		XMagnet & guideway pole & slot dimensions?			=IF(AND(MOD(LPV+0.0001,LPG+WG)<=0.001,MOD(WV+0.0001,LPG+WG)<=0.001),"OK","POOR")
151		XSlots and phases?			=IF(MOD((LPV+WV)/(LPG+WG)+0.0001,NP)<=0.001,"OK","POOR")
152		Guideway poles per mag. pole	---	Ng	=LPV/(LPG+WG)
153		*window height	m	hg	0.06
154		*magnet depth	m	dg	=DV+4*H1V
155		*coil packing factor	---	ffg	0.8
156		*number electrical phases	---	Np	3
157		*pole-coil clearance	m	zg	0.005
158		*number laminations	---	nlammg	400
159		lamination thickness	m	tmg	=DG/NLAMMG
160		skin depth	m	delg	=SQRT(2*RMG/(2*PI()*FS*MU*MUG))
161					
162		*Magnet Design*			
163		*amp turns/pole (mag seg)	A	Niv	6500
164		flux leakage coefficients			
165		fringing (across air gap)	---	nufv	=PFV/PUV
166		leakage (between poles)	---	nulv	=PLV/PUV
167		total	---	nutv	=1+(NULV+NUFV)
168		Xnom. lift field in air gap	T	B0v	=NIV*MU/H1V*TPV/LPV
169		Xmax B in yoke @2 h1v, lift only	T	Byv	=0.5*B0V*(1+2*(NUFV+NULV))*LPV/TYV
170		check field in yoke			=IF(BYV<=BSATV,"OK","SATURATED")
171		total lift force-Nmag magnets	N	Fv	=NMAGV*NSEGV*NG*LPG*DV*0.5*B0V^2/MU
172					
173		Xcore mass (1 mag)	kg	Mcorev	=ROVM*NSEGV*DV*(TYV*(LPV+WV)+TPV*(HV-ZV)+ZV*LPV)
174		mass core + coil (Nmagv mag)	kg	Mmagv	=NMAGV*(MCOREV+MCOILV)
175					
176		*Vehicle Coil Design*			
177		resist (1 magnet, 1 turn)	ohm	resv	=RCV*LCV/ACV
178		coil ohmic power (N mag)	W	qv	=RESV*NIV^2*NMAGV*NSEGV
179		temp. rise	deg C	Tv	=QV/(NMAGV*NSEGV*KV*ADISV)
180		mass (1 magnet)	kg	Mcoilv	=ROVC*NSEGV*ACV*LCV
181					
182		*Rail Coil Design*			
183		rail yoke thickness	m	tyg	0.1
184		*amp turns per phase (0-P)	A	Nlg	1200
185		flux leakage coefficients			
186		fringing (across air gap)	---	nufg	=PFG/PUG
187		leakage (between poles)	---	nulg	=PLG/PUG
188		total	---	nutg	=1+NUFG+NULG
189		B in air gap-1 phase	T	B0g	=MU*NIG/H1V
190		max. field in poles			

Table E-3. EMS III with formulas used to calculate the dependent parameters.

	A	B	C	D	E
1		ElectroMagnetic Suspension IIIA		filename:	Final EMS III, 134 m/s Optimization
2		(Separate vertical suspension & synchronous mc			
3		=NOW()			
4		Asterisk (*) before description indicates input.			
5					
6		DESCRIPTION	UNITS	SYMBOL	DESIGN 1
191		from 1 phase & h1v	T	Bp1g	=B0G*(1+NUFG+NULG)
192		from lift @ 2*h1v	T	Bp2g	=B0V*(1+2*NUFV)*DV/DG
193		check B in pole			=IF(BSATG>1.5*BP1G+BP2G,"OK","SATURATE")
194		max. field in yoke			
195		from 1 phase & h1v	T	By1g	=B0G*LPG/TYG*(1+(NUFG+NUTG))
196		X from lift @ 2*h1v	T	By2g	=0.5*B0V*(1+2*NUFV)*LPG*NG*DV/(TYG*DG)
197		check field in yoke			=IF(BSATG>1.5*BY1G+BY2G,"OK","SATURATE")
198					
199		core mass (2 rails)	kg/m	Mcoreg	=NSEGG*ROGM*2*(DG*TYG*(LPV+WV)+3*HG*WG*DG)/1000
200		mass core + coil (2 rails)	kg/m	Mmagg	=MCOREG+MCOILG/1000
201					
202		*Rail Winding Design-1 segment is 3 pole pieces*			
203		segments/km	1/km	nsegg	=1000/(LPV+WV)
204		resist (1 phase)	ohm/km	resg	=RCG*LCG*NSEGG/ACG
205		ohmic power (3 phase, 2rail)	W/km	Pohm	=3*2*0.5*NIG^2*RESG
206		temp. rise	deg C	Tg	=POHM/(2*NSEGG*ADISG*KG)
207		Xmass	kg/km	Mcoilg	=ROGC*6*NSEGG*ACG*LCG
208		freq. at nom speed	Hz	fs	=V/(2*(LPV+WV))
209					
210		track without vehicle			
211		Xtrack self L (1 rail)	H/km	Laax	=(0.5*PLG+PL2G)*MU*NSEGG
212		rail reactive impedance	ohms/km	Zlt	=2*PI()*FS*LAAX
213		mutual inductance	H/km	Mabt	0
214		voltage/phase/turn	V/km	Vt	=NIG*SQRT(RESG^2+ZLT^2)
215		Xmagnetic field in yoke	T	Bt	=1.5*MU*NIV*0.5*(PLG+PL2G)/(DG*TYG)
216		dB/dt amp. first harmonic	T/s	Btx	=4*FE*BT
217		guideway eddy losses	W/km	Pteddy	=BTX^2*TMG^3*TYG*NLAMMG*1000*2/(24*RMG)
218		Xreact. power (3ph-2 rails)	VA/km	Pzg	=2*1.5*NIG*VT
219					
220					
221		*Inductances*			
222	PR	Xinductance-self L field	H/(2 seg)	Lbasic	=4*(1+NUFV)*MU*DV*NG*LPG/(2*H1V)
223		X stator self L-mean value	H/(2 seg)	Laa	=LBASIC+4*0.25*PLG*MU
224		stator self L-second harm.	H/(2 seg)	Laa2	=0*LBASIC
225		mutual-first harmonic	H/(2 seg)	Mvg	=1.05*LBASIC
226		stator mutual-mean	H/(2 seg)	Mab	=0.21*LBASIC
227		stator mutual-second harm.	H/(2 seg)	Mab2	=0.614*LBASIC
228					
229		*Propulsive forces-maximum values*			
230		design force (Mvg calc)	N	Fl	=1.5*NMAGV*0.5*NSEGV*MVG*NIV*NIG*2*PI()/(2*(LPV+WV))
231		reluctance force (Mab2)	N		=1.5*NMAGV*0.5*NSEGV*MAB2*NIG^2*PI()/(2*(LPV+WV))
232		rail self induct (Laa2)	N		=1.5*0.5*NMAGV*0.5*NSEGV*LAA2*NIG^2*PI()/(2*(LPV+WV))
233					
234		hunting stiffness	N/m	Khunt	=FL*PI()/(LPV+WV)
235		hunting freq.	Hz	fhunt	=SQRT(KHUNT/M)/(2*PI())
236		Xmax. propel (B field)	N		=2*1.5*NMAGV*NSEGV*PI()*0.5*H1V*DV*(2*(1+NUFG)/PI())^2*B0G*B0V/MU

Table E-3. EMS III with formulas used to calculate the dependent parameters.

	A	B	C	D	E
1		ElectroMagnetic Suspension IIIA		filename:	Final EMS III, 134 m/s Optimization
2		(Separate vertical suspension & synchronous mc			
3		=NOW()			
4		Asterisk (*) before description indicates input.			
5					
6		DESCRIPTION	UNITS	SYMBOL	DESIGN 1
237					
238		*Losses from eddy currents*			
239		nom. rail B from vehicle	T	Br	=B0V*(1+NUFV)*(LPV/TYG)
240		eff. freq. for eddy anal.	Hz	Fe	=FS
241		dB/dt amp. first harmonic	T/s	B1x	=4*FE*BR
242		eddy current power	W	Pr	=B1X^2*TMG^3*TYG*LV*NMAGV*NLAMMG/(24*RMG)
243		rms eddy amp turn			
244		(upper bound, 1 magnet)	A	Nie	=B1X*TMG^2*TYV/(8*RMG)
245					
246		(ohmic+eddy)/wind power	%		=(QV+PR)/PD
247		(magnet+coil)/vehicle wt.	%		=MMAGV/M
248		eddy/lift amp-T (up. bound)	%		=0.5*NIE/NIV
249		wind drag/weight	%		=FD/(9.8*M)
250					
251		ratio propel F/weight	%		=FL/(9.8*M)
252		ratio propel/lift	%		=FL/FV
253		ratio lift/weight	%		=FV/(M*9.8)
254		ratio mag. weight/lift	%		=MMAGV*9.8/FV
255					
256		track losses/wind drag	%/km		=(POHM+PTEDDY)/PD
257					
258					
259					
260	AU				
261	Co	*Permeances*			
262		permeances-vehicle magnet		Pfv	=2*NG*((2*0.26+2*LN(2)/PI())*(DV+LPG))+4*NG*(0.308+0.5)*H1V
263		useful 1 air gap		Puv	=AUV/H1V
264		X		Plv	=2*(HV-H1V)*(DV/WCV+2*(0.26+LN(1+TPV/WCV)/PI()))
265		pole useful area	m^2	Auv	=LPG*DV*NG
266		Xcoil dimensions-1 coil on 1 pole		lcv	=2*(TPV+PI()*WCV/4+DV)
267		X 1 coil on 1 pole		acv	=(HV-ZV)*0.5*WCV*FFV
268		X 1 segments-1 pole		adisv	=2*TYV*(LPV+WV)+2*HV*(TPV+DV)+LPV*DV+(HV-ZV)*PI()*WCV+0.5*PI()*WCV^2
269					
270		permeances-guideway windings		Pfg	=PFV
271		vehicle in place		Pug	=PUV
272				Plg	=2*(HG-H1V)*(DG/WG+2*(0.26+LN(1+2*LPG/WG)/PI()))
273		X no vehicle magnets		Pl2g	=4*DG*(0.26+LN(1+2*LPG/WG)/PI())
274		*Coil dimensions*			
275		coil dimen.-1 phase-1 turn-3 pole pieces		lcg	=2*(3*LPG+3*WG+DG+WG*PI()/4)
276		1 -coil but 2 coils per slot		acg	=(HG-ZG)*WG*FFG/4
277		1 seg. 3 pole pieces		adisg	=6*(LPG+WG)*(TYG+HG-ZG+0.5*DG+2*WG)+6*ZG*(LPG+DG)
278					
279					
280		*Permeances*			
281	Gu	Air gap fringing permeance/length		Pf.l	1.92
282		Ideal air gap permeance/length		Pu.l	=LP.L/H1X.L

Table E-3. EMS III with formulas used to calculate the dependent parameters.

	A	B	C	D	E
1		**ElectroMagnetic Suspension IIIA**		filename:	**Final EMS III, 134 m/s Optimization**
2		(Separate vertical suspension & synchronous mc			
3		=NOW()			
4		Asterisk (*) before description indicates input.			
5					
6		DESCRIPTION	UNITS	SYMBOL	DESIGN 1
283		Inter-pole leakage perm./length		Pl.l	=(H.L-H1X.L)/W.L
284		*Coil dimensions*			
285		Mean turn length	m	lc.l	=2*(L.L+PI()*W.L/4+LP.L)
286		Coil crossectional area	m^2	ac.l	=(H.L-Z.L)*W.L/2*F.L
287		Coil Surface area	m^2	adis.l	=4*L.L*(LP.L+W.L+H.L)+4*H.L*LP.L+2*LP.L*(2*LP.L+W.L)+4*LP.L*W.L+PI()*W.L*W.L+2*(H.L-Z.L)*PI()*W.L
288					
289					
290					
291	El	Lift Magnets/LSM	kg		=MMAGV
292	*W*	Guidance Magnets	kg		=MMAG.L
293			kg		=SUM(E291:E292)
294		Magnet Weight/Vehicle Weight	%		=E293/M
295	To				
296		Lift Magnets/LSM	kg/m		=MMAGG
297	*W*	Guidance Magnets	kg/m		=MR.L
298			kg/m		=SUM(E296:E297)
299					
300	To				
301	*Re*	Lift Magnets/LSM	W		=QV
302	*Ol*	Guidance Magnets	W		=QC_SS.L
303			W		=SUM(E301:E302)
304					
305	*To*	Lift Magnets/LSM	W		=PR
306	*Ed*	Guidance Magnets	W		=PR.L
307			W		=SUM(E305:E306)
308			W		=SUM(E307,E303)
309	*To*		%		=E308/PD
310	To				
311	*El*	*Linear Synchronous Motor*	V-A		=PZG
312	Re		V-A		=SUM(E311)

APPENDIX F

COMPLETE SPREADSHEETS FOR ELECTROMAGNETIC SYSTEMS

Table F-1. Complete EMS I Spreadsheet; Design optimized for operation at 89 m/s
Separate Lift and guidance magnets and Linear Induction Motor

ElectroMagnetic Suspension I Optimized for operation at 89 m/s maximum speed
(Separate vertical & lateral suspensions & linear induction motor)

Asterisk (*) before description indicates input.
2 Asterisks (**) after description indicates output from MatLab Linear Induction Motor Analysis program.

DESCRIPTION	UNITS	SYMBOL	89 m/s Optimization			89 m/s Optimization @ 59 m/s		
			DESIGN 1 baseline (b/l)	DESIGN 2 slim pole (3/4 b/l)	DESIGN 3 small gap (0.8 b/l)	DESIGN 1 baseline	DESIGN 2 slim pole (3/4 b/l)	DESIGN 3 small gap (0.8 b/l)
VEHICLE PARAMETERS								
Design Parameters								
*Vehicle mass	kg	m	4.00E+04	4.00E+04	4.00E+04	4.00E+04	4.00E+04	4.00E+04
*Vehicle length	m	l_vehicle	3.00E+01	3.00E+01	3.00E+01	3.00E+01	3.00E+01	3.00E+01
*Design speed	m/s	V	8.90E+01	8.90E+01	8.90E+01	5.90E+01	5.90E+01	5.90E+01
*frontal area	m^2	Af	1.20E+01	1.20E+01	1.20E+01	1.20E+01	1.20E+01	1.20E+01
*air density	kg/m^3	roair	1.20E+00	1.20E+00	1.20E+00	1.20E+00	1.20E+00	1.20E+00
*drag coefficient	---	Cd	3.00E-01	3.00E-01	3.00E-01	3.00E-01	3.00E-01	3.00E-01
wind drag force	N	Fd	1.71E+04	1.71E+04	1.71E+04	7.52E+03	7.52E+03	7.52E+03
wind drag power	W	Pd	1.52E+06	1.52E+06	1.52E+06	4.44E+05	4.44E+05	4.44E+05
*Max. Lift Force(@Max disp.)	g	max_Fz	1.10E+00	1.10E+00	1.10E+00	1.10E+00	1.10E+00	1.10E+00
*Max. Lateral Force(*)(cont.)	g	max_F.l	1.80E-01	1.80E-01	1.80E-01	1.80E-01	1.80E-01	1.80E-01
*Max. Lateral Force(*)(short term)	g	max_sF.l	2.60E-01	2.60E-01	2.60E-01	2.60E-01	2.60E-01	2.60E-01
*Time of Max. (short)Lateral F	sec	t_max	5.00E+00	5.00E+00	5.00E+00	5.00E+00	5.00E+00	5.00E+00
*Max propulsive force	g	max_Fp	2.10E-01	2.10E-01	2.10E-01	2.10E-01	2.10E-01	2.10E-01
*Maximum ambient temperature	°C	maxTamb	5.00E+01	5.00E+01	5.00E+01	5.00E+01	5.00E+01	5.00E+01
Performance Parameters								
Power, (ohmic+eddy)/aero. drag	%		5.91E-01	7.79E-01	5.01E-01	1.67E+00	2.36E+00	1.39E+00
Weight, (magnet+coil)/vehicle	%		1.40E-01	1.67E-01	6.17E-02	1.40E-01	1.67E-01	6.17E-02
eddy/lift amp-T (up. bound)	%		1.25E-01	3.57E-02	1.07E-01	8.32E-02	2.37E-02	7.11E-02
Aerodynamic drag/lift force	%		4.36E-02	4.36E-02	4.36E-02	1.92E-02	1.92E-02	1.92E-02
CONSTANTS								
*air permeability	N/A^2	mu	1.26E-06	1.26E-06	1.26E-06	1.26E-06	1.26E-06	1.26E-06
Suspensions								
Construction materials								
*rail			steel	steel	steel	steel	steel	steel
*magnet			2V Perm.	2V Perm.	2V Perm.	2V Perm.	2V Perm.	2V Perm.
*coil			alum.	alum.	alum.	alum.	alum.	alum.
Materials properties								
mass density								
*rail	kg/m^3	ror	7.51E+03	7.51E+03	7.51E+03	7.51E+03	7.51E+03	7.51E+03
*magnet	kg/m^3	rom	7.78E+03	7.78E+03	7.78E+03	7.78E+03	7.78E+03	7.78E+03
*coil	kg/m^3	roc	2.78E+03	2.78E+03	2.78E+03	2.78E+03	2.78E+03	2.78E+03
maximum flux density								
*rail	T	Bsatr	1.60E+00	1.60E+00	1.60E+00	1.60E+00	1.60E+00	1.60E+00
*magnet	T	Bsatm	2.30E+00	2.30E+00	2.30E+00	2.30E+00	2.30E+00	2.30E+00
*Saturation Safety Factor(<1)	---	SF	1.00E+00	1.00E+00	1.00E+00	1.00E+00	1.00E+00	1.00E+00
electrical resistivity								
*rail @20°C	ohm-m	rr	4.06E-07	4.06E-07	4.06E-07	4.06E-07	4.06E-07	4.06E-07
*Temp. coefficient of rail	ohm-m/°C	rr_tc						
*coil @140 deg C	ohm-m	rc_	4.06E-08	4.06E-08	4.06E-08	4.06E-08	4.06E-08	4.06E-08
*Temp. coefficient of coil	ohm-m/°C	rc_tc						
Thermal								
*magnet heat transfer coef.	W/C-m^2	k	1.40E+01	1.40E+01	1.40E+01	1.40E+01	1.40E+01	1.40E+01
*Coil Specific heat	J/(kg°C)	cp	1.19E+02	1.19E+02	1.19E+02	1.19E+02	1.19E+02	1.19E+02
*Maximum wire insulation temp	°C	maxTins	2.00E+02	2.00E+02	2.00E+02	2.00E+02	2.00E+02	2.00E+02
Linear Induction Motor								
Construction materials								
*rail			steel	steel	steel	steel	steel	steel
*rail conductor(s)			aluminum	aluminum	aluminum	aluminum	aluminum	aluminum

Table F-1. (continued)

ElectroMagnetic Suspension I Optimized for operation at 89 m/s maximum speed

(Separate vertical & lateral suspensions & linear induction motor)

Asterisk (*) before description indicates input.
2 Asterisks (**) after description indicates output from MatLab Linear Induction Motor Analysis program.

DESCRIPTION	UNITS	SYMBOL	89 m/s Optimization			89 m/s Optimization @ 59 m/s		
			DESIGN 1	DESIGN 2	DESIGN 3	DESIGN 1	DESIGN 2	DESIGN 3
			baseline (b/l)	slim pole (3/4 b/l)	small gap (0.8 b/l)	baseline	slim pole (3/4 b/l)	small gap (0.8 b/l)
Materials properties								
Mass density								
*rail	kg/m^3	rom.g	7.51E+03	7.51E+03	7.51E+03	7.51E+03	7.51E+03	7.51E+03
*rail conductor(s)	kg/m^3	roc.g	2.78E+03	2.78E+03	2.78E+03	2.78E+03	2.78E+03	2.78E+03
*magnet	kg/m^3	rom.v	7.65E+03	7.65E+03	7.65E+03	7.65E+03	7.65E+03	7.65E+03
*coil	kg/m^3	roc.v	2.78E+03	2.78E+03	2.78E+03	2.78E+03	2.78E+03	2.78E+03
maximum flux densities								
*rail	T	bsat.g	1.60E+00	1.60E+00	1.60E+00	1.60E+00	1.60E+00	1.60E+00
*magnet	T	bsat.v	1.50E+00	1.50E+00	1.50E+00	1.50E+00	1.50E+00	1.50E+00
Magnetic permeability								
rail	---	mu.g	3.50E+03	3.50E+03	3.50E+03	3.50E+03	3.50E+03	3.50E+03
Vehicle (short) stator		mu.v						
Core Loss @ 1.0T, 100 Hz	W/kg	refc.loss	2.87E+00	2.87E+00	2.87E+00	2.87E+00	2.87E+00	2.87E+00
Core loss frequency exponent	-	freq.exp	1.50E+00	1.50E+00	1.50E+00	1.50E+00	1.50E+00	1.50E+00
Core loss induction exponent	-	B.exp	2.10E+00	2.10E+00	2.10E+00	2.10E+00	2.10E+00	2.10E+00
Core loss @ fsync & Bcore	W/kg	c.loss	1.05E+01	1.05E+01	1.36E+01	5.68E+00	5.68E+00	7.34E+00
electrical resistivity								
*Magnet laminations @ 140°C	ohm-m	rm.v	7.00E-07	7.00E-07	7.00E-07	7.00E-07	7.00E-07	7.00E-07
*rail @20 deg C	ohm-m	rm.g	4.06E-07	4.06E-07	4.06E-07	4.06E-07	4.06E-07	4.06E-07
*vehicle coil @20 deg C	ohm-m	rcRT.v	2.78E-08	2.78E-08	2.78E-08	2.78E-08	2.78E-08	2.78E-08
*vehicle coil temperature coefficie	1/°C	alpha.v	4.10E-03	4.10E-03	4.10E-03	4.10E-03	4.10E-03	4.10E-03
vehicle coil @operating temperatu	ohm-m	rc.v	4.73E-08	4.73E-08	4.75E-08	4.73E-08	4.73E-08	4.75E-08
*Guideway conductor @20 deg c	ohm-m	rc.g	2.80E-08	2.80E-08	2.80E-08	2.80E-08	2.80E-08	2.80E-08
Heat transfer coeffieients								
*magnet heat transfer coef.	W/C-m^2	k.v	4.19E+01	4.19E+01	4.19E+01	4.19E+01	4.19E+01	4.19E+01
*rail heat transfer coef.	W/C-m^2	k.g	1.40E+01	1.40E+01	1.40E+01	1.40E+01	1.40E+01	1.40E+01
COMPONENT DESIGN & ANALYSIS								
Vertical suspension								
Geometric dimensions								
*pole width	m	lp	3.14E-02	2.35E-02	2.79E-02	3.14E-02	2.35E-02	2.79E-02
*air gap	m	H1x	1.00E-02	1.00E-02	8.00E-03	1.00E-02	1.00E-02	8.00E-03
*window width	m	w	9.43E-02	8.51E-02	8.50E-02	9.43E-02	8.51E-02	8.50E-02
*window height	m	h	4.72E-02	4.25E-02	4.25E-02	4.72E-02	4.25E-02	4.25E-02
Window width/height	---		2.00E+00	2.00E+00	2.00E+00	2.00E+00	2.00E+00	2.00E+00
	---		OK	OK	OK	OK	OK	OK
*coil packing factor	---	f	7.00E-01	7.00E-01	7.00E-01	7.00E-01	7.00E-01	7.00E-01
*pole-coil clearance	m	z	5.08E-03	5.08E-03	5.08E-03	5.08E-03	5.08E-03	5.08E-03
*Number magnets required	---	nmag	4.00E+00	4.00E+00	4.00E+00	4.00E+00	4.00E+00	4.00E+00
magnet length	m	L	5.00E+00	9.52E+00	5.00E+00	5.00E+00	9.52E+00	5.00E+00
Magnet length/vehicle length ratio			OK	OK	OK	OK	OK	OK
Magnet design								
leakage/fringing flux ratios								
√ fringing (across air gap)	---	nuf	6.12E-01	8.16E-01	5.51E-01	6.12E-01	8.16E-01	5.51E-01
√ leakage (between poles)	---	nul	1.26E-01	1.63E-01	1.16E-01	1.26E-01	1.63E-01	1.16E-01
√total	---	nut	1.74E+00	1.98E+00	1.67E+00	1.74E+00	1.98E+00	1.67E+00
√nominal field in air gap(@2*H1x)	T	B0	9.29E-01	7.78E-01	9.85E-01	9.29E-01	7.78E-01	9.85E-01
√Max. Force per magnet(@2*H1x)	N	Fpm	1.08E+05	1.08E+05	1.08E+05	1.08E+05	1.08E+05	1.08E+05
√Max. vertical g's @ twice nom. gap	g		OK	OK	OK	OK	OK	OK
√Max amp turns per coil(@ 2H1x)	A	NI	1.48E+04	1.24E+04	1.25E+04	1.48E+04	1.24E+04	1.25E+04
√Max. steady state NI (1 coil@1g)		NI_ss	7.05E+03	5.90E+03	5.98E+03	7.05E+03	5.90E+03	5.98E+03

Table F-1. (continued)

ElectroMagnetic Suspension I Optimized for operation at 89 m/s maximum speed

(Separate vertical & lateral suspensions & linear induction motor)

Asterisk (*) before description indicates input.
2 Asterisks (**) after description indicates output from MatLab Linear Induction Motor Analysis program.

DESCRIPTION	UNITS	SYMBOL	89 m/s Optimization			89 m/s Optimization @ 59 m/s		
			DESIGN 1	DESIGN 2	DESIGN 3	DESIGN 1	DESIGN 2	DESIGN 3
			baseline (b/l)	slim pole (3/4 b/l)	small gap (0.8 b/l)	baseline	slim pole (3/4 b/l)	small gap (0.8 b/l)
√core mass (1 mag)	kg	Mcore	3.07E+02	3.79E+02	2.45E+02	3.07E+02	3.79E+02	2.45E+02
√mass core + coil (4 mag)	kg	Mmag	1.54E+03	1.99E+03	1.23E+03	1.54E+03	1.99E+03	1.23E+03
√Total magnet weight/vehicle wt.		%	3.86%	4.98%	3.08%	3.86%	4.98%	3.08%
Coil Design								
√resist (1 coil, of 2 on magnet)	ohm	resc	2.98E-04	6.99E-04	3.72E-04	2.98E-04	6.99E-04	3.72E-04
√Max. St. st. ohmic power(N mags)	W	qm_ss	1.19E+05	1.95E+05	1.06E+05	1.19E+05	1.95E+05	1.06E+05
√Max coil ohmic power (N magnets)	W	qc	5.22E+05	8.58E+05	4.68E+05	5.22E+05	8.58E+05	4.68E+05
√Maximum coil power(1 coil)	W	qc_max	6.52E+04	1.07E+05	5.85E+04	6.52E+04	1.07E+05	5.85E+04
√Max. steady state coil power(1 coi	W	qc_ss	1.48E+04	2.44E+04	1.33E+04	1.48E+04	2.44E+04	1.33E+04
√Steady state temperature rise	°C	Tm_ss	1.50E+02	1.50E+02	1.50E+02	1.50E+02	1.50E+02	1.50E+02
√Short term temperature rise	°C	Tm_st	5.57E+02	6.06E+02	6.24E+02	5.57E+02	6.06E+02	6.24E+02
Maximum coil temperature	°C	Tc_max	2.00E+02	2.00E+02	2.00E+02	2.00E+02	2.00E+02	2.00E+02
√mass(one coil)	kg	Mc	3.95E+01	5.96E+01	3.15E+01	3.95E+01	5.96E+01	3.15E+01
Rail design								
√rail thickness	m	tr	4.05E-02	3.01E-02	3.61E-02	4.05E-02	3.01E-02	3.61E-02
√rail pole tip width	m	lr	4.05E-02	3.01E-02	3.61E-02	4.05E-02	3.01E-02	3.61E-02
rail mass/length(2 rails)	kg/m	mr	1.13E+02	7.17E+01	8.94E+01	1.13E+02	7.17E+01	8.94E+01
nominal rail flux density	T	Br	1.16E+00	1.10E+00	1.18E+00	1.16E+00	1.10E+00	1.18E+00
eff. freq. for eddy anal.	Hz	Fe	8.90E+00	4.68E+00	8.90E+00	5.90E+00	3.10E+00	5.90E+00
dB/dt amp. first harmonic	T/s	B1x	4.13E+01	2.07E+01	4.20E+01	2.74E+01	1.37E+01	2.79E+01
eddy current power	W	Pr	2.93E+04	4.94E+03	1.93E+04	1.29E+04	2.17E+03	8.47E+03
rms eddy amp turn (upper bound, 1 magnet)	A	NIe	1.86E+03	4.42E+02	1.35E+03	1.23E+03	2.93E+02	8.92E+02
√Total continuous power	W	P.v	1.48E+05	2.00E+05	1.26E+05	1.31E+05	1.97E+05	1.15E+05
Lateral Suspension								
Geometric dimensions								
*pole width	m	lp.l	2.27E-02	1.70E-02	2.00E-02	2.27E-02	1.70E-02	2.00E-02
*window width	m	w.l	1.21E-01	1.09E-01	1.09E-01	1.21E-01	1.09E-01	1.09E-01
*window height	m	h.l	6.04E-02	5.45E-02	5.45E-02	6.04E-02	5.45E-02	5.45E-02
Window width/height ratio	---		2.00E+00	2.00E+00	2.00E+00	2.00E+00	2.00E+00	2.00E+00
*	---		OK	OK	OK	OK	OK	OK
*coil packing factor	---	f.l	7.00E-01	7.00E-01	7.00E-01	7.00E-01	7.00E-01	7.00E-01
*air gap	m	H1x.l	1.00E-02	1.00E-02	8.00E-03	1.00E-02	1.00E-02	8.00E-03
*pole-coil clearance	m	z.l	5.08E-03	5.08E-03	5.08E-03	5.08E-03	5.08E-03	5.08E-03
*Number magnets required	---	nmag.l	4.00E+00	4.00E+00	4.00E+00	4.00E+00	4.00E+00	4.00E+00
magnet length	m	L.l	5.00E+00	9.94E+00	5.00E+00	5.00E+00	9.94E+00	5.00E+00
Magnet length/vehicle length			OK	OK	OK	OK	OK	OK
Magnet design								
flux leakage coefficients								
fringing (across air gap)	---	nuf.l	8.46E-01	1.13E+00	7.67E-01	8.46E-01	1.13E+00	7.67E-01
leakage (between poles)	---	nul.l	1.84E-01	2.40E-01	1.70E-01	1.84E-01	2.40E-01	1.70E-01
total	---	nut.l	2.03E+00	2.37E+00	1.94E+00	2.03E+00	2.37E+00	1.94E+00
nominal field in air gap	T	B0.l	7.51E-01	6.15E-01	8.00E-01	7.51E-01	6.15E-01	8.00E-01
√Max. Force per magnet(@2*H1x.l)	N	Fpm.l	5.10E+04	5.10E+04	5.10E+04	5.10E+04	5.10E+04	5.10E+04
Max. lateral g's @ twice nom. gap	g		OK	OK	OK	OK	OK	OK
Max. amp turns per coil(@2H1x.l)	A	NI.l	1.20E+04	9.79E+03	1.02E+04	1.20E+04	9.79E+03	1.02E+04
√Max. steady state NI (one coil)		NI_ss.l	4.98E+03	4.07E+03	4.24E+03	4.98E+03	4.07E+03	4.24E+03
core mass (1 mag)	kg	Mcore.l	2.53E+02	3.32E+02	2.01E+02	2.53E+02	3.32E+02	2.01E+02
√mass core + coil (4 mag)	kg	Mmag.l	1.55E+03	2.17E+03	1.23E+03	1.55E+03	2.17E+03	1.23E+03
Total magnet weight/vehicle wt.		%	3.87%	5.43%	3.08%	3.87%	5.43%	3.08%
Coil design								

Table F-1. (continued)

ElectroMagnetic Suspension I Optimized for operation at 89 m/s maximum speed

(Separate vertical & lateral suspensions & linear induction motor)

Asterisk (*) before description indicates input.
2 Asterisks (**) after description indicates output from MatLab Linear Induction Motor Analysis program.

DESCRIPTION	UNITS	SYMBOL	89 m/s Optimization			89 m/s Optimization @ 59 m/s		
			DESIGN 1	DESIGN 2	DESIGN 3	DESIGN 1	DESIGN 2	DESIGN 3
			baseline (b/l)	slim pole (3/4 b/l)	small gap (0.8 b/l)	baseline	slim pole (3/4 b/l)	small gap (0.8 b/l)
√resist(1 coil, of 2 on magnet)	ohm	resc.l	1.77E-04	4.32E-04	2.20E-04	1.77E-04	4.32E-04	2.20E-04
√Max. St. st. ohmic power(N/2 mag:	W	qm_ss.l	1.76E+04	3.97E+04	2.18E+04	1.76E+04	3.97E+04	2.18E+04
√Max. ohmic power (N/2 magnets)	W	qc.l	1.02E+05	8.29E+04	4.56E+04	1.02E+05	8.29E+04	4.56E+04
√Maximum coil power(1 coil)	W	qc_max.l	2.54E+04	4.14E+04	2.28E+04	2.54E+04	4.14E+04	2.28E+04
√Max. steady state coil power(1 coi	W	qc_ss.l	4.39E+03	7.17E+03	3.94E+03	4.39E+03	7.17E+03	3.94E+03
√Steady state temperature rise	°C	Tm_ss.l	1.50E+02	1.41E+02	1.50E+02	1.50E+02	1.41E+02	1.50E+02
√Short term temperature rise	°C	Tm_st.l	6.41E+01	3.31E+01	3.58E+01	6.41E+01	3.31E+01	3.58E+01
Maximum coil temperature	°C	Tc_max.	2.00E+02	1.91E+02	2.00E+02	2.00E+02	1.91E+02	2.00E+02
√mass(one coil)	kg	Mc.l	6.66E+01	1.05E+02	5.36E+01	6.66E+01	1.05E+02	5.36E+01
Rail design								
√rail thickness	m	tr.l	2.87E-02	2.13E-02	2.54E-02	2.87E-02	2.13E-02	2.54E-02
√rail pole tip width (=tr)	m	lr.l	2.87E-02	2.13E-02	2.54E-02	2.87E-02	2.13E-02	2.54E-02
rail mass/length(two rails)	kg/m	mr.l	8.28E+01	5.36E+01	6.49E+01	8.28E+01	5.36E+01	6.49E+01
nominal rail flux density(centered?)	T	Br.l	9.13E-01	8.70E-01	9.28E-01	9.13E-01	8.70E-01	9.28E-01
eff. freq. for eddy anal.	Hz	Fe.l	8.90E+00	4.48E+00	8.90E+00	5.90E+00	2.97E+00	5.90E+00
dB/dt amp. first harmonic	T/s	B1x.l	3.25E+01	1.56E+01	3.30E+01	2.15E+01	1.03E+01	2.19E+01
eddy current power	W	Pr.l	7.34E+03	1.21E+03	4.72E+03	3.23E+03	5.31E+02	2.07E+03
rms eddy amp turn (upper bound, 1 magnet)	A	NIe.l	8.36E+02	1.94E+02	5.97E+02	5.54E+02	1.29E+02	3.96E+02
Maximum continuous Power	W	P.l	2.49E+04	2.99E+04	2.05E+04	2.08E+04	2.92E+04	1.78E+04
Linear Induction Motor								
Design maximum thrust	g	max.g	1.50E-01	1.50E-01	1.50E-01	1.50E-01	1.50E-01	1.50E-01
Design maximum thrust	N	max.thr	5.88E+04	5.88E+04	5.88E+04	5.88E+04	5.88E+04	5.88E+04
Nominal excitation frequency	Hz	fsync	1.35E+02	1.35E+02	1.60E+02	8.94E+01	8.94E+01	1.06E+02
Synchronous speed	m/s	vsync	8.99E+01	8.99E+01	8.99E+01	5.96E+01	5.96E+01	5.96E+01
Nominal slip		nom.slip	1.00E-02	1.00E-02	1.00E-02	1.00E-02	1.00E-02	1.00E-02
General								
*Number of motors		Nmotor	4.00E+00	4.00E+00	4.00E+00	4.00E+00	4.00E+00	4.00E+00
*Number of poles		Np.v	1.20E+01	1.20E+01	1.40E+01	1.20E+01	1.20E+01	1.40E+01
Geometric dimensions								
*Air gap (mechanical clearance)	m	cl.v	1.00E-02	1.00E-02	8.00E-03	1.00E-02	1.00E-02	8.00E-03
*Pole pitch	m	tau.v	3.33E-01	3.33E-01	2.81E-01	3.33E-01	3.33E-01	2.81E-01
*Slots/pole/phase		Nslots	2.00E+00	2.00E+00	2.00E+00	2.00E+00	2.00E+00	2.00E+00
*Core width	m	d.v	1.80E-01	1.80E-01	1.92E-01	1.80E-01	1.80E-01	1.92E-01
*Tooth width/slot width ratio		tsr.v	1.20E+00	1.20E+00	1.20E+00	1.20E+00	1.20E+00	1.20E+00
*Slot depth	m	h.v	5.00E-02	5.00E-02	5.00E-02	5.00E-02	5.00E-02	5.00E-02
*Lamination thickness	m	tlam.v	3.56E-04	3.56E-04	3.56E-04	3.56E-04	3.56E-04	3.56E-04
Magnetic gap (entrefer)	m	g.mag	1.50E-02	1.50E-02	1.30E-02	1.50E-02	1.50E-02	1.30E-02
Carter factor		Kcarter	1.19E+00	1.19E+00	1.18E+00	1.19E+00	1.19E+00	1.18E+00
Effective magnetic gap	m	ge.lim	1.78E-02	1.78E-02	1.54E-02	1.78E-02	1.78E-02	1.54E-02
Back iron thickness, vehicle	m	ty.v	5.74E-02	5.74E-02	4.69E-02	5.74E-02	5.74E-02	4.69E-02
Tooth width	m	lt.v	2.53E-02	2.53E-02	2.13E-02	2.53E-02	2.53E-02	2.13E-02
Slot width	m	w.v	3.03E-02	3.03E-02	2.55E-02	3.03E-02	3.03E-02	2.55E-02
Slot pitch (=tooth pitch)	m	sp.v	5.56E-02	5.56E-02	4.68E-02	5.56E-02	5.56E-02	4.68E-02
Number of laminations		Nlams.v	5.05E+02	5.05E+02	5.39E+02	5.05E+02	5.05E+02	5.39E+02
Motor effective length	m	Leff	4.00E+00	4.00E+00	3.93E+00	4.00E+00	4.00E+00	3.93E+00
Motor physical length	m	Lphys	4.56E+00	4.56E+00	4.40E+00	4.56E+00	4.56E+00	4.40E+00
Effective air gap area	m^2	Aface	7.20E-01	7.20E-01	7.55E-01	7.20E-01	7.20E-01	7.55E-01
Core exposed surface area	m^2	Acore	2.44E+00	2.44E+00	2.37E+00	2.44E+00	2.44E+00	2.37E+00
Winding parameters								
*Number of phases		Nphase.v	3.00E+00	3.00E+00	3.00E+00	3.00E+00	3.00E+00	3.00E+00
*Coil pitch/pole pitch ratio(fraction)		cp_tau	6.67E-01	6.67E-01	6.67E-01	6.67E-01	6.67E-01	6.67E-01
*Number of winding layers		Nlayers.v	2.00E+00	2.00E+00	2.00E+00	2.00E+00	2.00E+00	2.00E+00

Table F-1. (continued)

ElectroMagnetic Suspension I Optimized for operation at 89 m/s maximum speed

(Separate vertical & lateral suspensions & linear induction motor)

Asterisk (*) before description indicates input.
2 Asterisks (**) after description indicates output from MatLab Linear Induction Motor Analysis program.

DESCRIPTION	UNITS	SYMBOL	89 m/s Optimization			89 m/s Optimization @ 59 m/s		
			DESIGN 1	DESIGN 2	DESIGN 3	DESIGN 1	DESIGN 2	DESIGN 3
			baseline (b/l)	slim pole (3/4 b/l)	small gap (0.8 b/l)	baseline	slim pole (3/4 b/l)	small gap (0.8 b/l)
*Number of coils/pole/phase		ncoils.v	2.00E+00	2.00E+00	2.00E+00	2.00E+00	2.00E+00	2.00E+00
*Coil packing factor		f.v	7.85E-01	7.85E-01	7.85E-01	7.85E-01	7.85E-01	7.85E-01
*Pole/coil clearance	m	z.v	5.00E-03	5.00E-03	5.00E-03	5.00E-03	5.00E-03	5.00E-03
*Turns/coil		Npc.v	1.00E+00	1.00E+00	1.00E+00	1.00E+00	1.00E+00	1.00E+00
*End turn angle	degrees	alpha	3.00E+01	3.00E+01	3.00E+01	3.00E+01	3.00E+01	3.00E+01
*End turn projection	m	b	1.00E-02	1.00E-02	1.00E-02	1.00E-02	1.00E-02	1.00E-02
Distribution factor(distributed winding)		Kd	8.66E-01	8.66E-01	8.66E-01	8.66E-01	8.66E-01	8.66E-01
Pitch factor(fractional pitch coils)		Kp	8.66E-01	8.66E-01	8.66E-01	8.66E-01	8.66E-01	8.66E-01
Winding factor(for distributed windings)		Kw	7.50E-01	7.50E-01	7.50E-01	7.50E-01	7.50E-01	7.50E-01
Coil pitch	m	tau_c.v	2.22E-01	2.22E-01	1.87E-01	2.22E-01	2.22E-01	1.87E-01
Mean conductor length	m/coil	lcoil.v	9.13E-01	9.13E-01	8.57E-01	9.13E-01	9.13E-01	8.57E-01
Coil thickness	m	tcoil.v	2.25E-02	2.25E-02	2.25E-02	2.25E-02	2.25E-02	2.25E-02
Conductor x-section area/slot/layer	m^2	Acoil.v	5.35E-04	5.35E-04	4.51E-04	5.35E-04	5.35E-04	4.51E-04
Coil Resistance	ohm	Rcoil.v	8.08E-05	8.08E-05	9.02E-05	8.08E-05	8.08E-05	9.02E-05
Heat transfer area (1 coil)	m^2	Aht.v	7.74E-02	7.74E-02	6.39E-02	7.74E-02	7.74E-02	6.39E-02
Peak MMF per coil RMS amp-turns	-	MMFperN	4.05E+00	4.05E+00	4.05E+00	4.05E+00	4.05E+00	4.05E+00
Core operating flux density	T	Bcore.v	1.50E+00	1.50E+00	1.50E+00	1.50E+00	1.50E+00	1.50E+00
Coil RMS amp-turns @ Bsat of tooth	Amp-turn	NIcoil.v	2.38E+03	2.38E+03	2.06E+03	2.38E+03	2.38E+03	2.06E+03
Total flux per pole @ Bsat of tooth	Webers	Fpp	3.10E-02	3.10E-02	2.70E-02	3.10E-02	3.10E-02	2.70E-02
RMS phase current @ Bsat of tooth	A	Iphase.v	2.38E+03	2.38E+03	2.06E+03	2.38E+03	2.38E+03	2.06E+03
Total RMS slot current @ Bsat of tooth	A	Islot .v	4.77E+03	4.77E+03	4.12E+03	4.77E+03	4.77E+03	4.12E+03
Coil power (1coil)	W	Pcoil.v	4.59E+02	4.59E+02	3.82E+02	4.59E+02	4.59E+02	3.82E+02
Coil surface temperature rise	°C	delTavg.v	1.41E+02	1.41E+02	1.43E+02	1.41E+02	1.41E+02	1.43E+02
Maximum coil surface temperature	°C	Tw.lim	1.91E+02	1.91E+02	1.93E+02	1.91E+02	1.91E+02	1.93E+02
Slot current	A-conduct.	I.slot	4.77E+03	4.77E+03	4.12E+03	4.77E+03	4.77E+03	4.12E+03
Linear current loading	A/m	I.load	8.58E+04	8.58E+04	8.79E+04	8.58E+04	8.58E+04	8.79E+04
Stator Leakage Reactance Calculations								
Slot Leakage	ohm	Xslot	1.21E-02	1.21E-02	2.13E-02	8.05E-03	8.05E-03	1.41E-02
End turn leakage	ohm	Xec	3.60E-08	3.60E-08	2.64E-08	2.39E-08	2.39E-08	1.75E-08
Total Primary Leakage Reactance	ohm	Xleak	1.21E-02	1.21E-02	2.13E-02	8.05E-03	8.05E-03	1.41E-02
Stator Leakage Reactance @ 50 Hz.								
Leakage Reactance @ 50 Hz.	ohm/phase	X50_	4.50E-03	4.50E-03	6.65E-03	4.50E-03	4.50E-03	6.65E-03
Coil Resistance	ohm/phase	Rone	3.88E-03	3.88E-03	5.05E-03	3.88E-03	3.88E-03	5.05E-03
Reactance/Resistance ratio @ 50 Hz	-	alpha50	1.16E+00	1.16E+00	1.32E+00	1.16E+00	1.16E+00	1.32E+00
Series turns/phase		stp.lim	2.40E+01	2.40E+01	2.80E+01	2.40E+01	2.40E+01	2.80E+01
Resistance, Primary	ohm/phase	rp.lim	3.88E-03	3.88E-03	5.05E-03	3.88E-03	3.88E-03	5.05E-03
Motor iron weight, single stator	kg	mi.v	5.31E+02	5.31E+02	4.80E+02	5.31E+02	5.31E+02	4.80E+02
Motor conductor weight, single stator	kg	mc.v	9.78E+01	9.78E+01	9.03E+01	9.78E+01	9.78E+01	9.03E+01
Total motor weight(Nmotor motors)	kg	mmotor	2.52E+03	2.52E+03	2.28E+03	2.52E+03	2.52E+03	2.28E+03
Core loss power, single stator	W	Pcore	5.59E+03	5.59E+03	6.53E+03	3.02E+03	3.02E+03	3.52E+03
Core temperature rise	°C	delTcore	5.47E+01	5.47E+01	6.58E+01	2.95E+01	2.95E+01	3.55E+01
Core surface temperature	°C	Tcore	1.05E+02	1.05E+02	1.16E+02	7.95E+01	7.95E+01	8.55E+01
Motor Secondary (guideway) Design Parameters								
Iron								
Back iron thickness, guideway	m	ty.g	4.61E-02	4.61E-02	3.87E-02	4.61E-02	4.61E-02	3.87E-02
Back iron width	m	d.g	2.10E-01	2.10E-01	2.18E-01	2.10E-01	2.10E-01	2.18E-01
Guideway iron specific weight	kg/m	mi.g	7.27E+01	7.27E+01	6.34E+01	7.27E+01	7.27E+01	6.34E+01
Conductor								
*Conductor overlap factor		colf.g	4.00E-01	4.00E-01	4.00E-01	4.00E-01	4.00E-01	4.00E-01
*Conductor thickness	m	tc.g	5.00E-03	5.00E-03	5.00E-03	5.00E-03	5.00E-03	5.00E-03

Table F-1. (continued)

ElectroMagnetic Suspension I Optimized for operation at 89 m/s maximum speed

(Separate vertical & lateral suspensions & linear induction motor)

Asterisk (*) before description indicates input.
2 Asterisks (**) after description indicates output from MatLab Linear Induction Motor Analysis program.

DESCRIPTION	UNITS	SYMBOL	89 m/s Optimization			89 m/s Optimization @ 59 m/s		
			DESIGN 1	DESIGN 2	DESIGN 3	DESIGN 1	DESIGN 2	DESIGN 3
			baseline (b/l)	slim pole (3/4 b/l)	small gap (0.8 b/l)	baseline	slim pole (3/4 b/l)	small gap (0.8 b/l)
Conductor width	m	dc.g	4.77E-01	4.77E-01	4.43E-01	4.77E-01	4.77E-01	4.43E-01
Guideway conductor specific weight	kg/m	mc.g	6.63E+00	6.63E+00	6.16E+00	6.63E+00	6.63E+00	6.16E+00
Total guideway added weight	kg/m	m.gw	1.59E+02	1.59E+02	1.39E+02	1.59E+02	1.59E+02	1.39E+02
Performance Results from MatLab Analysis								
Individual Motor Parameters at Maximum Propulsive Force								
Thrust**	N	Thrust	1.47E+04	1.47E+04	1.46E+04	6.47E+03	6.47E+03	6.43E+03
Slip**	-	slip	1.50E-02	1.50E-02	1.50E-02	2.20E-02	2.20E-02	2.20E-02
Traction Power**	W	P.tract	1.31E+06	1.31E+06	1.29E+06	3.77E+05	3.77E+05	3.74E+05
Real input Power**	W	Pin.real	1.37E+06	1.37E+06	1.35E+06	4.03E+05	4.03E+05	3.98E+05
Reactive input Power**	V-A	Pin.reac	1.57E+06	1.57E+06	1.53E+06	4.68E+05	4.68E+05	4.57E+05
Efficiency**	%	eff.v	9.56E+01	9.56E+01	9.58E+01	9.36E+01	9.36E+01	9.41E+01
Power Factor		PwrFac	6.57E-01	6.57E-01	6.57E-01	6.57E-01	6.57E-01	6.57E-01
AUXILIARY CALCULATIONS								
LIFT MAGNETS								
permeances								
√Air gap fringing permeance/length		Pf	1.92E+00	1.92E+00	1.92E+00	1.92E+00	1.92E+00	1.92E+00
√Ideal air gap permeance/length		Pu	3.14E+00	2.35E+00	3.49E+00	3.14E+00	2.35E+00	3.49E+00
?Inter-pole leakage perm./length		Pl	3.94E-01	3.82E-01	4.06E-01	3.94E-01	3.82E-01	4.06E-01
coil dimensions								
√Mean turn length	m	lc	1.02E+01	1.92E+01	1.02E+01	1.02E+01	1.92E+01	1.02E+01
√Coil crossectional area(one coil)	m^2	ac	1.39E-03	1.12E-03	1.11E-03	1.39E-03	1.12E-03	1.11E-03
√Coil Surface area(for 1 coil)	m^2	adis	1.77E+00	2.91E+00	1.59E+00	1.77E+00	2.91E+00	1.59E+00
GUIDANCE MAGNETS								
permeances								
√Air gap fringing permeance/length		Pf.l	1.92E+00	1.92E+00	1.92E+00	1.92E+00	1.92E+00	1.92E+00
√Ideal air gap permeance/length		Pu.l	2.27E+00	1.70E+00	2.50E+00	2.27E+00	1.70E+00	2.50E+00
?Inter-pole leakage perm./length		Pl.l	4.17E-01	4.08E-01	4.27E-01	4.17E-01	4.08E-01	4.27E-01
coil dimensions								
√ Mean turn length(one coil)	m	lc.l	1.02E+01	2.01E+01	1.02E+01	1.02E+01	2.01E+01	1.02E+01
√Coil crossectional area(one coil)	m^2	ac.l	2.34E-03	1.89E-03	1.89E-03	2.34E-03	1.89E-03	1.89E-03
√Coil Surface area(for one coil)	m^2	adis.l	2.10E+00	3.63E+00	1.88E+00	2.10E+00	3.63E+00	1.88E+00
LINEAR INDUCTION MOTOR						0.00E+00	0.00E+00	0.00E+00
permeances						0.00E+00	0.00E+00	0.00E+00
Ideal air gap permeance/length		Pu.lim	1.01E+01	1.01E+01	1.25E+01	1.01E+01	1.01E+01	1.25E+01
Air gap fringing permeance/length		Pf.lim	1.92E+00	1.92E+00	1.92E+00	1.92E+00	1.92E+00	1.92E+00
Fringing permeance ratio		nuf.lim	1.90E-01	1.90E-01	1.54E-01	1.90E-01	1.90E-01	1.54E-01
EMS I Summary								
Weight on Vehicle								
Lift Magnets	kg		1.54E+03	1.99E+03	1.23E+03	1.54E+03	1.99E+03	1.23E+03
Guidance Magnets	kg		1.55E+03	2.17E+03	1.23E+03	1.55E+03	2.17E+03	1.23E+03
Linear Induction Motor	kg		2.52E+03	2.52E+03	2.28E+03	2.52E+03	2.52E+03	2.28E+03
Total	kg		5.61E+03	6.68E+03	4.75E+03	5.61E+03	6.68E+03	4.75E+03
Weight on Guideway								
Lift Magnets	kg/m		1.13E+02	7.17E+01	8.94E+01	1.13E+02	7.17E+01	8.94E+01
Guidance Magnets	kg/m		8.28E+01	5.36E+01	6.49E+01	8.28E+01	5.36E+01	6.49E+01
Linear Induction Motor	kg/m		1.59E+02	1.59E+02	1.39E+02	1.59E+02	1.59E+02	1.39E+02
Total	kg/m		3.55E+02	2.84E+02	2.93E+02	3.55E+02	2.84E+02	2.93E+02
Real Input Power Dissipation								
Ohmic Power Dissipation								

Table F-1. (continued)

ElectroMagnetic Suspension I Optimized for operation at 89 m/s maximum speed

(Separate vertical & lateral suspensions & linear induction motor)

Asterisk (*) before description indicates input.
2 Asterisks (**) after description indicates output from MatLab Linear Induction Motor Analysis program.

DESCRIPTION	UNITS	SYMBOL	89 m/s Optimization			89 m/s Optimization @ 59 m/s		
			DESIGN 1	DESIGN 2	DESIGN 3	DESIGN 1	DESIGN 2	DESIGN 3
			baseline (b/l)	slim pole (3/4 b/l)	small gap (0.8 b/l)	baseline	slim pole (3/4 b/l)	small gap (0.8 b/l)
Lift Magnets	W		1.19E+05	1.95E+05	1.06E+05	1.19E+05	1.95E+05	1.06E+05
Guidance Magnets	W		1.76E+04	3.97E+04	2.18E+04	1.76E+04	3.97E+04	2.18E+04
Linear Induction Motor	W		6.00E+04	6.00E+04	5.62E+04	2.56E+04	2.56E+04	2.35E+04
Total Ohmic Power	W		1.96E+05	2.95E+05	1.84E+05	1.62E+05	2.60E+05	1.52E+05
Eddy current Power								
Lift Magnets	W		2.93E+04	4.94E+03	1.93E+04	1.29E+04	2.17E+03	8.47E+03
Guidance Magnets	W		7.34E+03	1.21E+03	4.72E+03	3.23E+03	5.31E+02	2.07E+03
Total eddy current Power	W		3.66E+04	6.14E+03	2.40E+04	1.61E+04	2.70E+03	1.05E+04
Total Real Power Dissipation	W		2.33E+05	3.01E+05	2.08E+05	1.78E+05	2.63E+05	1.62E+05
Reactive Input Power								
Linear Induction Motor	V-A		1.57E+06	1.57E+06	1.53E+06	4.68E+05	4.68E+05	4.57E+05
Total	V-A		1.57E+06	1.57E+06	1.53E+06	4.68E+05	4.68E+05	4.57E+05

Table F-2. Complete EMS I Spreadsheet; Design optimized for operation at 134 m/s
Separate Lift and guidance magnets and Linear Induction Motor

ElectroMagnetic Suspension I Optimized for operation at 134 m/s maximum speed
(Separate vertical & lateral suspensions & linear induction motor)

Asterisk (*) before description indicates input.
2 Asterisks (**) after description indicates output from MatLab LIM program.

DESCRIPTION	UNITS	SYMBOL	134 m/s Optimization			134 m/s Optimization @ 89 m/s		
			DESIGN 1	DESIGN 2	DESIGN 3	DESIGN 1	DESIGN 2	DESIGN 3
			baseline	slim pole (3/4 b/l)	small gap (0.8 b/l)	baseline	slim pole (3/4 b/l)	small gap (0.8 b/l)
VEHICLE PARAMETERS								
Design Parameters								
*Vehicle mass	kg	m	4.00E+04	4.00E+04	4.00E+04	4.00E+04	4.00E+04	4.00E+04
*Vehicle length	m	l_vehicle	3.00E+01	3.00E+01	3.00E+01	3.00E+01	3.00E+01	3.00E+01
*Design speed	m/s	V	1.34E+02	1.34E+02	1.34E+02	8.90E+01	8.90E+01	8.90E+01
*frontal area	m^2	Af	1.20E+01	1.20E+01	1.20E+01	1.20E+01	1.20E+01	1.20E+01
*air density	kg/m^3	roair	1.20E+00	1.20E+00	1.20E+00	1.20E+00	1.20E+00	1.20E+00
*drag coefficient	---	Cd	3.00E-01	3.00E-01	3.00E-01	3.00E-01	3.00E-01	3.00E-01
wind drag force	N	Fd	3.88E+04	3.88E+04	3.88E+04	1.71E+04	1.71E+04	1.71E+04
wind drag power	W	Pd	5.20E+06	5.20E+06	5.20E+06	1.52E+06	1.52E+06	1.52E+06
*Max. Lift Force(@Max disp.)	g	max_Fz	1.10E+00	1.10E+00	1.10E+00	1.10E+00	1.10E+00	1.10E+00
*Max. Lateral Force(")(cont.)	g	max_F.l	2.60E-01	2.60E-01	2.60E-01	2.60E-01	2.60E-01	2.60E-01
*Max. Lateral Force(")(short term)	g	max_sF.l	4.20E-01	4.20E-01	4.20E-01	4.20E-01	4.20E-01	4.20E-01
*Time of Max. (short)Lateral F	sec	t_max	5.00E+00	5.00E+00	5.00E+00	5.00E+00	5.00E+00	5.00E+00
*Max propulsive force	g	max_Fp	2.10E-01	2.10E-01	2.10E-01	2.10E-01	2.10E-01	2.10E-01
*Maximum ambient temperature	°C	maxTamb	5.00E+01	5.00E+01	5.00E+01	5.00E+01	5.00E+01	5.00E+01
Performance Parameters								
Power, (ohmic+eddy)/aero. drag	%		2.07E-01	2.51E-01	1.75E-01	5.41E-01	7.24E-01	4.43E-01
Weight, (magnet+coil)/vehicle	%		1.80E-01	2.07E-01	6.93E-02	1.80E-01	2.07E-01	6.93E-02
eddy/lift amp-T (up. bound)	%		1.89E-01	5.38E-02	1.62E-01	1.25E-01	3.57E-02	1.07E-01
Aerodynamic drag/lift force	%		9.89E-02	9.89E-02	9.89E-02	4.36E-02	4.36E-02	4.36E-02
CONSTANTS								
*air permeability	N/A^2	mu	1.26E-06	1.26E-06	1.26E-06	1.26E-06	1.26E-06	1.26E-06
Suspensions								
Construction materials								
*rail			steel	steel	steel	steel	steel	steel
*magnet			2V Perm.	2V Perm.	2V Perm.	2V Perm.	2V Perm.	2V Perm.
*coil			alum.	alum.	alum.	alum.	alum.	alum.
Materials properties								
mass density								
*rail	kg/m^3	ror	7.51E+03	7.51E+03	7.51E+03	7.51E+03	7.51E+03	7.51E+03
*magnet	kg/m^3	rom	7.78E+03	7.78E+03	7.78E+03	7.78E+03	7.78E+03	7.78E+03
*coil	kg/m^3	roc	2.78E+03	2.78E+03	2.78E+03	2.78E+03	2.78E+03	2.78E+03
maximum flux density								
*rail	T	Bsatr	1.60E+00	1.60E+00	1.60E+00	1.60E+00	1.60E+00	1.60E+00
*magnet	T	Bsatm	2.30E+00	2.30E+00	2.30E+00	2.30E+00	2.30E+00	2.30E+00
*Saturation Safety Factor(<1)	---	SF	1.00E+00	1.00E+00	1.00E+00	1.00E+00	1.00E+00	1.00E+00
electrical resistivity								
*rail @20°C	ohm-m	rr	4.06E-07	4.06E-07	4.06E-07	4.06E-07	4.06E-07	4.06E-07
*Temp. coefficient of rail	ohm-m/°C	rr_tc						
*coil @140 deg C	ohm-m	rc_	4.06E-08	4.06E-08	4.06E-08	4.06E-08	4.06E-08	4.06E-08
*Temp. coefficient of coil	ohm-m/°C	rc_tc						
Thermal								
*magnet heat transfer coef.	W/C-m^2	k	1.40E+01	1.40E+01	1.40E+01	1.40E+01	1.40E+01	1.40E+01
*Coil Specific heat	J/(kg°C)	cp	1.19E+02	1.19E+02	1.19E+02	1.19E+02	1.19E+02	1.19E+02
*Maximum wire insulation temp	°C	maxTins	2.00E+02	2.00E+02	2.00E+02	2.00E+02	2.00E+02	2.00E+02
Linear Induction Motor								
Construction materials								
*rail			steel	steel	steel	steel	steel	steel
*rail conductor(s)			aluminum	aluminum	aluminum	aluminum	aluminum	aluminum

Table F-2. (continued)

ElectroMagnetic Suspension I Optimized for operation at 134 m/s maximum speed

(Separate vertical & lateral suspensions & linear induction motor)

Asterisk (*) before description indicates input.
2 Asterisks (**) after description indicates output from MatLab LIM program.

DESCRIPTION	UNITS	SYMBOL	134 m/s Optimization			134 m/s Optimization @ 89 m/s		
			DESIGN 1	DESIGN 2	DESIGN 3	DESIGN 1	DESIGN 2	DESIGN 3
			baseline	slim pole (3/4 b/l)	small gap (0.8 b/l)	baseline	slim pole (3/4 b/l)	small gap (0.8 b/l)
Materials properties								
Mass density								
*rail	kg/m^3	rom.g	7.51E+03	7.51E+03	7.51E+03	7.51E+03	7.51E+03	7.51E+03
*rail conductor(s)	kg/m^3	roc.g	2.78E+03	2.78E+03	2.78E+03	2.78E+03	2.78E+03	2.78E+03
*magnet	kg/m^3	rom.v	7.65E+03	7.65E+03	7.65E+03	7.65E+03	7.65E+03	7.65E+03
*coil	kg/m^3	roc.v	2.78E+03	2.78E+03	2.78E+03	2.78E+03	2.78E+03	2.78E+03
maximum flux densities								
*rail	T	bsat.g	1.60E+00	1.60E+00	1.60E+00	1.60E+00	1.60E+00	1.60E+00
*magnet	T	bsat.v	1.50E+00	1.50E+00	1.50E+00	1.50E+00	1.50E+00	1.50E+00
Magnetic permeability								
rail	---	mu.g	3.50E+03	3.50E+03	3.50E+03	3.50E+03	3.50E+03	3.50E+03
Vehicle (short) stator		mu.v						
Core Loss @ 1.0T, 100 Hz	W/kg	refc.loss	2.87E+00	2.87E+00	2.87E+00	2.87E+00	2.87E+00	2.87E+00
Core loss frequency exponent	-	freq.exp	1.50E+00	1.50E+00	1.50E+00	1.50E+00	1.50E+00	1.50E+00
Core loss Induction exponent	-	B.exp	2.10E+00	2.10E+00	2.10E+00	2.10E+00	2.10E+00	2.10E+00
Core loss @ fsync & Bcore	W/kg	c.loss	1.95E+01	1.95E+01	2.51E+01	1.05E+01	1.05E+01	1.36E+01
electrical resistivity								
*Magnet laminations @ 140°C	ohm-m	rm.v	7.00E-07	7.00E-07	7.00E-07	7.00E-07	7.00E-07	7.00E-07
*rail @20 deg C	ohm-m	rm.g	4.06E-07	4.06E-07	4.06E-07	4.06E-07	4.06E-07	4.06E-07
*vehicle coil @20 deg C	ohm-m	rcRT.v	2.78E-08	2.78E-08	2.78E-08	2.78E-08	2.78E-08	2.78E-08
*vehicle coil temperature coefficie	1/°C	alpha.v	4.10E-03	4.10E-03	4.10E-03	4.10E-03	4.10E-03	4.10E-03
vehicle coil @operating temperatu	ohm-m	rc.v	4.79E-08	4.79E-08	4.80E-08	4.79E-08	4.79E-08	4.80E-08
*Guideway conductor @20 deg c	ohm-m	rc.g	2.80E-08	2.80E-08	2.80E-08	2.80E-08	2.80E-08	2.80E-08
Heat transfer coeffieients								
*magnet heat transfer coef.	W/C-m^2	k.v	4.19E+01	4.19E+01	4.19E+01	4.19E+01	4.19E+01	4.19E+01
*rail heat transfer coef.	W/C-m^2	k.g	1.40E+01	1.40E+01	1.40E+01	1.40E+01	1.40E+01	1.40E+01
COMPONENT DESIGN & ANALYSIS								
Vertical suspension								
Geometric dimensions								
*pole width	m	lp	3.14E-02	2.35E-02	2.79E-02	3.14E-02	2.35E-02	2.79E-02
*air gap	m	H1x	1.00E-02	1.00E-02	8.00E-03	1.00E-02	1.00E-02	8.00E-03
*window width	m	w	9.43E-02	8.51E-02	8.50E-02	9.43E-02	8.51E-02	8.50E-02
*window height	m	h	4.72E-02	4.25E-02	4.25E-02	4.72E-02	4.25E-02	4.25E-02
Window width/height	---		2.00E+00	2.00E+00	2.00E+00	2.00E+00	2.00E+00	2.00E+00
	---		OK	OK	OK	OK	OK	OK
*coil packing factor	---	f	7.00E-01	7.00E-01	7.00E-01	7.00E-01	7.00E-01	7.00E-01
*pole-coil clearance	m	z	5.08E-03	5.08E-03	5.08E-03	5.08E-03	5.08E-03	5.08E-03
*Number magnets required	---	nmag	4.00E+00	4.00E+00	4.00E+00	4.00E+00	4.00E+00	4.00E+00
magnet length	m	L	5.00E+00	9.52E+00	5.00E+00	5.00E+00	9.52E+00	5.00E+00
Magnet length/vehicle length ratio			OK	OK	OK	OK	OK	OK
Magnet design								
leakage/fringing flux ratios								
√ fringing (across air gap)	---	nuf	6.12E-01	8.16E-01	5.51E-01	6.12E-01	8.16E-01	5.51E-01
√ leakage (between poles)	---	nul	1.26E-01	1.63E-01	1.16E-01	1.26E-01	1.63E-01	1.16E-01
√total	---	nut	1.74E+00	1.98E+00	1.67E+00	1.74E+00	1.98E+00	1.67E+00
√nominal field in air gap(@2*H1x)	T	B0	9.29E-01	7.78E-01	9.85E-01	9.29E-01	7.78E-01	9.85E-01
√Max. Force per magnet(@2*H1x)	N	Fpm	1.08E+05	1.08E+05	1.08E+05	1.08E+05	1.08E+05	1.08E+05
√Max. vertical g's @ twice nom. gap	g		OK	OK	OK	OK	OK	OK
√Max amp turns per coil(@ 2H1x)	A	NI	1.48E+04	1.24E+04	1.25E+04	1.48E+04	1.24E+04	1.25E+04
√Max. steady state NI (1 coil@1g)		NI_ss	7.05E+03	5.90E+03	5.98E+03	7.05E+03	5.90E+03	5.98E+03

Table F-2. (continued)

ElectroMagnetic Suspension I Optimized for operation at 134 m/s maximum speed

(Separate vertical & lateral suspensions & linear induction motor)

Asterisk (*) before description indicates input.
2 Asterisks (**) after description indicates output from MatLab LIM program.

DESCRIPTION	UNITS	SYMBOL	134 m/s Optimization			134 m/s Optimization @ 89 m/s		
			DESIGN 1	DESIGN 2	DESIGN 3	DESIGN 1	DESIGN 2	DESIGN 3
			baseline	slim pole (3/4 b/l)	small gap (0.8 b/l)	baseline	slim pole (3/4 b/l)	small gap (0.8 b/l)
√core mass (1 mag)	kg	Mcore	3.07E+02	3.79E+02	2.45E+02	3.07E+02	3.79E+02	2.45E+02
√mass core + coil (4 mag)	kg	Mmag	1.54E+03	1.99E+03	1.23E+03	1.54E+03	1.99E+03	1.23E+03
√Total magnet weight/vehicle wt.		%	3.86%	4.98%	3.08%	3.86%	4.98%	3.08%
Coil Design								
√resist (1 coil, of 2 on magnet)	ohm	resc	2.98E-04	6.99E-04	3.72E-04	2.98E-04	6.99E-04	3.72E-04
√Max. St. st. ohmic power(N mags)	W	qm_ss	1.19E+05	1.95E+05	1.06E+05	1.19E+05	1.95E+05	1.06E+05
√Max coil ohmic power (N magnets)	W	qc	5.22E+05	8.58E+05	4.68E+05	5.22E+05	8.58E+05	4.68E+05
√Maximum coil power(1 coil)	W	qc_max	6.52E+04	1.07E+05	5.85E+04	6.52E+04	1.07E+05	5.85E+04
√Max. steady state coil power(1 coi	W	qc_ss	1.48E+04	2.44E+04	1.33E+04	1.48E+04	2.44E+04	1.33E+04
√Steady state temperature rise	°C	Tm_ss	1.50E+02	1.50E+02	1.50E+02	1.50E+02	1.50E+02	1.50E+02
√Short term temperature rise	°C	Tm_st	5.57E+02	6.06E+02	6.24E+02	5.57E+02	6.06E+02	6.24E+02
Maximum coil temperature	°C	Tc_max	2.00E+02	2.00E+02	2.00E+02	2.00E+02	2.00E+02	2.00E+02
√mass(one coil)	kg	Mc	3.95E+01	5.96E+01	3.15E+01	3.95E+01	5.96E+01	3.15E+01
Rail design								
√rail thickness	m	tr	4.05E-02	3.01E-02	3.61E-02	4.05E-02	3.01E-02	3.61E-02
√rail pole tip width	m	lr	4.05E-02	3.01E-02	3.61E-02	4.05E-02	3.01E-02	3.61E-02
rail mass/length(2 rails)	kg/m	mr	1.13E+02	7.17E+01	8.94E+01	1.13E+02	7.17E+01	8.94E+01
nominal rail flux density	T	Br	1.16E+00	1.10E+00	1.18E+00	1.16E+00	1.10E+00	1.18E+00
eff. freq. for eddy anal.	Hz	Fe	1.34E+01	7.04E+00	1.34E+01	8.90E+00	4.68E+00	8.90E+00
dB/dt amp. first harmonic	T/s	B1x	6.22E+01	3.11E+01	6.33E+01	4.13E+01	2.07E+01	4.20E+01
eddy current power	W	Pr	6.63E+04	1.12E+04	4.37E+04	2.93E+04	4.94E+03	1.93E+04
rms eddy amp turn (upper bound, 1 magnet)	A	NIe	2.79E+03	6.66E+02	2.03E+03	1.86E+03	4.42E+02	1.35E+03
√Total continuous power	W	P.v	1.85E+05	2.06E+05	1.50E+05	1.48E+05	2.00E+05	1.26E+05
Lateral Suspension								
Geometric dimensions								
*pole width	m	lp.l	2.80E-02	2.10E-02	2.48E-02	2.80E-02	2.10E-02	2.48E-02
*window width	m	w.l	1.26E-01	1.13E-01	1.14E-01	1.26E-01	1.13E-01	1.14E-01
*window height	m	h.l	6.32E-02	5.64E-02	5.69E-02	6.32E-02	5.64E-02	5.69E-02
Window width/height ratio	---		2.00E+00	2.00E+00	2.00E+00	2.00E+00	2.00E+00	2.00E+00
"	---		OK	OK	OK	OK	OK	OK
*coil packing factor	---	f.l	7.00E-01	7.00E-01	7.00E-01	7.00E-01	7.00E-01	7.00E-01
*air gap	m	H1x.l	1.00E-02	1.00E-02	8.00E-03	1.00E-02	1.00E-02	8.00E-03
*pole-coil clearance	m	z.l	5.08E-03	5.08E-03	5.08E-03	5.08E-03	5.08E-03	5.08E-03
*Number magnets required	---	nmag.l	4.00E+00	4.00E+00	4.00E+00	4.00E+00	4.00E+00	4.00E+00
magnet length	m	L.l	5.00E+00	9.68E+00	5.00E+00	5.00E+00	9.68E+00	5.00E+00
Magnet length/vehicle length			OK	OK	OK	OK	OK	OK
Magnet design								
flux leakage coefficients								
fringing (across air gap)	---	nuf.l	6.87E-01	9.15E-01	6.20E-01	6.87E-01	9.15E-01	6.20E-01
leakage (between poles)	---	nul.l	1.51E-01	1.96E-01	1.39E-01	1.51E-01	1.96E-01	1.39E-01
total	---	nut.l	1.84E+00	2.11E+00	1.76E+00	1.84E+00	2.11E+00	1.76E+00
nominal field in air gap	T	B0.l	8.60E-01	7.14E-01	9.14E-01	8.60E-01	7.14E-01	9.14E-01
√Max. Force per magnet(@2*H1x.l)	N	Fpm.l	8.23E+04	8.23E+04	8.23E+04	8.23E+04	8.23E+04	8.23E+04
Max. lateral g's @ twice nom. gap	g		OK	OK	OK	OK	OK	OK
Max. amp turns per coil(@2H1x.l)	A	NI.l	1.37E+04	1.14E+04	1.16E+04	1.37E+04	1.14E+04	1.16E+04
√Max. steady state NI (one coil)		NI_ss.l	5.39E+03	4.47E+03	4.58E+03	5.39E+03	4.47E+03	4.58E+03
core mass (1 mag)	kg	Mcore.l	3.36E+02	4.23E+02	2.67E+02	3.36E+02	4.23E+02	2.67E+02
√mass core + coil (4 mag)	kg	Mmag.l	1.93E+03	2.58E+03	1.54E+03	1.93E+03	2.58E+03	1.54E+03
Total magnet weight/vehicle wt.		%	4.83%	6.44%	3.85%	4.83%	6.44%	3.85%

Table F-2. (continued)

ElectroMagnetic Suspension I Optimized for operation at 134 m/s maximum speed

(Separate vertical & lateral suspensions & linear induction motor)

Asterisk (*) before description indicates input.
2 Asterisks (**) after description indicates output from MatLab LIM program.

DESCRIPTION	UNITS	SYMBOL	134 m/s Optimization			134 m/s Optimization @ 89 m/s		
			DESIGN 1 baseline	DESIGN 2 slim pole (3/4 b/l)	DESIGN 3 small gap (0.8 b/l)	DESIGN 1 baseline	DESIGN 2 slim pole (3/4 b/l)	DESIGN 3 small gap (0.8 b/l)
Coil design								
√resist(1 coil, of 2 on magnet)	ohm	resc.l	1.62E-04	3.92E-04	2.01E-04	1.62E-04	3.92E-04	2.01E-04
√Max. St. st. ohmic power(N/2 mag:	W	qm_ss.l	1.88E+04	3.88E+04	2.08E+04	1.88E+04	3.88E+04	2.08E+04
√Max. ohmic power (N/2 magnets)	W	qc.l	1.21E+05	1.01E+05	5.44E+04	1.21E+05	1.01E+05	5.44E+04
√Maximum coil power(1 coil)	W	qc_max.l	3.03E+04	5.06E+04	2.72E+04	3.03E+04	5.06E+04	2.72E+04
√Max. steady state coil power(1 coi	W	qc_ss.l	4.69E+03	7.83E+03	4.21E+03	4.69E+03	7.83E+03	4.21E+03
√Steady state temperature rise	°C	Tm_ss.l	1.50E+02	1.50E+02	1.50E+02	1.50E+02	1.50E+02	1.50E+02
√Short term temperature rise	°C	Tm_st.l	6.96E+01	3.85E+01	3.89E+01	6.96E+01	3.85E+01	3.89E+01
Maximum coil temperature	°C	Tc_max.	2.00E+02	2.00E+02	2.00E+02	2.00E+02	2.00E+02	2.00E+02
√mass(one coil)	kg	Mc.l	7.33E+01	1.10E+02	5.88E+01	7.33E+01	1.10E+02	5.88E+01
Rail design								
√rail thickness	m	tr.l	3.57E-02	2.65E-02	3.17E-02	3.57E-02	2.65E-02	3.17E-02
√rail pole tip width (=tr)	m	lr.l	3.57E-02	2.65E-02	3.17E-02	3.57E-02	2.65E-02	3.17E-02
rail mass/length(two rails)	kg/m	mr.l	1.13E+02	7.17E+01	8.87E+01	1.13E+02	7.17E+01	8.87E+01
nominal rail flux density(centered?)	T	Br.l	8.95E-01	8.52E-01	9.10E-01	8.95E-01	8.52E-01	9.10E-01
eff. freq. for eddy anal.	Hz	Fe.l	1.34E+01	6.92E+00	1.34E+01	8.90E+00	4.59E+00	8.90E+00
dB/dt amp. first harmonic	T/s	B1x.l	4.80E+01	2.36E+01	4.88E+01	3.19E+01	1.57E+01	3.24E+01
eddy current power	W	Pr.l	3.31E+04	5.49E+03	2.16E+04	1.46E+04	2.42E+03	9.52E+03
rms eddy amp turn (upper bound, 1 magnet)	A	Nle.l	2.05E+03	4.82E+02	1.48E+03	1.36E+03	3.20E+02	9.83E+02
Maximum continuous Power	W	P.l	5.19E+04	3.68E+04	3.84E+04	3.34E+04	3.37E+04	2.63E+04
Peak Power(@ V, max F & displ.)	W							
Linear Induction Motor								
Design maximum thrust	g	max.g	2.10E-01	2.10E-01	2.10E-01	2.10E-01	2.10E-01	2.10E-01
Design maximum thrust	N	max.thr	8.23E+04	8.23E+04	8.23E+04	8.23E+04	8.23E+04	8.23E+04
Nominal excitation frequency	Hz	fsync	2.03E+02	2.03E+02	2.41E+02	1.35E+02	1.35E+02	1.60E+02
Synchronous speed	m/s	vsync	1.35E+02	1.35E+02	1.35E+02	8.99E+01	8.99E+01	8.99E+01
Nominal slip		nom.slip	1.00E-02	1.00E-02	1.00E-02	1.00E-02	1.00E-02	1.00E-02
General								
*Number of motors		Nmotor	4.00E+00	4.00E+00	4.00E+00	4.00E+00	4.00E+00	4.00E+00
*Number of poles		Np.v	1.60E+01	1.60E+01	1.60E+01	1.60E+01	1.60E+01	1.60E+01
Geometric dimensions								
*Air gap (mechanical clearance)	m	cl.v	1.00E-02	1.00E-02	8.00E-03	1.00E-02	1.00E-02	8.00E-03
*Pole pitch	m	tau.v	3.33E-01	3.33E-01	2.81E-01	3.33E-01	3.33E-01	2.81E-01
*Slots/pole/phase		Nslots	2.00E+00	2.00E+00	2.00E+00	2.00E+00	2.00E+00	2.00E+00
*Core width	m	d.v	2.10E-01	2.10E-01	2.20E-01	2.10E-01	2.10E-01	2.20E-01
*Tooth width/slot width ratio		tsr.v	1.20E+00	1.20E+00	1.20E+00	1.20E+00	1.20E+00	1.20E+00
*Slot depth	m	h.v	5.00E-02	5.00E-02	5.00E-02	5.00E-02	5.00E-02	5.00E-02
*Lamination thickness	m	tlam.v	3.56E-04	3.56E-04	3.56E-04	3.56E-04	3.56E-04	3.56E-04
Magnetic gap (entrefer)	m	g.mag	1.50E-02	1.50E-02	1.30E-02	1.50E-02	1.50E-02	1.30E-02
Carter factor		Kcarter	1.19E+00	1.19E+00	1.18E+00	1.19E+00	1.19E+00	1.18E+00
Effective magnetic gap	m	ge.lim	1.78E-02	1.78E-02	1.54E-02	1.78E-02	1.78E-02	1.54E-02
Back iron thickness, vehicle	m	ty.v	5.61E-02	5.61E-02	4.61E-02	5.61E-02	5.61E-02	4.61E-02
Tooth width	m	lt.v	2.53E-02	2.53E-02	2.13E-02	2.53E-02	2.53E-02	2.13E-02
Slot width	m	w.v	3.03E-02	3.03E-02	2.55E-02	3.03E-02	3.03E-02	2.55E-02
Slot pitch (=tooth pitch)	m	sp.v	5.56E-02	5.56E-02	4.68E-02	5.56E-02	5.56E-02	4.68E-02
Number of laminations		Nlams.v	5.89E+02	5.89E+02	6.17E+02	5.89E+02	5.89E+02	6.17E+02
Motor effective length	m	Leff	5.33E+00	5.33E+00	4.50E+00	5.33E+00	5.33E+00	4.50E+00
Motor physical length	m	Lphys	5.89E+00	5.89E+00	4.96E+00	5.89E+00	5.89E+00	4.96E+00
Effective air gap area	m^2	Aface	1.12E+00	1.12E+00	9.89E-01	1.12E+00	1.12E+00	9.89E-01
Core exposed surface area	m^2	Acore	3.48E+00	3.48E+00	2.94E+00	3.48E+00	3.48E+00	2.94E+00

Table F-2. (continued)

ElectroMagnetic Suspension I Optimized for operation at 134 m/s maximum speed

(Separate vertical & lateral suspensions & linear induction motor)

Asterisk (*) before description indicates input.
2 Asterisks (**) after description indicates output from MatLab LIM program.

DESCRIPTION	UNITS	SYMBOL	134 m/s Optimization			134 m/s Optimization @ 89 m/s		
			DESIGN 1 baseline	DESIGN 2 slim pole (3/4 b/l)	DESIGN 3 small gap (0.8 b/l)	DESIGN 1 baseline	DESIGN 2 slim pole (3/4 b/l)	DESIGN 3 small gap (0.8 b/l)
Winding parameters								
*Number of phases		Nphase.v	3.00E+00	3.00E+00	3.00E+00	3.00E+00	3.00E+00	3.00E+00
*Coil pitch/pole pitch ratio(fraction)		cp_tau	6.67E-01	6.67E-01	6.67E-01	6.67E-01	6.67E-01	6.67E-01
*Number of winding layers		Nlayers.v	2.00E+00	2.00E+00	2.00E+00	2.00E+00	2.00E+00	2.00E+00
*Number of coils/pole/phase		ncoils.v	2.00E+00	2.00E+00	2.00E+00	2.00E+00	2.00E+00	2.00E+00
*Coil packing factor		f.v	7.85E-01	7.85E-01	7.85E-01	7.85E-01	7.85E-01	7.85E-01
*Pole/coil clearance	m	z.v	5.00E-03	5.00E-03	5.00E-03	5.00E-03	5.00E-03	5.00E-03
*Turns/coil		Npc.v	1.00E+00	1.00E+00	1.00E+00	1.00E+00	1.00E+00	1.00E+00
*End turn angle	degrees	alpha	3.00E+01	3.00E+01	3.00E+01	3.00E+01	3.00E+01	3.00E+01
*End turn projection	m	b	1.00E-02	1.00E-02	1.00E-02	1.00E-02	1.00E-02	1.00E-02
Distribution factor(distributed winding)		Kd	8.66E-01	8.66E-01	8.66E-01	8.66E-01	8.66E-01	8.66E-01
Pitch factor(fractional pitch coils)		Kp	8.66E-01	8.66E-01	8.66E-01	8.66E-01	8.66E-01	8.66E-01
Winding factor(for distributed windings)		Kw	7.50E-01	7.50E-01	7.50E-01	7.50E-01	7.50E-01	7.50E-01
Coil pitch	m	tau_c.v	2.22E-01	2.22E-01	1.87E-01	2.22E-01	2.22E-01	1.87E-01
Mean conductor length	m/coil	lcoil.v	9.73E-01	9.73E-01	9.13E-01	9.73E-01	9.73E-01	9.13E-01
Coil thickness	m	tcoil.v	2.25E-02	2.25E-02	2.25E-02	2.25E-02	2.25E-02	2.25E-02
Conductor x-section area/slot/laye	m^2	Acoil.v	5.35E-04	5.35E-04	4.51E-04	5.35E-04	5.35E-04	4.51E-04
Coil Resistance	ohm	Rcoil.v	8.72E-05	8.72E-05	9.72E-05	8.72E-05	8.72E-05	9.72E-05
Heat transfer area (1 coil)	m^2	Aht.v	8.06E-02	8.06E-02	6.66E-02	8.06E-02	8.06E-02	6.66E-02
Peak MMF per coil RMS amp-turns	-	MMFperN	4.05E+00	4.05E+00	4.05E+00	4.05E+00	4.05E+00	4.05E+00
Core operating flux density	T	Bcore.v	1.50E+00	1.50E+00	1.50E+00	1.50E+00	1.50E+00	1.50E+00
Coil RMS amp-turns @ Bsat of tooth	Amp-turn	NIcoil.v	2.38E+03	2.38E+03	2.06E+03	2.38E+03	2.38E+03	2.06E+03
Total flux per pole @ Bsat of tooth	Webers	Fpp	3.53E-02	3.53E-02	3.04E-02	3.53E-02	3.53E-02	3.04E-02
RMS phase current @ Bsat of tooth	A	Iphase.v	2.38E+03	2.38E+03	2.06E+03	2.38E+03	2.38E+03	2.06E+03
Total RMS slot current @ Bsat of to	A	Islot .v	4.77E+03	4.77E+03	4.12E+03	4.77E+03	4.77E+03	4.12E+03
Coil power (1coil)	W	Pcoil.v	4.95E+02	4.95E+02	4.11E+02	4.95E+02	4.95E+02	4.11E+02
Coil surface temperature rise	°C	delTavg.	1.46E+02	1.46E+02	1.48E+02	1.46E+02	1.46E+02	1.48E+02
Maximum coil surface temperature	°C	Tw.lim	1.96E+02	1.96E+02	1.98E+02	1.96E+02	1.96E+02	1.98E+02
Slot current	A-conduct.	I.slot	4.77E+03	4.77E+03	4.12E+03	4.77E+03	4.77E+03	4.12E+03
Linear current loading	A/m	I.load	8.58E+04	8.58E+04	8.79E+04	8.58E+04	8.58E+04	8.79E+04
Stator Leakage Reactance Calculations								
Slot Leakage	ohm	Xslot	2.84E-02	2.84E-02	4.19E-02	1.89E-02	1.89E-02	2.78E-02
End turn leakage	ohm	Xec	3.05E-08	3.05E-08	3.05E-08	2.02E-08	2.02E-08	2.02E-08
Total Primary Leakage Reactance	ohm	Xleak	2.84E-02	2.84E-02	4.19E-02	1.89E-02	1.89E-02	2.78E-02
Stator Leakage Reactance @ 50 Hz.								
Leakage Reactance @ 50 Hz.	ohm/phase	X50_	7.00E-03	7.00E-03	8.70E-03	7.00E-03	7.00E-03	8.70E-03
Coil Resistance	ohm/phase	Rone	5.58E-03	5.58E-03	6.22E-03	5.58E-03	5.58E-03	6.22E-03
Reactance/Resistance ratio @ 50 Hz	-	alpha50	1.26E+00	1.26E+00	1.40E+00	1.26E+00	1.26E+00	1.40E+00
Series turns/phase		stp.lim	3.20E+01	3.20E+01	3.20E+01	3.20E+01	3.20E+01	3.20E+01
Resistance, Primary	ohm/phase	rp.lim	5.58E-03	5.58E-03	6.22E-03	5.58E-03	5.58E-03	6.22E-03
Weight								
Motor iron weight, single stator	kg	mi.v	7.89E+02	7.89E+02	6.13E+02	7.89E+02	7.89E+02	6.13E+02
Motor conductor weight, single stat	kg	mc.v	1.39E+02	1.39E+02	1.10E+02	1.39E+02	1.39E+02	1.10E+02
Total motor weight(Nmotor motors)	kg	mmotor	3.71E+03	3.71E+03	2.89E+03	3.71E+03	3.71E+03	2.89E+03
Power								
Core loss power, single stator	W	Pcore	1.53E+04	1.53E+04	1.54E+04	8.30E+03	8.30E+03	8.34E+03
Core temperature rise	°C	delTcore	1.05E+02	1.05E+02	1.25E+02	5.70E+01	5.70E+01	6.78E+01
Core surface temperature	°C	Tcore	1.55E+02	1.55E+02	1.75E+02	1.07E+02	1.07E+02	1.18E+02
Motor Secondary (guideway) Design Parameters								
Iron								
Back iron thickness, guideway	m	ty.g	4.60E-02	4.60E-02	3.87E-02	4.60E-02	4.60E-02	3.87E-02
Back iron width	m	d.g	2.40E-01	2.40E-01	2.46E-01	2.40E-01	2.40E-01	2.46E-01
Guideway iron specific weight	kg/m	mi.g	8.29E+01	8.29E+01	7.14E+01	8.29E+01	8.29E+01	7.14E+01

Table F-2. (continued)

ElectroMagnetic Suspension I Optimized for operation at 134 m/s maximum speed

(Separate vertical & lateral suspensions & linear induction motor)

Asterisk (*) before description indicates input.
2 Asterisks (**) after description indicates output from MatLab LIM program.

DESCRIPTION	UNITS	SYMBOL	134 m/s Optimization			134 m/s Optimization @ 89 m/s		
			DESIGN 1 baseline	DESIGN 2 slim pole (3/4 b/l)	DESIGN 3 small gap (0.8 b/l)	DESIGN 1 baseline	DESIGN 2 slim pole (3/4 b/l)	DESIGN 3 small gap (0.8 b/l)
Conductor								
*Conductor overlap factor		colf.g	4.00E-01	4.00E-01	4.00E-01	4.00E-01	4.00E-01	4.00E-01
*Conductor thickness	m	tc.g	5.00E-03	5.00E-03	5.00E-03	5.00E-03	5.00E-03	5.00E-03
Conductor width	m	dc.g	5.07E-01	5.07E-01	4.71E-01	5.07E-01	5.07E-01	4.71E-01
Guideway conductor specific weight	kg/m	mc.g	7.04E+00	7.04E+00	6.54E+00	7.04E+00	7.04E+00	6.54E+00
Total guideway added weight	kg/m	m.gw	1.80E+02	1.80E+02	1.56E+02	1.80E+02	1.80E+02	1.56E+02
Performance Results from MatLab Analysis								
Individual Motor Parameters at Maximum Propulsive Force								
Thrust**	N	Thrust	2.04E+04	2.04E+04	2.05E+04	9.02E+03	9.02E+03	9.05E+03
Slip**	-	slip	1.00E-02	1.00E-02	9.00E-03	1.50E-02	1.50E-02	1.40E-02
Traction Power**	W	P.tract	2.74E+06	2.74E+06	2.75E+06	7.98E+05	7.98E+05	8.03E+05
Real input Power**	W	Pin.real	2.82E+06	2.82E+06	2.83E+06	8.32E+05	8.32E+05	8.33E+05
Reactive input Power**	V-A	Pin.reac	3.22E+06	3.22E+06	3.27E+06	9.47E+05	9.47E+05	9.32E+05
Efficiency**	%	eff.v	9.65E+01	9.65E+01	9.69E+01	9.65E+01	9.65E+01	9.69E+01
Power Factor		PwrFac	6.59E-01	6.59E-01	6.54E-01	6.59E-01	6.59E-01	6.54E-01
AUXILIARY CALCULATIONS								
LIFT MAGNETS								
permeances								
√Air gap fringing permeance/length		Pf	1.92E+00	1.92E+00	1.92E+00	1.92E+00	1.92E+00	1.92E+00
√Ideal air gap permeance/length		Pu	3.14E+00	2.35E+00	3.49E+00	3.14E+00	2.35E+00	3.49E+00
?Inter-pole leakage perm./length		Pl	3.94E-01	3.82E-01	4.06E-01	3.94E-01	3.82E-01	4.06E-01
coil dimensions								
√Mean turn length	m	lc	1.02E+01	1.92E+01	1.02E+01	1.02E+01	1.92E+01	1.02E+01
√Coil crossectional area(one coil)	m^2	ac	1.39E-03	1.12E-03	1.11E-03	1.39E-03	1.12E-03	1.11E-03
√Coil Surface area(for 1 coil)	m^2	adis	1.77E+00	2.91E+00	1.59E+00	1.77E+00	2.91E+00	1.59E+00
GUIDANCE MAGNETS								
permeances								
√Air gap fringing permeance/length		Pf.l	1.92E+00	1.92E+00	1.92E+00	1.92E+00	1.92E+00	1.92E+00
√Ideal air gap permeance/length		Pu.l	2.80E+00	2.10E+00	3.10E+00	2.80E+00	2.10E+00	3.10E+00
?Inter-pole leakage perm./length		Pl.l	4.21E-01	4.11E-01	4.30E-01	4.21E-01	4.11E-01	4.30E-01
coil dimensions								
√ Mean turn length(one coil)	m	lc.l	1.03E+01	1.96E+01	1.02E+01	1.03E+01	1.96E+01	1.02E+01
√Coil crossectional area(one coil)	m^2	ac.l	2.57E-03	2.03E-03	2.07E-03	2.57E-03	2.03E-03	2.07E-03
√Coil Surface area(for one coil)	m^2	adis.l	2.24E+00	3.73E+00	2.01E+00	2.24E+00	3.73E+00	2.01E+00
LINEAR INDUCTION MOTOR						0.00E+00	0.00E+00	0.00E+00
permeances						0.00E+00	0.00E+00	0.00E+00
Ideal air gap permeance/length		Pu.lim	1.18E+01	1.18E+01	1.43E+01	1.18E+01	1.18E+01	1.43E+01
Air gap fringing permeance/length		Pf.lim	1.92E+00	1.92E+00	1.92E+00	1.92E+00	1.92E+00	1.92E+00
Fringing permeance ratio		nuf.lim	1.63E-01	1.63E-01	1.34E-01	1.63E-01	1.63E-01	1.34E-01
EMS I Summary								
Weight on Vehicle								
Lift Magnets	kg		1.54E+03	1.99E+03	1.23E+03	1.54E+03	1.99E+03	1.23E+03
Guidance Magnets	kg		1.93E+03	2.58E+03	1.54E+03	1.93E+03	2.58E+03	1.54E+03
Linear Induction Motor	kg		3.71E+03	3.71E+03	2.89E+03	3.71E+03	3.71E+03	2.89E+03
Total	kg		7.18E+03	8.28E+03	5.67E+03	7.18E+03	8.28E+03	5.67E+03
Weight on Guideway								
Lift Magnets	kg/m		1.13E+02	7.17E+01	8.94E+01	1.13E+02	7.17E+01	8.94E+01
Guidance Magnets	kg/m		1.13E+02	7.17E+01	8.87E+01	1.13E+02	7.17E+01	8.87E+01
Linear Induction Motor	kg/m		1.80E+02	1.80E+02	1.56E+02	1.80E+02	1.80E+02	1.56E+02
Total	kg/m		4.06E+02	3.23E+02	3.34E+02	4.06E+02	3.23E+02	3.34E+02
Real Input Power Dissipation								
Ohmic Power Dissipation								

Table F-2. (continued)

ElectroMagnetic Suspension I Optimized for operation at 134 m/s maximum speed

(Separate vertical & lateral suspensions & linear induction motor)

Asterisk (*) before description indicates input.
2 Asterisks (**) after description indicates output from MatLab LIM program.

DESCRIPTION	UNITS	SYMBOL	134 m/s Optimization			134 m/s Optimization @ 89 m/s		
			DESIGN 1	DESIGN 2	DESIGN 3	DESIGN 1	DESIGN 2	DESIGN 3
			baseline	slim pole (3/4 b/l)	small gap (0.8 b/l)	baseline	slim pole (3/4 b/l)	small gap (0.8 b/l)
Lift Magnets	W		1.19E+05	1.95E+05	1.06E+05	1.19E+05	1.95E+05	1.06E+05
Guidance Magnets	W		1.88E+04	3.88E+04	2.08E+04	1.88E+04	3.88E+04	2.08E+04
Linear Induction Motor	W		8.28E+04	8.28E+04	8.00E+04	3.40E+04	3.40E+04	3.08E+04
Total Ohmic Power	W		2.20E+05	3.16E+05	2.07E+05	1.71E+05	2.68E+05	1.58E+05
Eddy current Power								
Lift Magnets	W		6.63E+04	1.12E+04	4.37E+04	2.93E+04	4.94E+03	1.93E+04
Guidance Magnets	W		3.31E+04	5.49E+03	2.16E+04	1.46E+04	2.42E+03	9.52E+03
Total eddy current Power	W		9.94E+04	1.67E+04	6.52E+04	4.39E+04	7.36E+03	2.88E+04
Total Real Power Dissipation	W		3.20E+05	3.33E+05	2.72E+05	2.15E+05	2.75E+05	1.87E+05
Reactive Input Power								
Linear Induction Motor	V-A		3.22E+06	3.22E+06	3.27E+06	9.47E+05	9.47E+05	9.32E+05
Total	V-A		3.22E+06	3.22E+06	3.27E+06	9.47E+05	9.47E+05	9.32E+05

Table F-3. Complete EMS II Spreadsheet; Design optimized for operation at 89 m/s

Combined Lift and guidance magnets (staggered) and Linear Induction Motor

ElectroMagnetic Suspension II Optimized for operation at 89 m/s maximum speed

(Combined vertical & lateral suspensions(staggered), Linear Induction Motor)

Asterisk (*) before description indicates input.
2 Asterisks (**) after description indicates output from MatLab LIM program.

DESCRIPTION	UNITS	SYMBOL	89 m/s Optimization			89 m/s Optimization @ 59 m/s		
			DESIGN 1	DESIGN 2	DESIGN 3	DESIGN 1	DESIGN 2	DESIGN 3
VEHICLE PARAMETERS			baseline (b/l)	slim pole (3/4 b/l)	small gap (0.8 b/l)	baseline (b/l)	slim pole (3/4 b/l)	small gap (0.8 b/l)
Design Parameters								
* Vehicle mass	kg	m	4.00E+04	4.00E+04	4.00E+04	4.00E+04	4.00E+04	4.00E+04
* Vehicle length	m	l_vehicle	3.00E+01	3.00E+01	3.00E+01	3.00E+01	3.00E+01	3.00E+01
* Design speed	m/s	V	8.90E+01	8.90E+01	8.90E+01	5.90E+01	5.90E+01	5.90E+01
* frontal area	m^2	Af	1.20E+01	1.20E+01	1.20E+01	1.20E+01	1.20E+01	1.20E+01
* air density	kg/m^3	roair	1.20E+00	1.20E+00	1.20E+00	1.20E+00	1.20E+00	1.20E+00
* drag coefficient	---	Cd	3.00E-01	3.00E-01	3.00E-01	3.00E-01	3.00E-01	3.00E-01
wind drag force	N	Fd	1.71E+04	1.71E+04	1.71E+04	7.52E+03	7.52E+03	7.52E+03
wind drag power	W	Pd	1.52E+06	1.52E+06	1.52E+06	4.44E+05	4.44E+05	4.44E+05
* Max. Lift Force(@Max disp.)	g	max_Fz	1.10E+00	1.10E+00	1.10E+00	1.10E+00	1.10E+00	1.10E+00
* Max. Lateral Force(")(cont.)	g	max_F.l	1.80E-01	1.80E-01	1.80E-01	1.80E-01	1.80E-01	1.80E-01
* Max. Lateral Force(")(short term)	g	max_sF.l	2.60E-01	2.60E-01	2.60E-01	2.60E-01	2.60E-01	2.60E-01
* Time of Max. (short)Lateral F	sec	t_max	5.00E+00	5.00E+00	5.00E+00	5.00E+00	5.00E+00	5.00E+00
* Max propulsive force	g	max_Fp	1.50E-01	1.50E-01	1.50E-01	1.50E-01	1.50E-01	1.50E-01
* Maximum ambient temperature	°C	maxTamb	5.00E+01	5.00E+01	5.00E+01	5.00E+01	5.00E+01	5.00E+01
Performance Parameters								
Power, (ohmic+eddy)/aero. drag	%		1.53E-02	1.14E-02	1.26E-02	3.49E-02	3.43E-02	2.86E-02
Weight, (magnet+coil)/vehicle	%		1.19E-01	1.40E-01	9.00E-02	1.19E-01	1.40E-01	9.00E-02
eddy/lift amp-T (up. bound)	%		1.46E-01	5.80E-02	1.51E-01	9.68E-02	3.85E-02	9.99E-02
Aerodynamic drag/weight	%		4.36E-02	4.36E-02	4.36E-02	1.92E-02	1.92E-02	1.92E-02
CONSTANTS								
General								
*air permeability	N/A^2	mu	1.26E-06	1.26E-06	1.26E-06	1.26E-06	1.26E-06	1.26E-06
Suspensions								
Construction materials								
*rail			steel	steel	steel	steel	steel	steel
*magnet			2V Perm.	2V Perm.	2V Perm.	2V Perm.	2V Perm.	2V Perm.
*coil			alum.	alum.	alum.	alum.	alum.	alum.
Materials properties								
mass density								
*rail	kg/m^3	ror	7.85E+03	7.85E+03	7.85E+03	7.85E+03	7.85E+03	7.85E+03
*magnet	kg/m^3	rom	7.85E+03	7.85E+03	7.85E+03	7.85E+03	7.85E+03	7.85E+03
*coil	kg/m^3	roc	2.55E+03	2.55E+03	2.55E+03	2.55E+03	2.55E+03	2.55E+03
Saturation flux density								
*rail	T	BsatR	1.40E+00	1.40E+00	1.40E+00	1.40E+00	1.40E+00	1.40E+00
*magnet	T	BsatM	1.40E+00	1.40E+00	1.40E+00	1.40E+00	1.40E+00	1.40E+00
*Saturation Safety Factor(<1)	---	SF	1.00E+00	1.00E+00	1.00E+00	1.00E+00	1.00E+00	1.00E+00
Electrical resistivity								
*rail @20 deg C	ohm-m	rr	2.00E-07	2.00E-07	2.00E-07	2.00E-07	2.00E-07	2.00E-07
*coil @190 deg C	ohm-m	rc_	4.72E-08	4.72E-08	4.72E-08	4.72E-08	4.72E-08	4.72E-08
Thermal								
*magnet heat transfer coef.	W/°C-m	h_s	2.00E+01	2.00E+01	2.00E+01	2.00E+01	2.00E+01	2.00E+01
*Conductor thermal conductivity	W/(°C m	k_c	2.20E+02	2.20E+02	2.20E+02	2.20E+02	2.20E+02	2.20E+02
*Insulation thermal conductivity	W/°C-m	k_ins	1.73E-01	1.73E-01	1.73E-01	1.73E-01	1.73E-01	1.73E-01
*coil packing factor	---	f	7.85E-01	7.85E-01	7.85E-01	7.85E-01	7.85E-01	7.85E-01
*Coil Width packing factor	---	f_y	8.86E-01	8.86E-01	8.86E-01	8.86E-01	8.86E-01	8.86E-01
*Coil thickness packing factor	---	f_z	8.86E-01	8.86E-01	8.86E-01	8.86E-01	8.86E-01	8.86E-01
*Maximum ambient temperature	°C	T	5.50E+01	5.50E+01	5.50E+01	5.50E+01	5.50E+01	5.50E+01
*Coil Specific heat	J/(kg°C	cp	1.19E+02	1.19E+02	1.19E+02	1.19E+02	1.19E+02	1.19E+02
*Maximum wire insulation temp	°C	maxTins	2.20E+02	2.20E+02	2.20E+02	2.20E+02	2.20E+02	2.20E+02
Linear Induction Motor								

Table F-3. (continued)

ElectroMagnetic Suspension II Optimized for operation at 89 m/s maximum speed

(Combined vertical & lateral suspensions(staggered), Linear Induction Motor)

Asterisk (*) before description indicates input.
2 Asterisks (**) after description indicates output from MatLab LIM program.

DESCRIPTION	UNITS	SYMBOL	89 m/s Optimization			89 m/s Optimization @ 59 m/s		
			DESIGN 1	DESIGN 2	DESIGN 3	DESIGN 1	DESIGN 2	DESIGN 3
VEHICLE PARAMETERS			baseline (b/l)	slim pole (3/4 b/l)	small gap (0.8 b/l)	baseline (b/l)	slim pole (3/4 b/l)	small gap (0.8 b/l)
*rail			steel	steel	steel	steel	steel	steel
*rail conductor(s)			aluminum	aluminum	aluminum	aluminum	aluminum	aluminum
*magnet			M-19	M-19	M-19	M-19	M-19	M-19
*magnet coil			aluminum	aluminum	aluminum	aluminum	aluminum	aluminum
Materials properties								
Mass density								
*rail	kg/m^3	rom.g	7.51E+03	7.51E+03	7.51E+03	7.51E+03	7.51E+03	7.51E+03
*rail conductor(s)	kg/m^3	roc.g	2.78E+03	2.78E+03	2.78E+03	2.78E+03	2.78E+03	2.78E+03
*magnet	kg/m^3	rom.v	7.65E+03	7.65E+03	7.65E+03	7.65E+03	7.65E+03	7.65E+03
*coil	kg/m^3	roc.v	2.78E+03	2.78E+03	2.78E+03	2.78E+03	2.78E+03	2.78E+03
maximum flux densities								
*rail	T	bsat.g	1.60E+00	1.60E+00	1.60E+00	1.60E+00	1.60E+00	1.60E+00
*magnet	T	bsat.v	1.50E+00	1.50E+00	1.50E+00	1.50E+00	1.50E+00	1.50E+00
Magnetic permeability								
rail	---	mu.g	3.50E+03	3.50E+03	3.50E+03	3.50E+03	3.50E+03	3.50E+03
Vehicle (short) stator		mu.v						
Core loss								
Core Loss @ 1.0T, 100 Hz	W/kg	refc.loss	2.87E+00	2.87E+00	2.87E+00	2.87E+00	2.87E+00	2.87E+00
Core loss frequency exponent	-	freq.exp	1.50E+00	1.50E+00	1.50E+00	1.50E+00	1.50E+00	1.50E+00
Core loss induction exponent	-	B.exp	2.10E+00	2.10E+00	2.10E+00	2.10E+00	2.10E+00	2.10E+00
Core loss @ fsync & Bcore	W/kg	c.loss	1.05E+01	1.05E+01	1.36E+01	5.68E+00	5.68E+00	7.34E+00
Electrical resistivity								
*Magnet laminations @ 140°C	ohm-m	rm.v	7.00E-07	7.00E-07	7.00E-07	7.00E-07	7.00E-07	7.00E-07
*rail @20 deg C	ohm-m	rm.g	4.06E-07	4.06E-07	4.06E-07	4.06E-07	4.06E-07	4.06E-07
*vehicle coil @20 deg C	ohm-m	rcRT.v	2.78E-08	2.78E-08	2.78E-08	2.78E-08	2.78E-08	2.78E-08
*vehicle coil temperature coeffici	1/°C	alpha.v	4.10E-03	4.10E-03	4.10E-03	4.10E-03	4.10E-03	4.10E-03
vehicle coil @operating temperat	ohm-m	rc.v	4.73E-08	4.73E-08	4.75E-08	4.73E-08	4.73E-08	4.75E-08
*Guideway conductor @20 deg c	ohm-m	rc.g	2.80E-08	2.80E-08	2.80E-08	2.80E-08	2.80E-08	2.80E-08
Heat transfer coeffieients								
*magnet heat transfer coef.	W/C-m^	k.v	4.19E+01	4.19E+01	4.19E+01	4.19E+01	4.19E+01	4.19E+01
*rail heat transfer coef.	W/C-m^	k.g	1.40E+01	1.40E+01	1.40E+01	1.40E+01	1.40E+01	1.40E+01
COMPONENT DESIGN & ANALYSIS								
Vertical/lateral suspension								
Geometric dimensions								
*Lateral stagger	m	del	5.00E-03	1.50E-03	2.50E-03	1%	0%	0%
*pole width	m	lp	2.00E-02	1.50E-02	2.00E-02	2.00E-02	1.50E-02	2.00E-02
*window width	m	w	1.30E-01	1.19E-01	1.16E-01	1.30E-01	1.19E-01	1.16E-01
*window height	m	h (or d)	6.52E-02	5.97E-02	5.80E-02	6.52E-02	5.97E-02	5.80E-02
*air gap	m	H1x	1.00E-02	1.00E-02	8.00E-03	1.00E-02	1.00E-02	8.00E-03
*pole-coil clearance	m	z	5.08E-03	5.08E-03	5.08E-03	5.08E-03	5.08E-03	5.08E-03
*Number magnet sets required	---	nmag,N.se	4	4	4	4	4	4
*Number individual magnets/set	---	N.mags	2	2	2	2	2	2
Performance parameters								
Individual magnet total weight	kg	W_mag_c	5.93E+02	7.00E+02	4.50E+02	593.11891	700.30406	450.01616
Lift-to-weight ratio	---	LTWR	8.43E+00	7.14E+00	1.11E+01	8.43E+00	7.14E+00	1.11E+01
Power-to-lift ratio	kW/tonr	PTLR	1.86E+00	2.71E+00	1.52E+00	1.86E+00	2.71E+00	1.52E+00
Total weight of magnet assemblies	kg	M_magnet	4.74E+03	5.60E+03	3.60E+03	4.74E+03	5.60E+03	3.60E+03
Magnet-to-Vehicle weight ratio	---	MVWR	11.86%	14.01%	9.00%	1.19E-01	1.40E-01	9.00E-02
Max. lateral force @y*(1 set)	kg	F_y_star	6.50E+04	9.03E+04	5.21E+04	6.50E+04	9.03E+04	5.21E+04
Required max lateral force(1 set)	kg	F_ymax	2.55E+04	2.55E+04	2.55E+04	2.55E+04	2.55E+04	2.55E+04
Max. lift force @y*(1 set)	kg	Fz_y_star	1.08E+05	1.08E+05	1.08E+05	1.08E+05	1.08E+05	1.08E+05
Required max. lift force(1 set)	kg	F_zmax	1.08E+05	1.08E+05	1.08E+05	1.08E+05	1.08E+05	1.08E+05

Table F-3. (continued)

ElectroMagnetic Suspension II Optimized for operation at 89 m/s maximum speed

(Combined vertical & lateral suspensions(staggered), Linear Induction Motor)

Asterisk (*) before description indicates input.
2 Asterisks (**) after description indicates output from MatLab LIM program.

DESCRIPTION	UNITS	SYMBOL	89 m/s Optimization			89 m/s Optimization @ 59 m/s		
			DESIGN 1	DESIGN 2	DESIGN 3	DESIGN 1	DESIGN 2	DESIGN 3
			baseline (b/l)	slim pole (3/4 b/l)	small gap (0.8 b/l)	baseline (b/l)	slim pole (3/4 b/l)	small gap (0.8 b/l)
VEHICLE PARAMETERS								
Classical lift force (1 mag, y=0)	kg	F_class	4.11E+04	3.77E+04	4.16E+04	4.11E+04	3.77E+04	4.16E+04
Lateral stiffness (4 sets)	N/m	K_lateral	1.75E+07	2.40E+07	1.38E+07	1.75E+07	2.40E+07	1.38E+07
Magnet design		FFF	9.50E-01	9.90E-01	9.50E-01	9.50E-01	9.90E-01	9.50E-01
Decoupling displacement limit	m	y_star	1.49E-02	1.50E-02	1.51E-02	1.49E-02	1.50E-02	1.51E-02
magnet length	m	L	5.63E+00	8.88E+00	5.11E+00	5.63E+00	8.88E+00	5.11E+00
width of pole base	m	w_p	2.78E-02	2.21E-02	2.64E-02	2.78E-02	2.21E-02	2.64E-02
Magnet yoke length	m	L_y	5.50E+00	8.76E+00	4.99E+00	5.50E+00	8.76E+00	4.99E+00
Magnet yoke height	m	d_y	3.36E-02	2.69E-02	3.12E-02	3.36E-02	2.69E-02	3.12E-02
Yoke area	m^2	A_yoke	1.85E-01	2.36E-01	1.56E-01	1.85E-01	2.36E-01	1.56E-01
fringing (across air gap)	---	nuf	9.60E-01	1.28E+00	7.68E-01	9.60E-01	1.28E+00	7.68E-01
leakage (between poles)	---	nul	2.12E-01	2.78E-01	1.72E-01	2.12E-01	2.78E-01	1.72E-01
total	---	nut	2.17E+00	2.56E+00	1.94E+00	2.17E+00	2.56E+00	1.94E+00
Nominal air gap flux density	T	B0	6.78E-01	5.96E-01	7.15E-01	6.78E-01	5.96E-01	7.15E-01
Nominal pole tip flux density	T		8.68E-01	8.47E-01	8.89E-01			
Nominal pole base flux density	T		1.21E+00	1.25E+00	1.18E+00			
Nominal yoke flux density	T		1.42E+00	1.50E+00	1.36E+00			
Force per magnet	N	Fpm	4.11E+04	3.77E+04	4.16E+04	4.11E+04	3.77E+04	4.16E+04
amp turns per magnet	A	NI	1.08E+04	9.49E+03	9.11E+03	1.08E+04	9.49E+03	9.11E+03
core mass (1 mag)	kg	Mcore	4.02E+02	4.48E+02	3.12E+02	4.02E+02	4.48E+02	3.12E+02
mass core + coil (4 mag)	kg	Mmag	4.74E+03	5.60E+03	3.60E+03	4.74E+03	5.60E+03	3.60E+03
Coil design								
resistance (1 magnet, 1 turn)	ohm	resc	7.99E-05	1.50E-04	9.14E-05	7.99E-05	1.50E-04	9.14E-05
coil ohmic power (1 magnet)	W	qc	9.30E+03	1.35E+04	7.58E+03	9.30E+03	1.35E+04	7.58E+03
Surface temperature rise	°C	deltaT_su	1.58E+02	1.60E+02	1.60E+02	1.58E+02	1.60E+02	1.60E+02
Surface temperature	°C	T_s	2.08E+02	2.10E+02	2.10E+02	2.08E+02	2.10E+02	2.10E+02
Internal temperature rise	°C	deltaT_in	6.05E+00	4.71E+00	4.33E+00	6.05E+00	4.71E+00	4.33E+00
Maximum internal temperature	°C	T_int	2.19E+02	2.20E+02	2.19E+02	2.19E+02	2.20E+02	2.19E+02
mass(one coil)	kg	Mcoil	1.91E+02	2.53E+02	1.38E+02	1.91E+02	2.53E+02	1.38E+02
Total ohmic power, Nmag*n_mags	W	P_total	7.44E+04	1.08E+05	6.07E+04	7.44E+04	1.08E+05	6.07E+04
Rail design								
rail thickness	m	tr	2.83E-02	2.27E-02	2.59E-02	2.83E-02	2.27E-02	2.59E-02
rail mass/length	kg/m	mr	4.88E+01	3.54E+01	4.07E+01	4.88E+01	3.54E+01	4.07E+01
nominal rail flux density	T	Br	9.40E-01	8.97E-01	9.76E-01	9.40E-01	8.97E-01	9.76E-01
eff. freq. for eddy anal.	Hz	Fe	7.91E+00	5.01E+00	8.71E+00	5.24E+00	3.32E+00	5.78E+00
dB/dt amp. first harmonic	T/s	B1x	2.97E+01	1.80E+01	3.40E+01	1.97E+01	1.19E+01	2.25E+01
eddy current power	W	Pr	1.40E+04	3.77E+03	1.17E+04	6.17E+03	1.66E+03	5.12E+03
rms eddy amp turn (upper bound, 1 magnet)	A	NIe	1.58E+03	5.51E+02	1.37E+03	1.04E+03	3.65E+02	9.10E+02
Total continuous power	W	P.v	8.84E+04	1.12E+05	7.23E+04	8.05E+04	1.10E+05	6.58E+04
Linear Induction Motor								
Design maximum thrust	g	max.g	1.50E-01	1.50E-01	1.50E-01	1.50E-01	1.50E-01	1.50E-01
Design maximum thrust	N	max.thr	5.88E+04	5.88E+04	5.88E+04	5.88E+04	5.88E+04	5.88E+04
Nominal excitation frequency	Hz	fsync	1.35E+02	1.35E+02	1.60E+02	8.94E+01	8.94E+01	1.06E+02
Synchronous speed	m/s	vsync	8.99E+01	8.99E+01	8.99E+01	5.96E+01	5.96E+01	5.96E+01
Nominal slip		nom.slip	1.00E-02	1.00E-02	1.00E-02	1.00E-02	1.00E-02	1.00E-02
General								
*Number of motors		Nmotor	4.00E+00	4.00E+00	4.00E+00	4.00E+00	4.00E+00	4.00E+00
*Number of poles		Np.v	1.20E+01	1.20E+01	1.40E+01	1.20E+01	1.20E+01	1.40E+01
Geometric dimensions								
*Air gap (mechanical clearance)	m	cl.v	1.00E-02	1.00E-02	8.00E-03	1.00E-02	1.00E-02	8.00E-03
*Pole pitch	m	tau.v	3.33E-01	3.33E-01	2.81E-01	3.33E-01	3.33E-01	2.81E-01
*Slots/pole/phase		Nslots	2.00E+00	2.00E+00	2.00E+00	2.00E+00	2.00E+00	2.00E+00

Table F-3. (continued)

ElectroMagnetic Suspension II Optimized for operation at 89 m/s maximum speed

(Combined vertical & lateral suspensions(staggered), Linear Induction Motor)

Asterisk (*) before description indicates input.
2 Asterisks (**) after description indicates output from MatLab LIM program.

DESCRIPTION	UNITS	SYMBOL	89 m/s Optimization			89 m/s Optimization @ 59 m/s		
			DESIGN 1	DESIGN 2	DESIGN 3	DESIGN 1	DESIGN 2	DESIGN 3
			baseline (b/l)	slim pole (3/4 b/l)	small gap (0.8 b/l)	baseline (b/l)	slim pole (3/4 b/l)	small gap (0.8 b/l)
VEHICLE PARAMETERS								
*Core width	m	d.v	1.80E-01	1.80E-01	1.92E-01	1.80E-01	1.80E-01	1.92E-01
*Tooth width/slot width ratio		tsr.v	1.20E+00	1.20E+00	1.20E+00	1.20E+00	1.20E+00	1.20E+00
*Slot depth	m	h.v	5.00E-02	5.00E-02	5.00E-02	5.00E-02	5.00E-02	5.00E-02
*Lamination thickness	m	tlam.v	3.56E-04	3.56E-04	3.56E-04	3.56E-04	3.56E-04	3.56E-04
Magnetic gap (entrefer)	m	g.mag	1.50E-02	1.50E-02	1.30E-02	1.50E-02	1.50E-02	1.30E-02
Carter factor		Kcarter	1.19E+00	1.19E+00	1.18E+00	1.19E+00	1.19E+00	1.18E+00
Effective magnetic gap	m	ge.lim	1.78E-02	1.78E-02	1.54E-02	1.78E-02	1.78E-02	1.54E-02
Back iron thickness, vehicle	m	ty.v	5.74E-02	5.74E-02	4.69E-02	5.74E-02	5.74E-02	4.69E-02
Tooth width	m	lt.v	2.53E-02	2.53E-02	2.13E-02	2.53E-02	2.53E-02	2.13E-02
Slot width	m	w.v	3.03E-02	3.03E-02	2.55E-02	3.03E-02	3.03E-02	2.55E-02
Slot pitch (=tooth pitch)	m	sp.v	5.56E-02	5.56E-02	4.68E-02	5.56E-02	5.56E-02	4.68E-02
Number of laminations		Nlams.v	5.05E+02	5.05E+02	5.39E+02	5.05E+02	5.05E+02	5.39E+02
Motor effective length	m	Leff	4.00E+00	4.00E+00	3.93E+00	4.00E+00	4.00E+00	3.93E+00
Motor physical length	m	Lphys	4.56E+00	4.56E+00	4.40E+00	4.56E+00	4.56E+00	4.40E+00
Effective air gap area	m^2	Aface	7.20E-01	7.20E-01	7.55E-01	7.20E-01	7.20E-01	7.55E-01
Core exposed surface area	m^2	Acore	2.44E+00	2.44E+00	2.37E+00	2.44E+00	2.44E+00	2.37E+00
Winding parameters								
*Number of phases		Nphase.v	3.00E+00	3.00E+00	3.00E+00	3.00E+00	3.00E+00	3.00E+00
*Coil pitch/pole pitch ratio(fraction)		cp_tau	6.67E-01	6.67E-01	6.67E-01	6.67E-01	6.67E-01	6.67E-01
*Number of winding layers		Nlayers.v	2.00E+00	2.00E+00	2.00E+00	2.00E+00	2.00E+00	2.00E+00
*Number of coils/pole/phase		ncoils.v	2.00E+00	2.00E+00	2.00E+00	2.00E+00	2.00E+00	2.00E+00
*Coil packing factor		f.v	7.85E-01	7.85E-01	7.85E-01	7.85E-01	7.85E-01	7.85E-01
*Pole/coil clearance	m	z.v	5.00E-03	5.00E-03	5.00E-03	5.00E-03	5.00E-03	5.00E-03
*Turns/coil		Npc.v	1.00E+00	1.00E+00	1.00E+00	1.00E+00	1.00E+00	1.00E+00
*End turn angle	degrees	alpha	3.00E+01	3.00E+01	3.00E+01	3.00E+01	3.00E+01	3.00E+01
*End turn projection	m	b	1.00E-02	1.00E-02	1.00E-02	1.00E-02	1.00E-02	1.00E-02
Distribution factor(distributed winding)		Kd	8.66E-01	8.66E-01	8.66E-01	8.66E-01	8.66E-01	8.66E-01
Pitch factor(fractional pitch coils)		Kp	8.66E-01	8.66E-01	8.66E-01	8.66E-01	8.66E-01	8.66E-01
Winding factor(for distributed windings)		Kw	7.50E-01	7.50E-01	7.50E-01	7.50E-01	7.50E-01	7.50E-01
Coil pitch	m	tau_c.v	2.22E-01	2.22E-01	1.87E-01	2.22E-01	2.22E-01	1.87E-01
Mean conductor length	m/coil	lcoil.v	9.13E-01	9.13E-01	8.57E-01	9.13E-01	9.13E-01	8.57E-01
Coil thickness	m	tcoil.v	2.25E-02	2.25E-02	2.25E-02	2.25E-02	2.25E-02	2.25E-02
Conductor x-section area/slot/laye	m^2	Acoil.v	5.35E-04	5.35E-04	4.51E-04	5.35E-04	5.35E-04	4.51E-04
Coil Resistance	ohm	Rcoil.v	8.08E-05	8.08E-05	9.02E-05	8.08E-05	8.08E-05	9.02E-05
Heat transfer area (1 coil)	m^2	Aht.v	7.74E-02	7.74E-02	6.39E-02	7.74E-02	7.74E-02	6.39E-02
Peak MMF per coil RMS amp-turns	-	MMFperNI	4.05E+00	4.05E+00	4.05E+00	4.05E+00	4.05E+00	4.05E+00
Core operating flux density	T	Bcore.v	1.50E+00	1.50E+00	1.50E+00	1.50E+00	1.50E+00	1.50E+00
Coil RMS amp-turns @ Bsat of tooth	Amp-tu	NIcoil.v	2.38E+03	2.38E+03	2.06E+03	2.38E+03	2.38E+03	2.06E+03
Total flux per pole @ Bsat of tooth	Webers	Fpp	3.10E-02	3.10E-02	2.70E-02	3.10E-02	3.10E-02	2.70E-02
RMS phase current @ Bsat of tooth	A	Iphase.v	2.38E+03	2.38E+03	2.06E+03	2.38E+03	2.38E+03	2.06E+03
Total RMS slot current @ Bsat of t	A	Islot .v	4.77E+03	4.77E+03	4.12E+03	4.77E+03	4.77E+03	4.12E+03
Coil power (1coil)	W	Pcoil.v	4.59E+02	4.59E+02	3.82E+02	4.59E+02	4.59E+02	3.82E+02
Coil surface temperature rise	°C	delTavg.v	1.41E+02	1.41E+02	1.43E+02	1.41E+02	1.41E+02	1.43E+02
Maximum coil surface temperature	°C	Tw.lim	1.91E+02	1.91E+02	1.93E+02	1.91E+02	1.91E+02	1.93E+02
Slot current	A-cond	I.slot	4.77E+03	4.77E+03	4.12E+03	4.77E+03	4.77E+03	4.12E+03
Linear current loading	A/m	I.load	8.58E+04	8.58E+04	8.79E+04	8.58E+04	8.58E+04	8.79E+04
Stator Leakage Reactance Calculations								
Slot Leakage	ohm	Xslot	1.21E-02	1.21E-02	2.13E-02	8.05E-03	8.05E-03	1.41E-02
End turn leakage	ohm	Xec	3.60E-08	3.60E-08	2.64E-08	2.39E-08	2.39E-08	1.75E-08
Total Primary Leakage Reactance	ohm	Xleak	1.21E-02	1.21E-02	2.13E-02	8.05E-03	8.05E-03	1.41E-02
Stator Leakage Reactance @ 50 Hz.								
Leakage Reactance @ 50 Hz.	ohm/ph	X50_	4.50E-03	4.50E-03	6.65E-03	4.50E-03	4.50E-03	6.65E-03
Coil Resistance	ohm/ph	Rone	3.88E-03	3.88E-03	5.05E-03	3.88E-03	3.88E-03	5.05E-03
Reactance/Resistance ratio @ 50 H	-	alpha50	1.16E+00	1.16E+00	1.32E+00	1.16E+00	1.16E+00	1.32E+00

Table F-3. (continued)

ElectroMagnetic Suspension II Optimized for operation at 89 m/s maximum speed

(Combined vertical & lateral suspensions(staggered), Linear Induction Motor)

Asterisk (*) before description indicates input.
2 Asterisks (**) after description indicates output from MatLab LIM program.

			89 m/s Optimization			89 m/s Optimization @ 59 m/s		
DESCRIPTION	UNITS	SYMBOL	DESIGN 1	DESIGN 2	DESIGN 3	DESIGN 1	DESIGN 2	DESIGN 3
			baseline (b/l)	slim pole (3/4 b/l)	small gap (0.8 b/l)	baseline (b/l)	slim pole (3/4 b/l)	small gap (0.8 b/l)
VEHICLE PARAMETERS								
Series turns/phase		stp.lim	2.40E+01	2.40E+01	2.80E+01	2.40E+01	2.40E+01	2.80E+01
Resistance, Primary	ohm/ph	rp.lim	3.88E-03	3.88E-03	5.05E-03	3.88E-03	3.88E-03	5.05E-03
Weight								
Motor iron weight, single stator	kg	mi.v	5.31E+02	5.31E+02	4.80E+02	5.31E+02	5.31E+02	4.80E+02
Motor conductor weight, single sta	kg	mc.v	9.78E+01	9.78E+01	9.03E+01	9.78E+01	9.78E+01	9.03E+01
Total motor weight(Nmotor motors	kg	mmotor	2.52E+03	2.52E+03	2.28E+03	2.52E+03	2.52E+03	2.28E+03
Power								
Core loss power, single stator	W	Pcore	5.59E+03	5.59E+03	6.53E+03	3.02E+03	3.02E+03	3.52E+03
Core temperature rise	°C	delTcore	5.47E+01	5.47E+01	6.58E+01	2.95E+01	2.95E+01	3.55E+01
Core surface temperature	°C	Tcore	1.05E+02	1.05E+02	1.16E+02	7.95E+01	7.95E+01	8.55E+01
Motor Secondary (guideway) Design Parameters								
Iron								
Back iron thickness, guideway	m	ty.g	4.61E-02	4.61E-02	3.87E-02	4.61E-02	4.61E-02	3.87E-02
Back iron width	m	d.g	2.10E-01	2.10E-01	2.18E-01	2.10E-01	2.10E-01	2.18E-01
Guideway iron specific weight	kg/m	mi.g	7.27E+01	7.27E+01	6.34E+01	7.27E+01	7.27E+01	6.34E+01
Conductor								
*Conductor overlap factor		colf.g	4.00E-01	4.00E-01	4.00E-01	4.00E-01	4.00E-01	4.00E-01
*Conductor thickness	m	tc.g	5.00E-03	5.00E-03	5.00E-03	5.00E-03	5.00E-03	5.00E-03
Conductor width	m	dc.g	4.77E-01	4.77E-01	4.43E-01	4.77E-01	4.77E-01	4.43E-01
Guideway conductor specific weigh	kg/m	mc.g	6.63E+00	6.63E+00	6.16E+00	6.63E+00	6.63E+00	6.16E+00
Total guideway added weight	kg/m	m.gw	1.59E+02	1.59E+02	1.39E+02	1.59E+02	1.59E+02	1.39E+02
Performance Results from MatLab Analysis								
Individual Motor Parameters at Maximum Propulsive Force								
Thrust**	N	Thrust	1.47E+04	1.47E+04	1.46E+04	6.47E+03	6.47E+03	6.43E+03
Slip**	-	slip	1.50E-02	1.50E-02	1.50E-02	2.20E-02	2.20E-02	2.20E-02
Traction Power**	W	P.tract	1.31E+06	1.31E+06	1.29E+06	3.77E+05	3.77E+05	3.74E+05
Real input Power**	W	Pin.real	1.37E+06	1.37E+06	1.35E+06	4.03E+05	4.03E+05	3.98E+05
Reactive input Power**	V-A	Pin.react	1.57E+06	1.57E+06	1.53E+06	4.68E+05	4.68E+05	4.57E+05
Efficiency**	%	eff.v	9.50E+01	9.50E+01	9.54E+01	9.27E+01	9.27E+01	9.36E+01
Power Factor		PwrFac	6.57E-01	6.57E-01	6.61E-01	6.52E-01	6.52E-01	6.57E-01
AUXILIARY CALCULATIONS								
Lift/guidance magnets								
permeances								
√Air gap fringing permeance/lengtl	---	Pf	1.92E+00	1.92E+00	1.92E+00	1.92E+00	1.92E+00	1.92E+00
√Ideal air gap permeance/length	---	Pu	2.00E+00	1.50E+00	2.50E+00	2.00E+00	1.50E+00	2.50E+00
?Inter-pole leakage perm./length	---	Pl	4.25E-01	4.18E-01	4.31E-01	4.25E-01	4.18E-01	4.31E-01
alpha(g,delta)		alpha_g.del	1.24E+00	1.41E+00	1.23E+00	1.24E+00	1.41E+00	1.23E+00
alpha(g,delta+y*)		'alpha_g.del.y_star	1.24E+00	1.41E+00	1.23E+00	1.24E+00	1.41E+00	1.23E+00
example using function "alpha(y,g,l_p)"		0	0	0	0			
Coil dimensions								
Average turn length		lc	1.13E+01	1.78E+01	1.02E+01	1.13E+01	1.78E+01	1.02E+01
Coil conductor crossectional area		ac	6.66E-03	5.58E-03	5.28E-03	6.66E-03	5.58E-03	5.28E-03
Effective surface area/heat trans.		adis	4.97E+00	6.98E+00	4.06E+00	4.97E+00	6.98E+00	4.06E+00
Coil volume	m^3	V_coil	9.55E-02	1.26E-01	6.88E-02	9.55E-02	1.26E-01	6.88E-02
Magnet parameters								
Magnet volume	m^3	V_mag	5.12E-02	5.70E-02	3.98E-02	5.12E-02	5.70E-02	3.98E-02
flux leakage coefficients								
Gap fringing flux coefficient	---	nu_g	1.28E+00	1.42E+00	1.24E+00	1.28E+00	1.42E+00	1.24E+00
Pole leakage flux coefficient	---	nu_l.p	5.02E-01	6.69E-01	4.00E-01	5.02E-01	6.69E-01	4.00E-01
Yoke leakage flux coefficient	---	nu_l.y	3.18E-01	4.24E-01	2.55E-01	3.18E-01	4.24E-01	2.55E-01
Total leakage & fringing flux coef.	---	nu_t	2.10E+00	2.51E+00	1.90E+00	2.10E+00	2.51E+00	1.90E+00

Table F-3. (continued)

ElectroMagnetic Suspension II Optimized for operation at 89 m/s maximum speed

(Combined vertical & lateral suspensions{staggered}, Linear Induction Motor)

Asterisk (*) before description indicates input.
2 Asterisks (**) after description indicates output from MatLab LIM program.

DESCRIPTION	UNITS	SYMBOL	89 m/s Optimization			89 m/s Optimization @ 59 m/s		
			DESIGN 1	DESIGN 2	DESIGN 3	DESIGN 1	DESIGN 2	DESIGN 3
VEHICLE PARAMETERS			baseline (b/l)	slim pole (3/4 b/l)	small gap (0.8 b/l)	baseline (b/l)	slim pole (3/4 b/l)	small gap (0.8 b/l)
Total leakage flux coefficient	---	nu_l	8.20E-01	1.09E+00	6.55E-01	8.20E-01	1.09E+00	6.55E-01
Total leakage flux/gap flux	---	Lambda	6.40E-01	7.70E-01	5.27E-01	6.40E-01	7.70E-01	5.27E-01
nu_t @ g=2ge, y=0		nu_t.max1	3.28E+00	4.04E+00	2.82E+00	3.28E+00	4.04E+00	2.82E+00
nu_t @ g=ge, y=y_star		nu_t.max2	3.39E+00	4.15E+00	2.99E+00	3.39E+00	4.15E+00	2.99E+00
Linear induction motor								
permeances								
Ideal air gap permeance/length		Pu.lim	1.01E+01	1.01E+01	1.25E+01	1.01E+01	1.01E+01	1.25E+01
Air gap fringing permeance/length		Pf.lim	1.92E+00	1.92E+00	1.92E+00	1.92E+00	1.92E+00	1.92E+00
Fringing permeance ratio		nuf.lim	1.90E-01	1.90E-01	1.54E-01	1.90E-01	1.90E-01	1.54E-01
EMS II Summary								
Weight on Vehicle								
Lift/Guidance Magnets	kg		4.74E+03	5.60E+03	3.60E+03	4.74E+03	5.60E+03	3.60E+03
Linear Induction Motor	kg		2.52E+03	2.52E+03	2.28E+03	2.52E+03	2.52E+03	2.28E+03
Total	kg		7.26E+03	8.12E+03	5.88E+03	7.26E+03	8.12E+03	5.88E+03
Weight on Guideway								
Lift/Guidance Magnets	kg/m		4.88E+01	3.54E+01	4.07E+01	4.88E+01	3.54E+01	4.07E+01
Linear Induction Motor	kg/m		1.59E+02	1.59E+02	1.39E+02	1.59E+02	1.59E+02	1.39E+02
Total	kg/m		2.07E+02	1.94E+02	1.80E+02	2.07E+02	1.94E+02	1.80E+02
Real Input Power Dissipation								
Ohmic Power Dissipation								
Lift/Guidance Magnets	W		7.44E+04	1.08E+05	6.07E+04	7.44E+04	1.08E+05	6.07E+04
Linear Induction Motor	W		6.00E+04	6.00E+04	5.62E+04	2.56E+04	2.56E+04	2.35E+04
Total Ohmic Power	W		1.34E+05	1.68E+05	1.17E+05	1.00E+05	1.34E+05	8.41E+04
Eddy current Power								
Lift/Guidance Magnets	W		1.40E+04	3.77E+03	1.17E+04	6.17E+03	1.66E+03	5.12E+03
Total eddy current Power	W		1.40E+04	3.77E+03	1.17E+04	6.17E+03	1.66E+03	5.12E+03
Total Real Power Dissipation	W		1.48E+05	1.72E+05	1.29E+05	1.06E+05	1.36E+05	8.92E+04
Reactive Input Power								
Linear Induction Motor	V-A		1.57E+06	1.57E+06	1.53E+06	4.68E+05	4.68E+05	4.57E+05
Total	V-A		1.57E+06	1.57E+06	1.53E+06	4.68E+05	4.68E+05	4.57E+05

Table F-4. Complete EMS II Spreadsheet; Design optimized for operation at 134 m/s
Combined Lift and guidance magnets (staggered) and Linear Induction Motor

ElectroMagnetic Suspension II — Optimized for operation at 134 m/s maximum speed

(Combined vertical & lateral suspensions(staggered), Linear Induction Motor)

Asterisk (*) before description indicates input.
2 Asterisks (**) after description indicates output from MatLab LIM program.

DESCRIPTION	UNITS	SYMBOL	134 m/s Optimization			134 m/s Optimization @ 89 m/s		
			DESIGN 1	DESIGN 2	DESIGN 3	DESIGN 1	DESIGN 2	DESIGN 3
VEHICLE PARAMETERS			baseline (b/l)	slim pole (3/4 b/l)	small gap (0.8 b/l)	baseline (b/l)	slim pole (3/4 b/l)	small gap (0.8 b/l)
Design Parameters								
*Vehicle mass	kg	m	4.00E+04	4.00E+04	4.00E+04	4.00E+04	4.00E+04	4.00E+04
*Vehicle length	m	l_vehicle	3.00E+01	3.00E+01	3.00E+01	3.00E+01	3.00E+01	3.00E+01
*Design speed	m/s	V	1.34E+02	1.34E+02	1.34E+02	8.90E+01	8.90E+01	8.90E+01
*frontal area	m^2	Af	1.20E+01	1.20E+01	1.20E+01	1.20E+01	1.20E+01	1.20E+01
*air density	kg/m^3	roair	1.20E+00	1.20E+00	1.20E+00	1.20E+00	1.20E+00	1.20E+00
*drag coefficient	---	Cd	3.00E-01	3.00E-01	3.00E-01	3.00E-01	3.00E-01	3.00E-01
wind drag force	N	Fd	3.88E+04	3.88E+04	3.88E+04	1.71E+04	1.71E+04	1.71E+04
wind drag power	W	Pd	5.20E+06	5.20E+06	5.20E+06	1.52E+06	1.52E+06	1.52E+06
*Max. Lift Force(@Max disp.)	g	max_Fz	1.10E+00	1.10E+00	1.10E+00	1.10E+00	1.10E+00	1.10E+00
*Max. Lateral Force(")(cont.)	g	max_F.l	2.60E-01	2.60E-01	2.60E-01	2.60E-01	2.60E-01	2.60E-01
*Max. Lateral Force(")(short term)	g	max_sF.l	4.20E-01	4.20E-01	4.20E-01	4.20E-01	4.20E-01	4.20E-01
*Time of Max. (short)Lateral F	sec	t_max	5.00E+00	5.00E+00	5.00E+00	5.00E+00	5.00E+00	5.00E+00
*Max propulsive force	g	max_Fp	2.10E-01	2.10E-01	2.10E-01	2.10E-01	2.10E-01	2.10E-01
*Maximum ambient temperature	°C	maxTamb	5.00E+01	5.00E+01	5.00E+01	5.00E+01	5.00E+01	5.00E+01
Performance Parameters								
Power, (ohmic+eddy)/aero. drag	%		7.89E-03	4.25E-03	6.56E-03	1.53E-02	1.14E-02	1.27E-02
Weight, (magnet+coil)/vehicle	%		1.20E-01	1.40E-01	8.99E-02	1.20E-01	1.40E-01	8.99E-02
eddy/lift amp-T (up. bound)	%		2.18E-01	8.74E-02	2.27E-01	1.45E-01	5.80E-02	1.51E-01
Aerodynamic drag/weight	%		9.89E-02	9.89E-02	9.89E-02	4.36E-02	4.36E-02	4.36E-02
CONSTANTS								
General								
*air permeability	N/A^2	mu	1.26E-06	1.26E-06	1.26E-06	1.26E-06	1.26E-06	1.26E-06
Suspensions								
Construction materials								
*rail			steel	steel	steel	steel	steel	steel
*magnet			2V Perm.	2V Perm.	2V Perm.	2V Perm.	2V Perm.	2V Perm.
*coil			alum.	alum.	alum.	alum.	alum.	alum.
Materials properties								
mass density								
*rail	kg/m^3	ror	7.85E+03	7.85E+03	7.85E+03	7.85E+03	7.85E+03	7.85E+03
*magnet	kg/m^3	rom	7.85E+03	7.85E+03	7.85E+03	7.85E+03	7.85E+03	7.85E+03
*coil	kg/m^3	roc	2.55E+03	2.55E+03	2.55E+03	2.55E+03	2.55E+03	2.55E+03
Saturation flux density								
*rail	T	BsatR	1.40E+00	1.40E+00	1.40E+00	1.40E+00	1.40E+00	1.40E+00
*magnet	T	BsatM	1.40E+00	1.40E+00	1.40E+00	1.40E+00	1.40E+00	1.40E+00
*Saturation Safety Factor(<1)	---	SF	1.00E+00	1.00E+00	1.00E+00	1.00E+00	1.00E+00	1.00E+00
Electrical resistivity								
*rail @20 deg C	ohm-m	rr	2.00E-07	2.00E-07	2.00E-07	2.00E-07	2.00E-07	2.00E-07
*coil @190 deg C	ohm-m	rc_	4.72E-08	4.72E-08	4.72E-08	4.72E-08	4.72E-08	4.72E-08
Thermal								
*magnet heat transfer coef.	W/°C-m	h_s	2.00E+01	2.00E+01	2.00E+01	2.00E+01	2.00E+01	2.00E+01
*Conductor thermal conductivity	W/(°C	k_c	2.20E+02	2.20E+02	2.20E+02	2.20E+02	2.20E+02	2.20E+02
*Insulation thermal conductivity	W/°C-m	k_ins	1.73E-01	1.73E-01	1.73E-01	1.73E-01	1.73E-01	1.73E-01
*coil packing factor	---	f	7.85E-01	7.85E-01	7.85E-01	7.85E-01	7.85E-01	7.85E-01
*Coil Width packing factor	---	f_y	8.86E-01	8.86E-01	8.86E-01	8.86E-01	8.86E-01	8.86E-01
*Coil thickness packing factor	---	f_z	8.86E-01	8.86E-01	8.86E-01	8.86E-01	8.86E-01	8.86E-01
*Maximum ambient temperature	°C	T	5.50E+01	5.50E+01	5.50E+01	5.50E+01	5.50E+01	5.50E+01
*Coil Specific heat	J/(kg°C	cp	1.19E+02	1.19E+02	1.19E+02	1.19E+02	1.19E+02	1.19E+02
*Maximum wire insulation temp	°C	maxTins	2.20E+02	2.20E+02	2.20E+02	2.20E+02	2.20E+02	2.20E+02
Linear Induction Motor								

Table F-4. (continued)

ElectroMagnetic Suspension II Optimized for operation at 134 m/s maximum speed

(Combined vertical & lateral suspensions(staggered), Linear Induction Motor)

Asterisk (*) before description indicates input.
2 Asterisks (**) after description indicates output from MatLab LIM program.

DESCRIPTION	UNITS	SYMBOL	134 m/s Optimization			134 m/s Optimization @ 89 m/s		
			DESIGN 1	DESIGN 2	DESIGN 3	DESIGN 1	DESIGN 2	DESIGN 3
VEHICLE PARAMETERS			baseline (b/l)	slim pole (3/4 b/l)	small gap (0.8 b/l)	baseline (b/l)	slim pole (3/4 b/l)	small gap (0.8 b/l)
*rail			steel	steel	steel	steel	steel	steel
*rail conductor(s)			aluminum	aluminum	aluminum	aluminum	aluminum	aluminum
*magnet			M-19	M-19	M-19	M-19	M-19	M-19
*magnet coil			aluminum	aluminum	aluminum	aluminum	aluminum	aluminum
Materials properties								
Mass density								
*rail	kg/m^3	rom.g	7.51E+03	7.51E+03	7.51E+03	7.51E+03	7.51E+03	7.51E+03
*rail conductor(s)	kg/m^3	roc.g	2.78E+03	2.78E+03	2.78E+03	2.78E+03	2.78E+03	2.78E+03
*magnet	kg/m^3	rom.v	7.65E+03	7.65E+03	7.65E+03	7.65E+03	7.65E+03	7.65E+03
*coil	kg/m^3	roc.v	2.78E+03	2.78E+03	2.78E+03	2.78E+03	2.78E+03	2.78E+03
maximum flux densities								
*rail	T	bsat.g	1.60E+00	1.60E+00	1.60E+00	1.60E+00	1.60E+00	1.60E+00
*magnet	T	bsat.v	1.50E+00	1.50E+00	1.50E+00	1.50E+00	1.50E+00	1.50E+00
Magnetic permeability								
rail	---	mu.g	3.50E+03	3.50E+03	3.50E+03	3.50E+03	3.50E+03	3.50E+03
Vehicle (short) stator		mu.v						
Core loss								
Core Loss @ 1.0T, 100 Hz	W/kg	refc.loss	2.87E+00	2.87E+00	2.87E+00	2.87E+00	2.87E+00	2.87E+00
Core loss frequency exponent	-	freq.exp	1.50E+00	1.50E+00	1.50E+00	1.50E+00	1.50E+00	1.50E+00
Core loss Induction exponent	-	B.exp	2.10E+00	2.10E+00	2.10E+00	2.10E+00	2.10E+00	2.10E+00
Core loss @ fsync & Bcore	W/kg	c.loss	1.95E+01	1.95E+01	2.51E+01	1.05E+01	1.05E+01	1.36E+01
Electrical resistivity								
*Magnet laminations @ 140°C	ohm-m	rm.v	7.00E-07	7.00E-07	7.00E-07	7.00E-07	7.00E-07	7.00E-07
*rail @20 deg C	ohm-m	rm.g	4.06E-07	4.06E-07	4.06E-07	4.06E-07	4.06E-07	4.06E-07
*vehicle coil @20 deg C	ohm-m	rcRT.v	2.78E-08	2.78E-08	2.78E-08	2.78E-08	2.78E-08	2.78E-08
*vehicle coil temperature coeffici	1/°C	alpha.v	4.10E-03	4.10E-03	4.10E-03	4.10E-03	4.10E-03	4.10E-03
vehicle coil @operating temperat	ohm-m	rc.v	4.79E-08	4.79E-08	4.80E-08	4.79E-08	4.79E-08	4.80E-08
*Guideway conductor @20 deg c	ohm-m	rc.g	2.80E-08	2.80E-08	2.80E-08	2.80E-08	2.80E-08	2.80E-08
Heat transfer coeffieients								
*magnet heat transfer coef.	W/C-m	k.v	4.19E+01	4.19E+01	4.19E+01	4.19E+01	4.19E+01	4.19E+01
*rail heat transfer coef.	W/C-m	k.g	1.40E+01	1.40E+01	1.40E+01	1.40E+01	1.40E+01	1.40E+01
COMPONENT DESIGN & ANALYSIS								
<u>*Vertical/lateral suspension*</u>								
Geometric dimensions								
*Lateral stagger	m	del	5.00E-03	1.50E-03	2.50E-03	5.00E-03	1.50E-03	2.50E-03
*pole width	m	lp	2.00E-02	1.50E-02	2.00E-02	2.00E-02	1.50E-02	2.00E-02
*window width	m	w	1.30E-01	1.19E-01	1.16E-01	1.30E-01	1.19E-01	1.16E-01
*window height	m	h (or d)	6.52E-02	5.97E-02	5.80E-02	6.52E-02	5.97E-02	5.80E-02
*air gap	m	H1x	1.00E-02	1.00E-02	8.00E-03	1.00E-02	1.00E-02	8.00E-03
*pole-coil clearance	m	z	5.08E-03	5.08E-03	5.08E-03	5.08E-03	5.08E-03	5.08E-03
*Number magnet sets required	---	nmag,N.s	4	4	4	4	4	4
*Number individual magnets/set	---	N.mags	2	2	2	2	2	2
<u>*Performance parameters*</u>								
Individual magnet total weight	kg	W_mag_c	5.98E+02	7.00E+02	4.49E+02	598.45475	700.33698	449.41394
Lift-to-weight ratio	---	LTWR	8.35E+00	7.14E+00	1.11E+01	8.35E+00	7.14E+00	1.11E+01
Power-to-lift ratio	kW/ton	PTLR	1.88E+00	2.71E+00	1.52E+00	1.88E+00	2.71E+00	1.52E+00
Total weight of magnet assemblies	kg	M_magne	4.79E+03	5.60E+03	3.60E+03	4.79E+03	5.60E+03	3.60E+03
Magnet-to-Vehicle weight ratio	---	MVWR	11.97%	14.01%	8.99%	1.20E-01	1.40E-01	8.99E-02
Max. lateral force @y*(1 set)	kg	F_y_star	6.55E+04	9.03E+04	5.20E+04	6.55E+04	9.03E+04	5.20E+04
Required max lateral force(1 set)	kg	F_ymax	4.12E+04	4.12E+04	4.12E+04	4.12E+04	4.12E+04	4.12E+04
Max. lift force @y*(1 set)	kg	Fz_y_sta	1.08E+05	1.08E+05	1.08E+05	1.08E+05	1.08E+05	1.08E+05
Required max. lift force(1 set)	kg	F_zmax	1.08E+05	1.08E+05	1.08E+05	1.08E+05	1.08E+05	1.08E+05

Table F-4. (continued)

ElectroMagnetic Suspension II Optimized for operation at 134 m/s maximum speed

(Combined vertical & lateral suspensions(staggered), Linear Induction Motor)

Asterisk (*) before description indicates input.
2 Asterisks (**) after description indicates output from MatLab LIM program.

DESCRIPTION	UNITS	SYMBOL	134 m/s Optimization DESIGN 1 baseline (b/l)	134 m/s Optimization DESIGN 2 slim pole (3/4 b/l)	134 m/s Optimization DESIGN 3 small gap (0.8 b/l)	134 m/s Optimization @ 89 m/s DESIGN 1 baseline (b/l)	134 m/s Optimization @ 89 m/s DESIGN 2 slim pole (3/4 b/l)	134 m/s Optimization @ 89 m/s DESIGN 3 small gap (0.8 b/l)
VEHICLE PARAMETERS								
Classical lift force (1 mag, y=0)	kg	F_class	4.16E+04	3.77E+04	4.16E+04	4.16E+04	3.77E+04	4.16E+04
Lateral stiffness (4 sets)	N/m	K_lateral	1.76E+07	2.40E+07	1.38E+07	1.76E+07	2.40E+07	1.38E+07
Magnet design		FFF	9.60E-01	9.90E-01	9.50E-01	9.60E-01	9.90E-01	9.50E-01
Decoupling displacement limit	m	y_star	1.49E-02	1.50E-02	1.51E-02	1.49E-02	1.50E-02	1.51E-02
magnet length	m	L	5.68E+00	8.88E+00	5.10E+00	5.68E+00	8.88E+00	5.10E+00
width of pole base	m	w_p	2.78E-02	2.21E-02	2.64E-02	2.78E-02	2.21E-02	2.64E-02
Magnet yoke length	m	L_y	5.55E+00	8.76E+00	4.99E+00	5.55E+00	8.76E+00	4.99E+00
Magnet yoke height	m	d_y	3.36E-02	2.69E-02	3.12E-02	3.36E-02	2.69E-02	3.12E-02
Yoke area	m^2	A_yoke	1.86E-01	2.36E-01	1.56E-01	1.86E-01	2.36E-01	1.56E-01
fringing (across air gap)	---	nuf	9.60E-01	1.28E+00	7.68E-01	9.60E-01	1.28E+00	7.68E-01
leakage (between poles)	---	nul	2.12E-01	2.78E-01	1.72E-01	2.12E-01	2.78E-01	1.72E-01
total	---	nut	2.17E+00	2.56E+00	1.94E+00	2.17E+00	2.56E+00	1.94E+00
Nominal air gap flux density	T	B0	6.78E-01	5.96E-01	7.16E-01	6.78E-01	5.96E-01	7.16E-01
Nominal pole tip flux density	T		8.68E-01	8.47E-01	8.89E-01			
Nominal pole base flux density	T		1.21E+00	1.25E+00	1.18E+00			
Nominal yoke flux density	T		1.42E+00	1.50E+00	1.36E+00			
Force per magnet	N	Fpm	4.16E+04	3.77E+04	4.16E+04	4.16E+04	3.77E+04	4.16E+04
amp turns per magnet	A	NI	1.08E+04	9.49E+03	9.12E+03	1.08E+04	9.49E+03	9.12E+03
core mass (1 mag)	kg	Mcore	4.05E+02	4.48E+02	3.12E+02	4.05E+02	4.48E+02	3.12E+02
mass core + coil (4 mag)	kg	Mmag	4.79E+03	5.60E+03	3.60E+03	4.79E+03	5.60E+03	3.60E+03
Coil design								
resistance (1 magnet, 1 turn)	ohm	resc	8.06E-05	1.50E-04	9.12E-05	8.06E-05	1.50E-04	9.12E-05
coil ohmic power (1 magnet)	W	qc	9.39E+03	1.35E+04	7.58E+03	9.39E+03	1.35E+04	7.58E+03
Surface temperature rise	°C	deltaT_s	1.59E+02	1.60E+02	1.60E+02	1.59E+02	1.60E+02	1.60E+02
Surface temperature	°C	T_s	2.09E+02	2.10E+02	2.10E+02	2.09E+02	2.10E+02	2.10E+02
Internal temperature rise	°C	deltaT_i	6.06E+00	4.71E+00	4.33E+00	6.06E+00	4.71E+00	4.33E+00
Maximum internal temperature	°C	T_int	2.20E+02	2.20E+02	2.19E+02	2.20E+02	2.20E+02	2.19E+02
mass(one coil)	kg	Mcoil	1.93E+02	2.53E+02	1.38E+02	1.93E+02	2.53E+02	1.38E+02
Total ohmic power, Nmag*n_mags	W	P_total	7.51E+04	1.08E+05	6.07E+04	7.51E+04	1.08E+05	6.07E+04
Rail design								
rail thickness	m	tr	2.83E-02	2.27E-02	2.59E-02	2.83E-02	2.27E-02	2.59E-02
rail mass/length	kg/m	mr	4.89E+01	3.54E+01	4.07E+01	4.89E+01	3.54E+01	4.07E+01
nominal rail flux density	T	Br	9.40E-01	8.97E-01	9.76E-01	9.40E-01	8.97E-01	9.76E-01
eff. freq. for eddy anal.	Hz	Fe	1.18E+01	7.54E+00	1.31E+01	7.84E+00	5.01E+00	8.72E+00
dB/dt amp. first harmonic	T/s	B1x	4.44E+01	2.71E+01	5.13E+01	2.95E+01	1.80E+01	3.41E+01
eddy current power	W	Pr	3.16E+04	8.55E+03	2.65E+04	1.40E+04	3.77E+03	1.17E+04
rms eddy amp turn (upper bound, 1 magnet)	A	NIe	2.35E+03	8.29E+02	2.07E+03	1.56E+03	5.51E+02	1.38E+03
Total continuous power	W	P.v	4.10E+04	2.21E+04	3.41E+04	2.33E+04	1.73E+04	1.93E+04
Linear Induction Motor								
Design maximum thrust	g	max.g	2.10E-01	2.10E-01	2.10E-01	2.10E-01	2.10E-01	2.10E-01
Design maximum thrust	N	max.thr	8.23E+04	8.23E+04	8.23E+04	8.23E+04	8.23E+04	8.23E+04
Nominal excitation frequency	Hz	fsync	2.03E+02	2.03E+02	2.41E+02	1.35E+02	1.35E+02	1.60E+02
Synchronous speed	m/s	vsync	1.35E+02	1.35E+02	1.35E+02	8.99E+01	8.99E+01	8.99E+01
Nominal slip		nom.slip	1.00E-02	1.00E-02	1.00E-02	1.00E-02	1.00E-02	1.00E-02
General								
*Number of motors		Nmotor	4.00E+00	4.00E+00	4.00E+00	4.00E+00	4.00E+00	4.00E+00
*Number of poles		Np.v	1.60E+01	1.60E+01	1.60E+01	1.60E+01	1.60E+01	1.60E+01
Geometric dimensions								
*Air gap (mechanical clearance)	m	cl.v	1.00E-02	1.00E-02	8.00E-03	1.00E-02	1.00E-02	8.00E-03

Table F-4. (continued)

ElectroMagnetic Suspension II Optimized for operation at 134 m/s maximum speed

(Combined vertical & lateral suspensions(staggered), Linear Induction Motor)

Asterisk (*) before description indicates input.
2 Asterisks (**) after description indicates output from MatLab LIM program.

DESCRIPTION	UNITS	SYMBOL	134 m/s Optimization			134 m/s Optimization @ 89 m/s		
			DESIGN 1	DESIGN 2	DESIGN 3	DESIGN 1	DESIGN 2	DESIGN 3
			baseline (b/l)	slim pole (3/4 b/l)	small gap (0.8 b/l)	baseline (b/l)	slim pole (3/4 b/l)	small gap (0.8 b/l)
VEHICLE PARAMETERS								
*Pole pitch	m	tau.v	3.33E-01	3.33E-01	2.81E-01	3.33E-01	3.33E-01	2.81E-01
*Slots/pole/phase		Nslots	2.00E+00	2.00E+00	2.00E+00	2.00E+00	2.00E+00	2.00E+00
*Core width	m	d.v	2.10E-01	2.10E-01	2.20E-01	2.10E-01	2.10E-01	2.20E-01
*Tooth width/slot width ratio		tsr.v	1.20E+00	1.20E+00	1.20E+00	1.20E+00	1.20E+00	1.20E+00
*Slot depth	m	h.v	5.00E-02	5.00E-02	5.00E-02	5.00E-02	5.00E-02	5.00E-02
*Lamination thickness	m	tlam.v	3.56E-04	3.56E-04	3.56E-04	3.56E-04	3.56E-04	3.56E-04
Magnetic gap (entrefer)	m	g.mag	1.50E-02	1.50E-02	1.30E-02	1.50E-02	1.50E-02	1.30E-02
Carter factor		Kcarter	1.19E+00	1.19E+00	1.18E+00	1.19E+00	1.19E+00	1.18E+00
Effective magnetic gap	m	ge.lim	1.78E-02	1.78E-02	1.54E-02	1.78E-02	1.78E-02	1.54E-02
Back iron thickness, vehicle	m	ty.v	5.61E-02	5.61E-02	4.61E-02	5.61E-02	5.61E-02	4.61E-02
Tooth width	m	lt.v	2.53E-02	2.53E-02	2.13E-02	2.53E-02	2.53E-02	2.13E-02
Slot width	m	w.v	3.03E-02	3.03E-02	2.55E-02	3.03E-02	3.03E-02	2.55E-02
Slot pitch (=tooth pitch)	m	sp.v	5.56E-02	5.56E-02	4.68E-02	5.56E-02	5.56E-02	4.68E-02
Number of laminations		Nlams.v	5.89E+02	5.89E+02	5.89E+02	5.89E+02	5.89E+02	5.89E+02
Motor effective length	m	Leff	5.33E+00	5.33E+00	4.50E+00	5.33E+00	5.33E+00	4.50E+00
Motor physical length	m	Lphys	5.89E+00	5.89E+00	4.96E+00	5.89E+00	5.89E+00	4.96E+00
Effective air gap area	m^2	Aface	1.12E+00	1.12E+00	9.89E-01	1.12E+00	1.12E+00	9.89E-01
Core exposed surface area	m^2	Acore	3.48E+00	3.48E+00	2.94E+00	3.48E+00	3.48E+00	2.94E+00
Winding parameters								
*Number of phases		Nphase.v	3.00E+00	3.00E+00	3.00E+00	3.00E+00	3.00E+00	3.00E+00
*Coil pitch/pole pitch ratio(fraction)		cp_tau	6.67E-01	6.67E-01	6.67E-01	6.67E-01	6.67E-01	6.67E-01
*Number of winding layers		Nlayers.v	2.00E+00	2.00E+00	2.00E+00	2.00E+00	2.00E+00	2.00E+00
*Number of coils/pole/phase		ncoils.v	2.00E+00	2.00E+00	2.00E+00	2.00E+00	2.00E+00	2.00E+00
*Coil packing factor		f.v	7.85E-01	7.85E-01	7.85E-01	7.85E-01	7.85E-01	7.85E-01
*Pole/coil clearance	m	z.v	5.00E-03	5.00E-03	5.00E-03	5.00E-03	5.00E-03	5.00E-03
*Turns/coil		Npc.v	1.00E+00	1.00E+00	1.00E+00	1.00E+00	1.00E+00	1.00E+00
*End turn angle	degrees	alpha	3.00E+01	3.00E+01	3.00E+01	3.00E+01	3.00E+01	3.00E+01
*End turn projection	m	b	1.00E-02	1.00E-02	1.00E-02	1.00E-02	1.00E-02	1.00E-02
Distribution factor(distributed winding)		Kd	8.66E-01	8.66E-01	8.66E-01	8.66E-01	8.66E-01	8.66E-01
Pitch factor(fractional pitch coils)		Kp	8.66E-01	8.66E-01	8.66E-01	8.66E-01	8.66E-01	8.66E-01
Winding factor(for distributed windings)		Kw	7.50E-01	7.50E-01	7.50E-01	7.50E-01	7.50E-01	7.50E-01
Coil pitch	m	tau_c.v	2.22E-01	2.22E-01	1.87E-01	2.22E-01	2.22E-01	1.87E-01
Mean conductor length	m/coil	lcoil.v	9.73E-01	9.73E-01	9.13E-01	9.73E-01	9.73E-01	9.13E-01
Coil thickness	m	tcoil.v	2.25E-02	2.25E-02	2.25E-02	2.25E-02	2.25E-02	2.25E-02
Conductor x-section area/slot/lay	m^2	Acoil.v	5.35E-04	5.35E-04	4.51E-04	5.35E-04	5.35E-04	4.51E-04
Coil Resistance	ohm	Rcoil.v	8.72E-05	8.72E-05	9.72E-05	8.72E-05	8.72E-05	9.72E-05
Heat transfer area (1 coil)	m^2	Aht.v	8.06E-02	8.06E-02	6.66E-02	8.06E-02	8.06E-02	6.66E-02
Peak MMF per coil RMS amp-turns	-	MMFperNI	4.05E+00	4.05E+00	4.05E+00	4.05E+00	4.05E+00	4.05E+00
Core operating flux density	T	Bcore.v	1.50E+00	1.50E+00	1.50E+00	1.50E+00	1.50E+00	1.50E+00
Coil RMS amp-turns @ Bsat of toot	Amp-tu	NIcoil.v	2.38E+03	2.38E+03	2.06E+03	2.38E+03	2.38E+03	2.06E+03
Total flux per pole @ Bsat of tooth	Webers	Fpp	3.53E-02	3.53E-02	3.04E-02	3.53E-02	3.53E-02	3.04E-02
RMS phase current @ Bsat of tooth	A	Iphase.v	2.38E+03	2.38E+03	2.06E+03	2.38E+03	2.38E+03	2.06E+03
Total RMS slot current @ Bsat of t	A	Islot .v	4.77E+03	4.77E+03	4.12E+03	4.77E+03	4.77E+03	4.12E+03
Coil power (1coil)	W	Pcoil.v	4.95E+02	4.95E+02	4.11E+02	4.95E+02	4.95E+02	4.11E+02
Coil surface temperature rise	°C	delTavg.v	1.46E+02	1.46E+02	1.48E+02	1.46E+02	1.46E+02	1.48E+02
Maximum coil surface temperature	°C	Tw.lim	1.96E+02	1.96E+02	1.98E+02	1.96E+02	1.96E+02	1.98E+02
Slot current	A-cond	I.slot	4.77E+03	4.77E+03	4.12E+03	4.77E+03	4.77E+03	4.12E+03
Linear current loading	A/m	I.load	8.58E+04	8.58E+04	8.79E+04	8.58E+04	8.58E+04	8.79E+04
Stator Leakage Reactance Calculations								
Slot Leakage	ohm	Xslot	2.84E-02	2.84E-02	4.19E-02	1.89E-02	1.89E-02	2.78E-02
End turn leakage	ohm	Xec	3.05E-08	3.05E-08	3.05E-08	2.02E-08	2.02E-08	2.02E-08
Total Primary Leakage Reactance	ohm	Xleak	2.84E-02	2.84E-02	4.19E-02	1.89E-02	1.89E-02	2.78E-02

Stator Leakage Reactance @ 50 Hz.

Table F-4. (continued)

ElectroMagnetic Suspension II Optimized for operation at 134 m/s maximum speed

(Combined vertical & lateral suspensions(staggered), Linear Induction Motor)

Asterisk (*) before description indicates input.
2 Asterisks (**) after description indicates output from MatLab LIM program.

DESCRIPTION	UNITS	SYMBOL	134 m/s Optimization			134 m/s Optimization @ 89 m/s		
			DESIGN 1	DESIGN 2	DESIGN 3	DESIGN 1	DESIGN 2	DESIGN 3
VEHICLE PARAMETERS			baseline (b/l)	slim pole (3/4 b/l)	small gap (0.8 b/l)	baseline (b/l)	slim pole (3/4 b/l)	small gap (0.8 b/l)
Leakage Reactance @ 50 Hz.	ohm/ph	X50_	7.00E-03	7.00E-03	8.70E-03	7.00E-03	7.00E-03	8.70E-03
Coil Resistance	ohm/ph	Rone	5.58E-03	5.58E-03	6.22E-03	5.58E-03	5.58E-03	6.22E-03
Reactance/Resistance ratio @ 50 H	-	alpha50	1.26E+00	1.26E+00	1.40E+00	1.26E+00	1.26E+00	1.40E+00
Series turns/phase		stp.lim	3.20E+01	3.20E+01	3.20E+01	3.20E+01	3.20E+01	3.20E+01
Resistance, Primary	ohm/ph	rp.lim	5.58E-03	5.58E-03	6.22E-03	5.58E-03	5.58E-03	6.22E-03
Weight								
Motor iron weight, single stator	kg	mi.v	7.89E+02	7.89E+02	6.13E+02	7.89E+02	7.89E+02	6.13E+02
Motor conductor weight, single sta	kg	mc.v	1.39E+02	1.39E+02	1.10E+02	1.39E+02	1.39E+02	1.10E+02
Total motor weight(Nmotor motors	kg	mmotor	3.71E+03	3.71E+03	2.89E+03	3.71E+03	3.71E+03	2.89E+03
Power								
Core loss power, single stator	W	Pcore	1.53E+04	1.53E+04	1.54E+04	8.30E+03	8.30E+03	8.34E+03
Core temperature rise	°C	delTcore	1.05E+02	1.05E+02	1.25E+02	5.70E+01	5.70E+01	6.78E+01
Core surface temperature	°C	Tcore	1.55E+02	1.55E+02	1.75E+02	1.07E+02	1.07E+02	1.18E+02
Motor Secondary (guideway) Design Parameters								
Iron								
Back iron thickness, guideway	m	ty.g	4.60E-02	4.60E-02	3.87E-02	4.60E-02	4.60E-02	3.87E-02
Back iron width	m	d.g	2.40E-01	2.40E-01	2.46E-01	2.40E-01	2.40E-01	2.46E-01
Guideway iron specific weight	kg/m	mi.g	8.29E+01	8.29E+01	7.14E+01	8.29E+01	8.29E+01	7.14E+01
Conductor								
*Conductor overlap factor		colf.g	4.00E-01	4.00E-01	4.00E-01	4.00E-01	4.00E-01	4.00E-01
*Conductor thickness	m	tc.g	5.00E-03	5.00E-03	5.00E-03	5.00E-03	5.00E-03	5.00E-03
Conductor width	m	dc.g	5.07E-01	5.07E-01	4.71E-01	5.07E-01	5.07E-01	4.71E-01
Guideway conductor specific weig	kg/m	mc.g	7.04E+00	7.04E+00	6.54E+00	7.04E+00	7.04E+00	6.54E+00
Total guideway added weight	kg/m	m.gw	1.80E+02	1.80E+02	1.56E+02	1.80E+02	1.80E+02	1.56E+02
Performance Results from MatLab Analysis								
Individual Motor Parameters at Maximum Propulsive Force								
Thrust**	N	Thrust	2.04E+04	2.04E+04	2.05E+04	9.02E+03	9.02E+03	9.05E+03
Slip**	-	slip	1.00E-02	1.00E-02	9.00E-03	1.50E-02	1.50E-02	1.40E-02
Traction Power**	W	P.tract	2.74E+06	2.74E+06	2.75E+06	7.98E+05	7.98E+05	8.03E+05
Real input Power**	W	Pin.real	2.82E+06	2.82E+06	2.83E+06	8.32E+05	8.32E+05	8.33E+05
Reactive input Power**	V-A	Pin.react	3.22E+06	3.22E+06	3.27E+06	9.47E+05	9.47E+05	9.32E+05
Efficiency**	%	eff.v	9.65E+01	9.65E+01	9.69E+01	9.59E+01	9.59E+01	9.59E+01
Power Factor		PwrFac	6.59E-01	6.59E-01	6.54E-01	6.59E-01	6.59E-01	6.59E-01
AUXILIARY CALCULATIONS								
Lift/guidance magnets								
permeances								
√Air gap fringing permeance/lengt	---	Pf	1.92E+00	1.92E+00	1.92E+00	1.92E+00	1.92E+00	1.92E+00
√Ideal air gap permeance/length	---	Pu	2.00E+00	1.50E+00	2.50E+00	2.00E+00	1.50E+00	2.50E+00
?Inter-pole leakage perm./length	---	Pl	4.25E-01	4.18E-01	4.31E-01	4.25E-01	4.18E-01	4.31E-01
alpha(g,delta)		alpha_g.del	1.24E+00	1.41E+00	1.23E+00			
alpha(g,delta+y*)		lpha_g.del.y_star	1.24E+00	1.41E+00	1.23E+00			
example using function "alpha(y,g,l_p)"		0						
Coil dimensions								
Average turn length		lc	1.14E+01	1.78E+01	1.02E+01	1.14E+01	1.78E+01	1.02E+01
Coil conductor crossectional area		ac	6.66E-03	5.58E-03	5.28E-03	6.66E-03	5.58E-03	5.28E-03
Effective surface area/heat trans.		adis	5.01E+00	6.98E+00	4.06E+00	5.01E+00	6.98E+00	4.06E+00
Coil volume	m^3	V_coil	9.64E-02	1.26E-01	6.87E-02			
Magnet parameters						0.00E+00	0.00E+00	0.00E+00
Magnet volume	m^3	V_mag	5.17E-02	5.70E-02	3.97E-02	5.17E-02	5.70E-02	3.97E-02
flux leakage coefficients								
Gap fringing flux coefficient	---	nu_g	1.28E+00	1.42E+00	1.24E+00	1.28E+00	1.42E+00	1.24E+00
Pole leakage flux coefficient	---	nu_l.p	5.02E-01	6.69E-01	4.00E-01	5.02E-01	6.69E-01	4.00E-01

Table F-4. (continued)

ElectroMagnetic Suspension II Optimized for operation at 134 m/s maximum speed

(Combined vertical & lateral suspensions(staggered), Linear Induction Motor)

Asterisk (*) before description indicates input.
2 Asterisks (**) after description indicates output from MatLab LIM program.

DESCRIPTION	UNITS	SYMBOL	134 m/s Optimization			134 m/s Optimization @ 89 m/s		
			DESIGN 1	DESIGN 2	DESIGN 3	DESIGN 1	DESIGN 2	DESIGN 3
VEHICLE PARAMETERS			baseline (b/l)	slim pole (3/4 b/l)	small gap (0.8 b/l)	baseline (b/l)	slim pole (3/4 b/l)	small gap (0.8 b/l)
Yoke leakage flux coefficient	---	nu_l.y	3.18E-01	4.24E-01	2.55E-01	3.18E-01	4.24E-01	2.55E-01
Total leakage & fringing flux coef.	---	nu_t	2.10E+00	2.51E+00	1.90E+00	2.10E+00	2.51E+00	1.90E+00
Total leakage flux coefficient	---	nu_l	8.20E-01	1.09E+00	6.55E-01	8.20E-01	1.09E+00	6.55E-01
Total leakage flux/gap flux	---	Lambda	6.40E-01	7.70E-01	5.27E-01	6.40E-01	7.70E-01	5.27E-01
nu_t @ g=2ge, y=0		nu_t.max1	3.28E+00	4.04E+00	2.82E+00	3.28E+00	4.04E+00	2.82E+00
nu_t @ g=ge, y=y_star		nu_t.max2	3.39E+00	4.16E+00	2.99E+00	3.39E+00	4.16E+00	2.99E+00
Linear induction motor								
permeances								
Ideal air gap permeance/length		Pu.lim	1.18E+01	1.18E+01	1.43E+01	1.18E+01	1.18E+01	1.43E+01
Air gap fringing permeance/length		Pf.lim	1.92E+00	1.92E+00	1.92E+00	1.92E+00	1.92E+00	1.92E+00
Fringing permeance ratio		nuf.lim	1.63E-01	1.63E-01	1.34E-01	1.63E-01	1.63E-01	1.34E-01
EMS II Summary								
Weight on Vehicle								
Lift/Guidance Magnets	kg		4.79E+03	5.60E+03	3.60E+03	4.79E+03	5.60E+03	3.60E+03
Linear Induction Motor	kg		3.71E+03	3.71E+03	2.89E+03	3.71E+03	3.71E+03	2.89E+03
Total	kg		8.50E+03	9.31E+03	6.49E+03	8.50E+03	9.31E+03	6.49E+03
Weight on Guideway								
Lift/Guidance Magnets	kg/m		4.89E+01	3.54E+01	4.07E+01	4.89E+01	3.54E+01	4.07E+01
Linear Induction Motor	kg/m		1.80E+02	1.80E+02	1.56E+02	1.80E+02	1.80E+02	1.56E+02
Total	kg/m		2.29E+02	2.15E+02	1.97E+02	2.29E+02	2.15E+02	1.97E+02
Real Input Power Dissipation								
Ohmic Power Dissipation								
Lift/Guidance Magnets	W		7.51E+04	1.08E+05	6.07E+04	7.51E+04	1.08E+05	6.07E+04
Linear Induction Motor	W		8.28E+04	8.28E+04	8.00E+04	3.40E+04	3.40E+04	3.08E+04
Total Ohmic Power	W		1.58E+05	1.91E+05	1.41E+05	1.09E+05	1.42E+05	9.14E+04
Eddy current Power								
Lift/Guidance Magnets	W		3.16E+04	8.55E+03	2.65E+04	1.40E+04	3.77E+03	1.17E+04
Total eddy current Power	W		3.16E+04	8.55E+03	2.65E+04	1.40E+04	3.77E+03	1.17E+04
Total Real Power Dissipation	W		1.90E+05	2.00E+05	1.67E+05	1.23E+05	1.46E+05	1.03E+05
Reactive Input Power								
Linear Induction Motor	V-A		3.22E+06	3.22E+06	3.27E+06	9.47E+05	9.47E+05	9.32E+05
Total	V-A		3.22E+06	3.22E+06	3.27E+06	9.47E+05	9.47E+05	9.32E+05

Table F-5 Complete EMS III Spreadsheet; Design optimized for operation at 89 m/s
Separate guidance magnet,Combined lift magnet and Linear Synchronous Motor

ElectroMagnetic Suspension III Optimized for operation at 89 m/s maximum speed
(Separate vertical suspension & synchronous motor, lateral suspension)
12/09/92
Asterisk (*) before description indicates input.

DESCRIPTION	UNITS	SYMBOL	89 m/s Optimization			89 m/s Optimization @ 59 m/s		
			DESIGN 1	DESIGN 2	DESIGN 3	DESIGN 1	DESIGN 2	DESIGN 3
			baseline	slim pole (3/4 b/l)	small gap (0.8 b/l)	baseline	slim pole (3/4 b/l)	small gap (0.8 b/l)
VEHICLE PARAMETERS								
Design Parameters								
*Vehicle mass	kg	m	4.00E+04	4.00E+04	4.00E+04	4.00E+04	4.00E+04	4.00E+04
*Design speed	m/s	V	8.90E+01	8.90E+01	8.90E+01	5.90E+01	5.90E+01	5.90E+01
*frontal area	m^2	Af	1.20E+01	1.20E+01	1.20E+01	1.20E+01	1.20E+01	1.20E+01
*air density	kg/m^3	roair	1.20E+00	1.20E+00	1.20E+00	1.20E+00	1.20E+00	1.20E+00
*drag coefficient	---	Cd	3.00E-01	3.00E-01	3.00E-01	3.00E-01	3.00E-01	3.00E-01
wind drag force	N	Fd	1.71E+04	1.71E+04	1.71E+04	7.52E+03	7.52E+03	7.52E+03
wind drag power	W	Pd	1.52E+06	1.52E+06	1.52E+06	4.44E+05	4.44E+05	4.44E+05
*Max. Lift Force(@Max disp.)	g	max_Fz	1.10E+00	1.10E+00	1.10E+00	1.10E+00	1.10E+00	1.10E+00
*Max. Lateral Force(")(cont.)	g	max_F.l	1.80E-01	1.80E-01	1.80E-01	1.80E-01	1.80E-01	1.80E-01
*Max. Lateral Force(")(short)	g	max_sF.l	2.60E-01	2.60E-01	2.60E-01	2.60E-01	2.60E-01	2.60E-01
*Time of Max. (short)Lateral F	sec	t_max	5.00E+00	5.00E+00	5.00E+00	5.00E+00	5.00E+00	5.00E+00
*Maximum ambient temp.	°C	maxTamb	5.00E+01	5.00E+01	5.00E+01	5.00E+01	5.00E+01	5.00E+01
CONSTANTS								
General								
*air permeability	N/A^2	mu	1.26E-06	1.26E-06	1.26E-06	1.26E-06	1.26E-06	1.26E-06
Lateral Suspension								
Construction materials								
*rail			steel	steel	steel	steel	steel	steel
*magnet			2V Perm.	2V Perm.	2V Perm.	2V Perm.	2V Perm.	2V Perm.
*coil			alum.	alum.	alum.	alum.	alum.	alum.
Materials properties								
mass density								
*rail	kg/m^3	ror	7.51E+03	7.51E+03	7.51E+03	7.51E+03	7.51E+03	7.51E+03
*magnet	kg/m^3	rom	7.78E+03	7.78E+03	7.78E+03	7.78E+03	7.78E+03	7.78E+03
*coil	kg/m^3	roc	2.78E+03	2.78E+03	2.78E+03	2.78E+03	2.78E+03	2.78E+03
maximum flux density								
*rail	T	Bsatr	1.60E+00	1.60E+00	1.60E+00	1.60E+00	1.60E+00	1.60E+00
*magnet	T	Bsatm	2.30E+00	2.30E+00	2.30E+00	2.30E+00	2.30E+00	2.30E+00
*Saturation Safety Factor(<1)	---	SF	1.00E+00	1.00E+00	1.00E+00	1.00E+00	1.00E+00	1.00E+00
Electrical resistivity								
*rail @20 deg C	ohm-m	rr	4.06E-07	4.06E-07	4.06E-07	4.06E-07	4.06E-07	4.06E-07
*coil @140 deg C	ohm-m	rc_	4.06E-08	4.06E-08	4.06E-08	4.06E-08	4.06E-08	4.06E-08
*coil @220 deg C	ohm-m	rc_220						
Thermal								
*magnet heat transfer coef.	W/C-m^2	k	1.40E+01	1.40E+01	1.40E+01	1.40E+01	1.40E+01	1.40E+01
*Coil Specific heat	J/(kg°C)	cp	1.19E+02	1.19E+02	1.19E+02	1.19E+02	1.19E+02	1.19E+02
*Maximum wire insulation tem	°C	maxTins	2.00E+02	2.00E+02	2.00E+02	2.00E+02	2.00E+02	2.00E+02
Lift Magnet & Linear Synchronous Motor								
Construction materials								
*rail			steel	steel	steel	steel	steel	steel
*rail windings			copper	copper	copper	copper	copper	copper
*magnet			2V Perm.	2V Perm.	2V Perm.	2V Perm.	2V Perm.	2V Perm.
*magnet coil			aluminum	aluminum	aluminum	aluminum	aluminum	aluminum
Densities								
*rail	kg/m^3	rogm	7.51E+03	7.51E+03	7.51E+03	7.51E+03	7.51E+03	7.51E+03
*rail windings	kg/m^3	rogc	8.90E+03	8.90E+03	8.90E+03	8.90E+03	8.90E+03	8.90E+03
*magnet	kg/m^3	rovm	7.78E+03	7.78E+03	7.78E+03	7.78E+03	7.78E+03	7.78E+03
*coil	kg/m^3	rovc	2.78E+03	2.78E+03	2.78E+03	2.78E+03	2.78E+03	2.78E+03
Maximum flux densities								
*rail	T	bsatg	1.60E+00	1.60E+00	1.60E+00	1.60E+00	1.60E+00	1.60E+00
*magnet	T	bsatv	2.30E+00	2.30E+00	2.30E+00	2.30E+00	2.30E+00	2.30E+00
Magnetic permeabilities								

Table F-5 (continued)

ElectroMagnetic Suspension III Optimized for operation at 89 m/s maximum speed

(Separate vertical suspension & synchronous motor, lateral suspension)

12/09/92

Asterisk (*) before description indicates input.

DESCRIPTION	UNITS	SYMBOL	89 m/s Optimization			89 m/s Optimization @ 59 m/s		
			DESIGN 1 baseline	DESIGN 2 slim pole (3/4 b/l)	DESIGN 3 small gap (0.8 b/l)	DESIGN 1 baseline	DESIGN 2 slim pole (3/4 b/l)	DESIGN 3 small gap (0.8 b/l)
Electrical Resistivity								
*rail @20 deg C	ohm-m	rmg	4.06E-07	4.06E-07	4.06E-07	4.06E-07	4.06E-07	4.06E-07
*vehicle coil @140 deg C	ohm-m	rcv	4.06E-08	4.06E-08	4.06E-08	4.06E-08	4.06E-08	4.06E-08
*rail coil *140 deg c	ohm-m	rcg	2.46E-08	2.46E-08	2.46E-08	2.46E-08	2.46E-08	2.46E-08
Thermal								
*magnet heat transfer coeffic	W/C-m^2	kv	1.40E+01	1.40E+01	1.40E+01	1.40E+01	1.40E+01	1.40E+01
*rail heat transfer coef.	W/C-m^2	kg	1.40E+01	1.40E+01	1.40E+01	1.40E+01	1.40E+01	1.40E+01
COMPONENT DESIGN & ANALYSIS								
Lateral Suspension								
Geometric dimensions								
*pole width	m	lp.l	2.27E-02	1.70E-02	2.00E-02	2.27E-02	1.70E-02	2.00E-02
*window width	m	w.l	1.21E-01	1.09E-01	1.09E-01	1.21E-01	1.09E-01	1.09E-01
*window height	m	h.l	6.04E-02	5.45E-02	5.45E-02	6.04E-02	5.45E-02	5.45E-02
window width/height ratio	---		2.00E+00	2.00E+00	2.00E+00	2.00E+00	2.00E+00	2.00E+00
*coil packing factor	---	f.l	7.00E-01	7.00E-01	7.00E-01	7.00E-01	7.00E-01	7.00E-01
*air gap	m	H1x.l	1.00E-02	1.00E-02	8.00E-03	1.00E-02	1.00E-02	8.00E-03
*pole-coil clearance	m	z.l	5.08E-03	5.08E-03	5.08E-03	5.08E-03	5.08E-03	5.08E-03
*Number magnets required	---	nmag.l	4.00E+00	4.00E+00	4.00E+00	4.00E+00	4.00E+00	4.00E+00
magnet length	m	L.l	5.00E+00	9.94E+00	5.00E+00	5.00E+00	9.94E+00	5.00E+00
Magnet Design								
flux leakage coefficients								
fringing (across air gap)	---	nuf.l	8.46E-01	1.13E+00	7.67E-01	8.46E-01	1.13E+00	7.67E-01
leakage (between poles)	---	nul.l	1.84E-01	2.40E-01	1.70E-01	1.84E-01	2.40E-01	1.70E-01
total	---	nut.l	2.03E+00	2.37E+00	1.94E+00	2.03E+00	2.37E+00	1.94E+00
nominal field in air gap	T	B0.l	7.51E-01	6.15E-01	8.00E-01	7.51E-01	6.15E-01	8.00E-01
Force per magnet	N	Fpm.l	5.10E+04	5.10E+04	5.10E+04	5.10E+04	5.10E+04	5.10E+04
amp turns per magnet	A	NI.l	1.20E+04	9.79E+03	1.02E+04	1.20E+04	9.79E+03	1.02E+04
core mass (1 mag)	kg	Mcore.l	2.53E+02	3.32E+02	2.01E+02	2.53E+02	3.32E+02	2.01E+02
mass core + coil (4 mag)	kg	Mmag.l	1.55E+03	2.17E+03	1.23E+03	1.55E+03	2.17E+03	1.23E+03
Coil Design								
resist (1 magnet, 1 turn)	ohm	resc.l	1.77E-04	4.32E-04	2.20E-04	1.77E-04	4.32E-04	2.20E-04
St. state coil power(N/2 mags	W	qc_ss.l	1.76E+04	2.87E+04	1.58E+04	1.76E+04	2.87E+04	1.58E+04
Max. coil power (N/2 magnets)	W	qc.l	1.02E+05	1.66E+05	9.11E+04	1.02E+05	1.66E+05	9.11E+04
Steady state temperature rise	°C	Tm_ss.l	1.50E+02	1.41E+02	1.50E+02	1.50E+02	1.41E+02	1.50E+02
Short term temperature rise	°C	Tm_st.l	3.20E+01	3.31E+01	3.58E+01	3.20E+01	3.31E+01	3.58E+01
Maximum coil temperature	°C	Tc_max.l	2.00E+02	1.91E+02	2.00E+02	2.00E+02	1.91E+02	2.00E+02
mass(one coil)	kg	Mc.l	6.66E+01	1.05E+02	5.36E+01	6.66E+01	1.05E+02	5.36E+01
Rail Design								
rail thickness	m	tr.l	2.87E-02	2.13E-02	2.54E-02	2.87E-02	2.13E-02	2.54E-02
rail pole tip width (=tr)	m	lr.l	2.87E-02	2.13E-02	2.54E-02	2.87E-02	2.13E-02	2.54E-02
rail mass/length(two rails)	kg/m	mr.l	8.28E+01	5.36E+01	6.49E+01	8.28E+01	5.36E+01	6.49E+01
nominal rail flux density	T	Br.l	9.13E-01	8.70E-01	9.28E-01	9.13E-01	8.70E-01	9.28E-01
eff. freq. for eddy anal.	Hz	Fe.l	8.90E+00	4.48E+00	8.90E+00	5.90E+00	2.97E+00	5.90E+00
dB/dt amp. first harmonic	T/s	B1x.l	3.25E+01	1.56E+01	3.30E+01	2.15E+01	1.03E+01	2.19E+01
eddy current power	W	Pr.l	7.34E+03	1.21E+03	4.72E+03	3.23E+03	5.31E+02	2.07E+03
rms eddy amp turn								
(upper bound, 1 magnet)	A	NIe.l	8.36E+02	1.94E+02	5.97E+02	5.54E+02	1.29E+02	3.96E+02
Total power	W	P.l	2.49E+04	2.99E+04	2.05E+04	2.08E+04	2.92E+04	1.78E+04
Lift Magnet & Synchronous Motor - 2 guideway poles per vehicle pole								
Geometric Dimensions-on board magnet								
*Xpole thickness	m	tpv	2.00E-01	2.00E-01	2.00E-01	2.00E-01	2.00E-01	2.00E-01

Table F-5 (continued)

ElectroMagnetic Suspension III Optimized for operation at 89 m/s maximum speed

(Separate vertical suspension & synchronous motor, lateral suspension)

12/09/92

Asterisk (*) before description indicates input.

DESCRIPTION	UNITS	SYMBOL	89 m/s Optimization			89 m/s Optimization @ 59 m/s		
			DESIGN 1	DESIGN 2	DESIGN 3	DESIGN 1	DESIGN 2	DESIGN 3
			baseline	slim pole (3/4 b/l)	small gap (0.8 b/l)	baseline	slim pole (3/4 b/l)	small gap (0.8 b/l)
Xpole to pole distance	m	wcv	1.00E-01	1.00E-01	1.00E-01	1.00E-01	1.00E-01	1.00E-01
*pole face width	m	lpv	2.00E-01	2.00E-01	2.00E-01	2.00E-01	2.00E-01	2.00E-01
Xface to face dist.	m	wv	1.00E-01	1.00E-01	1.00E-01	1.00E-01	1.00E-01	1.00E-01
*window height	m	hv	8.00E-02	8.00E-02	8.00E-02	8.00E-02	8.00E-02	8.00E-02
*magnet depth	m	dv	1.00E-01	1.00E-01	1.00E-01	1.00E-01	1.00E-01	1.00E-01
*yoke thickness	m	tyv	8.50E-02	8.50E-02	8.50E-02	8.50E-02	8.50E-02	8.50E-02
*coil packing factor	---	ffv	7.00E-01	7.00E-01	7.00E-01	7.00E-01	7.00E-01	7.00E-01
*air gap	m	H1v	1.00E-02	1.00E-02	1.00E-02	1.00E-02	1.00E-02	1.00E-02
*pole-coil clearance	m	zv	5.08E-03	5.08E-03	5.08E-03	5.08E-03	5.08E-03	5.08E-03
*number laminations	---	nlammv	5.00E+00	5.00E+00	5.00E+00	5.00E+00	5.00E+00	5.00E+00
lamination thickness	m	tmv	2.00E-02	2.00E-02	2.00E-02	2.00E-02	2.00E-02	2.00E-02
*Number magnets required	---	nmagv	1.00E+01	1.00E+01	1.00E+01	1.00E+01	1.00E+01	1.00E+01
*number of poles per mag	---	nsegv	1.50E+01	1.40E+01	9.00E+00	1.50E+01	1.40E+01	9.00E+00
magnet length	m	Lv	4.50E+00	4.20E+00	2.70E+00	4.50E+00	4.20E+00	2.70E+00
Geometric Dimensions-guideway								
*pole width	m	lpg	8.00E-02	8.00E-02	8.00E-02	8.00E-02	8.00E-02	8.00E-02
*slot width	m	wg	2.00E-02	2.00E-02	2.00E-02	2.00E-02	2.00E-02	2.00E-02
XMagnet & guideway pole & slot dimensions?			OK	OK	OK	OK	OK	OK
XSlots and phases?			OK	OK	OK	OK	OK	OK
Guideway poles per mag. pole	---	Ng	2.00E+00	2.00E+00	2.00E+00	2.00E+00	2.00E+00	2.00E+00
*window height	m	hg	6.00E-02	6.00E-02	6.00E-02	6.00E-02	6.00E-02	6.00E-02
*magnet depth	m	dg	1.40E-01	1.40E-01	1.40E-01	1.40E-01	1.40E-01	1.40E-01
*coil packing factor	---	ffg	8.00E-01	8.00E-01	8.00E-01	8.00E-01	8.00E-01	8.00E-01
*number electrical phases	---	Np	3.00E+00	3.00E+00	3.00E+00	3.00E+00	3.00E+00	3.00E+00
*pole-coil clearance	m	zg	5.00E-03	5.00E-03	5.00E-03	5.00E-03	5.00E-03	5.00E-03
*number laminations	---	nlammg	4.00E+02	4.00E+02	4.00E+02	4.00E+02	4.00E+02	4.00E+02
lamination thickness	m	tmg	3.50E-04	3.50E-04	3.50E-04	3.50E-04	3.50E-04	3.50E-04
skin depth	m	delg	4.45E-04	4.45E-04	4.45E-04	5.47E-04	5.47E-04	5.47E-04
Magnet Design								
*amp turns/pole (mag seg)	A	Niv	5.40E+03	5.40E+03	5.29E+03	5.40E+03	5.40E+03	5.29E+03
flux leakage coefficients								
fringing (across air gap)	---	nufv	4.73E-01	4.73E-01	4.73E-01	4.73E-01	4.73E-01	4.73E-01
leakage (between poles)	---	nulv	1.94E-01	1.94E-01	1.94E-01	1.94E-01	1.94E-01	1.94E-01
total	---	nutv	1.67E+00	1.67E+00	1.67E+00	1.67E+00	1.67E+00	1.67E+00
Xnom. lift field in air gap	T	B0v	6.79E-01	6.79E-01	6.65E-01	6.79E-01	6.79E-01	6.65E-01
Xmax B in yoke @2 h1v, lift onl	T	Byv	1.86E+00	1.86E+00	1.83E+00	1.86E+00	1.86E+00	1.83E+00
check field in yoke			OK	OK	OK	OK	OK	OK
total lift force-Nmag magnets	N	Fv	4.40E+05	4.10E+05	2.53E+05	4.40E+05	4.10E+05	2.53E+05
Xcore mass (1 mag)	kg	Mcorev	4.85E+02	4.52E+02	2.91E+02	4.85E+02	4.52E+02	2.91E+02
mass core + coil (Nmagv mag)	kg	Mmagv	5.67E+03	5.30E+03	3.40E+03	5.67E+03	5.30E+03	3.40E+03
Vehicle Coil Design								
resist (1 magnet, 1 turn)	ohm	resv	1.17E-05	1.17E-05	1.17E-05	1.17E-05	1.17E-05	1.17E-05
coil ohmic power (N mag)	W	qv	5.13E+04	4.79E+04	2.95E+04	5.13E+04	4.79E+04	2.95E+04
temp. rise	deg C	Tv	1.55E+02	1.55E+02	1.48E+02	1.55E+02	1.55E+02	1.48E+02
mass (1 magnet)	kg	Mcoilv	8.28E+01	7.73E+01	4.97E+01	8.28E+01	7.73E+01	4.97E+01
Rail Coil Design								
rail yoke thickness	m	tyg	1.00E-01	1.00E-01	1.00E-01	1.00E-01	1.00E-01	1.00E-01
*amp turns per phase (0-P)	A	NIg	1.20E+03	1.20E+03	1.20E+03	1.20E+03	1.20E+03	1.20E+03
flux leakage coefficients								
fringing (across air gap)	---	nufg	4.73E-01	4.73E-01	4.73E-01	4.73E-01	4.73E-01	4.73E-01
leakage (between poles)	---	nulg	5.57E-01	5.57E-01	5.57E-01	5.57E-01	5.57E-01	5.57E-01
total	---	nutg	2.03E+00	2.03E+00	2.03E+00	2.03E+00	2.03E+00	2.03E+00

Table F-5 (continued)

ElectroMagnetic Suspension III Optimized for operation at 89 m/s maximum speed

(Separate vertical suspension & synchronous motor, lateral suspension)

12/09/92

Asterisk (*) before description indicates input.

DESCRIPTION	UNITS	SYMBOL	89 m/s Optimization DESIGN 1 baseline	89 m/s Optimization DESIGN 2 slim pole (3/4 b/l)	89 m/s Optimization DESIGN 3 small gap (0.8 b/l)	89 m/s Optimization @ 59 m/s DESIGN 1 baseline	89 m/s Optimization @ 59 m/s DESIGN 2 slim pole (3/4 b/l)	89 m/s Optimization @ 59 m/s DESIGN 3 small gap (0.8 b/l)
B in air gap-1 phase	T	B0g	1.51E-01	1.51E-01	1.51E-01	1.51E-01	1.51E-01	1.51E-01
max. field in poles								
from 1 phase & h1v	T	Bp1g	3.06E-01	3.06E-01	3.06E-01	3.06E-01	3.06E-01	3.06E-01
from lift @ 2*h1v	T	Bp2g	9.43E-01	9.43E-01	9.24E-01	9.43E-01	9.43E-01	9.24E-01
check B in pole			OK	OK	OK	OK	OK	OK
max. field in yoke								
from 1 phase & h1v	T	By1g	4.23E-01	4.23E-01	4.23E-01	4.23E-01	4.23E-01	4.23E-01
X from lift @ 2*h1v	T	By2g	7.55E-01	7.55E-01	7.39E-01	7.55E-01	7.55E-01	7.39E-01
check field in yoke			OK	OK	OK	OK	OK	OK
core mass (2 rails)	kg/m	Mcoreg	2.35E+02	2.35E+02	2.35E+02	2.35E+02	2.35E+02	2.35E+02
mass core + coil (2 rails)	kg/m	Mmagg	2.71E+02	2.71E+02	2.71E+02	2.71E+02	2.71E+02	2.71E+02
Rail Winding Design-1 segment is 3 pole pieces								
segments/km	1/km	nsegg	3.33E+03	3.33E+03	3.33E+03	3.33E+03	3.33E+03	3.33E+03
resist (1 phase)	ohm/km	resg	3.40E-01	3.40E-01	3.40E-01	3.40E-01	3.40E-01	3.40E-01
ohmic power (3 phase, 2rail)	W/km	Pohm	1.47E+06	1.47E+06	1.47E+06	1.47E+06	1.47E+06	1.47E+06
temp. rise	deg C	Tg	9.51E+01	9.51E+01	9.51E+01	9.51E+01	9.51E+01	9.51E+01
Xmass	kg/km	Mcoilg	3.57E+04	3.57E+04	3.57E+04	3.57E+04	3.57E+04	3.57E+04
freq. at nom speed	Hz	fs	1.48E+02	1.48E+02	1.48E+02	9.83E+01	9.83E+01	9.83E+01
track without vehicle								
Xtrack self L (1 rail)	H/km	Laax	4.12E-03	4.12E-03	4.12E-03	4.12E-03	4.12E-03	4.12E-03
rail reactive impedance	ohms/km	Zlt	3.84E+00	3.84E+00	3.84E+00	2.54E+00	2.54E+00	2.54E+00
mutual inductance	H/km	Mabt	0.00E+00	0.00E+00	0.00E+00	0.00E+00	0.00E+00	0.00E+00
voltage/phase/turn	V/km	Vt	4.62E+03	4.62E+03	4.62E+03	3.08E+03	3.08E+03	3.08E+03
Xmagnetic field in yoke	T	Bt	5.20E-01	5.20E-01	5.09E-01	5.20E-01	5.20E-01	5.09E-01
dB/dt amp. first harmonic	T/s	Btx	3.08E+02	3.08E+02	3.02E+02	2.04E+02	2.04E+02	2.00E+02
guideway eddy losses	W/km	Pteddy	3.34E+04	3.34E+04	3.21E+04	1.47E+04	1.47E+04	1.41E+04
Xreact. power (3ph-2 rails)	VA/km	Pzg	1.66E+07	1.66E+07	1.66E+07	1.11E+07	1.11E+07	1.11E+07
PROPULSIVE FORCE CALCULATIONS								
Inductances								
Xinductance-self L field	H/(2 seg)	Lbasic	5.92E-06	5.92E-06	5.92E-06	5.92E-06	5.92E-06	5.92E-06
X stator self L-mean value	H/(2 seg)	Laa	7.04E-06	7.04E-06	7.04E-06	7.04E-06	7.04E-06	7.04E-06
stator self L-second harm.	H/(2 seg)	Laa2	0.00E+00	0.00E+00	0.00E+00	0.00E+00	0.00E+00	0.00E+00
mutual-first harmonic	H/(2 seg)	Mvg	6.22E-06	6.22E-06	6.22E-06	6.22E-06	6.22E-06	6.22E-06
stator mutual-mean	H/(2 seg)	Mab	1.24E-06	1.24E-06	1.24E-06	1.24E-06	1.24E-06	1.24E-06
stator mutual-second harm.	H/(2 seg)	Mab2	3.64E-06	3.64E-06	3.64E-06	3.64E-06	3.64E-06	3.64E-06
Propulsive forces-maximum values								
design force (Mvg calc)	N	Fl	4.75E+04	4.43E+04	2.79E+04	4.75E+04	4.43E+04	2.79E+04
reluctance force (Mab2)	N		3.08E+03	2.88E+03	1.85E+03	3.08E+03	2.88E+03	1.85E+03
rail self induct (Laa2)	N		0.00E+00	0.00E+00	0.00E+00	0.00E+00	0.00E+00	0.00E+00
hunting stiffness	N/m	Khunt	4.97E+05	4.64E+05	2.92E+05	4.97E+05	4.64E+05	2.92E+05
hunting freq.	Hz	fhunt	5.61E-01	5.42E-01	4.30E-01	5.61E-01	5.42E-01	4.30E-01
Xmax. propel (B field)	N		5.06E+04	4.72E+04	2.97E+04	5.06E+04	4.72E+04	2.97E+04
Losses from eddy currents								
nom. rail B from vehicle	T	Br	2.00E+00	2.00E+00	1.96E+00	2.00E+00	2.00E+00	1.96E+00
eff. freq. for eddy anal.	Hz	Fe	1.48E+02	1.48E+02	1.48E+02	9.83E+01	9.83E+01	9.83E+01
dB/dt amp. first harmonic	T/s	B1x	1.19E+03	1.19E+03	1.16E+03	7.86E+02	7.86E+02	7.70E+02
eddy current power	W	Pr	1.11E+04	1.04E+04	6.41E+03	4.90E+03	4.57E+03	2.82E+03
rms eddy amp turn								
(upper bound, 1 magnet)	A	Nle	3.80E+00	3.80E+00	3.72E+00	2.52E+00	2.52E+00	2.47E+00

Table F-5 (continued)

ElectroMagnetic Suspension III

Optimized for operation at 89 m/s maximum speed

(Separate vertical suspension & synchronous motor, lateral suspension)

12/09/92

Asterisk (*) before description indicates input.

DESCRIPTION	UNITS	SYMBOL	89 m/s Optimization			89 m/s Optimization @ 59 m/s		
			DESIGN 1	DESIGN 2	DESIGN 3	DESIGN 1	DESIGN 2	DESIGN 3
			baseline	slim pole (3/4 b/l)	small gap (0.8 b/l)	baseline	slim pole (3/4 b/l)	small gap (0.8 b/l)
(ohmic+eddy)/wind power	%		4.10%	3.83%	2.36%	12.66%	11.82%	7.29%
(magnet+coil)/vehicle wt.	%		14.18%	13.24%	8.51%	14.18%	13.24%	8.51%
eddy/lift amp-T (up. bound)	%		0.04%	0.04%	0.04%	0.02%	0.02%	0.02%
wind drag/weight	%		4.36%	4.36%	4.36%	1.92%	1.92%	1.92%
ratio propel F/weight	%		12.11%	11.30%	7.12%	1.21E-01	1.13E-01	7.12E-02
ratio propel/lift	%		10.80%	10.80%	11.02%	1.08E-01	1.08E-01	1.10E-01
ratio lift/weight	%		112.17%	104.70%	64.59%	1.12E+00	1.05E+00	6.46E-01
ratio mag. weight/lift	%		12.64%	12.64%	13.18%	1.26E-01	1.26E-01	1.32E-01
track losses/wind drag	%/km		98.54%	98.54%	98.46%	334.03%	334.03%	333.90%
AUXILIARY CALCULATIONS								
Combined lift magnets & synchronous motor								
Permeances								
permeances-vehicle magnet		Pfv	7.57E-01	7.57E-01	7.57E-01	7.57E-01	7.57E-01	7.57E-01
useful 1 air gap		Puv	1.60E+00	1.60E+00	1.60E+00	1.60E+00	1.60E+00	1.60E+00
X		Plv	3.11E-01	3.11E-01	3.11E-01	3.11E-01	3.11E-01	3.11E-01
pole useful area	m^2	Auv	1.60E-02	1.60E-02	1.60E-02	1.60E-02	1.60E-02	1.60E-02
Xcoil dimensions-1 coil on 1 pole		lcv	7.57E-01	7.57E-01	7.57E-01	7.57E-01	7.57E-01	7.57E-01
X 1 coil on 1 pole		acv	2.62E-03	2.62E-03	2.62E-03	2.62E-03	2.62E-03	2.62E-03
X 1 segments-1 pole		adisv	1.58E-01	1.58E-01	1.58E-01	1.58E-01	1.58E-01	1.58E-01
permeances-guideway windings		Pfg	7.57E-01	7.57E-01	7.57E-01	7.57E-01	7.57E-01	7.57E-01
vehicle in place		Pug	1.60E+00	1.60E+00	1.60E+00	1.60E+00	1.60E+00	1.60E+00
		Plg	8.92E-01	8.92E-01	8.92E-01	8.92E-01	8.92E-01	8.92E-01
X no vehicle magnets		Pl2g	5.37E-01	5.37E-01	5.37E-01	5.37E-01	5.37E-01	5.37E-01
Coil dimensions						0.00E+00	0.00E+00	0.00E+00
coil dimen.-1 phase-1 turn-3 pole pieces		lcg	9.11E-01	9.11E-01	9.11E-01	9.11E-01	9.11E-01	9.11E-01
1 -coil but 2 coils per slot		acg	2.20E-04	2.20E-04	2.20E-04	2.20E-04	2.20E-04	2.20E-04
1 seg. 3 pole pieces		adisg	1.66E-01	1.66E-01	1.66E-01	1.66E-01	1.66E-01	1.66E-01
Guidance Magnets								
Permeances								
Air gap fringing permeance/length		Pf.l	1.92E+00	1.92E+00	1.92E+00	1.92E+00	1.92E+00	1.92E+00
Ideal air gap permeance/length		Pu.l	2.27E+00	1.70E+00	2.50E+00	2.27E+00	1.70E+00	2.50E+00
Inter-pole leakage perm./length		Pl.l	4.17E-01	4.08E-01	4.27E-01	4.17E-01	4.08E-01	4.27E-01
Coil dimensions								
Mean turn length	m	lc.l	1.02E+01	2.01E+01	1.02E+01	1.02E+01	2.01E+01	1.02E+01
Coil crossectional area	m^2	ac.l	2.34E-03	1.89E-03	1.89E-03	2.34E-03	1.89E-03	1.89E-03
Coil Surface area	m^2	adis.l	4.19E+00	7.27E+00	3.76E+00	4.19E+00	7.27E+00	3.76E+00
EMS III Summary								
Weight on Vehicle								
Lift Magnets/LSM	kg		5.67E+03	5.30E+03	3.40E+03	5.67E+03	5.30E+03	3.40E+03
Guidance Magnets	kg		1.55E+03	2.17E+03	1.23E+03	1.55E+03	2.17E+03	1.23E+03
Total	kg		7.22E+03	7.47E+03	4.64E+03	7.22E+03	7.47E+03	4.64E+03
Magnet Weight/Vehicle Weight	%		18.05%	18.67%	11.59%	18.05%	18.67%	11.59%
Weight on Guideway								
Lift Magnets/LSM	kg/m		2.71E+02	2.71E+02	2.71E+02	2.71E+02	2.71E+02	2.71E+02
Guidance Magnets	kg/m		8.28E+01	5.36E+01	6.49E+01	8.28E+01	5.36E+01	6.49E+01
Total	kg/m		3.54E+02	3.25E+02	3.36E+02	3.54E+02	3.25E+02	3.36E+02
Vehicle Real Power								
Ohmic Power Dissipation								
Lift Magnets/LSM	W		5.13E+04	4.79E+04	2.95E+04	5.13E+04	4.79E+04	2.95E+04
Guidance Magnets	W		1.76E+04	2.87E+04	1.58E+04	1.76E+04	2.87E+04	1.58E+04

Table F-5 (continued)

ElectroMagnetic Suspension III Optimized for operation at 89 m/s maximum speed

(Separate vertical suspension & synchronous motor, lateral suspension)

12/09/92

Asterisk (*) before description indicates input.

DESCRIPTION	UNITS	SYMBOL	89 m/s Optimization			89 m/s Optimization @ 59 m/s		
			DESIGN 1	DESIGN 2	DESIGN 3	DESIGN 1	DESIGN 2	DESIGN 3
			baseline	slim pole (3/4 b/l)	small gap (0.8 b/l)	baseline	slim pole (3/4 b/l)	small gap (0.8 b/l)
Total Ohmic Power	W		6.88E+04	7.65E+04	4.53E+04	6.88E+04	7.65E+04	4.53E+04
Eddy current Power Dissipation								
Lift Magnets/LSM	W		1.11E+04	1.04E+04	6.41E+03	4.90E+03	4.57E+03	2.82E+03
Guidance Magnets	W		7.34E+03	1.21E+03	4.72E+03	3.23E+03	5.31E+02	2.07E+03
Total eddy current Power	W		1.85E+04	1.16E+04	1.11E+04	8.12E+03	5.10E+03	4.89E+03
Total Vehicle Power Dissipatic	W		8.73E+04	8.81E+04	5.64E+04	7.70E+04	8.16E+04	5.02E+04
Electrical Power/Aero Drag Powe	%		5.73%	5.79%	3.71%	17.35%	18.40%	11.31%
Guideway Power								
Real Power Dissipation								
Guideway LSM Winding	kW/m		1.47E+00	1.47E+00	1.47E+00	1.47E+00	1.47E+00	1.47E+00
Total	kW/m		1.47E+00	1.47E+00	1.47E+00	1.47E+00	1.47E+00	1.47E+00
Reactive Input Power								
Linear Synchronous Motor	kVA/m		1.66E+01	1.66E+01	1.66E+01	1.11E+01	1.11E+01	1.11E+01
Total	kVA/m		1.66E+01	1.66E+01	1.66E+01	1.11E+01	1.11E+01	1.11E+01

Table F-6 Complete EMS III Spreadsheet; Design optimized for operation at 134 m/s
Separate guidance magnet,Combined lift magnet and LSM

ElectroMagnetic Suspension III Optimized for operation at 134 m/s maximum speed

(Separate vertical suspension & synchronous motor, lateral suspension)

Asterisk (*) before description indicates input.

DESCRIPTION	UNITS	SYMBOL	134 m/s Optimization			134 m/s Optimization @ 89 m/s		
			DESIGN 1	DESIGN 2	DESIGN 3	DESIGN 1	DESIGN 2	DESIGN 3
			baseline (b/l)	slim pole (3/4 b/l)	small gap (0.8 b/l)	baseline (b/l)	slim pole (3/4 b/l)	small gap (0.8 b/l)
VEHICLE PARAMETERS								
<u>Design Parameters</u>								
*Vehicle mass	kg	m	4.00E+04	4.00E+04	4.00E+04	4.00E+04	4.00E+04	4.00E+04
*Vehicle length	m	l_vehicle	3.00E+01	3.00E+01	3.00E+01	3.00E+01	3.00E+01	3.00E+01
*Design speed	m/s	V	1.34E+02	1.34E+02	1.34E+02	8.90E+01	8.90E+01	8.90E+01
*frontal area	m^2	Af	1.20E+01	1.20E+01	1.20E+01	1.20E+01	1.20E+01	1.20E+01
*air density	kg/m^3	roair	1.20E+00	1.20E+00	1.20E+00	1.20E+00	1.20E+00	1.20E+00
*drag coefficient	---	Cd	3.00E-01	3.00E-01	3.00E-01	3.00E-01	3.00E-01	3.00E-01
wind drag force	N	Fd	3.88E+04	3.88E+04	3.88E+04	1.71E+04	1.71E+04	1.71E+04
wind drag power	W	Pd	5.20E+06	5.20E+06	5.20E+06	1.52E+06	1.52E+06	1.52E+06
*Max. Lift Force(@Max disp.)	g	max_Fz	1.10E+00	1.10E+00	1.10E+00	1.10E+00	1.10E+00	1.10E+00
*Max. Lateral Force(")(cont.)	g	max_F.l	2.60E-01	2.60E-01	2.60E-01	2.60E-01	2.60E-01	2.60E-01
*Max. Lateral Force(")(short)	g	max_sF.l	4.20E-01	4.20E-01	4.20E-01	4.20E-01	4.20E-01	4.20E-01
*Time of Max. (short)Lateral F	sec	t_max	5.00E+00	5.00E+00	5.00E+00	5.00E+00	5.00E+00	5.00E+00
*Maximum ambient temp.	°C	maxTamb	5.00E+01	5.00E+01	5.00E+01	5.00E+01	5.00E+01	5.00E+01
CONSTANTS								
*air permeability	N/A^2	mu	1.26E-06	1.26E-06	1.26E-06	1.26E-06	1.26E-06	1.26E-06
<u>General</u>								
<u>Construction materials</u>								
<u>Lateral Suspension</u>								
*rail			steel	steel	steel	steel	steel	steel
*magnet			2V Perm.	2V Perm.	2V Perm.	2V Perm.	2V Perm.	2V Perm.
*coil			alum.	alum.	alum.	alum.	alum.	alum.
<u>Materials properties</u>								
mass density								
*rail	kg/m^3	ror	7.51E+03	7.51E+03	7.51E+03	7.51E+03	7.51E+03	7.51E+03
*magnet	kg/m^3	rom	7.78E+03	7.78E+03	7.78E+03	7.78E+03	7.78E+03	7.78E+03
*coil	kg/m^3	roc	2.78E+03	2.78E+03	2.78E+03	2.78E+03	2.78E+03	2.78E+03
maximum flux density								
*rail	T	Bsatr	1.60E+00	1.60E+00	1.60E+00	1.60E+00	1.60E+00	1.60E+00
*magnet	T	Bsatm	2.30E+00	2.30E+00	2.30E+00	2.30E+00	2.30E+00	2.30E+00
*Saturation Safety Factor(<1)	---	SF	1.00E+00	1.00E+00	1.00E+00	1.00E+00	1.00E+00	1.00E+00
Electrical resistivity								
*rail @20 deg C	ohm-m	rr	4.06E-07	4.06E-07	4.06E-07	4.06E-07	4.06E-07	4.06E-07
*coil @140 deg C	ohm-m	rc_	4.06E-08	4.06E-08	4.06E-08	4.06E-08	4.06E-08	4.06E-08
*coil @220 deg C	ohm-m	rc_220						
Thermal								
*magnet heat transfer coef.	W/C-m^2	k	1.40E+01	1.40E+01	1.40E+01	1.40E+01	1.40E+01	1.40E+01
*Coil Specific heat	J/(kg°C)	cp	1.19E+02	1.19E+02	1.19E+02	1.19E+02	1.19E+02	1.19E+02
*Maximum wire insulation tem	°C	maxTins	2.00E+02	2.00E+02	2.00E+02	2.00E+02	2.00E+02	2.00E+02
<u>Construction materials</u>								
<u>Lift Magnet & Linear Synchronous Motor</u>								
*rail			steel	steel	steel	steel	steel	steel
*rail windings			copper	copper	copper	copper	copper	copper
*magnet			2V Perm.	2V Perm.	2V Perm.	2V Perm.	2V Perm.	2V Perm.
*magnet coil			aluminum	aluminum	aluminum	aluminum	aluminum	aluminum
Densities								
*rail	kg/m^3	rogm	7.51E+03	7.51E+03	7.51E+03	7.51E+03	7.51E+03	7.51E+03
*rail windings	kg/m^3	rogc	8.90E+03	8.90E+03	8.90E+03	8.90E+03	8.90E+03	8.90E+03
*magnet	kg/m^3	rovm	7.78E+03	7.78E+03	7.78E+03	7.78E+03	7.78E+03	7.78E+03
*coil	kg/m^3	rovc	2.78E+03	2.78E+03	2.78E+03	2.78E+03	2.78E+03	2.78E+03
Maximum flux densities								
*rail	T	bsatg	1.60E+00	1.60E+00	1.60E+00	1.60E+00	1.60E+00	1.60E+00
*magnet	T	bsatv	2.30E+00	2.30E+00	2.30E+00	2.30E+00	2.30E+00	2.30E+00

Table F-6 (continued)

ElectroMagnetic Suspension III Optimized for operation at 134 m/s maximum speed

(Separate vertical suspension & synchronous motor, lateral suspension)

Asterisk (*) before description indicates input.

DESCRIPTION	UNITS	SYMBOL	134 m/s Optimization			134 m/s Optimization @ 89 m/s		
			DESIGN 1	DESIGN 2	DESIGN 3	DESIGN 1	DESIGN 2	DESIGN 3
			baseline (b/l)	slim pole (3/4 b/l)	small gap (0.8 b/l)	baseline (b/l)	slim pole (3/4 b/l)	small gap (0.8 b/l)
Rail	---	mug	3.50E+03	3.50E+03	3.50E+03	3.50E+03	3.50E+03	3.50E+03
Electrical Resistivity								
*rail @20 deg C	ohm-m	rmg	4.06E-07	4.06E-07	4.06E-07	4.06E-07	4.06E-07	4.06E-07
*vehicle coil @140 deg C	ohm-m	rcv	4.06E-08	4.06E-08	4.06E-08	4.06E-08	4.06E-08	4.06E-08
*rail coil *140 deg c	ohm-m	rcg	2.46E-08	2.46E-08	2.46E-08	2.46E-08	2.46E-08	2.46E-08
Thermal								
*magnet heat transfer coeffic	W/C-m^2	kv	1.40E+01	1.40E+01	1.40E+01	1.40E+01	1.40E+01	1.40E+01
*rail heat transfer coef.	W/C-m^2	kg	1.40E+01	1.40E+01	1.40E+01	1.40E+01	1.40E+01	1.40E+01
COMPONENT DESIGN & ANALYSIS								
Lateral Suspension								
Geometric dimensions								
*pole width	m	lp.l	2.80E-02	2.10E-02	2.48E-02	2.80E-02	2.10E-02	2.48E-02
*window width	m	w.l	1.26E-01	1.13E-01	1.14E-01	1.26E-01	1.13E-01	1.14E-01
*window height	m	h.l	6.32E-02	5.64E-02	5.69E-02	6.32E-02	5.64E-02	5.69E-02
Window width/height ratio	---		2.00E+00	2.00E+00	2.00E+00	2.00E+00	2.00E+00	2.00E+00
*coil packing factor	---	f.l	7.00E-01	7.00E-01	7.00E-01	7.00E-01	7.00E-01	7.00E-01
*air gap	m	H1x.l	1.00E-02	1.00E-02	8.00E-03	1.00E-02	1.00E-02	8.00E-03
*pole-coil clearance	m	z.l	5.08E-03	5.08E-03	5.08E-03	5.08E-03	5.08E-03	5.08E-03
*Number magnets required	---	nmag.l	4.00E+00	4.00E+00	4.00E+00	4.00E+00	4.00E+00	4.00E+00
magnet length	m	L.l	5.00E+00	9.68E+00	5.00E+00	5.00E+00	9.68E+00	5.00E+00
Magnet length/vehicle length			OK	OK	OK	OK	OK	OK
Magnet Design								
flux leakage coefficients								
fringing (across air gap)	---	nuf.l	6.87E-01	9.15E-01	6.20E-01	6.87E-01	9.15E-01	6.20E-01
leakage (between poles)	---	nul.l	1.51E-01	1.96E-01	1.39E-01	1.51E-01	1.96E-01	1.39E-01
total	---	nut.l	1.84E+00	2.11E+00	1.76E+00	1.84E+00	2.11E+00	1.76E+00
nominal field in air gap	T	B0.l	8.60E-01	7.14E-01	9.14E-01	8.60E-01	7.14E-01	9.14E-01
Force per magnet	N	Fpm.l	8.23E+04	8.23E+04	8.23E+04	8.23E+04	8.23E+04	8.23E+04
amp turns per magnet	A	NI.l	1.37E+04	1.14E+04	1.16E+04	1.37E+04	1.14E+04	1.16E+04
core mass (1 mag)	kg	Mcore.l	3.36E+02	4.23E+02	2.67E+02	3.36E+02	4.23E+02	2.67E+02
mass core + coil (4 mag)	kg	Mmag.l	1.93E+03	2.58E+03	1.54E+03	1.93E+03	2.58E+03	1.54E+03
Coil Design								
resist (1 magnet, 1 turn)	ohm	resc.l	1.62E-04	3.92E-04	2.01E-04	1.62E-04	3.92E-04	2.01E-04
St. state coil power(N/2 mags	W	qc_ss.l	1.88E+04	3.13E+04	1.68E+04	1.88E+04	3.13E+04	1.68E+04
Max. coil power (N/2 magnets)	W	qc.l	1.21E+05	2.02E+05	1.09E+05	1.21E+05	2.02E+05	1.09E+05
Steady state temperature rise	°C	Tm_ss.l	1.50E+02	1.50E+02	1.50E+02	1.50E+02	1.50E+02	1.50E+02
Short term temperature rise	°C	Tm_st.l	3.48E+01	3.85E+01	3.89E+01	3.48E+01	3.85E+01	3.89E+01
Maximum coil temperature	°C	Tc_max.l	2.00E+02	2.00E+02	2.00E+02	2.00E+02	2.00E+02	2.00E+02
mass(one coil)	kg	Mc.l	7.33E+01	1.10E+02	5.88E+01	7.33E+01	1.10E+02	5.88E+01
Rail Design								
rail thickness	m	tr.l	3.57E-02	2.65E-02	3.17E-02	3.57E-02	2.65E-02	3.17E-02
rail pole tip width (=tr)	m	lr.l	3.57E-02	2.65E-02	3.17E-02	3.57E-02	2.65E-02	3.17E-02
rail mass/length(two rails)	kg/m	mr.l	1.13E+02	7.17E+01	8.87E+01	1.13E+02	7.17E+01	8.87E+01
nominal rail flux density	T	Br.l	8.95E-01	8.52E-01	9.10E-01	8.95E-01	8.52E-01	9.10E-01
eff. freq. for eddy anal.	Hz	Fe.l	1.34E+01	6.92E+00	1.34E+01	8.90E+00	4.59E+00	8.90E+00
dB/dt amp. first harmonic	T/s	B1x.l	4.80E+01	2.36E+01	4.88E+01	3.19E+01	1.57E+01	3.24E+01
eddy current power	W	Pr.l	3.31E+04	5.49E+03	2.16E+04	1.46E+04	2.42E+03	9.52E+03
rms eddy amp turn (upper bound, 1 magnet)	A	NIe.l	2.05E+03	4.82E+02	1.48E+03	1.36E+03	3.20E+02	9.83E+02
Total power	W	P.l	5.19E+04	3.68E+04	3.84E+04	3.34E+04	3.37E+04	2.63E+04
Lift Magnet & Synchronous Motor - 2 guideway poles per vehicle pole								
Geometric Dimensions-on board magnet								

Table F-6 (continued)

ElectroMagnetic Suspension III Optimized for operation at 134 m/s maximum speed

(Separate vertical suspension & synchronous motor, lateral suspension)

Asterisk (*) before description indicates input.

DESCRIPTION	UNITS	SYMBOL	134 m/s Optimization			134 m/s Optimization @ 89 m/s		
			DESIGN 1	DESIGN 2	DESIGN 3	DESIGN 1	DESIGN 2	DESIGN 3
			baseline (b/l)	slim pole (3/4 b/l)	small gap (0.8 b/l)	baseline (b/l)	slim pole (3/4 b/l)	small gap (0.8 b/l)
*Xpole thickness	m	tpv	2.00E-01	2.00E-01	2.00E-01	2.00E-01	2.00E-01	2.00E-01
Xpole to pole distance	m	wcv	1.00E-01	1.00E-01	1.00E-01	1.00E-01	1.00E-01	1.00E-01
*pole face width	m	lpv	2.00E-01	2.00E-01	2.00E-01	2.00E-01	2.00E-01	2.00E-01
Xface to face dist.	m	wv	1.00E-01	1.00E-01	1.00E-01	1.00E-01	1.00E-01	1.00E-01
*window height	m	hv	8.00E-02	8.00E-02	8.00E-02	8.00E-02	8.00E-02	8.00E-02
*magnet depth	m	dv	1.00E-01	7.50E-02	1.00E-01	1.00E-01	7.50E-02	1.00E-01
*yoke thickness	m	tyv	8.50E-02	8.50E-02	8.50E-02	8.50E-02	8.50E-02	8.50E-02
*coil packing factor	---	ffv	7.00E-01	7.00E-01	7.00E-01	7.00E-01	7.00E-01	7.00E-01
*air gap	m	H1v	1.00E-02	1.00E-02	8.00E-03	1.00E-02	1.00E-02	8.00E-03
*pole-coil clearance	m	zv	5.08E-03	5.08E-03	5.08E-03	5.08E-03	5.08E-03	5.08E-03
*number laminations	---	nlammv	5.00E+00	5.00E+00	5.00E+00	5.00E+00	5.00E+00	5.00E+00
lamination thickness	m	tmv	2.00E-02	1.50E-02	2.00E-02	2.00E-02	1.50E-02	2.00E-02
*Number magnets required	---	nmagv	1.00E+01	1.00E+01	1.00E+01	1.00E+01	1.00E+01	1.00E+01
*number of poles per mag	---	nsegv	1.40E+01	1.90E+01	1.00E+01	1.40E+01	1.90E+01	1.00E+01
magnet length	m	Lv	4.20E+00	5.70E+00	3.00E+00	4.20E+00	5.70E+00	3.00E+00
Geometric Dimensions-guideway								
*pole width	m	lpg	8.00E-02	8.00E-02	8.00E-02	8.00E-02	8.00E-02	8.00E-02
*slot width	m	wg	2.00E-02	2.00E-02	2.00E-02	2.00E-02	2.00E-02	2.00E-02
XMagnet & guideway pole & slot dimensions?			OK	OK	OK	OK	OK	OK
XSlots and phases?			OK	OK	OK	OK	OK	OK
Guideway poles per mag. pole	---	Ng	2.00E+00	2.00E+00	2.00E+00	2.00E+00	2.00E+00	2.00E+00
*window height	m	hg	6.00E-02	6.00E-02	6.00E-02	6.00E-02	6.00E-02	6.00E-02
*magnet depth	m	dg	1.40E-01	1.15E-01	1.32E-01	1.40E-01	1.15E-01	1.32E-01
*coil packing factor	---	ffg	8.00E-01	8.00E-01	8.00E-01	8.00E-01	8.00E-01	8.00E-01
*number electrical phases	---	Np	3.00E+00	3.00E+00	3.00E+00	3.00E+00	3.00E+00	3.00E+00
*pole-coil clearance	m	zg	5.00E-03	5.00E-03	5.00E-03	5.00E-03	5.00E-03	5.00E-03
*number laminations	---	nlammg	4.00E+02	4.00E+02	4.00E+02	4.00E+02	4.00E+02	4.00E+02
lamination thickness	m	tmg	3.50E-04	2.88E-04	3.30E-04	3.50E-04	2.88E-04	3.30E-04
skin depth	m	delg	3.63E-04	3.63E-04	3.63E-04	4.45E-04	4.45E-04	4.45E-04
Magnet Design								
*amp turns/pole (mag seg)	A	Niv	5.40E+03	5.40E+03	5.29E+03	5.40E+03	5.40E+03	5.29E+03
flux leakage coefficients								
fringing (across air gap)	---	nufv	4.73E-01	5.51E-01	3.72E-01	4.73E-01	5.51E-01	3.72E-01
leakage (between poles)	---	nulv	1.94E-01	2.30E-01	1.60E-01	1.94E-01	2.30E-01	1.60E-01
total	---	nutv	1.67E+00	1.78E+00	1.53E+00	1.67E+00	1.78E+00	1.53E+00
Xnom. lift field in air gap	T	B0v	6.79E-01	6.79E-01	8.31E-01	6.79E-01	6.79E-01	8.31E-01
Xmax B in yoke @2 h1v, lift onl	T	Byv	1.86E+00	2.04E+00	2.02E+00	1.86E+00	2.04E+00	2.02E+00
check field in yoke			OK	OK	OK	OK	OK	OK
total lift force-Nmag magnets	N	Fv	4.10E+05	4.18E+05	4.40E+05	4.10E+05	4.18E+05	4.40E+05
Xcore mass (1 mag)	kg	Mcorev	4.52E+02	4.60E+02	3.23E+02	4.52E+02	4.60E+02	3.23E+02
mass core + coil (Nmagv mag)	kg	Mmagv	5.30E+03	5.58E+03	3.78E+03	5.30E+03	5.58E+03	3.78E+03
Vehicle Coil Design								
resist (1 magnet, 1 turn)	ohm	resv	1.17E-05	1.09E-05	1.17E-05	1.17E-05	1.09E-05	1.17E-05
coil ohmic power (N mag)	W	qv	4.79E+04	6.07E+04	3.28E+04	4.79E+04	6.07E+04	3.28E+04
temp. rise	deg C	Tv	1.55E+02	1.53E+02	1.48E+02	1.55E+02	1.53E+02	1.48E+02
mass (1 magnet)	kg	Mcoilv	7.73E+01	9.79E+01	5.52E+01	7.73E+01	9.79E+01	5.52E+01
Rail Coil Design								
rail yoke thickness	m	tyg	1.00E-01	1.00E-01	1.00E-01	1.00E-01	1.00E-01	1.00E-01
*amp turns per phase (0-P)	A	NIg	1.20E+03	1.20E+03	1.20E+03	1.20E+03	1.20E+03	1.20E+03
flux leakage coefficients								
fringing (across air gap)	---	nufg	4.73E-01	5.51E-01	3.72E-01	4.73E-01	5.51E-01	3.72E-01
leakage (between poles)	---	nulg	5.57E-01	6.39E-01	4.43E-01	5.57E-01	6.39E-01	4.43E-01

Table F-6 (continued)

ElectroMagnetic Suspension III Optimized for operation at 134 m/s maximum speed

(Separate vertical suspension & synchronous motor, lateral suspension)

Asterisk (*) before description indicates input.

DESCRIPTION	UNITS	SYMBOL	134 m/s Optimization			134 m/s Optimization @ 89 m/s		
			DESIGN 1	DESIGN 2	DESIGN 3	DESIGN 1	DESIGN 2	DESIGN 3
			baseline (b/l)	slim pole (3/4 b/l)	small gap (0.8 b/l)	baseline (b/l)	slim pole (3/4 b/l)	small gap (0.8 b/l)
total	---	nutg	2.03E+00	2.19E+00	1.81E+00	2.03E+00	2.19E+00	1.81E+00
B in air gap-1 phase	T	B0g	1.51E-01	1.51E-01	1.88E-01	1.51E-01	1.51E-01	1.88E-01
max. field in poles								
from 1 phase & h1v	T	Bp1g	3.06E-01	3.30E-01	3.42E-01	3.06E-01	3.30E-01	3.42E-01
from lift @ 2*h1v	T	Bp2g	9.43E-01	9.30E-01	1.10E+00	9.43E-01	9.30E-01	1.10E+00
check B in pole			OK	OK	SATURATE	OK	OK	SATURATE
max. field in yoke								
from 1 phase & h1v	T	By1g	4.23E-01	4.51E-01	4.81E-01	4.23E-01	4.51E-01	4.81E-01
X from lift @ 2*h1v	T	By2g	7.55E-01	7.44E-01	8.78E-01	7.55E-01	7.44E-01	8.78E-01
check field in yoke			OK	OK	OK	OK	OK	OK
core mass (2 rails)	kg/m	Mcoreg	2.35E+02	1.93E+02	2.22E+02	2.35E+02	1.93E+02	2.22E+02
mass core + coil (2 rails)	kg/m	Mmagg	2.71E+02	2.27E+02	2.57E+02	2.71E+02	2.27E+02	2.57E+02
Rail Winding Design-1 segment is 3 pole pieces								
segments/km	1/km	nsegg	3.33E+03	3.33E+03	3.33E+03	3.33E+03	3.33E+03	3.33E+03
resist (1 phase)	ohm/km	resg	3.40E-01	3.21E-01	3.34E-01	3.40E-01	3.21E-01	3.34E-01
ohmic power (3 phase, 2rail)	W/km	Pohm	1.47E+06	1.39E+06	1.44E+06	1.47E+06	1.39E+06	1.44E+06
temp. rise	deg C	Tg	9.51E+01	9.46E+01	9.50E+01	9.51E+01	9.46E+01	9.50E+01
Xmass	kg/km	Mcoilg	3.57E+04	3.37E+04	3.51E+04	3.57E+04	3.37E+04	3.51E+04
freq. at nom speed	Hz	fs	2.23E+02	2.23E+02	2.23E+02	1.48E+02	1.48E+02	1.48E+02
track without vehicle								
Xtrack self L (1 rail)	H/km	Laax	4.12E-03	3.45E-03	3.98E-03	4.12E-03	3.45E-03	3.98E-03
rail reactive impedance	ohms/km	Zlt	5.78E+00	4.85E+00	5.58E+00	3.84E+00	3.22E+00	3.71E+00
mutual inductance	H/km	Mabt	0.00E+00	0.00E+00	0.00E+00	0.00E+00	0.00E+00	0.00E+00
voltage/phase/turn	V/km	Vt	6.95E+03	5.83E+03	6.71E+03	4.62E+03	3.88E+03	4.47E+03
Xmagnetic field in yoke	T	Bt	5.20E-01	5.35E-01	5.26E-01	5.20E-01	5.35E-01	5.26E-01
dB/dt amp. first harmonic	T/s	Btx	4.64E+02	4.78E+02	4.70E+02	3.08E+02	3.17E+02	3.12E+02
guideway eddy losses	W/km	Pteddy	7.58E+04	4.45E+04	6.51E+04	3.34E+04	1.96E+04	2.87E+04
Xreact. power (3ph-2 rails)	VA/km	Pzg	2.50E+07	2.10E+07	2.42E+07	1.66E+07	1.40E+07	1.61E+07
PROPULSIVE FORCE CALCULATIONS								
Inductances								
Xinductance-self L field	H/(2 seg)	Lbasic	5.92E-06	4.68E-06	6.90E-06	5.92E-06	4.68E-06	6.90E-06
X stator self L-mean value	H/(2 seg)	Laa	7.04E-06	5.64E-06	8.01E-06	7.04E-06	5.64E-06	8.01E-06
stator self L-second harm.	H/(2 seg)	Laa2	0.00E+00	0.00E+00	0.00E+00	0.00E+00	0.00E+00	0.00E+00
mutual-first harmonic	H/(2 seg)	Mvg	6.22E-06	4.91E-06	7.24E-06	6.22E-06	4.91E-06	7.24E-06
stator mutual-mean	H/(2 seg)	Mab	1.24E-06	9.82E-07	1.45E-06	1.24E-06	9.82E-07	1.45E-06
stator mutual-second harm.	H/(2 seg)	Mab2	3.64E-06	2.87E-06	4.23E-06	3.64E-06	2.87E-06	4.23E-06
Propulsive forces-maximum values								
design force (Mvg calc)	N	Fl	4.43E+04	4.75E+04	3.61E+04	4.43E+04	4.75E+04	3.61E+04
reluctance force (Mab2)	N		2.88E+03	3.08E+03	2.39E+03	2.88E+03	3.08E+03	2.39E+03
rail self induct (Laa2)	N		0.00E+00	0.00E+00	0.00E+00	0.00E+00	0.00E+00	0.00E+00
hunting stiffness	N/m	Khunt	4.64E+05	4.97E+05	3.78E+05	4.64E+05	4.97E+05	3.78E+05
hunting freq.	Hz	fhunt	5.42E-01	5.61E-01	4.89E-01	5.42E-01	5.61E-01	4.89E-01
Xmax. propel (B field)	N		4.72E+04	5.33E+04	3.58E+04	4.72E+04	5.33E+04	3.58E+04
Losses from eddy currents								
nom. rail B from vehicle	T	Br	2.00E+00	2.10E+00	2.28E+00	2.00E+00	2.10E+00	2.28E+00
eff. freq. for eddy anal.	Hz	Fe	2.23E+02	2.23E+02	2.23E+02	1.48E+02	1.48E+02	1.48E+02
dB/dt amp. first harmonic	T/s	B1x	1.79E+03	1.88E+03	2.04E+03	1.19E+03	1.25E+03	1.35E+03
eddy current power	W	Pr	2.36E+04	1.96E+04	1.84E+04	1.04E+04	8.67E+03	8.10E+03
rms eddy amp turn								
(upper bound, 1 magnet)	A	Nle	5.72E+00	4.07E+00	5.80E+00	3.80E+00	2.70E+00	3.85E+00

Table F-6 (continued)

ElectroMagnetic Suspension III Optimized for operation at 134 m/s maximum speed

(Separate vertical suspension & synchronous motor, lateral suspension)

Asterisk (*) before description indicates input.

DESCRIPTION	UNITS	SYMBOL	134 m/s Optimization			134 m/s Optimization @ 89 m/s		
			DESIGN 1	DESIGN 2	DESIGN 3	DESIGN 1	DESIGN 2	DESIGN 3
			baseline (b/l)	slim pole (3/4 b/l)	small gap (0.8 b/l)	baseline (b/l)	slim pole (3/4 b/l)	small gap (0.8 b/l)
(ohmic+eddy)/wind power	%		1.37%	1.55%	0.98%	3.83%	4.55%	2.69%
(magnet+coil)/vehicle wt.	%		13.24%	13.96%	9.46%	13.24%	13.96%	9.46%
eddy/lift amp-T (up. bound)	%		0.05%	0.04%	0.05%	0.04%	0.03%	0.04%
wind drag/weight	%		9.89%	9.89%	9.89%	4.36%	4.36%	4.36%
ratio propel F/weight	%		11.30%	12.11%	9.21%	1.13E-01	1.21E-01	9.21E-02
ratio propel/lift	%		10.80%	11.37%	8.21%	1.08E-01	1.14E-01	8.21E-02
ratio lift/weight	%		104.70%	106.57%	112.14%	1.05E+00	1.07E+00	1.12E+00
ratio mag. weight/lift	%		12.64%	13.10%	8.43%	1.26E-01	1.31E-01	8.43E-02
track losses/wind drag	%/km		29.69%	27.54%	28.99%	98.54%	92.35%	96.54%
AUXILIARY CALCULATIONS								
<u>*Combined lift magnets & synchronous motor*</u>								
Permeances								
permeances-vehicle magnet		Pfv	7.57E-01	6.61E-01	7.44E-01	7.57E-01	6.61E-01	7.44E-01
useful 1 air gap		Puv	1.60E+00	1.20E+00	2.00E+00	1.60E+00	1.20E+00	2.00E+00
X		Plv	3.11E-01	2.76E-01	3.20E-01	3.11E-01	2.76E-01	3.20E-01
pole useful area	m^2	Auv	1.60E-02	1.20E-02	1.60E-02	1.60E-02	1.20E-02	1.60E-02
Xcoil dimensions-1 coil on 1 pole		lcv	7.57E-01	7.07E-01	7.57E-01	7.57E-01	7.07E-01	7.57E-01
X 1 coil on 1 pole		acv	2.62E-03	2.62E-03	2.62E-03	2.62E-03	2.62E-03	2.62E-03
X 1 segments-1 pole		adisv	1.58E-01	1.49E-01	1.58E-01	1.58E-01	1.49E-01	1.58E-01
permeances-guideway windings		Pfg	7.57E-01	6.61E-01	7.44E-01	7.57E-01	6.61E-01	7.44E-01
vehicle in place		Pug	1.60E+00	1.20E+00	2.00E+00	1.60E+00	1.20E+00	2.00E+00
		Plg	8.92E-01	7.67E-01	8.86E-01	8.92E-01	7.67E-01	8.86E-01
X no vehicle magnets		Pl2g	5.37E-01	4.41E-01	5.07E-01	5.37E-01	4.41E-01	5.07E-01
Coil dimensions						0.00E+00	0.00E+00	0.00E+00
coil dimen.-1 phase-1 turn-3 pole pieces		lcg	9.11E-01	8.61E-01	8.95E-01	9.11E-01	8.61E-01	8.95E-01
1 -coil but 2 coils per slot		acg	2.20E-04	2.20E-04	2.20E-04	2.20E-04	2.20E-04	2.20E-04
1 seg. 3 pole pieces		adisg	1.66E-01	1.57E-01	1.63E-01	1.66E-01	1.57E-01	1.63E-01
<u>*Guidance Magnets*</u>								
Permeances								
Air gap fringing permeance/length		Pf.l	1.92E+00	1.92E+00	1.92E+00	1.92E+00	1.92E+00	1.92E+00
Ideal air gap permeance/length		Pu.l	2.80E+00	2.10E+00	3.10E+00	2.80E+00	2.10E+00	3.10E+00
Inter-pole leakage perm./length		Pl.l	4.21E-01	4.11E-01	4.30E-01	4.21E-01	4.11E-01	4.30E-01
Coil dimensions								
Mean turn length	m	lc.l	1.03E+01	1.96E+01	1.02E+01	1.03E+01	1.96E+01	1.02E+01
Coil crossectional area	m^2	ac.l	2.57E-03	2.03E-03	2.07E-03	2.57E-03	2.03E-03	2.07E-03
Coil Surface area	m^2	adis.l	4.48E+00	7.47E+00	4.02E+00	4.48E+00	7.47E+00	4.02E+00
<u>EMS III Summary</u>								
<u>*Weight on Vehicle*</u>								
Lift Magnets/LSM	kg		5.30E+03	5.58E+03	3.78E+03	2.22E+03	2.22E+03	2.22E+03
Guidance Magnets	kg		1.93E+03	2.58E+03	1.54E+03	1.93E+03	2.58E+03	1.54E+03
Total			7.23E+03	8.16E+03	5.32E+03	4.15E+03	4.80E+03	3.76E+03
Magnet Weight/Vehicle Weight	%		18.07%	20.40%	13.31%	10.38%	12.00%	9.41%
<u>*Weight on Guideway*</u>								
Lift Magnets/LSM	kg/m		2.71E+02	2.27E+02	2.57E+02	2.71E+02	2.27E+02	2.57E+02
Guidance Magnets	kg/m		1.13E+02	7.17E+01	8.87E+01	1.13E+02	7.17E+01	8.87E+01
Total	kg/m		3.84E+02	2.99E+02	3.46E+02	3.84E+02	2.99E+02	3.46E+02
<u>*Vehicle Real Power*</u>								
Ohmic Power Dissipation								
Lift Magnets/LSM	W		4.79E+04	6.07E+04	3.28E+04	4.79E+04	6.07E+04	3.28E+04
Guidance Magnets	W		1.88E+04	3.13E+04	1.68E+04	1.88E+04	3.13E+04	1.68E+04

Table F-6 (continued)

ElectroMagnetic Suspension III Optimized for operation at 134 m/s maximum speed

(Separate vertical suspension & synchronous motor, lateral suspension)

Asterisk (*) before description indicates input.

DESCRIPTION	UNITS	SYMBOL	134 m/s Optimization			134 m/s Optimization @ 89 m/s		
			DESIGN 1	DESIGN 2	DESIGN 3	DESIGN 1	DESIGN 2	DESIGN 3
			baseline (b/l)	slim pole (3/4 b/l)	small gap (0.8 b/l)	baseline (b/l)	slim pole (3/4 b/l)	small gap (0.8 b/l)
Total Ohmic Power	W		6.66E+04	9.20E+04	4.96E+04	6.66E+04	9.20E+04	4.96E+04
Eddy current Power								
Lift Magnets/LSM	W		2.36E+04	1.96E+04	1.84E+04	1.04E+04	8.67E+03	8.10E+03
Guidance Magnets	W		3.31E+04	5.49E+03	2.16E+04	1.46E+04	2.42E+03	9.52E+03
Total eddy current Power	W		5.67E+04	2.51E+04	3.99E+04	2.50E+04	1.11E+04	1.76E+04
Total Real Power Dissipation	W		1.23E+05	1.17E+05	8.96E+04	9.16E+04	1.03E+05	6.72E+04
Guideway Power								
Real Power Dissipation								
Guideway LSM Winding	kW/m		1.47E+00	1.39E+00	1.44E+00	1.47E+00	1.39E+00	1.44E+00
Total	kW/m		1.47E+00	1.39E+00	1.44E+00	1.47E+00	1.39E+00	1.44E+00
Reactive Input Power								
Linear Synchronous Motor	kVA/m		2.50E+01	2.10E+01	2.42E+01	1.66E+01	1.40E+01	1.61E+01
Total	kVA/m		2.50E+01	2.10E+01	2.42E+01	1.66E+01	1.40E+01	1.61E+01

APPENDIX G

SPREADSHEETS FOR ELECTRODYNAMIC SYSTEMS WITH FORMULAS

Table G-1. Hybrid null flux spreadsheet.

Operating Parameters			
*Velocity	m/s	v	134
*Vehicle Vertical Position	m	delh	0.01503
*Differential Vertical Position (produces t	m	difh	0
*Vehicle Lateral Position	m	dely	0
*Lateral Force Required	g	latg	0
*Lateral Force Arm above Levitation She	m	LFarm	2
Torque from Lateral Force	Nm		+LATG*9.8*MV*(LFARM+A/2)
Vehicle Description			
*Vehicle Frontal Area	m^2	Af	12.7
*Vehicle Length	m	Lv	
*Drag Coefficient		Cd	0.3
*Vehicle Weight	kg	Mv	40000
*Mechanical Clearance, Vehicle to Guid	m	mcl	0.08
Vehicle Magnets			
*Magnet Length	m	L	1.7
*Pole Pitch	m	P	2
*"Width"	m	A	1
*Main Conductor Current	A	I	800000
Radius of Main Superconductor	m	Rm	@IF(4.0000000E−14*JM*I*@PI*PD>BD^2,0.0000002*I/BD,(I/(@PI*JM*PD))^0.5)
Radius of "Shield" Superconductor	m	Rs	@IF(4.0000000E−14*I/4*JM*PD>BD^2,0.0000002*I/4/BD,(I/4/@PI/JM/PD)^0.5)
*Number of Magnet Units per Bogie		nu	3
*Number of Bogies		nb	2
*Superconducting Current Density	A/m^	Jm	200000000
*Superconducting Wire Density	kg/m^	dm	8000
*"Technology" Factor		T	5
*Max B Field Seen by Superconductors	Vs/m^	Bd	4
*Superconductor Wire Packing Density		pd	0.5
*Spacing, SC Surface to Vehicle Surface	m	cins	0.06
Guideway			
*Levitation Sheet Thickness	m	dl	0.006
*Guidance Sheet Thickness	m	dg	0.006
*Levitation Sheet Width	m	Wl	2*A−0.3−RM*2
*Guidance Sheet Width	m	Wg	+WL/2
*Guideway Conductivity	A/Vm	cg	37000000
*Guideway Density	kg/m^	dng	2700
Motor			
Winding to Superconducting Magnet Sp	m	S	+MCL+CINS+RM+R+2^0.5*(0.015−DELH)
*Winding Width	m	Am	+A/@SQRT(2)
*Number of Magnet Units (per Vehicle)		n	+NB*NU
*Radius of Conductor	m	R	0.02
*Number of Phases		nph	3
*Turns per Phase		tu	5
*Block Length	m	Lb	1000
*Insulation Spacing between Turns	m	Si	0.014
Current Density	A/m^	Jmm	+AMOT/@PI/R^2
B and C (winding geometry)	m	bpc	2*R*(TU+1)+SI*(TU−1)
Calculated parameters			
Cryosystem Weight	kg	Mss	+T*NU*NB*DM*I*(5*L+6.13*A)/JM
First Harmonic, Open Circuit Motor V	V	v1oc	+N*TU*V*I*0.0000002/(3*((S/A)^2−0.05*S/A+0.05))
Motor Resistance per Phase−Block	V/A	Rph	2*$LB*$TU*($A*0.707+$P)/$P/(3.14159*$R^2*$CG)
Motor Phase Inductance	H	Lmw	+LB/P*TU^2*2*0.0000002*(1−2*0.0018+AM*@LN(AM*2/BPC)+1.2*P*@LN(1.2*P*2/BPC))
Motor Phase Reactance	V/A	X	@PI*V*LMW/P
Guideway Levitation Mass per Meter	kg/m	Mgl	+WL*DL*DNG
Guideway Gudance Mass per Meter	kg/m	Mgg	+DNG*WG*DG
Guideway Motor Mass per Meter	kg/m	Mgm	2*TU*@PI*R^2*(AM+P)*DNG/P
Max Passenger Compartment Magnetic	G	Bp	
Lift	N	Fl	+P*A*NU*NB*VMUL/2/0.0000004/@PI*(BUN^2−BLN^2)
Magnetic Drag, No Lateral Force	N	Fd	+P*A*NU*NB/2/0.0000004/@PI*V/VA*((BUN−BLN)^2/(1+(V/VA)^2)+(K3D*(DL+DG/2)*(BUN+BLN))^2/12)
Magnetic Lift to Drag Ratio, No Lateral Force			+FL/FD
Required Propulsive Force	n	Fp	+PWD*1000000/V+FD+FLD+FTD
Required Motor Output	w	Pmo	+FP*V
Required In−Phase Motor Current	Arms	Amot	+PMO/V1OC/NPH
Reactive Voltage	V	Vrea	+V*@PI/P*LMW*AMOT
Motor Constant per Phase	N/A	kmot	+V1OC/V
Motor Current per .15g per Phase	A	I.15g	0.15*9.8*MV/KMOT/NPH
Motor Current per .21g per Phase	A	I.21g	0.21*9.8*MV/KMOT/NPH
Best Dynamic Breaking Deceleration	g	Ddbo	+KMOT^2*P/2/@PI/LMW/MV*NPH/9.8
Reactive kVA	kVA		+VREA*AMOT*NPH/1000
Lateral Force	N	Flat	0.5*(BLL^2−BRL^2)*P*A*NU*NB*VMUL/2/0.0000004/@PI
Lateral Drag	N	Fld	4*P*A*NU*NB/2/0.0000004/@PI*V/VA*(BLL−BRL)^2/(1+(V/VA)^2)
Torque for Lateral Force	Nm	Tlat	0.5*(BUD^2−BLD^2)*P*A^2*NU*NB*VMUL/2/0.0000004/@PI
Drag for Lateral Torque	N	Ftd	4*P*A*NU*NB/2/0.0000004/@PI*V/VA*(BUD−BLD)^2/(1+(V/VA)^2)
Lift Loss	MW	Pld	+FD*V/1000000
Loss from Lateral Drag	MW	Psd	+V*FLD/1000000
Loss from Lateral Torque	MW	Ptd	+FTD*V/1000000
Total Magnetic Losses	MW		(PLD+PDS+PTD)
Total Motor Winding Losses	MW	Pdw	+AMOT^2*RPH*NPH/1000000
Wind Drag Loss	MW	Pwd	1.23*V^3*CD*AF/2/1000000
Primary Suspension Natural Frequency	Hz		1/2/@PI*(FL/DELH/MV)^0.5
Intermediate results, levitation			
Richards and Tinkham interpreted by Marc then modified by using 3D ks			
wave number	1/m	k3D	@PI/(1/P^2+1/A^2)^0.5
speed for g'way L*omega/R=1	m/s	va	2/0.0000004/@PI/CG/DL
speed and thickness factor		vmul	(V/VA)^2/(1+(V/VA)^2)
upper B scalar, rms	T	Bun	32^0.5*I*0.0000004*@PI/P*@EXP(−K3D*(HNOT−DELH))
lower B scalar, rms	T	Bln	32^0.5*I*0.0000004*@PI/P*@EXP(−K3D*(HNOT+DELH))
for debugging, spacing, normally A/2	m	hnot	+A/2
left B scalar, rms	T	Bll	32^0.5*I*0.0000004*@PI/P*@EXP(−K3D*(A/2−DELY))
right B scalar, rms	T	Brl	32^0.5*I*0.0000004*@PI/P*@EXP(−K3D*(A/2+DELY))
upper differential B scalar, rms	T	Bud	32^0.5*I*0.0000004*@PI/P*@EXP(−K3D*(A/2−DIFH))
lower differential scalar, rms	T	Bld	32^0.5*I*0.0000004*@PI/P*@EXP(−K3D*(A/2+DIFH))

Table G-2. Image flux spreadsheet.

Operating Parameters	Units		
*velocity	m/s	v	80
*lateral force	g	Flat	0.26
*vehicle vertical position, + = up, 0 = norm		delh	0
Vehicle Description			
*assumed frontal area	m^2	Af	+G26
*drag coefficient		Cd	0.3
*total vehicle operating mass	kg	Mv	40000
*height above arc (headroom)	m	ht	1.87
Vehicle Magnet Parameters			
*pole pitch	m	P	15
*magnet length	m	L	13
*center angle	degree	pvc	30
*total angle	degree	pvt	112
*vehicle skin outer bottom radius	m	rv	2.1
*central current	A	Im	+IL*4
*outer current	A	Il	145756
*central coils per cluster (3)		nc	3
*outer coil pairs per cluster (1 or 3)		nl	3
*clusters per vehicle		nb	3
*superconducting current density	A/m^2	Jm	200000000
*superconducting wire density	kg/m^3	dm	8000
*"technology" factor		T	5
*superconductor to skin distance	m	ins	0.06
*max B field in superconductor	Vs/m^2	Bd	4
*superconductor wire packing density		pd	0.5
Guideway Levitation Parameters			
radius, upper guideway surface	m	rg	+RV+0.15
*central angle	degrees	pgc	40
*total angle	degrees	pgt	140
*levitation sheet thickness	m	dl	0.01
*levitation sheet conductivity	A/Vm	cg	37000000
*guideway density	kg/m^3	dg	2700
Guideway Motor Parameters			
*motor wire radius	m	rgm	0.02
*number of phases		np	3
*turns per phase		tu	5
*turn to turn spacing	m	gmws	1.00E+99
*block length	m	mbl	1000
*spacing, windings to g'way surface	m	lgm	0.01
*winding width angle	degrees	pgw	30
*winding conductivity	A/Vm	cgm	37000000
*winding density	kg/m^3	dgm	2700
Calculated Parameters			
vehicle frontal area	m^2	Afc	+RV^2*(@PI*PVT/360-@SIN(PVT*@PI/360)*@COS(PVT*@PI/360))+2*@SIN(PVT*@PI/360)*RV*HT-0.75^2*(2-@PI/2)
cryosystem weight	kg	Mss	+T*DM*PD*(SCL+SCMT+SCML)
first harmonic, open circuit motor V	Vrms	V1oc	+NB*NC*IM*M1H*0.0000001*V*TU
motor resistance per phase - block	V/A	Rph	+TU*MBL/P*(P+(RG+IGM+RGM)*PGW*@PI/180)/CGM/@PI/RGM^2
motor inductance per phase - block	H	Lph	+LPP*MBL/P
motor reactance per phase - block	V/A	Xph	+LPH*V*@PI/P
guideway levitation mass per meter	kg/m	Mgl	+DG*(RG+0.5*DL)*(PGT-PGC)*@PI/180*DL
guideway motor mass per meter	kg/m	Mgm	+DGM*@PI*RGM^2*TU*(1+(RG+IGM+RGM)*PGW*@PI/180/P)
levitation force	N	Fl	+FHUP*(V/DE)^2/(1+(V/DE)^2)
magnetic drag force	N	Fd	+FL*DE/V
motor constant per phase	N/A	kmot	+V1OC/V
maximum deceleration	g		+E79^2*NP*P/2/@PI/LPH/MV/9.8
motor current per phase	Arms	Ip	(PWD*1000000/V+FD)/E79/NP
motor reactive power, total	KVA		+XPH*IP^2*NP/1000
motor winding losses	MW		+RPH*IP^2*NP/1000000
lift loss	MW		+FD*V/1000000
lateral loss	MW		+FLAT*9.8*MV/@SIN(PVT*@PI/360)*DE/1000000
wind drag power	MW	Pwd	1.23*V^3*CD/2*AF/1000000
primary suspension natural frequency	Hz		@SQRT(9.8/H)/2/@PI
Not included in summary spreadsheet			
levitation superconductor radius	m	rl	@IF(4.0000000E-14*$JM*$IL*@PI*PD>$BD^2,0.0000002*$IL/$BD,($IL/@PI/$JM/PD)^0.5)
motor sc radius, transverse	m	rmt	@IF(4.0000000E-14*$JM*$IM*@PI*PD>$BD^2,0.0000002*$IM/$BD,($IM/@PI/$JM/PD)^0.5)
motor sc radius, longitudinal	m	rml	@IF(4.0000000E-14*JM*(IM-IL)*@PI>BD^2,0.0000002*(IM-IL)/BD,((IM-IL)/@PI/JM/PD)^0.5)
vertical distance, levitation to g-way	m	h	+RG-RV+RL+INS+DELH
levitation force, thick guideway	N	Flt	+FHUP/(1+(1/0.0000002/CG/V/P)^0.5)
magnetic drag force, thick guideway	N	Fdt	+FHNOR/(1+(0.0000002*CG*V*P)^0.5)
Intermediate Results, Lift Force			
levitation current, front and back coils, if any		Ila	@IF(NL=1,0,IL)
levitation current, center		Ilb	+IL
active transverse levitation coil length		La	(RV-INS-RL)*(PVT-PGC)*@PI/360
"geometrical" curvature corrention, longitudinal		gcl	@COS(PVT*@PI/360)
"geometrical" curvature correction, transverse		gct	(@SIN(PVT*@PI/360)-@SIN(PGC*@PI/360))*360/(PVT-PGC)/@PI
total, high speed limit, levitation force		Fhup	+NB*2*(GCT*(-F11A*(4*ILA^2+2*ILB^2)-4*F34A*LA*ILB+F13A*(4*ILA^2+2*ILB^2)+8*F14A*ILA*ILB+2*F37A*ILA^2-4*F16A*LA*ILB-4*F17A*ILA^2+2*F19A*ILA^2)+GCL*(-F22A*(2*ILA^2+ILB^2)+4*F56A*ILA*ILB-2*F28A*ILA^2))
total, high speed limit, normal force		Fhnor	+NB*2*(-F11A*(4*ILA^2+2*ILB^2)-F22A*(2*ILA^2+ILB^2)-F34A*4*ILA*ILB+F13A*(4*ILA^2+2*ILB^2)+8*F14A*ILA*ILB+2*F37A*ILA^2-4*F16A*ILA*ILB-4*F17A*ILA^2+2*F19A*ILA^2+4*F56A*ILA*ILB-2*F28A*ILA^2)
speed for g'way wL/R=1	m/s	va	2/0.0000004/@PI/CG/DL
speed for skin depth = g'way thickness	m/s	vb	2*P/0.0000004/@PI^2/CG/DL^2
speed for skin depth = pole pitch/pi	m/s	vc	1/0.0000002/P/CG
effective va	m/s	vae	@IF(V<VB,VA,(V/0.0000002/CG/P)^0.5)

Table G-2. Image flux spreadsheet. (Cont.)

```
                           +LA                        +LA
(4*H^2+E123^2)^0.5             0
F11a          (0.0000004*E122*H/D123)*((-E122/D123^2-E122^2/(D123^3*(1+(E122/D123)^2)^0.5))/(E122/D123+(1+(E122/D123)^2)^0.5)-D123/(E122^2*(1+(D123/E122)^2)^0.5)+1/E122)
              +L
(4*$H^2+E126^2)^0.5            0
F22a          (0.0000004*E122*H/D126)*((-E122/D126^2-E122^2/(D126^3*(1+(E122/D126)^2)^0.5))/(E122/D126+(1+(E122/D126)^2)^0.5)-D126/(E122^2*(1+(D126/E122)^2)^0.5)+1/E122)
              +LA
(4*H^2+E129^2)^0.5  +P-L
F34a          (0.0000004*E128*H/D129)*((-E128/D129^2-E128^2/(D129^3*(1+(E128/D129)^2)^0.5))/(E128/D129+(1+(E128/D129)^2)^0.5)-D129/(E128^2*(1+(D129/E128)^2)^0.5)+1/E128)
              +LA
(4*H^2+E132^2)^0.5  +L
F13a          (0.0000004*E131*H/D132)*((-E131/D132^2-E131^2/(D132^3*(1+(E131/D132)^2)^0.5))/(E131/D132+(1+(E131/D132)^2)^0.5)-D132/(E131^2*(1+(D132/E131)^2)^0.5)+1/E131)
              +LA
(4*H^2+E135^2)^0.5  +P
F14a          (0.0000004*E134*H/D135)*((-E134/D135^2-E134^2/(D135^3*(1+(E134/D135)^2)^0.5))/(E134/D135+(1+(E134/D135)^2)^0.5)-D135/(E134^2*(1+(D135/E134)^2)^0.5)+1/E134)
              +LA
(4*H^2+E138^2)^0.5  2*P-L
F37a          (0.0000004*E137*H/D138)*((-E137/D138^2-E137^2/(D138^3*(1+(E137/D138)^2)^0.5))/(E137/D138+(1+(E137/D138)^2)^0.5)-D138/(E137^2*(1+(D138/E137)^2)^0.5)+1/E137)
              +LA
(4*H^2+E141^2)^0.5  +P+L
F16a          (0.0000004*E140*H/D141)*((-E140/D141^2-E140^2/(D141^3*(1+(E140/D141)^2)^0.5))/(E140/D141+(1+(E140/D141)^2)^0.5)-D141/(E140^2*(1+(D141/E140)^2)^0.5)+1/E140)
              +LA
(4*H^2+E144^2)^0.5  2*P
F17a          (0.0000004*E143*H/D144)*((-E143/D144^2-E143^2/(D144^3*(1+(E143/D144)^2)^0.5))/(E143/D144+(1+(E143/D144)^2)^0.5)-D144/(E143^2*(1+(D144/E143)^2)^0.5)+1/E143)
              +LA
(4*H^2+E147^2)^0.5  2*P+L
F19a          (0.0000004*E146*H/D147)*((-E146/D147^2-E146^2/(D147^3*(1+(E146/D147)^2)^0.5))/(E146/D147+(1+(E146/D147)^2)^0.5)-D147/(E146^2*(1+(D147/E146)^2)^0.5)+1/E146)
              +P+L
(4*H^2+E150^2)^0.5             0
F56b          (0.0000004*E149*H/D150)*((-E149/D150^2-E149^2/(D150^3*(1+(E149/D150)^2)^0.5))/(E149/D150+(1+(E149/D150)^2)^0.5)-D150/(E149^2*(1+(D150/E149)^2)^0.5)+1/E149)
              +P-L
(4*H^2+E153^2)^0.5             0
F56c          (0.0000004*E152*H/D153)*((-E152/D153^2-E152^2/(D153^3*(1+(E152/D153)^2)^0.5))/(E152/D153+(1+(E152/D153)^2)^0.5)-D153/(E152^2*(1+(D153/E152)^2)^0.5)+1/E152)
              +P
(4*H^2+E156^2)^0.5             0
F56d          (0.0000004*E155*H/D156)*((-E155/D156^2-E155^2/(D156^3*(1+(E155/D156)^2)^0.5))/(E155/D156+(1+(E155/D156)^2)^0.5)-D156/(E155^2*(1+(D156/E155)^2)^0.5)+1/E155)
F56a          (F56B+F56C-2*F56D)*0.5
              2*P+L
(4*H^2+E160^2)^0.5             0
F26b          (0.0000004*E159*H/D160)*((-E159/D160^2-E159^2/(D160^3*(1+(E159/D160)^2)^0.5))/(E159/D160+(1+(E159/D160)^2)^0.5)-D160/(E159^2*(1+(D160/E159)^2)^0.5)+1/E159)
              2*P-L
(4*H^2+E163^2)^0.5             0
F26c          (0.0000004*E162*H/D163)*((-E162/D163^2-E162^2/(D163^3*(1+(E162/D163)^2)^0.5))/(E162/D163+(1+(E162/D163)^2)^0.5)-D163/(E162^2*(1+(D163/E162)^2)^0.5)+1/E162)
              2*P
(4*H^2+E166^2)^0.5             0
F26d          (0.0000004*E165*H/D166)*((-E165/D166^2-E165^2/(D166^3*(1+(E165/D166)^2)^0.5))/(E165/D166+(1+(E165/D166)^2)^0.5)-D166/(E165^2*(1+(D166/E165)^2)^0.5)+1/E165)
F26a          (F26B+F26C-2*F26D)*0.5

                         +LT*1000000
                         +LLE*1000000
                         +LLO*1000000
                         +LPP*1000000
```

Intermediate results, motor inductance

transverse inductance per pole pirtch	H	Lt	`+TU^2*0.0000002*(RG+IGM+RGM)*PGW*@PI/180*(@LN((RG+IGM+RGM)*PGW*@PI/180/RGM/(1+TU))+0.5)`
longitudinal inductance per P, even	H	Lle	`+TU^2*0.0000001*P*(@LN(P/RGM/(1+TU/2))+0.5)`
longitudinal inductance per P, odd	H	Llo	`(TU+1)^2*0.00000005*P*(@LN(P/RGM/(1.5+TU/2))+0.5)+(TU-1)^2*0.00000005*P*(@LN(P/RGM/(0.5+TU/2))+0.5)`
inductance per pole pitch	H	LpP	`@IF(@ROUND(TU/2,0)=TU/2,LT+LLE,LT+LLO)`

Intermediate Results, Superconducting Weight

levitation SC volume	m ^ 3	SCl	`@PI*RL^2*2*(L+(RV-INS)*(PVT-PVC)*@PI/180)*NL*NB`
motor transverse volume	m ^ 3	SCmt	`@PI*RMT^2*6*(RV-INS)*PVC*@PI/180*NB`
motor longitudinal volume	m ^ 3	SCml	`@PI*L*NB*@IF(NL=3,RML^2*6,RML^2*2+RMT^2*4)`

Table G-3. Sidewall null flux spreadsheet.

This spreadsheet assumes two magnet coils per bogie per side.
Run macro "1" to get fresh levitation force values.

Operating Parameters	Units			
*Velocity	m/s	v	134.00	
*Vehicle Vertical Position	m	delh	0.02710	
*Vehicle Lateral Position	m	dely	+<<C:\123WORK\MAGLEV\SWNF-G.WK1>>D13	!!! LINKED FROM SWNF-G.WK1.
*Lateral Force	N	flat	101920	.26 g's for 134, .18 g's for 89, for worst case comparisons.
		DELY(CALC)	0.00000	This value is used to calculate lift forces. Either use DELY(CALC)=0 or average results with + and - some non-zero value.

Vehicle Description			
*Vehicle Weight	kg	Mv	40000
*Vehicle Frontal Area	m^2	Afr	12.164184
*Coefficient of Drag		Cd	0.3
*Mechanical Clearance, Vehicle to Gm		Cmec	0.08

Vehicle Magnets			
*Magnet Pitch	m	P	1.35
*Magnet Height	m	H	0.5
*Magnet Length	m	L	1.2
Magnet Spacing, Side to Side	m	W	+E-2*(INS+RLC+RSC+CMEC)
*Magnet Current	A	Isc	800000
*Maximum SC Curent Density	A/m^2	Jscm	200000000
*Maximum SC B Field	T	Bscm	4
*Superconductor Wire Packing Density		SCPD	0.5
*Superconductor Wire Density	kg/m^3	SCD	8000
*Spacing, SC Surface to Vehicle Surm		ins	0.06
*"Technology" Factor		T	5
*Number of Bogies		nb	4
Number of SC Coils per Bogie, each side		nsc	2
Radius of superconductor cable		Rsc	@IF(4.0000000E-14*JSCM*ISC*@PI*SCPD>BSCM^2,0.0000002*ISC/BSCM,(ISC/@PI/JSCM/SCPD)^0.5)

Sidewall Levitation Coils			
*Coil Pitch	m	C	0.9
Coil Length	m	B	+C-2*RLC-0.02
*Half Height	m	A	0.4
*Half Inner Spacing	m	D	0.1
*side-to-side spacing	m	E	3.2
*Coil Conductor Radius	m	Rlc	0.028
*Coil Conductivity	A/V/m	clc	37000000
*Coil Density	kg/m^3	dlc	2700
*winding efficiency (lev. & guid.)		gcwe	0.75

Sidewall Guidance Coils			
*Coil Pitch	m	CG	+C
*Coil Length	m	BG	+CG-2*RGC-0.02
*Half Height	m	AG	+H/2
*Coil Conductor Radius	m	Rgc	0.02
*Coil Conductivity	A/V/m^2	cgc	37000000
*Coil Density	kg/m^3	dgc	2700
**Lateral Spacing	m	Eg	+EP+RPW+RGC+0.01

Motor			
Winding Pitch (same as vehicle magnet pitch)			+P
*Winding Half Height	m	Ap	0.35
*Number of Turns per Phase		nt	6
*Number of Phases		np	3
*Radius of Conductor	m		0.015
*Block Length	m	Lb	1000
**Lateral Spacing	m	Ep	+E+RLC+RPW+0.01
*Insulation spacing between turns	m	Si	0.01
center-to-center turn spacing	m	Sx	+SI+2*RPW
*conductivity	A/(V*m)	cpw	37000000
*density	kg/m^3	dpw	2700

Calculated Parameters			
Aerodynamic Drag Power	W	Paero	1.23*V^3*CD*AFR/2
Weight of Cryogenic System	kg		2*$NB*$NSC*(2*$L+2*$H)*$ISC*$SCD/$JSCM*$T
Motor Constant	Vs/m, N/A	Kmot	+<<C:\123WORK\MAGLEV\SWNF-P.WK1>>D72 !!!linked from SWNF-P.WK1
Motor Resistance per Block	V/A	Rmot	2*$NT*(2*$AP+$P+0.3)*$LB/$P/@PI/$RPW^2/$CPW
Motor Inductance per Block	H	Lblock	See below.
Motor Open Circuit Voltage per Pha	Vrms		+KMOT*V
Motor Losses	W		+IMOT^2*RMOT*NP
Motor Reactive VA	VA		+NP*LBLOCK*V*@PI/P*IMOT^2
Lift Force	N		@SUM(E234..E1234)*2*NB*DELT*V/C
Drag Force	N	FD	@SUM(F234..F734)*2*NB*DELT*V/C
Lift/Drag (no guidance forces)			+D76/FD
Lift Losses	W		+FD*V
Lateral guidance force	N		+<<C:\123WORK\MAGLEV\SWNF-G.WK1>>D187!!! linked from SWNF-G.WK1
Lateral Losses	W	Plat	+<<C:\123WORK\MAGLEV\SWNF-G.WK1>>D189!!! linked from SWNF-G.WK1
Passenger Compartment B Field	Gauss		
Guideway Levitation Aluminum	kg/m		4*(A+B-D)*@PI*RLC^2*DLC/C*2*GCWE
Guideway Guidance Aluminum	kg/m		4*(BG+2*AG)*@PI*RGC^2*DGC*GCWE/C
Guideway Propulsion Alumnium	kg/m		2*NP*NT*(P+2*AP*1.3)*@PI*RPW^2*DPW/P
Motor Current	A	Imot	((PAERO+PLAT)/V+FD)/KMOT/NP
Vehicle width	m		+W+2*RSC+2*INS
Maximum Dynamic Breaking	g		+KMOT^2*P/2/@PI/LBLOCK/MV/9.8
Primary Natural Frequency	Hz		(9.8/DELH)^0.5/2/@PI

Motor inductance per block formula:
0.0000002*(2*$AP*(@LN(4*$AP/(2*($NT+1)*$RPW+($NT-1)*$SI))+0.4978)+($P+0.3)/2*(@LN(2*($P+0.3)/(($NT+2)*$RPW+($NT/2-1)*$SI))+0.4978))*NT^2*LB/$P

Table G-3. Sidewall null flux spreadsheet. (Cont.)

Sidewall Levitation Coil Inductance		Llc	@SUM(D102..D113)
L11 + L33 + L55 + L77	H		0.0000002*(A-D)*(@LN(2*(A-D)/RLC)-0.75)
L22 + L44 + L66 + L88	H		0.0000002*B*(@LN(B/RLC)-0.75)
2 * (M15 + M37)	H		-0.0000002*(A*@LN(2*A)+D*@LN(2*D)-(A+D)*@LN(A+D))
2 * (M13 + M57)	H		-0.0000002*(A-D)*(@LN((A-D)/B+(1+((A-D)/B)^2)^0.5)-(1+(B/(A-D))^2)^0.5+B/(A-D))
2 * (M17 + M35)	H		0.0000004*(C107+C108+C109)
		2*A*(@LN(2*A/B+(1+(2*A/B)^2)^0.5)-(1+(B/2/A)^2)^0.5+B/2/A)	
		2*D*(@LN(2*D/B+(1+(2*D/B)^2)^0.5)-(1+(B/2/D)^2)^0.5+B/2/D)	
		-2*(A+D)*(@LN((A+D)/B+(1+((A+D)/B)^2)^0.5)-(1+(B/(A+D))^2)^0.5+B/(A+D))	
2 * (M24 + M68)	H		-0.0000002*B*(@LN(B/(A-D)+(1+(B/(A-D))^2)^0.5)-(1+((A-D)/B)^2)^0.5+(A-D)/B)
2 * (M26 + M48)	H		-0.0000002*B*(@LN(B/(A+D)+(1+(B/(A+D))^2)^0.5)-(1+((A+D)/B)^2)^0.5+(A+D)/B)
2 * M28	H		0.0000004*B*(@LN(B/2/A+(1+(B/2/A)^2)^0.5)-(1+(2*A/B)^2)^0.5+2*A/B)
2 * M46	H		0.0000004*B*(@LN(B/2/D+(1+(B/2/D)^2)^0.5)-(1+(2*D/B)^2)^0.5+2*D/B)
Sidewall Levitation Coil Resistance	V/A	Rsl	4*(A+B-D)/@PI/RLC^2/CLC/OCWE
sidewall time constant L/R	s		+LLC/RSL

Sidewall-Vehicle Mutual Inductances

Vertical Pairs

			le	dx	Horizontal Pairs		ln	dh	
M11a	zv	-$H/2	+SUG-ZLV+(($E/2-$W/2	+LE*@LN(LE0.0000001*(F120+F121-RM22	xv	+$P/2+$L/2	+XRG+ERR-(($E/2+$DE		+L120*@L*0.0000001*(N120+N121-N122-N123)
b	zuv	+$H/2	+ZUV-ZLG-+DX	+D121*@LN(D121/E121+(1+D121^2/E121^2)^	xuv	+$P/2-$L/2	+XLG+ERR-+M120		+L121*@LN(L121/M121+(1+L121^2/M121^2)^0.5)-(L121^2+M121^2)^0.5+M121
c	xv	($P+$L)/2	+SUG-ZUV-+E121	+D122*@LN(D122/E122+(1+D122^2/E122^2)^	zv	+$H/2	+XRG+ERR-+M121		+L122*@LN(L122/M122+(1+L122^2/M122^2)^0.5)-(L122^2+M122^2)^0.5+M122
d	zg	+$D	+ZLG-ZLV-+E122	+D123*@LN(D123/E123+(1+D123^2/E123^2)^	xg	+$B/2	+XLG+ERR-+M122		+L123*@LN(L123/M123+(1+L123^2/M123^2)^0.5)-(L123^2+M123^2)^0.5+M123
	zug	+$A			xug	-$B/2			
	xg	+$B/2			zg	+$A			
M13	zv	-$H/2	+C130-C12(($E/2-$W/2	+D126*@LN0.0000001*(F126+F127-RM24	xv	+XLV	+L120	(($E/2+$DE	+L126*@L*0.0000001*(N126+N127-N128-N129)*-1
	zuv	+$H/2	+C127-C12+E126	+D127*@LN(D127/E127+(1+D127^2/E127^2)^	xuv	+XRV	+L121	+M126	+L127*@LN(L127/M127+(1+L127^2/M127^2)^0.5)-(L127^2+M127^2)^0.5+M127
	xv	($P+$L)/2	+C130-C12+E127	+D128*@LN(D128/E128+(1+D128^2/E128^2)^	zv	+ZV	+L122	+M127	+L128*@LN(L128/M128+(1+L128^2/M128^2)^0.5)-(L128^2+M128^2)^0.5+M128
	zg	+$D	+C129-C12+E128	+D129*@LN(D129/E129+(1+D129^2/E129^2)^	xg	+$B/2	+L123	+M128	+L129*@LN(L129/M129+(1+L129^2/M129^2)^0.5)-(L129^2+M129^2)^0.5+M129
	zug	+$A			xug	-$B/2			
	xg	-$B/2			zg	+$D			
M15	zv	-$H/2	+C136-C13(($E/2-$W/2	+D132*@LN0.0000001*(F132+F133-RM26	xv	+K126	+L120	(($E/2+$DE	+L132*@L*0.0000001*(N132+N133-N134-N135)*-1
	zuv	+$H/2	+C133-C13+E132	+D133*@LN(D133/E133+(1+D133^2/E133^2)^	xuv	+K127	+L121	+M132	+L133*@LN(L133/M133+(1+L133^2/M133^2)^0.5)-(L133^2+M133^2)^0.5+M133
	xv	($P+$L)/2	+C136-C13+E133	+D134*@LN(D134/E134+(1+D134^2/E134^2)^	zv	+K128	+L122	+M133	+L134*@LN(L134/M134+(1+L134^2/M134^2)^0.5)-(L134^2+M134^2)^0.5+M134
	zg	-$A	+C135-C13+E134	+D135*@LN(D135/E135+(1+D135^2/E135^2)^	xg	+$B/2	+L123	+M134	+L135*@LN(L135/M135+(1+L135^2/M135^2)^0.5)-(L135^2+M135^2)^0.5+M135
	zug	-$D			xug	-$B/2			
	xg	+$B/2			zg	-$D			
M17	zv	-$H/2	+C142-C13(($E/2-$W/2	+D138*@LN0.0000001*(F138+F139-RM28	xv	+K132	+L120	(($E/2+$DE	+L138*@L*0.0000001*(N138+N139-N140-N141)
	zuv	+$H/2	+C139-C14+E138	+D139*@LN(D139/E139+(1+D139^2/E139^2)^	xuv	+K133	+L121	+M138	+L139*@LN(L139/M139+(1+L139^2/M139^2)^0.5)-(L139^2+M139^2)^0.5+M139
	xv	($P+$L)/2	+C142-C13+E139	+D140*@LN(D140/E140+(1+D140^2/E140^2)^	zv	+K134	+L122	+M139	+L140*@LN(L140/M140+(1+L140^2/M140^2)^0.5)-(L140^2+M140^2)^0.5+M140
	zg	-$A	+C141-C13+E140	+D141*@LN(D141/E141+(1+D141^2/E141^2)^	xg	+$B/2	+L123	+M140	+L141*@LN(L141/M141+(1+L141^2/M141^2)^0.5)-(L141^2+M141^2)^0.5+M141
	zug	-$D			xug	-$B/2			
	xg	-$B/2			zg	-$A			
M31	zv	-$H/2	+C148-C14(($E/2-$W/2	+D144*@LN0.0000001*(F144+F145-RM42	xv	+K138	+L120	(($E/2+$DE	+L144*@L*0.0000001*(N144+N145-N146-N147)*-1
	zuv	+$H/2	+C145-C14+E144	+D145*@LN(D145/E145+(1+D145^2/E145^2)^	xuv	+K139	+L121	+M144	+L145*@LN(L145/M145+(1+L145^2/M145^2)^0.5)-(L145^2+M145^2)^0.5+M145
	xv	+$P/2-$L/2	+C148-C14+E145	+D146*@LN(D146/E146+(1+D146^2/E146^2)^	zv	-$H/2	+L122	+M145	+L146*@LN(L146/M146+(1+L146^2/M146^2)^0.5)-(L146^2+M146^2)^0.5+M146
	zg	+$D	+C147-C14+E146	+D147*@LN(D147/E147+(1+D147^2/E147^2)^	xg	+XLG	+L123	+M146	+L147*@LN(L147/M147+(1+L147^2/M147^2)^0.5)-(L147^2+M147^2)^0.5+M147
	zug	+$A			xug	+XRG			
	xg	+$B/2			zg	+ZG			
M33	zv	-$H/2	+C154-C15(($E/2-$W/2	+D150*@LN0.0000001*(F150+F151-RM44	xv	+K144	+L120	(($E/2+$DE	+L150*@L*0.0000001*(N150+N151-N152-N153)
	zuv	+$H/2	+C151-C15+E150	+D151*@LN(D151/E151+(1+D151^2/E151^2)^	xuv	+K145	+L121	+M150	+L151*@LN(L151/M151+(1+L151^2/M151^2)^0.5)-(L151^2+M151^2)^0.5+M151
	xv	+$P/2-$L/2	+C154-C15+E151	+D152*@LN(D152/E152+(1+D152^2/E152^2)^	zv	+K146	+L122	+M151	+L152*@LN(L152/M152+(1+L152^2/M152^2)^0.5)-(L152^2+M152^2)^0.5+M152
	zg	+$D	+C153-C15+E152	+D153*@LN(D153/E153+(1+D153^2/E153^2)^	xg	+K129	+L123	+M152	+L153*@LN(L153/M153+(1+L153^2/M153^2)^0.5)-(L153^2+M153^2)^0.5+M153
	zug	+$A			xug	+K130			
	xg	-$B/2			zg	+K131			
M35	zv	-$H/2	+C160-C15(($E/2-$W/2	+D156*@LN0.0000001*(F156+F157-RM46	xv	+K150	+L120	(($E/2+$DE	+L156*@L*0.0000001*(N156+N157-N158-N159)
	zuv	+$H/2	+C157-C15+E156	+D157*@LN(D157/E157+(1+D157^2/E157^2)^	xuv	+K151	+L121	+M156	+L157*@LN(L157/M157+(1+L157^2/M157^2)^0.5)-(L157^2+M157^2)^0.5+M157
	xv	+$P/2-$L/2	+C160-C15+E157	+D158*@LN(D158/E158+(1+D158^2/E158^2)^	zv	+K152	+L122	+M157	+L158*@LN(L158/M158+(1+L158^2/M158^2)^0.5)-(L158^2+M158^2)^0.5+M158
	zg	-$A	+C159-C15+E158	+D159*@LN(D159/E159+(1+D159^2/E159^2)^	xg	+K135	+L123	+M158	+L159*@LN(L159/M159+(1+L159^2/M159^2)^0.5)-(L159^2+M159^2)^0.5+M159
	zug	-$D			xug	+K136			
	xg	+$B/2			zg	+K137			
M37	zv	-$H/2	+C166-C16(($E/2-$W/2	+D162*@LN0.0000001*(F162+F163-RM48	xv	+K156	+L120	(($E/2+$DE	+L162*@L*0.0000001*(N162+N163-N164-N165)*-1
	zuv	+$H/2	+C163-C16+E162	+D163*@LN(D163/E163+(1+D163^2/E163^2)^	xuv	+K157	+L121	+M162	+L163*@LN(L163/M163+(1+L163^2/M163^2)^0.5)-(L163^2+M163^2)^0.5+M163
	xv	+$P/2-$L/2	+C166-C16+E163	+D164*@LN(D164/E164+(1+D164^2/E164^2)^	zv	+K158	+L122	+M163	+L164*@LN(L164/M164+(1+L164^2/M164^2)^0.5)-(L164^2+M164^2)^0.5+M164
	zg	-$A	+C165-C16+E164	+D165*@LN(D165/E165+(1+D165^2/E165^2)^	xg	+K141	+L123	+M164	+L165*@LN(L165/M165+(1+L165^2/M165^2)^0.5)-(L165^2+M165^2)^0.5+M165
	zug	-$D			xug	+K142			
	xg	-$B/2			zg	+K143			
M51	zv	-$H/2	+C172-C16(($E/2-$W/2	+D168*@LN0.0000001*(F168+F169-RM62	xv	-$P/2+$L/2	+K172+ERR+M120		+L168*@L*0.0000001*(N168+N169-N170-N171)*-1
	zuv	+$H/2	+C169-C17+E168	+D169*@LN(D169/E169+(1+D169^2/E169^2)^	xuv	-$P/2-$L/2	+K171+ERR+M121		+L169*@LN(L169/M169+(1+L169^2/M169^2)^0.5)-(L169^2+M169^2)^0.5+M169
	xv	-$P/2+$L/2	+C172-C16+E169	+D170*@LN(D170/E170+(1+D170^2/E170^2)^	zv	+$H/2	+K172+ERR+M122		+L170*@LN(L170/M170+(1+L170^2/M170^2)^0.5)-(L170^2+M170^2)^0.5+M170
	zg	+$D	+C171-C16+E170	+D171*@LN(D171/E171+(1+D171^2/E171^2)^	xg	+XLG	+K171+ERR+M123		+L171*@LN(L171/M171+(1+L171^2/M171^2)^0.5)-(L171^2+M171^2)^0.5+M171
	zug	+$A			xug	+XRG			
	xg	+$B/2			zg	+ZG			
M53	zv	-$H/2	+C178-C17(($E/2-$W/2	+D174*@LN0.0000001*(F174+F175-RM64	xv	+K168	+L168	+M126	+L174*@L*0.0000001*(N174+N175-N176-N177)
	zuv	+$H/2	+C175-C17+E174	+D175*@LN(D175/E175+(1+D175^2/E175^2)^	xuv	+K169	+L169	+M127	+L175*@LN(L175/M175+(1+L175^2/M175^2)^0.5)-(L175^2+M175^2)^0.5+M175
	xv	-$P/2+$L/2	+C178-C17+E175	+D176*@LN(D176/E176+(1+D176^2/E176^2)^	zv	+K170	+L170	+M128	+L176*@LN(L176/M176+(1+L176^2/M176^2)^0.5)-(L176^2+M176^2)^0.5+M176
	zg	+$D	+C177-C17+E176	+D177*@LN(D177/E177+(1+D177^2/E177^2)^	xg	+K129	+L171	+M129	+L177*@LN(L177/M177+(1+L177^2/M177^2)^0.5)-(L177^2+M177^2)^0.5+M177
	zug	+$A			xug	+K130			
	xg	-$B/2			zg	+K131			
M55	zv	-$H/2	+C184-C18(($E/2-$W/2	+D180*@LN0.0000001*(F180+F181-RM66	xv	+K168	+L168	+M132	+L180*@L*0.0000001*(N180+N181-N182-N183)
	zuv	+$H/2	+C181-C18+E180	+D181*@LN(D181/E181+(1+D181^2/E181^2)^	xuv	+K169	+L169	+M180	+L181*@LN(L181/M181+(1+L181^2/M181^2)^0.5)-(L181^2+M181^2)^0.5+M181
	xv	-$P/2+$L/2	+C184-C18+E181	+D182*@LN(D182/E182+(1+D182^2/E182^2)^	zv	+K170	+L170	+M181	+L182*@LN(L182/M182+(1+L182^2/M182^2)^0.5)-(L182^2+M182^2)^0.5+M182
	zg	-$A	+C183-C18+E182	+D183*@LN(D183/E183+(1+D183^2/E183^2)^	xg	+K135	+L171	+M182	+L183*@LN(L183/M183+(1+L183^2/M183^2)^0.5)-(L183^2+M183^2)^0.5+M183
	zug	-$D			xug	+K136			
	xg	+$B/2			zg	+K137			
M57	zv	-$H/2	+C190-C18(($E/2-$W/2	+D186*@LN0.0000001*(F186+F187-RM68	xv	+K168	+L168	+M138	+L186*@L*0.0000001*(N186+N187-N188-N189)*-1
	zuv	+$H/2	+C187-C18+E186	+D187*@LN(D187/E187+(1+D187^2/E187^2)^	xuv	+K169	+L169	+M186	+L187*@LN(L187/M187+(1+L187^2/M187^2)^0.5)-(L187^2+M187^2)^0.5+M187
	xv	-$P/2+$L/2	+C190-C18+E187	+D188*@LN(D188/E188+(1+D188^2/E188^2)^	zv	+K170	+L170	+M187	+L188*@LN(L188/M188+(1+L188^2/M188^2)^0.5)-(L188^2+M188^2)^0.5+M188
	zg	-$A	+C189-C18+E188	+D189*@LN(D189/E189+(1+D189^2/E189^2)^	xg	+K141	+L171	+M188	+L189*@LN(L189/M189+(1+L189^2/M189^2)^0.5)-(L189^2+M189^2)^0.5+M189
	zug	-$D			xug	+K142			
	xg	-$B/2			zg	+K143			
M71	zv	-$H/2	+C196-C19(($E/2-$W/2	+D192*@LN0.0000001*(F192+F193-RM82	xv	+K168	+L168	+M144	+L192*@L*0.0000001*(N192+N193-N194-N195)
	zuv	+$H/2	+C193-C19+E192	+D193*@LN(D193/E193+(1+D193^2/E193^2)^	xuv	+K169	+L169	+M192	+L193*@LN(L193/M193+(1+L193^2/M193^2)^0.5)-(L193^2+M193^2)^0.5+M193
	xv	-$P/2-$L/2	+C196-C19+E193	+D194*@LN(D194/E194+(1+D194^2/E194^2)^	zv	-$H/2	+L170	+M193	+L194*@LN(L194/M194+(1+L194^2/M194^2)^0.5)-(L194^2+M194^2)^0.5+M194
	zg	+$D	+C195-C19+E194	+D195*@LN(D195/E195+(1+D195^2/E195^2)^	xg	+XLG	+L171	+M194	+L195*@LN(L195/M195+(1+L195^2/M195^2)^0.5)-(L195^2+M195^2)^0.5+M195
	zug	+$A			xug	+XRG			
	xg	+$B/2			zg	+ZG			
M73	zv	-$H/2	+C202-C19(($E/2-$W/2	+D198*@LN0.0000001*(F198+F199-RM84	xv	+K192	+L168	+M150	+L198*@L*0.0000001*(N198+N199-N200-N201)*-1
	zuv	+$H/2	+C199-C20+E198	+D199*@LN(D199/E199+(1+D199^2/E199^2)^	xuv	+K193	+L169	+M198	+L199*@LN(L199/M199+(1+L199^2/M199^2)^0.5)-(L199^2+M199^2)^0.5+M199
	xv	-$P/2-$L/2	+C202-C19+E199	+D200*@LN(D200/E200+(1+D200^2/E200^2)^	zv	+K194	+L170	+M199	+L200*@LN(L200/M200+(1+L200^2/M200^2)^0.5)-(L200^2+M200^2)^0.5+M200
	zg	+$D	+C201-C19+E200	+D201*@LN(D201/E201+(1+D201^2/E201^2)^	xg	+K129	+L171	+M200	+L201*@LN(L201/M201+(1+L201^2/M201^2)^0.5)-(L201^2+M201^2)^0.5+M201
	zug	+$A			xug	+K130			
	xg	-$B/2			zg	+K131			
M75	zv	-$H/2	+C208-C20(($E/2-$W/2	+D204*@LN0.0000001*(F204+F205-RM86	xv	+K192	+L168	+M156	+L204*@L*0.0000001*(N204+N205-N206-N207)*-1
	zuv	+$H/2	+C205-C20+E204	+D205*@LN(D205/E205+(1+D205^2/E205^2)^	xuv	+K193	+L169	+M204	+L205*@LN(L205/M205+(1+L205^2/M205^2)^0.5)-(L205^2+M205^2)^0.5+M205
	xv	-$P/2-$L/2	+C208-C20+E205	+D206*@LN(D206/E206+(1+D206^2/E206^2)^	zv	+K194	+L170	+M205	+L206*@LN(L206/M206+(1+L206^2/M206^2)^0.5)-(L206^2+M206^2)^0.5+M206
	zg	-$A	+C207-C20+E206	+D207*@LN(D207/E207+(1+D207^2/E207^2)^	xg	+K135	+L171	+M206	+L207*@LN(L207/M207+(1+L207^2/M207^2)^0.5)-(L207^2+M207^2)^0.5+M207
	zug	-$D			xug	+K136			
	xg	+$B/2			zg	+K137			
M77	zv	-$H/2	+C214-C21(($E/2-$W/2	+D210*@LN0.0000001*(F210+F211-RM88	xv	+K192	+L168	+M162	+L210*@L*0.0000001*(N210+N211-N212-N213)
	zuv	+$H/2	+C211-C21+E210	+D211*@LN(D211/E211+(1+D211^2/E211^2)^	xuv	+K193	+L169	+M210	+L211*@LN(L211/M211+(1+L211^2/M211^2)^0.5)-(L211^2+M211^2)^0.5+M211
	xv	-$P/2-$L/2	+C214-C21+E211	+D212*@LN(D212/E212+(1+D212^2/E212^2)^	zv	+K194	+L170	+M211	+L212*@LN(L212/M212+(1+L212^2/M212^2)^0.5)-(L212^2+M212^2)^0.5+M212
	zg	-$A	+C213-C21+E212	+D213*@LN(D213/E213+(1+D213^2/E213^2)^	xg	+K141	+L171	+M212	+L213*@LN(L213/M213+(1+L213^2/M213^2)^0.5)-(L213^2+M213^2)^0.5+M213
	zug	-$D			xug	+K142			
	xg	-$B/2			zg	+K143			

Parameters for Levitation Calculation

* step size	m	xstep	0.02	
initial position (< 0)	m	xstart	-XSTEP*ENDSTEP	
* increment for calculating dM/dz	m	dz	0.001	
step counter		step	251	+XSTEP/V
* (number of steps - 1)/2		endstep	250	
time for a step	s	delt	+XSTEP/V	check.
guideway-vehicle M for current step	H	Mvg	@SUM(G120..G210,O120..sum I^2*r*delt+.5LI^2	
previous guideway-vehicle M	H	Mvgp	3.30E-13	+RI^2*DELT+D734^2/2*LLC
		Ig	((MVGP-MVG)*ISC-RSL*sum drag*V*dt=	
		Igp	-696.8982	@SUM(F234..F734)*V*DELT
		dMvg/dz	(MVG-MVGP)/DZ	
		RI^2	2308638.0	
lift to drag ratio			@SUM(E234	

Levitation Macro (named "1")

Initial conditions		{let igp,0}
		{let mvgp,0}
		{let x,xstart-xstep}~
for.. do loop		{for step,-endstep,endstep,1,loop}
calculate losses		{let RI^2,+Rsl*(2*endstep+1)*(@var(d234..d1250)+@avg(d234..d1250)^2)}~
calculate drag column		/c235~f236..f733~/rvf236..f733~f236~
increment x	loop	{let x,x+xstep}~
put mutual inductance in table		{put lev_table,0,step+endstep,Mvg}
put guideway current in table		{put lev_table,2,step+endstep,Ig}
store current Mvg as previous		{let Mvgp,Mvg}
store current Ig as previous		{let Igp,Ig}
increase height a small delta		{let delh,delh+dz}~
put dM/dz in table		{put lev_table,1,step+endstep,dMvg/dz}
put force in table		{put lev_table,3,step+endstep,-Isc*Igp*dMvg/dz}
return height		{let delh,delh-dz}
		{return}

intermediate results table

	Mvg	dMvg/dz	Ig	Flift	drag		time
lev-table	-3.30E-13	-1.23E-11	0.1603216	0.0000015			
The table continues	-3.41E-13	-1.26E-11	0.1636121	0.0000016	-(B236-B23	0.0000138	-0.0498
for 500 rows.	-3.51E-13	-1.29E-11	0.1670160	0.0000017	0.0000000	0.0000149	-0.0496
	-3.60E-13	-1.33E-11	0.1705374	0.0000018	0.0000000	0.0000162	-0.0494
	-3.70E-13	-1.36E-11	0.1741806	0.0000018	0.0000000	0.0000175	-0.0492
	-3.80E-13	-1.40E-11	0.1779502	0.0000019	0.0000000	0.0000190	-0.049
	-3.90E-13	-1.44E-11	0.1818508	0.0000020	0.0000000	0.0000207	-0.0488
	-4.00E-13	-1.48E-11	0.1858875	0.0000021	0.0000000	0.0000225	-0.0486
	-4.11E-13	-1.52E-11	0.1900653	0.0000023	0.0000000	0.0000245	-0.0484
	-4.23E-13	-1.56E-11	0.1943896	0.0000024	0.0000000	0.0000268	-0.0482

Table G-3. Sidewall null flux spreadsheet. (Cont.)

Miscelleneous Calculations

Guidance Coil Inductance Vs/A	Lgc	(D89 + D90 - D91 - D92)*4
(inductance of a connected pair)	L1	0.0000002*BG*(@LN(2*BG/RGC) - 0.75)
	L2	0.0000004*AG*(@LN(4*AG/RGC) - 0.75)
	M13	0.0000002*(2*AG*@LN(2*AG/BG + (1 + (2*AG/BG) ^ 2) ^ 0.5) - (4*AG ^ 2 + BG ^ 2) ^ 0.5 + BG)
	M24	0.0000002*(BG*@LN(BG/2*AG + (1 + (BG/2/AG) ^ 2) ^ 0.5) - (4*AG ^ 2 + BG ^ 2) ^ 0.5 + 2*AG)
Guidance Coil Resistance V/A	Rg	4*(2*AG + BG)/@PI/RGC ^ 2/CLC/GCWE
(resistance of a connected pair)		
guidance coil time constans		+LGC/RG

Mutual Inductance Calculations

Vertical pairs

			Le	Dx
M11	Xv - (P + L)/2	Xg - BG/2	+ ZGU + $DEL((($EG - $W)	+ LE* @LN(l0.0000001*(H101 + H102 - H103 - H104)
	Zvu + H/2	Zgu + AG	+ ZVU - ZGL - + DX	+ F102*@LN(F102/G102 + (1 + (F102/G102) ^2) ^ 0.5) - (F102 ^ 2 + G102 ^ 2) ^ 0.5 + G102
	Zvl - H/2	Zgl - AG	+ ZVL - ZGL - + G102	+ F103*@LN(F103/G103 + (1 + (F103/G103) ^2) ^ 0.5) - (F103 ^ 2 + G103 ^ 2) ^ 0.5 + G103
			+ ZGU + $DEL + G103	+ F104*@LN(F104/G104 + (1 + (F104/G104) ^2) ^ 0.5) - (F104 ^ 2 + G104 ^ 2) ^ 0.5 + G104
M13	Xv + XV	Xg - XG	+ E106 + $DE((($EG - $W)	+ F105*@Ll0.0000001*(H105 + H106 - H107 - H108)* - 1
	Zvu + ZVU	Zgu + ZGU	+ C106 - E107 + G105	+ F106*@LN(F106/G106 + (1 + (F106/G106) ^2) ^ 0.5) - (F106 ^ 2 + G106 ^ 2) ^ 0.5 + G106
	Zvl + ZVL	Zgl + ZGL	+ C107 - E107 + G106	+ F107*@LN(F107/G107 + (1 + (F107/G107) ^2) ^ 0.5) - (F107 ^ 2 + G107 ^ 2) ^ 0.5 + G107
			+ E106 + $DEl + G107	+ F108*@LN(F108/G108 + (1 + (F108/G108) ^2) ^ 0.5) - (F108 ^ 2 + G108 ^ 2) ^ 0.5 + G108
M31	Xv - (P - L)/2	Xg - E105	+ E110 + $DE((($EG - $W)	+ F109*@Ll0.0000001*(H109 + H110 - H111 - H112)* - 1
	Zvu + C106	Zgu + E106	+ C110 - E11 + G109	+ F110*@LN(F110/G110 + (1 + (F110/G110) ^2) ^ 0.5) - (F110 ^ 2 + G110 ^ 2) ^ 0.5 + G110
	Zvl + C107	Zgl + E107	+ C111 - E11 + G110	+ F111*@LN(F111/G111 + (1 + (F111/G111) ^2) ^ 0.5) - (F111 ^ 2 + G111 ^ 2) ^ 0.5 + G111
			+ E110 + $DEl + G111	+ F112*@LN(F112/G112 + (1 + (F112/G112) ^2) ^ 0.5) - (F112 ^ 2 + G112 ^ 2) ^ 0.5 + G112
M33	Xv + C109	Xg - E109	+ E114 + $DE((($EG - $W)	+ F113*@Ll0.0000001*(H113 + H114 - H115 - H116)
	Zvu + C110	Zgu + E110	+ C114 - E11 + G113	+ F114*@LN(F114/G114 + (1 + (F114/G114) ^2) ^ 0.5) - (F114 ^ 2 + G114 ^ 2) ^ 0.5 + G114
	Zvl + C111	Zgl + E111	+ C115 - E11 + G114	+ F115*@LN(F115/G115 + (1 + (F115/G115) ^2) ^ 0.5) - (F115 ^ 2 + G115 ^ 2) ^ 0.5 + G115
			+ E114 + $DEl + G115	+ F116*@LN(F116/G116 + (1 + (F116/G116) ^2) ^ 0.5) - (F116 ^ 2 + G116 ^ 2) ^ 0.5 + G116
M51	Xv (P - L)/2	Xg - E113	+ E118 + $DE((($EG - $W)	+ F117*@Ll0.0000001*(H117 + H118 - H119 - H120)* - 1
	Zvu + C114	Zgu + E114	+ C118 - E11 + G117	+ F118*@LN(F118/G118 + (1 + (F118/G118) ^2) ^ 0.5) - (F118 ^ 2 + G118 ^ 2) ^ 0.5 + G118
	Zvl + C115	Zgl + E115	+ C119 - E11 + G118	+ F119*@LN(F119/G119 + (1 + (F119/G119) ^2) ^ 0.5) - (F119 ^ 2 + G119 ^ 2) ^ 0.5 + G119
			+ E118 + $DEl + G119	+ F120*@LN(F120/G120 + (1 + (F120/G120) ^2) ^ 0.5) - (F120 ^ 2 + G120 ^ 2) ^ 0.5 + G120
M53	Xv + C117	Xg - E117	+ E122 + $DE((($EG - $W)	+ F121*@Ll0.0000001*(H121 + H122 - H123 - H124)
	Zvu + C118	Zgu + E118	+ C122 - E12 + G121	+ F122*@LN(F122/G122 + (1 + (F122/G122) ^2) ^ 0.5) - (F122 ^ 2 + G122 ^ 2) ^ 0.5 + G122
	Zvl + C119	Zgl + E119	+ C123 - E12 + G122	+ F123*@LN(F123/G123 + (1 + (F123/G123) ^2) ^ 0.5) - (F123 ^ 2 + G123 ^ 2) ^ 0.5 + G123
			+ E122 + $DEl + G123	+ F124*@LN(F124/G124 + (1 + (F124/G124) ^2) ^ 0.5) - (F124 ^ 2 + G124 ^ 2) ^ 0.5 + G124
M71	Xv (P + L)/2	Xg - E121	+ E126 + $DE((($EG - $W)	+ F125*@Ll0.0000001*(H125 + H126 - H127 - H128)
	Zvu + C122	Zgu + E122	+ C126 - E12 + G125	+ F126*@LN(F126/G126 + (1 + (F126/G126) ^2) ^ 0.5) - (F126 ^ 2 + G126 ^ 2) ^ 0.5 + G126
	Zvl + C123	Zgl + E123	+ C127 - E12 + G126	+ F127*@LN(F127/G127 + (1 + (F127/G127) ^2) ^ 0.5) - (F127 ^ 2 + G127 ^ 2) ^ 0.5 + G127
			+ E126 + $DEl + G127	+ F128*@LN(F128/G128 + (1 + (F128/G128) ^2) ^ 0.5) - (F128 ^ 2 + G128 ^ 2) ^ 0.5 + G128
M73	Xv + C125	Xg - E125	+ E130 + $DE((($EG - $W)	+ F129*@Ll0.0000001*(H129 + H130 - H131 - H132)* - 1
	Zvu + C126	Zgu + E126	+ C130 - E13 + G129	+ F130*@LN(F130/G130 + (1 + (F130/G130) ^2) ^ 0.5) - (F130 ^ 2 + G130 ^ 2) ^ 0.5 + G130
	Zvl + C127	Zgl + E127	+ C131 - E13 + G130	+ F131*@LN(F131/G131 + (1 + (F131/G131) ^2) ^ 0.5) - (F131 ^ 2 + G131 ^ 2) ^ 0.5 + G131
			+ E130 + $DEl + G131	+ F132*@LN(F132/G132 + (1 + (F132/G132) ^2) ^ 0.5) - (F132 ^ 2 + G132 ^ 2) ^ 0.5 + G132

Horizontal pairs

M22	Xvl - (P + L)/2	Xgl - BG/2	+ $X + XGR - X($DELH + Z	+ F134*@Ll0.0000001*(H134 + H135 - H136 - H137)
	Xvr - (P - L)/2	Xgr + BG/2	- $X + XGL - X + G134	+ F135*@LN(F135/G135 + (1 + (F135/G135) ^2) ^ 0.5) - (F135 ^ 2 + G135 ^ 2) ^ 0.5 + G135
	Zv + H/2	Zg + AG	- $X + XGL - X + G135	+ F136*@LN(F136/G136 + (1 + (F136/G136) ^2) ^ 0.5) - (F136 ^ 2 + G136 ^ 2) ^ 0.5 + G136
			+ $X + XGR -) + G136	+ F137*@LN(F137/G137 + (1 + (F137/G137) ^2) ^ 0.5) - (F137 ^ 2 + G137 ^ 2) ^ 0.5 + G137
M24	Xvl + XVL	Xgl + XGL	+ $X + E139 - (($DELH + E	+ F138*@Ll0.0000001*(H138 + H139 - H140 - H141)* - 1
	Xvr + XVR	Xgr + XGR	+ $X + E138 - + G138	+ F139*@LN(F139/G139 + (1 + (F139/G139) ^2) ^ 0.5) - (F139 ^ 2 + G139 ^ 2) ^ 0.5 + G139
	Zv + ZV	Zg - ZG	+ $X + E138 - + G139	+ F140*@LN(F140/G140 + (1 + (F140/G140) ^2) ^ 0.5) - (F140 ^ 2 + G140 ^ 2) ^ 0.5 + G140
			+ $X + E139 - + G140	+ F141*@LN(F141/G141 + (1 + (F141/G141) ^2) ^ 0.5) - (F141 ^ 2 + G141 ^ 2) ^ 0.5 + G141
M42	Xvl + C138	Xgl + E138	+ $X + E143 - (($DELH + E	+ F142*@Ll0.0000001*(H142 + H143 - H144 - H145)* - 1
	Xvr + C139	Xgr + E139	+ $X + E142 - + G142	+ F143*@LN(F143/G143 + (1 + (F143/G143) ^2) ^ 0.5) - (F143 ^ 2 + G143 ^ 2) ^ 0.5 + G143
	Zv - C140	Zg - E140	+ $X + E142 - + G143	+ F144*@LN(F144/G144 + (1 + (F144/G144) ^2) ^ 0.5) - (F144 ^ 2 + G144 ^ 2) ^ 0.5 + G144
			+ $X + E143 - + G144	+ F145*@LN(F145/G145 + (1 + (F145/G145) ^2) ^ 0.5) - (F145 ^ 2 + G145 ^ 2) ^ 0.5 + G145
M44	Xvl + C142	Xgl + E142	+ $X + E147 - (($DELH + E	+ F146*@Ll0.0000001*(H146 + H147 - H148 - H149)
	Xvr + C143	Xgr + E143	+ $X + E146 - + G146	+ F147*@LN(F147/G147 + (1 + (F147/G147) ^2) ^ 0.5) - (F147 ^ 2 + G147 ^ 2) ^ 0.5 + G147
	Zv + C144	Zg - E144	+ $X + E146 - + G147	+ F148*@LN(F148/G148 + (1 + (F148/G148) ^2) ^ 0.5) - (F148 ^ 2 + G148 ^ 2) ^ 0.5 + G148
			+ $X + E147 - + G148	+ F149*@LN(F149/G149 + (1 + (F149/G149) ^2) ^ 0.5) - (F149 ^ 2 + G149 ^ 2) ^ 0.5 + G149
M62	Xvl (P - L)/2	Xgl + E146	+ $X + E151 - (($DELH + E	+ F150*@Ll0.0000001*(H150 + H151 - H152 - H153)* - 1
	Xvr (P + L)/2	Xgr + E147	+ $X + E150 - + G150	+ F151*@LN(F151/G151 + (1 + (F151/G151) ^2) ^ 0.5) - (F151 ^ 2 + G151 ^ 2) ^ 0.5 + G151
	Zv - C148	Zg - E148	+ $X + E150 - + G151	+ F152*@LN(F152/G152 + (1 + (F152/G152) ^2) ^ 0.5) - (F152 ^ 2 + G152 ^ 2) ^ 0.5 + G152
			+ $X + E151 - + G152	+ F153*@LN(F153/G153 + (1 + (F153/G153) ^2) ^ 0.5) - (F153 ^ 2 + G153 ^ 2) ^ 0.5 + G153
M64	Xvl + C150	Xgl + E150	+ $X + E155 - (($DELH + E	+ F154*@Ll0.0000001*(H154 + H155 - H156 - H157)
	Xvr + C151	Xgr + E151	+ $X + E154 - + G154	+ F155*@LN(F155/G155 + (1 + (F155/G155) ^2) ^ 0.5) - (F155 ^ 2 + G155 ^ 2) ^ 0.5 + G155
	Zv + C152	Zg - E152	+ $X + E154 - + G155	+ F156*@LN(F156/G156 + (1 + (F156/G156) ^2) ^ 0.5) - (F156 ^ 2 + G156 ^ 2) ^ 0.5 + G156
			+ $X + E155 - + G156	+ F157*@LN(F157/G157 + (1 + (F157/G157) ^2) ^ 0.5) - (F157 ^ 2 + G157 ^ 2) ^ 0.5 + G157
M82	Xvl + C154	Xgl + E154	+ $X + E159 - (($DELH + E	+ F158*@Ll0.0000001*(H158 + H159 - H160 - H161)
	Xvr + C155	Xgr + E155	+ $X + E158 - + G158	+ F159*@LN(F159/G159 + (1 + (F159/G159) ^2) ^ 0.5) - (F159 ^ 2 + G159 ^ 2) ^ 0.5 + G159
	Zv - C156	Zg - E156	+ $X + E158 - + G159	+ F160*@LN(F160/G160 + (1 + (F160/G160) ^2) ^ 0.5) - (F160 ^ 2 + G160 ^ 2) ^ 0.5 + G160
			+ $X + E159 - + G160	+ F161*@LN(F161/G161 + (1 + (F161/G161) ^2) ^ 0.5) - (F161 ^ 2 + G161 ^ 2) ^ 0.5 + G161
M84	Xvl + C158	Xgl + E158	+ $X + E163 - (($DELH + E	+ F162*@Ll0.0000001*(H162 + H163 - H164 - H165)* - 1
	Xvr + C159	Xgr + E159	+ $X + E162 - + G162	+ F163*@LN(F163/G163 + (1 + (F163/G163) ^2) ^ 0.5) - (F163 ^ 2 + G163 ^ 2) ^ 0.5 + G163
	Zv + C160	Zg - E160	+ $X + E162 - + G163	+ F164*@LN(F164/G164 + (1 + (F164/G164) ^2) ^ 0.5) - (F164 ^ 2 + G164 ^ 2) ^ 0.5 + G164
			+ $X + E163 - + G164	+ F165*@LN(F165/G165 + (1 + (F165/G165) ^2) ^ 0.5) - (F165 ^ 2 + G165 ^ 2) ^ 0.5 + G165

Macro Variables:

*(number of steps - 1)/2		endstep	250
*step size	m	delx	0.02
*increment for cal. dM/dy		dy	0.001
		delt	+DELX/V
		Ma	1.82E-10
		Mb	1.82E-10
		Mc	1.83E-10
		Mp	-9.36E-13
		Mn	+MA-MC
		Ip	206.7
		In	205.4
		x	5.0
		dely	-0.0
		Fg	0.5
		step	251.0
		M	@SUM(I101..I162)

Macro Outputs

average guidance drag	N	451.9
average guidance force	N	-101939
guidance force/guidance drag		225.59
guidance losses	W	60552

Guidance Macro

Macro 1: Turn off screen.	{FRAMEOFF}{WINDOWSOFF}
Set initial conditions.	{let Ip,0}{let mp,0}{let x,-endstep*delx}
Do a subroutine 2*endstep + 1 times.	{for step,-endstep,endstep,1,loop}
Calculate drag at time.	/ce201 ~ e201..e699 ~
Calculate average guidance drag.	{let d186,@sum(e201..e699)/20*delt*v/c*nb}
Calculate average guidance force.	{let d187,@sum(d200..d700)*delt*v/c*nb}
Calculate guidance losses.	{let d189,d186*v}
Set drag table to values.	/rve202..e699 ~ e202 ~
The end	{quit}
loop: Calculate M with y=yo.	{let dely,delyo} ~ {let Ma,M}
Calculate M with y=yo+dy.	{let dely,delyo+dy} ~ {let Mb,M}
Calculate M with y= -yo.	{let dely,-delyo} ~ {let Mc,M}
Calculate M with y= -yo-dy	{let dely,-delyo-dy} ~
Put Mtotal in table.	{put mactab,0,step+endstep,Mn}
Put I in table.	{put mactab,1,step+endstep,In}
Put guidanced force in table.	{put mactab,2,step+endstep,Fg}
Put now values in past positions.	{let Ip,In}{let Mp,Mn}{let x,x+delx}
	{return}

Table G-3. Sidewall null flux spreadsheet. (Cont.)

```
Calculated Parameters
Motor Constant                      Vs/m, N/A  Kmot   @SUM(I751..I850)/100*$ISC*$NB*2/@SQRT(2)*CTM
Motor Resistance per Block          V/A               +$NT*($AP+$P+0.3)*$LB/$P/@PI/$RPW^2/$CPW
Motor Inductance per Block          H                 0.0000002*(2*$AP*(@LN(4*$AP/(2*$NT+1)*$RPW+($NT-1)*$S$))+0.4978)+($P+0.3)/2*(@LN(2*($P+0.3)/(($NT+2)*$RPW+($NT/2-1)*$S$))+0.4978))*$NT^2*$LB/$P

Motor Constant Calculations (minor)          radians    dp     @PI*$SX/$P
(turns multipliers, phase inaccuracy degredation)       c2tm   2*@COS($DP/2)
                                                        c3tm   1+2*@COS($DP)
                                                        c4tm   +$C2TM+2*@COS($DP*1.5)
                                                        c5tm   +$C3TM+2*@COS($DP*2)
                                                        c6tm   +$C4TM+2*@COS($DP*2.5)
                                                        ctm    @IF(NT=1,1,@IF(NT=2,$C2TM,@IF(NT=3,$C3TM,@IF(NT=4,$C4TM,@IF(NT=5,$C5TM,@IF(NT=6,$C6TM,0))))))

Propulsion Calculations
Mutual inductance between vertical segments
                                        Lv              Dv
        M11   +$H/2+$AP-(((SEP-$W)/2+Lv*@LN(Lv    4.35E-09
              +$H/2+$AP++DV          +C103*@LN(C103/D103+(1+(C103/D103)^2)^0.5)-(C103^2+D103^2)^0.5+D103
              -$H/2+$AP-+D103        +C104*@LN(C104/D104+(1+(C104/D104)^2)^0.5)-(C104^2+D104^2)^0.5+D104
              -$H/2+$AP++D104        +C105*@LN(C105/D105+(1+(C105/D105)^2)^0.5)-(C105^2+D105^2)^0.5+D105

        M31   +LV     (((SEP-$W)/2+C107*@LN   -5.11E-09
              +C103   +D107     +C108*@LN(C108/D108+(1+(C108/D108)^2)^0.5)-(C108^2+D108^2)^0.5+D108
              +C104   +D108     +C109*@LN(C109/D109+(1+(C109/D109)^2)^0.5)-(C109^2+D109^2)^0.5+D109
              +C105   +D109     +C110*@LN(C110/D110+(1+(C110/D110)^2)^0.5)-(C110^2+D110^2)^0.5+D110

        M51   +C107   (((SEP-$W)/2+C112*@LN   -5.23E-09
              +C108   +D112     +C113*@LN(C113/D113+(1+(C113/D113)^2)^0.5)-(C113^2+D113^2)^0.5+D113
              +C109   +D113     +C114*@LN(C114/D114+(1+(C114/D114)^2)^0.5)-(C114^2+D114^2)^0.5+D114
              +C110   +D114     +C115*@LN(C115/D115+(1+(C115/D115)^2)^0.5)-(C115^2+D115^2)^0.5+D115

        M71   +C112   (((SEP-$W)/2+C117*@LN   6.36E-09
              +C113   +D117     +C118*@LN(C118/D118+(1+(C118/D118)^2)^0.5)-(C118^2+D118^2)^0.5+D118
              +C114   +D118     +C119*@LN(C119/D119+(1+(C119/D119)^2)^0.5)-(C119^2+D119^2)^0.5+D119
              +C115   +D119     +C120*@LN(C120/D120+(1+(C120/D120)^2)^0.5)-(C120^2+D120^2)^0.5+D120


Mutual inductance, upper horizontal winding
        M22   Xvl -($P+$L)/2   Xgl -$P      +$X+XGR-X(((SEP-$W)/2+G124*@LN  -2.41E-08
              Xvr -($P-$L)/2   Xgr        0 +$X+XGL-X+H124   -G125*@LN(G125/H125+(1+(G125/H125)^2)^0.5)-(G125^2+H125^2)^0.5+H125
              Zv +$H/2         Zg +$AP      +$X+XGL-X+H125   -G126*@LN(G126/H126+(1+(G126/H126)^2)^0.5)-(G126^2+H126^2)^0.5+H126
                                            +$X+XGR-)+H126   -G127*@LN(G127/H127+(1+(G127/H127)^2)^0.5)-(G127^2+H127^2)^0.5+H127

        M42   Xvl -($P+$L)/2   Xgl -$P      +$X+F130-I(((SEP-$W)/2-G129*@LN  2.40E-08
              Xvr -($P-$L)/2   Xgr        0 +$X+F129-I+H129  -G130*@LN(G130/H130+(1+(G130/H130)^2)^0.5)-(G130^2+H130^2)^0.5+H130
              Zv -$H/2         Zg +$AP      +$X+F129-I+H130  -G131*@LN(G131/H131+(1+(G131/H131)^2)^0.5)-(G131^2+H131^2)^0.5+H131
                                            +$X+F130-I+H131  -G132*@LN(G132/H132+(1+(G132/H132)^2)^0.5)-(G132^2+H132^2)^0.5+H132

        M62   Xvl ($P-$L)/2    Xgl -$P      +$X+F135-I(((SEP-$W)/2-G134*@LN  3.02E-08
              Xvr ($P+$L)/2    Xgr        0 +$X+F134-I+H134  -G135*@LN(G135/H135+(1+(G135/H135)^2)^0.5)-(G135^2+H135^2)^0.5+H135
              Zv +$H/2         Zg +$AP      +$X+F134-I+H135  -G136*@LN(G136/H136+(1+(G136/H136)^2)^0.5)-(G136^2+H136^2)^0.5+H136
                                            +$X+F135-I+H136  -G137*@LN(G137/H137+(1+(G137/H137)^2)^0.5)-(G137^2+H137^2)^0.5+H137

        M82   Xvl ($P-$L)/2    Xgl -$P      +$X+F140-I(((SEP-$W)/2-G139*@LN  -3.00E-08
              Xvr ($P+$L)/2    Xgr        0 +$X+F139-I+H139  -G140*@LN(G140/H140+(1+(G140/H140)^2)^0.5)-(G140^2+H140^2)^0.5+H140
              Zv -$H/2         Zg +$AP      +$X+F139-I+H140  -G141*@LN(G141/H141+(1+(G141/H141)^2)^0.5)-(G141^2+H141^2)^0.5+H141
                                            +$X+F140-I+H141  -G142*@LN(G142/H142+(1+(G142/H142)^2)^0.5)-(G142^2+H142^2)^0.5+H142


Mutual inductance, lower horizontal winding
        M24   Xvl -($P+$L)/2   Xgl        0 +$X+F147-I(((SEP-$W)/2-G146*@LN  -2.00E-08
              Xvr -($P-$L)/2   Xgr +$P      +$X+F146-I+H146  -G147*@LN(G147/H147+(1+(G147/H147)^2)^0.5)-(G147^2+H147^2)^0.5+H147
              Zv +$H/2         Zg -$AP      +$X+F146-I+H147  -G148*@LN(G148/H148+(1+(G148/H148)^2)^0.5)-(G148^2+H148^2)^0.5+H148
                                            +$X+F147-I+H148  -G149*@LN(G149/H149+(1+(G149/H149)^2)^0.5)-(G149^2+H149^2)^0.5+H149

        M44   Xvl -($P+$L)/2   Xgl        0 +$X+F152-I(((SEP-$W)/2-G151*@LN  2.00E-08
              Xvr -($P-$L)/2   Xgr +$P      +$X+F151-I+H151  -G152*@LN(G152/H152+(1+(G152/H152)^2)^0.5)-(G152^2+H152^2)^0.5+H152
              Zv -$H/2         Zg -$AP      +$X+F151-I+H152  -G153*@LN(G153/H153+(1+(G153/H153)^2)^0.5)-(G153^2+H153^2)^0.5+H153
                                            +$X+F152-I+H153  -G154*@LN(G154/H154+(1+(G154/H154)^2)^0.5)-(G154^2+H154^2)^0.5+H154

        M64   Xvl ($P-$L)/2    Xgl        0 +$X+F157-I(((SEP-$W)/2-G156*@LN  2.40E-08
              Xvr ($P+$L)/2    Xgr +$P      +$X+F156-I+H156  -G157*@LN(G157/H157+(1+(G157/H157)^2)^0.5)-(G157^2+H157^2)^0.5+H157
              Zv +$H/2         Zg -$AP      +$X+F156-I+H157  -G158*@LN(G158/H158+(1+(G158/H158)^2)^0.5)-(G158^2+H158^2)^0.5+H158
                                            +$X+F157-I+H158  -G159*@LN(G159/H159+(1+(G159/H159)^2)^0.5)-(G159^2+H159^2)^0.5+H159

        M84   Xvl ($P-$L)/2    Xgl        0 +$X+F162-I(((SEP-$W)/2-G161*@LN  -2.41E-08
              Xvr ($P+$L)/2    Xgr +$P      +$X+F161-I+H161  -G162*@LN(G162/H162+(1+(G162/H162)^2)^0.5)-(G162^2+H162^2)^0.5+H162
              Zv -$H/2         Zg -$AP      +$X+F161-I+H162  -G163*@LN(G163/H163+(1+(G163/H163)^2)^0.5)-(G163^2+H163^2)^0.5+H163
                                            +$X+F162-I+H163  -G164*@LN(G164/H164+(1+(G164/H164)^2)^0.5)-(G164^2+H164^2)^0.5+H164

Parameters for propulsion macro
*(number of steps - 1)/2                             endstep     500
*x step size                          m                xstep +P/100
starting x for table                  m               xstart -ENDSTEP*XSTEP
macro for loop counter                                  step     501
guideway - vehicle position           m      x                6.7635
vertical mutual inductance            H      Mpv            3.77E-10
horizontal mutual inductance, upper   H      Mphu           9.95E-11
horizontal mutual inductance, lower   H      Mphl          -3.70E-11
seed for expanding secondary table                       2*(B175-ERI+$E$800*@X-@PI*$E$80(E197-E174)@SIN(A175*@PI/$P)*H175

                 Macro that fills the mutual inductance table.
                       The macro's name is "tablefill.
                       The table name is mtable, at b300..d1301.
erase old table             /reb300..h1300
initial condition           {let x,xstart}~
for..do..loop               {for step,-endstep,endstep,1,loop}
expand central section      /cseed~e749..h851~
erase a starting problem    /reb300..d300~

store mutual inductances:   loop
   vertical                 {put mtable,0,endstep+step,mpv}
   horizontal upper         {put mtable,1,endstep+step,mphu}
   horizontal lower         {put mtable,2,endstep+step,mphl}
increment position          {let x,x+xstep}~
                            {return}
```

Table G-4. B field spreadsheet.

Three Dimensional B Field Calculation for fields generated by air core conducting filaments.

Each line of the bulk spreadsheet body represents a straight filament segment and calculates the field from this segment.

Point A is the beginning, current in, end of the segment. Point A is the other end of the segment. The field is calculated at point P.

The bulk of the calculations consist of transforming various points into a special coordinate system in which the B field is easy to calculate for that segment. The x axis of the transformed coordinates is parallel to line A–B.

The field for each segment is calculated for the transformed coordinates and then transformed back to the normal coordinate system.

Finally the B field components from each segment are summed.

For setting up the spreadsheet, each segment normally begins where the previous segment ended, and the current of each segment is normally the current of the previous segment.

Dimensions are meters and teslas.

xp	2		
yp	0		
zp	2.5		
Bx	@SUM(C63	Sum Bx	
By	@SUM(C64	Sum By	
Bz	@SUM(C65	Sum Bz	@SUM(Y91.@SUM(Y141..Y189)
Bmag	(C35^2+C:+C38*1000	gauss	

The core, repeated once for each straight filament, begins below.

xb	0.85
yb	0.5
zb	0.5
xa	−0.85
ya	0.5
za	0.5
I	600000
phi	@IF(XA=XB,@PI/2,@ATAN((YB−YA)/(XB−XA)))
test	@COS(PHI)*(XA−XB)+@SIN(PHI)*(YA−YB)
the	@IF(TEST=0,@PI/2,@ATAN((ZA−ZB)/(@COS(PHI)*(XA−XB)+@SIN(PHI)*(YA−YB))))
xta	@COS(THE)*@COS(PHI)*XA+@COS(THE)*@SIN(PHI)*YA+@SIN(THE)*ZA
yta	−@SIN(PHI)*XA+@COS(PHI)*YA
zta	−@COS(PHI)*@SIN(THE)*XA−@SIN(PHI)*@SIN(THE)*YA+@COS(THE)*ZA
xtb	@COS(THE)*@COS(PHI)*XB+@COS(THE)*@SIN(PHI)*YB+@SIN(THE)*ZB
xtp	@COS(THE)*@COS(PHI)*$XP+@COS(THE)*@SIN(PHI)*$YP+@SIN(THE)*$ZP
ytp	−@SIN(PHI)*$XP+@COS(PHI)*$YP
ztp	−@COS(PHI)*@SIN(THE)*$XP−@SIN(PHI)*@SIN(THE)*$YP+@COS(THE)*$ZP
rr	(YTP−YTA)^2+(ZTP−ZTA)^2
A	+XTA−XTP
B	+XTB−XTP
Byt	@IF(RR=0,0,0.0000001*I*(ZTA−ZTP)/RR*(B/(B^2+RR)^0.5−A/(A^2+RR)^0.5))
Bzt	@IF(RR=0,0,0.0000001*I*(YTP−YTA)/RR*(B/(B^2+RR)^0.5−A/(A^2+RR)^0.5))
Bx	−@SIN(PHI)*BYT−@COS(PHI)*@SIN(THE)*BZT
By	@COS(PHI)*BYT−@SIN(PHI)*@SIN(THE)*BZT
Bz	@COS(THE)*BZT

APPENDIX H

COMPLETE SPREADSHEETS FOR ELECTRODYNAMIC SYSTEMS

Table H-1. Summary of sidewall null flux calculations (134 m/s).

Operating Parameters	Units	baseline	J-single	J-10 car	BL-aero	5cm clear	600 kA	Rlc<BL	Rpw<BL
*Velocity	m/s	134	134	134	134	134	134	134	134
*Vehicle Vertical Position	m	0.0271	0.0292	0.0292	0.0271	0.0181	0.0459	0.0284	0.0271
*Vehicle Lateral Position	m	0.0136	0.0000	0.0000	0.0136	0.0000	0.0224	0.0000	0.0000
*Lateral Force	N	101920	0	0	101920	0	101920	0	0
Vehicle Description									
*Vehicle Weight	kg	40,000	40,000	400,000	40,000	40,000	40,000	40,000	40,000
*Vehicle Frontal Area	m^2	12.16	12.16	12.16	8.16	12.16	12.16	12.16	12.16
*Coefficient of Drag		0.3	0.3	1	0.3	0.3	0.3	0.3	0.3
*Mechanical Clearance, Vehicle to G'way	m	0.08	0.08	0.08	0.08	0.05	0.08	0.08	0.08
Vehicle Magnets									
*Magnet Pitch	m	1.35	2.7	2.7	1.35	1.35	1.35	1.35	1.35
*Magnet Height	m	0.5	0.5	0.5	0.5	0.5	0.5	0.5	0.5
*Magnet Length	m	1.2	2.2	2.2	1.2	1.2	1.2	1.2	1.2
Magnet Spacing, Side to Side	m	2.76	2.76	2.76	2.76	2.82	2.78	2.77	2.76
*Magnet Current	A	8E+05	8E+05	8E+05	8E+05	8E+05	6E+05	8E+05	8E+05
*Maximum SC Curent Density	A/m^2	2E+08	2E+08	2E+08	2E+08	2E+08	2E+08	2E+08	2E+08
*Maximum SC B Field	T	4	4	4	4	4	4	4	4
*Superconductor Wire Packing Density		0.5	0.5	0.5	0.5	0.5	0.5	0.5	0.5
*Superconductor Wire Density	kg/m^3	8000	8000	8000	8000	8000	8000	8000	8000
*Spacing, SC Surface to Vehicle Surface	m	0.06	0.06	0.06	0.06	0.06	0.06	0.06	0.06
*"Technology" Factor		5	5	5	5	5	5	5	5
*Number of Bogies		4	2	20	4	4	4	4	4
*Number of SC Coils per Bogie, each side		2	2	2	2	2	2	2	2
Radius of superconductor cable		0.0505	0.0505	0.0505	0.0505	0.0505	0.0437	0.0505	0.0505
Sidewall Levitation Coils									
*Coil Pitch	m	0.9	1.8	1.8	0.9	0.9	0.9	0.9	0.9
Coil Length	m	0.824	1.724	1.724	0.824	0.824	0.824	0.832	0.824
*Half Height	m	0.4	0.4	0.4	0.4	0.4	0.4	0.4	0.4
*Half Inner Spacing	m	0.1	0.1	0.1	0.1	0.1	0.1	0.1	0.1
*side-to-side spacing	m	3.2	3.2	3.2	3.2	3.2	3.2	3.2	3.2
*Coil Conductor Radius	m	0.028	0.028	0.028	0.028	0.028	0.028	0.024	0.028
*Coil Conductivity	A/V/m	3.7E+07	3.7E+07	3.7E+07	3.7E+07	3.7E+07	3.7E+07	3.7E+07	3.7E+07
*Coil Density	kg/m^3	2700	2700	2700	2700	2700	2700	2700	2700
*winding efficiency (lev. & guid.)		0.75	0.75	0.75	0.75	0.75	0.75	0.75	0.75

Table H-1. Summary of sidewall null flux calculations (134 m/s). (Cont.)

page 2

Sidewall Guidance Coils	Units	baseline	J-single	J-10 car	BL-aero	5cm clear	600 kA	Rlc<BL	Rpw<BL
*Coil Pitch	m	0.9	1.8	1.8	0.9	0.9	0.9	0.9	0.9
*Coil Length	m	0.84	1.74	1.74	0.84	0.84	0.84	0.84	0.84
*Half Height	m	0.25	0.25	0.25	0.25	0.25	0.25	0.25	0.25
*Coil Conductor Radius	m	0.02	0.02	0.02	0.02	0.02	0.02	0.02	0.02
*Coil Conductivity	A/V/m ^ 2	3.7E+07	3.7E+07	3.7E+07	3.7E+07	3.7E+07	3.7E+07	3.7E+07	3.7E+07
*Coil Density	kg/m ^ 3	2700	2700	2700	2700	2700	2700	2700	2700
Lateral Spacing	m	3.298	3.298	3.298	3.298	3.298	3.298	3.294	3.294
Motor									
Winding Pitch (same as vehicle magent pitch)		1.35	2.7	2.7	1.35	1.35	1.35	1.35	1.35
*Winding Half Height	m	0.35	0.35	0.35	0.35	0.35	0.35	0.35	0.35
*Number of Turns per Phase		6	6	6	6	6	6	6	6
*Number of Phases		3	3	3	3	3	3	3	3
*Radius of Conductor	m	0.015	0.015	0.015	0.015	0.015	0.015	0.015	0.013
*Block Length	m	1000	1000	1000	1000	1000	1000	1000	1000
Lateral Spacing	m	3.253	3.253	3.253	3.253	3.253	3.253	3.249	3.251
*Insulation spacing between turns	m	0.01	0.01	0.01	0.01	0.01	0.01	0.01	0.01
center-to-center turn spacing	m	0.04	0.04	0.04	0.04	0.04	0.04	0.04	0.036
*conductivity	A/(V*m)	3.7E+07	3.7E+07	3.7E+07	3.7E+07	3.7E+07	3.7E+07	3.7E+07	3.7E+07
*density	kg/m ^ 3	2700	2700	2700	2700	2700	2700	2700	2700
Calculated Parameters									
Aerodynamic Drag Power	W	5,400,000	5,400,000	18,000,000	3,622,438	5,400,000	5,400,000	5,400,000	5,400,000
Weight of Cryogenic System	kg	8,704	6,912	69,120	8,704	8,704	6,528	8,704	8,704
Motor Constant	Vs/m, N/A	30.2	13.4	133.8	30.2	34.0	23.1	30.9	30.4
Motor Resistance per Block	V/A	0.799	0.629	0.629	0.799	0.799	0.799	0.799	1.063
Motor Inductance per Block	H	0.024	0.021	0.021	0.024	0.024	0.024	0.024	0.025
Motor Open Circuit Voltage per Phase	Vrms	4,050	1,794	17,935	4,050	4,550	3,093	4,141	4,075
Motor Losses	W	562,560	2,212,851	323,345	274,116	415,357	1,082,383	551,777	724,598
Motor Reactive VA	VA	5,323,637	11,575,184	1,691,384	2,594,022	3,930,623	10,242,845	5,221,590	5,354,257
Lift Force	N	392,000	392,000	3,920,000	392,000	392,000	392,000	392,000	392,000
Drag Force	N	3,181	3,192	31,916	3,181	2,112	5,507	4,192	3,181
Lift/Drag (no guidance forces)		123.23	122.82	122.82	123.23	185.59	71.19	93.50	123.23
Lift Losses	W	426,258	427,680	4,276,799	426,258	283,027	737,899	561,793	426,258
Lateral guidance force	N	(101,920)	0	0	(101,920)	0	(101,920)	0	0
Lateral Losses	W	60,561	0	0	60,561	0	98,922	0	0
Guideway Levitation Aluminum	kg/m	49.8	44.9	44.9	49.8	49.8	49.8	36.9	49.8
Guideway Guidance Aluminum	kg/m	15.2	12.7	12.7	15.2	15.2	15.2	15.2	15.2
Guideway Propulsion Alumnium	kg/m	115.0	91.9	91.9	115.0	115.0	115.0	115.0	86.4
Motor Current	A	485	1083	414	338	416	672	480	477
Maximum Dynamic Breaking	g	0.021	0.009	0.093	0.021	0.026	0.012	0.022	0.020
Primary Natural Frequency	Hz	3.03	2.92	2.92	3.03	3.70	2.32	2.96	3.03

Table H-1. Summary of sidewall null flux calculations (89 m/s). (Cont.)

Operating Parameters	Units	baseline	J–single	J–10 car	BL–aero	5cm clear	600 kA	Rlc<BL	Rpw<BL
*Velocity	m/s	89	89	89	89	89	89	89	89
*Vehicle Vertical Position	m	0.0285	0.0332	0.0332	0.0285	0.0190	0.0487	0.0306	0.0285
*Vehicle Lateral Position	m	0.0099	0.0000	0.0000	0.0099	0.0000	0.0164	0.0000	0.0000
*Lateral Force	N	70560	0	0	70560	0	70560	0	0
Vehicle Description									
*Vehicle Weight	kg	40,000	40,000	400,000	40,000	40,000	40,000	40,000	40,000
*Vehicle Frontal Area	m^2	12.16	12.16	12.16	8.16	12.16	12.16	12.16	12.16
*Coefficient of Drag		0.3	0.3	1	0.3	0.3	0.3	0.3	0.3
*Mechanical Clearance, Vehicle to G'way	m	0.08	0.08	0.08	0.08	0.05	0.08	0.08	0.08
Vehicle Magnets									
*Magnet Pitch	m	1.35	2.7	2.7	1.35	1.35	1.35	1.35	1.35
*Magnet Height	m	0.5	0.5	0.5	0.5	0.5	0.5	0.5	0.5
*Magnet Length	m	1.2	2.2	2.2	1.2	1.2	1.2	1.2	1.2
Magnet Spacing, Side to Side	m	2.76	2.76	2.76	2.76	2.82	2.78	2.77	2.76
*Magnet Current	A	8E+05	8E+05	8E+05	8E+05	8E+05	6E+05	8E+05	8E+05
*Maximum SC Curent Density	A/m^2	2E+08	2E+08	2E+08	2E+08	2E+08	2E+08	2E+08	2E+08
*Maximum SC B Field	T	4	4	4	4	4	4	4	4
*Superconductor Wire Packing Density		0.5	0.5	0.5	0.5	0.5	0.5	0.5	0.5
*Superconductor Wire Density	kg/m^3	8000	8000	8000	8000	8000	8000	8000	8000
*Spacing, SC Surface to Vehicle Surface	m	0.06	0.06	0.06	0.06	0.06	0.06	0.06	0.06
*"Technology" Factor		5	5	5	5	5	5	5	5
*Number of Bogies		4	2	20	4	4	4	4	4
*Number of SC Coils per Bogie, each side		2	2	2	2	2	2	2	2
Radius of superconductor cable		0.0505	0.0505	0.0505	0.0505	0.0505	0.0437	0.0505	0.0505
Sidewall Levitation Coils									
*Coil Pitch	m	0.9	1.8	1.8	0.9	0.9	0.9	0.9	0.9
Coil Length	m	0.824	1.724	1.724	0.824	0.824	0.824	0.832	0.824
*Half Height	m	0.4	0.4	0.4	0.4	0.4	0.4	0.4	0.4
*Half Inner Spacing	m	0.1	0.1	0.1	0.1	0.1	0.1	0.1	0.1
*side–to–side spacing	m	3.2	3.2	3.2	3.2	3.2	3.2	3.2	3.2
*Coil Conductor Radius	m	0.028	0.028	0.028	0.028	0.028	0.028	0.024	0.028
*Coil Conductivity	A/V/m	3.7E+07	3.7E+07	3.7E+07	3.7E+07	3.7E+07	3.7E+07	3.7E+07	3.7E+07
*Coil Density	kg/m^3	2700	2700	2700	2700	2700	2700	2700	2700
*winding efficiency (lev. & guid.)		0.75	0.75	0.75	0.75	0.75	0.75	0.75	0.75

Table H-1. Summary of sidewall null flux calculations (89 m/s). (Cont.)

Sidewall Guidance Coils	Units	baseline	J-single	J-10 car	BL-aero	5cm clear	600 kA	Rlc<BL	Rpw<BL
*Coil Pitch	m	0.9	1.8	1.8	0.9	0.9	0.9	0.9	0.9
*Coil Length	m	0.84	1.74	1.74	0.84	0.84	0.84	0.84	0.84
*Half Height	m	0.25	0.25	0.25	0.25	0.25	0.25	0.25	0.25
*Coil Conductor Radius	m	0.02	0.02	0.02	0.02	0.02	0.02	0.02	0.02
*Coil Conductivity	A/V/m ^ 2	3.7E+07	3.7E+07	3.7E+07	3.7E+07	3.7E+07	3.7E+07	3.7E+07	3.7E+07
*Coil Density	kg/m ^ 3	2700	2700	2700	2700	2700	2700	2700	2700
Lateral Spacing	m	3.298	3.298	3.298	3.298	3.298	3.298	3.294	3.294
Motor									
Winding Pitch (same as vehicle magent pitch)		1.35	2.7	2.7	1.35	1.35	1.35	1.35	1.35
*Winding Half Height	m	0.35	0.35	0.35	0.35	0.35	0.35	0.35	0.35
*Number of Turns per Phase		6	6	6	6	6	6	6	6
*Number of Phases		3	3	3	3	3	3	3	3
*Radius of Conductor	m	0.015	0.015	0.015	0.015	0.015	0.015	0.015	0.013
*Block Length	m	1000	1000	1000	1000	1000	1000	1000	1000
Lateral Spacing	m	3.253	3.253	3.253	3.253	3.253	3.253	3.249	3.251
*Insulation spacing between turns	m	0.01	0.01	0.01	0.01	0.01	0.01	0.01	0.01
center-to-center turn spacing	m	0.04	0.04	0.04	0.04	0.04	0.04	0.04	0.036
*conductivity	A/(V*m)	3.7E+07	3.7E+07	3.7E+07	3.7E+07	3.7E+07	3.7E+07	3.7E+07	3.7E+07
*density	kg/m ^ 3	2700	2700	2700	2700	2700	2700	2700	2700
Calculated Parameters									
Aerodynamic Drag Power	W	1,582,156	1,582,156	5,273,854	1,061,345	1,582,156	1,582,156	1,582,156	1,582,156
Weight of Cryogenic System	kg	8,704	6,912	69,120	8,704	8,704	6,528	8,704	8,704
Motor Constant	Vs/m, N/A	30.2	13.4	133.6	30.2	33.9	23.1	30.9	30.4
Motor Resistance per Block	V/A	0.799	0.629	0.629	0.799	0.799	0.799	0.799	1.063
Motor Inductance per Block	H	0.024	0.021	0.021	0.024	0.024	0.024	0.024	0.025
Motor Open Circuit Voltage per Phase	Vrms	2,689	1,189	11,895	2,689	3,021	2,052	2,749	2,705
Motor Losses	W	156,685	634,869	152,739	87,548	103,091	369,637	168,858	199,967
Motor Reactive VA	VA	984,811	2,205,694	530,654	550,261	647,953	2,323,271	1,061,320	981,398
Lift Force	N	392,000	392,000	3,920,000	392,000	392,000	392,000	392,000	392,000
Drag Force	N	5,054	5,483	54,834	5,054	3,348	8,819	6,818	5,054
Lift/Drag (no guidance forces)		77.56	71.49	71.49	77.56	117.10	44.45	57.50	77.56
Lift Losses	W	449,813	488,024	4,880,245	449,813	297,944	784,915	606,799	449,813
Lateral guidance force	N	(70,560)	0	0	(70,560)	0	(70,560)	0	0
Lateral Losses	W	30,606	0	0	30,606	0	50,278	0	0
Guideway Levitation Aluminum	kg/m	49.8	44.9	44.9	49.8	49.8	49.8	36.9	49.8
Guideway Guidance Aluminum	kg/m	15.2	12.7	12.7	15.2	15.2	15.2	15.2	15.2
Guideway Propulsion Alumnium	kg/m	115.0	91.9	91.9	115.0	115.0	115.0	115.0	86.4
Motor Current	A	256	580	285	191	207	393	265	250
Maximum Dynamic Breaking	g	0.021	0.009	0.093	0.021	0.026	0.012	0.022	0.020
Primary Natural Frequency	Hz	2.95	2.74	2.74	2.95	3.61	2.26	2.85	2.95

Table H-2. Summary of hybrid null flux calculations. (Cont.)

page 2

Motor	Units	134 m/s	134, no T	89 m/s	89, no T	134 Aero	5 cm clear	600 kA	d=.004	4mm, 89m/s	P=1m	P&d<BL	P,d,89
Winding to Superconducting Magnet Spacing	m	0.210	0.210	0.210	0.210	0.210	0.180	0.187	0.210	0.210	0.224	0.224	0.224
*Winding Width	m	0.707	0.707	0.707	0.707	0.707	0.707	0.707	0.707	0.707	0.707	0.707	0.707
*Number of Magnet Units (per Vehicle)		6	6	6	6	6	6	6	6	6	6	6	6
*Radius of Conductor	m	0.02	0.02	0.02	0.02	0.02	0.02	0.02	0.02	0.02	0.02	0.02	0.02
*Number of Phases		3	3	3	3	3	3	3	3	3	3	3	3
*Turns per Phase		5	5	5	5	5	5	5	5	5	5	5	5
*Block Length	m	1000	1000	1000	1000	1000	1000	1000	1000	1000	1000	1000	1000
*Insulation Spacing between Turns	m	0.014	0.014	0.014	0.014	0.014	0.014	0.014	0.014	0.014	0.014	0.014	0.014
Current Density	A/m ^ 2	7.42E+05	6.58E+05	3.84E+05	3.22E+05	6.82E+05	6.52E+05	9.39E+05	7.31E+05	3.84E+05	8.29E+05	6.99E+05	3.38E+05
Calculated parameters													
Cryosystem Weight	kg	14,045	14,045	14,045	14,045	14,045	14,045	10,534	14,045	14,045	9,245	9,245	9,245
First Harmonic, Open Circuit Motor V	V	2560	2560	1701	1701	2560	2916	2124	2561	1702	2408	2408	1600
Motor Resistance per Phase–Block	V/A	0.291	0.291	0.291	0.291	0.291	0.291	0.291	0.291	0.291	0.367	0.367	0.367
Motor Phase Inductance	H	0.044	0.044	0.044	0.044	0.044	0.044	0.044	0.044	0.044	0.046	0.046	0.046
Motor Phase Reactance	V/A	9.25	9.25	6.14	6.14	9.25	9.25	9.25	9.25	6.14	19.42	19.42	12.90
Guideway Levitation Mass per Meter	kg/m	25.9	25.9	25.9	25.9	25.9	25.9	26.1	17.3	17.3	25.9	17.3	17.3
Guideway Gudance Mass per Meter	kg/m	13.0	13.0	13.0	13.0	13.0	13.0	13.1	8.6	8.6	13.0	8.6	8.6
Guideway Motor Mass per Meter	kg/m	45.9	45.9	45.9	45.9	45.9	45.9	45.9	45.9	45.9	57.9	57.9	57.9
Magnetic Drag, No Lateral Force	N	7068	7067	5444	5443	7067	7068	5056	3164	3239	14150	4490	3298
Magnetic Lift to Drag Ratio, No Lateral Force		55.5	55.5	72.0	72.0	55.5	55.5	77.5	123.9	121.0	27.7	87.3	118.8
Required Propulsive Force	n	53,463	47,365	27,643	23,220	49,141	53,463	56,124	52,640	27,703	56,145	47,343	22,934
Required Motor Output	w	7,164,039	6,346,974	2,460,218	2,066,621	6,584,836	7,164,039	7,520,656	7,053,788	2,465,527	7,523,447	6,343,969	2,041,131
Required In–Phase Motor Current	Arms	933	826	482	405	857	819	1180	918	483	1042	878	425
Reactive Voltage	V	8629	7645	2962	2488	7931	7575	10915	8493	2966	20232	17058	5487
Motor Constant per Phase	N/A	19.1	19.1	19.1	19.1	19.1	21.8	15.9	19.1	19.1	18.0	18.0	18.0
Motor Current per .15g per Phase	A	1026	1026	1026	1026	1026	901	1236	1026	1025	1091	1091	1091
Motor Current per .21g per Phase	A	1436	1436	1436	1436	1436	1261	1731	1436	1435	1527	1527	1527
Best Dynamic Breaking Deceleration	g	0.020	0.020	0.020	0.020	0.020	0.026	0.014	0.020	0.020	0.009	0.009	0.009
Reactive kVA	kVA	24,149	18,954	4,285	3,024	20,402	18,612	38,640	23,395	4,297	63,228	44,946	7,002
Lateral Drag	N	120	0	87	0	0	120	213	180	131	33	50	36
Torque for Lateral Force	Nm	3E+05	0E+00	2E+05	0E+00	0E+00	3E+05	3E+05	3E+05	2E+05	3E+05	3E+05	2E+05
Drag for Lateral Torque	N	5977	0	4335	0	0	5977	10557	8997	6555	1664	2504	1822
Lift Loss	MW	0.947	0.947	0.484	0.484	0.947	0.947	0.677	0.424	0.288	1.896	0.602	0.294
Loss from Lateral Drag	MW	0.016	0.000	0.008	0.000	0.000	0.016	0.029	0.024	0.012	0.004	0.007	0.003
Loss from Lateral Torque	MW	0.801	0.000	0.386	0.000	0.000	0.801	1.415	1.206	0.583	0.223	0.336	0.162
Total Magnetic Losses	MW	1.764	0.947	0.878	0.484	0.947	1.764	2.121	1.654	0.883	2.123	0.944	0.459
Total Motor Winding Losses	MW	0.760	0.597	0.203	0.143	0.642	0.586	1.216	0.736	0.204	1.195	0.850	0.199
Wind Drag Loss	MW	5.400	5.400	1.582	1.582	5.638	5.400	5.400	5.400	1.582	5.400	5.400	1.582
Primary Suspension Natural Frequency	Hz	4.06	4.06	4.06	4.06	4.06	4.06	3.05	4.06	4.04	6.85	6.84	6.81

Table H-2. Summary of hybrid null flux calculations.

Operating Parameters	Units	134 m/s	134, no T	89 m/s	89, no T	134 Aero	5 cm clear	600 kA	d=.004	4mm, 89m/s	P=1m	P&d<BL	P,d,89
*Velocity	m/s	134	134	89	89	134	134	134	134	89	134	134	89
*Vehicle Vertical Position	m	0.0150	0.0150	0.0151	0.0151	0.0150	0.0150	0.0267	0.0151	0.0152	0.0053	0.0053	0.0053
*Differential Vertical Position (produces torque)	m	0.0195	0.0000	0.0136	0.0000	0.0000	0.0195	0.0346	0.0196	0.0137	0.0069	0.0069	0.0048
*Vehicle Lateral Position	m	0.0078	0.0000	0.0054	0.0000	0.0000	0.0078	0.0139	0.0079	0.0055	0.0027	0.0028	0.0019
*Lateral Force Required	g	0.26	0	0.18	0	0	0.26	0.26	0.26	0.18	0.26	0.26	0.18
*Lateral Force Arm above Levitation Sheet	m	2	2	2	2	2	2	2	2	2	2	2	2
Torque from Lateral Force	Nm	254,800	0	176,400	0	0	254,800	254,800	254,800	176,400	254,800	254,800	176,400
Vehicle Description													
*Vehicle Frontal Area	m^2	12.16	12.16	12.16	12.16	12.70	12.16	12.16	12.16	12.16	12.16	12.16	12.16
*Drag Coefficient		0.3	0.3	0.3	0.3	0.3	0.3	0.3	0.3	0.3	0.3	0.3	0.3
*Vehicle Weight	kg	40,000	40,000	40,000	40,000	40,000	40,000	40,000	40,000	40,000	40,000	40,000	40,000
*Mechanical Clearance, Vehicle to Guideway	m	0.08	0.08	0.08	0.08	0.08	0.05	0.08	0.08	0.08	0.08	0.08	0.08
Vehicle Magnets													
*Magnet Length	m	1.7	1.7	1.7	1.7	1.7	1.7	1.7	1.7	1.7	0.7	0.7	0.7
*Pole Pitch	m	2	2	2	2	2	2	2	2	2	1	1	1
*"Width"	m	1	1	1	1	1	1	1	1	1	1	1	1
*Main Conductor Current	A	8E+05	8E+05	8E+05	8E+05	8E+05	8E+05	6E+05	8E+05	8E+05	8E+05	8E+05	8E+05
Radius of Main Superconductor	m	0.0505	0.0505	0.0505	0.0505	0.0505	0.0505	0.0437	0.0505	0.0505	0.0505	0.0505	0.0505
Radius of "Shield" Superconductor	m	0.0252	0.0252	0.0252	0.0252	0.0252	0.0252	0.0219	0.0252	0.0252	0.0252	0.0252	0.0252
*Number of Magnet Units per Bogie		3	3	3	3	3	3	3	3	3	3	3	3
*Number of Bogies		2	2	2	2	2	2	2	2	2	2	2	2
*Superconducting Current Density	A/m^2	2E+08	2E+08	2E+08	2E+08	2E+08	2E+08	2E+08	2E+08	2E+08	2E+08	2E+08	2E+08
*Superconducting Wire Density	kg/m^3	8E+03	8E+03	8E+03	8E+03	8E+03	8E+03	8E+03	8E+03	8E+03	8E+03	8E+03	8E+03
*"Technology" Factor		5	5	5	5	5	5	5	5	5	5	5	5
*Max B Field Seen by Superconductors	Vs/m^2	4	4	4	4	4	4	4	4	4	4	4	4
*Superconductor Wire Packing Density		0.5	0.5	0.5	0.5	0.5	0.5	0.5	0.5	0.5	0.5	0.5	0.5
*Spacing, SC Surface to Vehicle Surface	m	0.06	0.06	0.06	0.06	0.06	0.06	0.06	0.06	0.06	0.06	0.06	0.06
Guideway													
*Levitation Sheet Thickness	m	0.006	0.006	0.006	0.006	0.006	0.006	0.006	0.004	0.004	0.006	0.004	0.004
*Guidance Sheet Thickness	m	0.006	0.006	0.006	0.006	0.006	0.006	0.006	0.004	0.004	0.006	0.004	0.004
*Levitation Sheet Width	m	1.60	1.60	1.60	1.60	1.60	1.60	1.61	1.60	1.60	1.60	1.60	1.60
*Guidance Sheet Width	m	0.80	0.80	0.80	0.80	0.80	0.80	0.81	0.80	0.80	0.80	0.80	0.80
*Guideway Conductivity	A/Vm	4E+07	4E+07	4E+07	4E+07	4E+07	4E+07	4E+07	4E+07	4E+07	4E+07	4E+07	4E+07
*Guideway Density	kg/m^3	3E+03	3E+03	3E+03	3E+03	3E+03	3E+03	3E+03	3E+03	3E+03	3E+03	3E+03	3E+03

Table H-2.1. Hybrid null flux optimizations.

Operating Parameters	Units	op1@.26	op1@.09	op2@.09	op2@.26	op3@.18	op3@.06	op4@.06	op4@.18
*Velocity	m/s	134	134	134	134	89	89	89	89
*Vehicle Vertical Position	m	0.0150	0.0150	0.0151	0.0151	0.0151	0.0151	0.0152	0.0152
*Differential Vertical Position (produces torque)	m	0.0195	0.0068	0.0068	0.0196	0.0136	0.0045	0.0046	0.0137
*Vehicle Lateral Position	m	0.0080	0.0028	0.0028	0.0082	0.0056	0.0019	0.0020	0.0060
*Lateral Force Required	g	0.26	0.09	0.09	0.26	0.18	0.06	0.06	0.18
*Lateral Force Arm above Levitation Sheet	m	2	2	2	2	2	2	2	2
Torque from Lateral Force	Nm	254,800	88,200	88,200	254,800	176,400	58,800	58,800	176,400
Vehicle Description									
*Vehicle Frontal Area	m^2	12.16	12.16	12.16	12.16	12.16	12.16	12.16	12.16
*Drag Coefficient		0.3	0.3	0.3	0.3	0.3	0.3	0.3	0.3
*Vehicle Weight	kg	40,000	40,000	40,000	40,000	40,000	40,000	40,000	40,000
*Mechanical Clearance, Vehicle to Guideway	m	0.08	0.08	0.08	0.08	0.08	0.08	0.08	0.08
Vehicle Magnets									
*Magnet Length	m	1.7	1.7	1.7	1.7	1.7	1.7	1.7	1.7
*Pole Pitch	m	2	2	2	2	2	2	2	2
*"Width"	m	1	1	1	1	1	1	1	1
*Main Conductor Current	A	8E+05	8E+05	8E+05	8E+05	8E+05	8E+05	8E+05	8E+05
Radius of Main Superconductor	m	0.0505	0.0505	0.0505	0.0505	0.0505	0.0505	0.0505	0.0505
Radius of "Shield" Superconductor	m	0.0252	0.0252	0.0252	0.0252	0.0252	0.0252	0.0252	0.0252
*Number of Magnet Units per Bogie		3	3	3	3	3	3	3	3
*Number of Bogies		2	2	2	2	2	2	2	2
*Superconducting Current Density	A/m^2	2E+08	2E+08	2E+08	2E+08	2E+08	2E+08	2E+08	2E+08
*Superconducting Wire Density	kg/m^3	8E+03	8E+03	8E+03	8E+03	8E+03	8E+03	8E+03	8E+03
*"Technology" Factor		5	5	5	5	5	5	5	5
*Max B Field Seen by Superconductors	Vs/m^2	4	4	4	4	4	4	4	4
*Superconductor Wire Packing Density		0.5	0.5	0.5	0.5	0.5	0.5	0.5	0.5
*Spacing, SC Surface to Vehicle Surface	m	0.06	0.06	0.06	0.06	0.06	0.06	0.06	0.06
Guideway									
*Levitation Sheet Thickness	m	0.0052	0.0052	0.0036	0.0036	0.0055	0.0055	0.0042	0.0042
*Guidance Sheet Thickness	m	0.0023	0.0023	0.0014	0.0014	0.0024	0.0024	0.0014	0.0014
*Levitation Sheet Width	m	1.60	1.60	1.60	1.60	1.60	1.60	1.60	1.60
*Guidance Sheet Width	m	0.80	0.80	0.80	0.80	0.80	0.80	0.80	0.80
*Guideway Conductivity	A/Vm	4E+07	4E+07	4E+07	4E+07	4E+07	4E+07	4E+07	4E+07
*Guideway Density	kg/m^3	3E+03	3E+03	3E+03	3E+03	3E+03	3E+03	3E+03	3E+03

Table H-2.1. Hybrid null flux optimizations. (Cont.)

Motor	Units	op1@.26	op1@.09	op2@.09	op2@.26	op3@.18	op3@.06	op4@.06	op4@.18
Winding to Superconducting Magnet Spacing	m	0.210	0.210	0.210	0.210	0.210	0.210	0.210	0.210
*Winding Width	m	0.707	0.707	0.707	0.707	0.707	0.707	0.707	0.707
*Number of Magnet Units (per Vehicle)		6	6	6	6	6	6	6	6
*Radius of Conductor	m	0.02	0.02	0.02	0.02	0.02	0.02	0.02	0.02
*Number of Phases		3	3	3	3	3	3	3	3
*Turns per Phase		5	5	5	5	5	5	5	5
*Block Length	m	1000	1000	1000	1000	1000	1000	1000	1000
*Insulation Spacing between Turns	m	0.014	0.014	0.014	0.014	0.014	0.014	0.014	0.014
Current Density	A/m^2	7.13E+05	6.25E+05	6.10E+05	7.39E+05	3.66E+05	3.05E+05	2.97E+05	3.79E+05

Calculated parameters

Cryosystem Weight	kg	14,045	14,045	14,045	14,045	14,045	14,045	14,045	14,045
First Harmonic, Open Circuit Motor V	V	2560	2560	2561	2561	1701	1701	1702	1702
Motor Resistance per Phase–Block	V/A	0.291	0.291	0.291	0.291	0.291	0.291	0.291	0.291
Motor Phase Inductance	H	0.044	0.044	0.044	0.044	0.044	0.044	0.044	0.044
Motor Phase Reactance	V/A	9.25	9.25	9.25	9.25	6.14	6.14	6.14	6.14
Guideway Levitation Mass per Meter	kg/m	22.5	22.5	15.5	15.5	23.7	23.7	18.1	18.1
Guideway Gudance Mass per Meter	kg/m	5.0	5.0	3.0	3.0	5.2	5.2	3.0	3.0
Guideway Motor Mass per Meter	kg/m	45.9	45.9	45.9	45.9	45.9	45.9	45.9	45.9
Magnetic Drag, No Lateral Force	N	3823	3823	2400	2400	3658	3658	2880	2880
Magnetic Lift to Drag Ratio, No Lateral Force		102.5	102.5	163.4	163.4	107.2	107.2	136.1	136.1
Required Propulsive Force	n	51,342	44,989	43,966	53,249	26,395	21,987	21,397	27,306
Required Motor Output	w	6,879,779	6,028,462	5,891,391	7,135,314	2,349,125	1,956,831	1,904,341	2,430,218
Required In–Phase Motor Current	Arms	896	785	767	929	460	383	373	476
Reactive Voltage	V	8286	7260	7093	8590	2828	2356	2291	2924
Motor Constant per Phase	N/A	19.1	19.1	19.1	19.1	19.1	19.1	19.1	19.1
Motor Current per .15g per Phase	A	1026	1026	1026	1026	1026	1026	1025	1025
Motor Current per .21g per Phase	A	1436	1436	1436	1436	1436	1436	1435	1435
Best Dynamic Breaking Deceleration	g	0.020	0.020	0.020	0.020	0.020	0.020	0.020	0.020
Reactive kVA	kVA	22,266	17,097	16,315	23,933	3,906	2,710	2,564	4,176
Lateral Drag	N	318	38	65	539	224	25	46	414
Torque for Lateral Force	Nm	3E+05	9E+04	9E+04	3E+05	2E+05	6E+04	6E+04	2E+05
Drag for Lateral Torque	N	6903	829	1203	10011	4735	527	694	6235
Lift Loss	MW	0.512	0.512	0.322	0.322	0.326	0.326	0.256	0.256
Loss from Lateral Drag	MW	0.043	0.005	0.009	0.072	0.020	0.002	0.004	0.037
Loss from Lateral Torque	MW	0.925	0.111	0.161	1.342	0.421	0.047	0.062	0.555
Total Magnetic Losses	MW	1.480	0.628	0.491	1.735	0.767	0.375	0.322	0.848
Total Motor Winding Losses	MW	0.701	0.538	0.513	0.753	0.185	0.128	0.122	0.198
Wind Drag Loss	MW	5.400	5.400	5.400	5.400	1.582	1.582	1.582	1.582
Primary Suspension Natural Frequency	Hz	4.06	4.06	4.05	4.05	4.05	4.05	4.04	4.04

Table H-3. Summary of image flux calculations.

Operating Parameters	Units	134 m/s	134, no T	134 Aero	89 m/s	89,HSI	d=.01	10mm, 89	P=1 m
*velocity	m/s	134	134	134	89	89	134	89	134
*lateral force	g	0.26	0	0.26	0.18	0.18	0.26	0.18	0.26
*vehicle vertical position, +=up, 0=norrm		0	0	0	0	−0.00005	0	0	0
Vehicle Description									
*assumed frontal area	m ^ 2	12.16	12.16	8.54	12.16	12.16	12.16	12.16	12.16
*drag coefficient		0.3	0.3	0.35	0.3	0.3	0.3	0.3	0.3
*total vehicle operating mass	kg	40,000	40,000	40,000	40,000	40,000	40,000	40,000	40,000
*height above arc (headroom)	m	1.87	1.87	1.87	1.87	1.87	1.87	1.87	1.87
Vehicle Magnet Parameters									
*pole pitch	m	1.5	1.5	1.5	1.5	1.5	1.5	1.5	1
*magnet length	m	1.3	1.3	1.3	1.3	1.3	1.3	1.3	0.8
*center angle	degree	30	30	30	30	30	30	30	30
*total angle	degree	112	112	112	112	112	112	112	112
*vehicle skin outer bottom radius	m	2.1	2.1	2.1	2.1	2.1	2.1	2.1	2.1
*central current	A	582,528	582,528	582,528	582,632	582,528	582,636	583,032	620,540
*outer current	A	145,632	145,632	145,632	145,658	145,632	145,659	145,758	155,135
*central coils per cluster (3)		3	3	3	3	3	3	3	3
*outter coil pairs per cluster (1 or 3)		3	3	3	3	3	3	3	3
*clusters per vehicle		3	3	3	3	3	3	3	3
*superconducting current density	A/m ^ 2	2.0E+08	2.0E+08	2.0E+08	2.0E+08	2.0E+08	2.0E+08	2E+08	2.0E+08
*superconducting wire density	kg/m ^ 3	8E+03	8E+03	8E+03	8E+03	8E+03	8E+03	8E+03	8E+03
*"technology" factor		5	5	5	5	5	5	5	5
*superconductor to skin distance	m	0.06	0.06	0.06	0.06	0.06	0.06	0.06	0.06
*max B field in superconductor	Vs/m ^ 2	4	4	4	4	4	4	4	4
*superconductor wire packing density		0.5	0.5	0.5	0.5	0.5	0.5	0.5	0.5
Guideway Levitation Parameters									
radius, upper guideway surface	m	2.25	2.25	2.25	2.25	2.25	2.25	2.25	2.25
*central angle	degrees	40	40	40	40	40	40	40	40
*total angle	degrees	140	140	140	140	140	140	140	140
*levitation sheet thickness	m	0.02	0.02	0.02	0.02	0.02	0.01	0.01	0.02
*levitation sheet conductivity	A/Vm	3.7E+07	3.7E+07	3.7E+07	3.7E+07	3.7E+07	3.7E+07	3.7E+07	3.7E+07
*guideway density	kg/m ^ 3	2.7E+03	2.7E+03	2.7E+03	2.7E+03	2.7E+03	2.7E+03	2.7E+03	2.7E+03

Table H-3. Summary of image flux calculations. (Cont.)

Guideway Motor Parameters	Units	134 m/s	134, no T	134 Aero	89 m/s	89,HSI	d=.01	10mm, 89	P=1 m
*motor wire radius	m	0.02	0.02	0.02	0.02	0.02	0.02	0.02	0.02
*number of phases		3	3	3	3	3	3	3	3
*turns per phase		5	5	5	5	5	5	5	5
*block length	m	1000	1000	1000	1000	1000	1000	1000	1000
*spacing, windings to g'way surface	m	0.01	0.01	0.01	0.01	0.01	0.01	0.01	0.01
*winding width angle	degrees	30	30	30	30	30	30	30	30
*winding conductivity	A/Vm	3.7E+07	3.7E+07	3.7E+07	3.7E+07	3.7E+07	3.7E+07	3.7E+07	3.7E+07
*winding density	kg/m^3	2.7E+03	2.7E+03	2.7E+03	2.7E+03	2.7E+03	2.7E+03	2.7E+03	2.7E+03
Calculated Parameters									
vehicle frontal area	m^2	8.54	8.54	8.54	8.54	8.54	8.54	8.54	8.54
cryosystem weight	kg	6,497	6,497	6,497	6,498	6,497	6,498	6,503	5,804
first harmonic, open circuit motor V	Vrms	4,144	4,144	4,144	2,753	2,753	4,145	2,755	4,491
motor resistance per phase–block	V/A	0.193	0.193	0.193	0.193	0.193	0.193	0.193	0.236
motor inductance per phase–block	H	0.020	0.020	0.020	0.020	0.020	0.020	0.020	0.025
motor reactance per phase–block	V/A	5.69	5.69	5.69	3.78	3.78	5.69	3.78	10.44
guideway levitation mass per meter	kg/m	213.0	213.0	213.0	213.0	213.0	106.3	106.3	213.0
guideway motor mass per meter	kg/m	30.5	30.5	30.5	30.5	30.5	30.5	30.5	37.2
levitation force	N	391,998	391,998	391,998	391,999	392,000	391,998	392,000	392,001
magnetic drag force	N	10,164	10,164	10,164	12,472	12,472	12,583	18,946	12,449
motor constant per phase	N/A	30.9	30.9	30.9	30.9	30.9	30.9	31.0	33.5
maximum deceleration	g	0.086	0.086	0.086	0.086	0.086	0.086	0.086	0.055
motor current per phase	Arms	544	544	465	326	326	570	395	525
motor reactive power, total	kVA	5,052	5,052	3,695	1,205	1,205	5,546	1,774	8,619
motor winding losses	MW	0.171	0.171	0.125	0.062	0.062	0.188	0.091	0.195
lift loss	MW	1.362	1.362	1.362	1.110	1.110	1.686	1.686	1.668
lateral loss	MW	0.427	0.000	0.427	0.241	0.241	0.529	0.366	0.523
wind drag power	MW	5.40	5.40	4.42	1.58	1.58	5.40	1.58	5.40
primary suspension natural frequency	Hz	1.04	1.04	1.04	1.04	1.04	1.04	1.04	1.03
		134 m/s	134, no T	134 Aero	89 m/s	89,HSI	d=.01	10mm, 89	P=1 m

REFERENCES

EMS Vertical Magnets (or Lateral Magnets)

1. Weinberg, M.S., "Electromagnetic Suspensions for Ground Transportation", Ph.D. Thesis, M.I.T., Cambridge, MA, December, 1973.

2. Wormley, D.N. et al, "Noncontacting Suspension and Propulsion for Ground Transportation," Final First Year Report, U.S.D.O.T. Report DOT/RSPA/DPB-50/79/34(NTIS PB 80-176274), December, 1979.

3. Yamamura, S., and Ito, T., "Analysis of Speed Characteristics of Attracting Magnetic Levitation of Vehicles," IEEE Transactions on Magnetics Vol. Mag-ll, No. 5, September, 1975, pp. 1504-7.

4. Roters, H.C., "Electromagnetic Devices", J. Wiley and Sons, N.Y., 1941.

5. Borcherts, R.H., Davis, L.C., Wan, C.C., Mahdulla, A.V., Reitz, J.R., "Parameter Optimizations Studies of Magnetic Suspensions for High Speed Ground Transportation," Ford Motor Co. and FRA, Report No. FRA/ORD-74/42(NTIS PB 238773), April, 1974.

6. Sinha, P. K., "Design of a Magnetically Levitated Vehicle," IEEE Transactions on Magnetics. Vol. Mag-20, No. 5, September, 1984, pp 1672-2.

7. Sabnis, A.V., "Analysis of Forces in Rectangular-Pole Geometries Using Numerical Integration Techniques," IEEE Transactions on Magnetics. Vol. MAG-12, No. 4, July 1976.

8. Heinrich, K., and Kretzschmar, R., Editors., "Transrapid MagLev System," Hestra-Verlag, Darmstadt, 1989.

9. Bohn, G. and Steinmetz, G., "The Electromagnetic Levitation and Guidance Technology of the 'Transrapid' Test Facility Emsland," IEEE Transactions on Magnetics. Vol. Mag-20, No. 5, September, 1984, pp 1666-71.

10. Heger, F., Heger, W., Roth, R., "Three-Dimemsional Finite Element Analysis of Radial Magnetic Bearing," Draper Laboratory report CSDL-P-3085, August, 1991.

EMS Staggered Vertical Magnets(with lateral Force capability)

11. Brzezina, W., Langerholc, J., "Lift and Side Forces on Rectangular Poles in Two Dimensions," J. Applied Physics, Vol. 45, No. 4,1974.

Wormley, D.N. et al, op. cit.

Yamamura, S., and Ito, T., op. cit.

Sabnis, A.V., op. cit.

EMS Vertical Lift Magnets /Synchronous Motor

12. Mischler, W.R. and Nondahl, T.A., "Performance of a Linear Synchronous Motor with Laminated Track Poles and with Various Misalignments. Phase 1, Vol. 1," GE and FRA, Report No. RFA/ORD-80/52-1, SRD-78-102, September, 1980.

Roters, H.C., op. cit.

Weinberg, M.S., op. cit.

EMS Linear Induction Motor

13. Stickler, J. J., "Comparison of Theories for High-Speed Linear Induction Motors," IEEE Trans. Vehicular Technology, Vol. VT-29, No. 1, Feb., 1980, pp. 65-71.

14. Nondahl, T. A. and Richter, E., "Comparison between Designs for Single-Sided Linear Electric Motors, Homopolar Synchronous and Induction, Phase III," GE and FRA, Report No. RFA/ORD-80/54 (NTIS PB 81 116188), September, 1980.

15. Elliot, D.G., "Matrix Analysis of Linear Induction Machines," Jet Propulsion Lab. and FRA, Report No JPL-SP-43-24, FRA/ORD-75/77 (NTIS PB 254574), September, 1975.

16. Kliman, G.B. and Mischler, W.R., "Performance of a Single-Sided Linear Induction Motor with Solid Back Iron and with Various Misalignments, Phase II," Vol. 1, GE and FRA, Report No. RFA/ORD-80/53-1; SRD-78-069, September, 1980.

17. Lipkis, R.S. and Wang, T.S., "Single Sided Linear Induction Motor (SLIM); A Study of Thrust and Lateral Forces," TRW and FRA, Report No. FRA/RT72125 (NTIS PB 205029), June, 1971.

18. Nonaka, S. and Higuchi, T., "Design Strategy of Single-Sided Linear Induction Motors for Propulsion of Vehicles," IEEE International Conference on Maglev and Linear Drives, Las Vegas, 1987, pp 1-5.

19. Yamamura, S., "Theory of Linear Induction Motors," 2d Ed., John Wiley & Sons, New York, 1978.

20. Nasar, S.A. and Boldea, I., "Linear Motion Electromagnetic Systems," John Wiles & Sons, New York, 1985.

21. Gieras, J.F., "Linear Induction Motors," WNT, Warsaw, 1990.

22. Nonaka, S., and Furukawa, T., "Finite Element Analysis of Linear Induction Motors Taking into Account Discontinuity of Secondary Rails," Proc. 11th International Conference on Magnetically Levitated Systems and Linear Drives (Maglev'89), July 7-11, 1989, Yokohama, Japan, pp 339-344.

23. Tevan, G., and Toth, F., "A Clear Algorithm for the Calculation of the Linear Induction Motor Based on Field Theory," Acta Technica, Academiae Scientiarum Hungaricae, Tom 8b(3-4), 1978, pp 331-362.

24. Tevan, G., "Computation of a Double-Sided Linear Induction Motor by Undamped Travelling Waves," Periodica Polytechnia-Electrical Engineering, Vol. 23, No. 2, 1979, pp.113-135.

25. Tevan, G., "Optimizing Analyses of a Double-Sided Linear Induction Motor," Periodica Polytechnia-Electrical Engineering, Vol. 23, No. 2, pp.137-147.

26. Nonaka, S., Fujii, N., Watanabe, T., and Kojima, T., "Test Facility and Test Results of Single-Sided LIM for Urban Transit," Proc. International Conference on Magnetically Levitated Systems and Linear Drives(Maglev'85), 1985, pp 111-120.

27. Gieras, J. F., Dawson, G. E., and Eastham, A. R., "Performance Calculation for Single-Sided Linear Induction Motors with a Double-Layer Reaction Rail Under Constant Current Excitation," IEEE Transactions on Magnetics, Vol. Mag-22, No. 1, January, 1986, pp. 54-62.

28. Gieras, J. F., Eastham, A. R. and Dawson, G. E., Performance Calculation for Single-Sided Linear Induction Motors with a Solid Steel Reaction Plate Under Constant Current Excitation," IEE Proceedings, Vol. 132, Pt. B, No. 4, July 1985, pp. 185-194.

29. Gieras, J. F., Dawson, G. E., and Eastham, A. R., "A New Longitudinal End Effect Factor for Linear Induction Motors," IEEE Trans. Energy Conversion, Vol. EC-2, No. 1, March 1987, pp. 152-159.

30. Dawson, G. E., and Eastham, A. R., "Comparative Performance of Single-Sided Linear Induction Motors with Squirrel-Cage, Solid-Steel and Aluminum-Capped Reaction Rails," Conference Record-IEEE Industry Applications Society Annual Meeting, Oct. 8-9, 1981, pp. 323-329.

31. Heger, F., "Electromagnetic Processes in a Conducting Medium with Non Linear Parameters (Application of Lie Groups to Maxwell's Equations)," Draper Laboratory Report CSDL-P-2968, July, 1990.

32. Ogarkov, E.M., Korotaev, A.D., "The Quadrature Effect of Linear Induction Motors with Account Taken of Secondary Element Anisotropy," Elektrichestvo, No. 4, 1991, pp 36-40.

33. Epifanov, A.P., Lebedev, A.M., "Method for Calculation of Characteristics of Linear Induction Motors," Eleсktroteknika, Vol. 4, No. 5, 1991, pp 26-29, translated in Soviet Electrical Engineering, pp. 46-51, Allerton Press, New York, 1992.

34. Skobelev, V. E.,"Influence of Longitudinal Fringe Effect on the Operation of High Speed Traction Induction Motors," Rail International, Dec. 1974, pp. 767-781.

35. Skobelev, V. E.,"The Problems of using the Asynchronous Linear Motor for High-Speed Ground Transport," Rail International, June 1977, pp. 297-308.

36. Skobelev, V. E., Solovyev, G. I. and Epifanov, A. P. "The Analysis of Means of Improving Characteristics of Linear Induction Traction Motors for High-Speed Ground Transport," Rail International, June, 1980, pp. 369-380.

37. Poloujadoff, M., "The Theory of Linear Induction Machinery," Clarendon Press, Oxford, 1980.

EDS Levitation/Guidance

38. Richards, P.L. and Tinkham, M., "Magnetic Suspension and Propulsion Systems for High-Speed Transportation," J. Appl. Phys., Vol. 43, No. 6, June 1972, pp. 2680-91.

39. Heger, F. and Gorman, J., "Superconducting Materials for Magnetic Field Shaping and Shielding in Electrical Machinery," Draper Laboratory Memo EEF-5027-89.

40. Grover, F.W., "Inductance Calculations, Working Formulas and Tables," Dover Publications, New York, 1962.

41. Urankar, L. and Mierícke, J. "Forces on Arbitrary Plane Multiple Excitation Current Systems Used in Magnetic Levitation," Siemens Forsch.- u. Entwickl.-Ber. Bd. 2, Nr. 3 (1974), pp. 142-148.

42. Miericke, J. and Urankar, L. "Theory of Electrodynamic Levitation with a Continuous Sheet Track - Part I," Appl. Phys., No. 2, 1973, pp. 201-211.

43. Urankar, L. and Miericke, J. "Forces on Null-Flux Magnetic Levitation Systems," J. Appl. Phys., Vol. 44, No. 4, April 1973, pp. 1907-1909.

44. Powell and Danby, "Magnetic Suspennsion for Levitated Tracked Vehicles", Cryogenics, June 1971

Ride Quality (both EMS & EDS)

45. Pepler, R.D., et al, "Development of Techniques and Data for Evaluating Ride Quality, Vol. II, U.S. Dept. of Trans. Report DOT-TSC-RSPD-77-1, II, February, 1978.

46. Hedrick, J.K. and Wormley, D.N., "Active Suspensions for Ground Transport Vehicled-A State of the Art Review", Mechanics of Transportation Suspension Systems, ASME Monograph AMD-V0115, 1975.

47. Wormley, D. N. , et al, "Magnetic Levitation Vehicle-Suspension Guideway Interaction", Technical Memorandum, Center for Transportation Studies, Massachusetts Institute of Technology (Contract DTFR 53-91-C-00062, Federal Railroad Administration), January, 1992.

48. Wormley, D. N., et al, "Interactions Between Magnetically Levitated Vehicles and Elevated Guideway Structures", Center for Transportation Studies, Massachusetts Institute of Technology, contract DTFR 52-91-C-00062, July, 1992.

Weinberg, M.S., op. cit.

Wormley, D.N. et al, op. cit.

General

49. Beltramo, M. N., D. L. Trapp, B. W. Kimoto, and D. P. Marsh, "Parametric Study of Transport Aircraft Systems Cost and Weight," NASA Report CR 151970 (NTIS N77-26106), April 1977

50. Baumeister, T., Avallone, E. A. , and Baumeister III, T., eds., "Marks Standard Handbook for Mechanical Engineers", 8th Ed., McGraw-Hill, 1978

Comparison of Major Parameters in Electrodynamic and Electromagnetic Levitation Transport Systems, US DOT, FRA, NMI, WE Brown, CR Dauwalter, F Heger, MS Weinberg, 1992 -11-Advanced Systems